frontiers | Research Topics

Metabolic estimates during glucose challenge tests and continuous glucose monitoring – innovative and broad approaches to assessing glucose and insulin metabolism in diverse populations

Edited by
Joon Ha, Stephanie Therese Chung, Melanie Cree-Green and Cecilia Diniz Behn

Published in
Frontiers in Endocrinology
Frontiers in Physiology

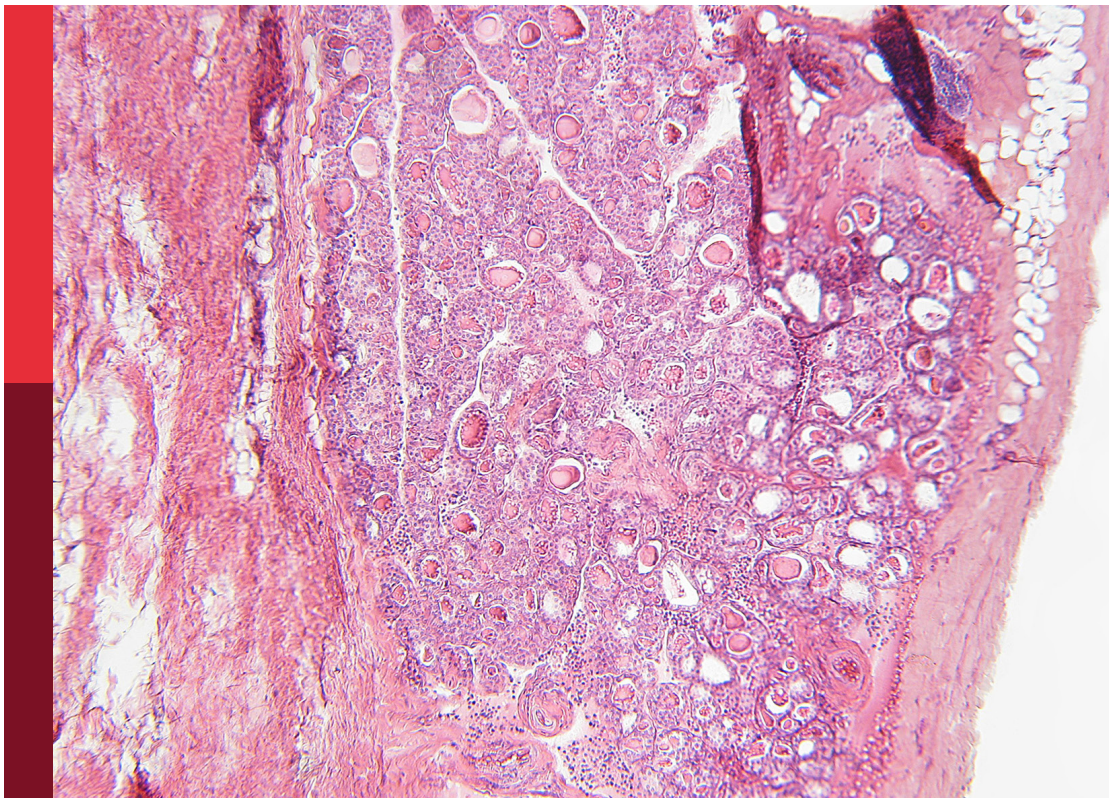

ISSN 1664-8714
ISBN 978-2-83251-214-2
DOI 10.3389/978-2-83251-214-2

About Frontiers

Frontiers is more than just an open access publisher of scholarly articles: it is a pioneering approach to the world of academia, radically improving the way scholarly research is managed. The grand vision of Frontiers is a world where all people have an equal opportunity to seek, share and generate knowledge. Frontiers provides immediate and permanent online open access to all its publications, but this alone is not enough to realize our grand goals.

Frontiers journal series

The Frontiers journal series is a multi-tier and interdisciplinary set of open-access, online journals, promising a paradigm shift from the current review, selection and dissemination processes in academic publishing. All Frontiers journals are driven by researchers for researchers; therefore, they constitute a service to the scholarly community. At the same time, the *Frontiers journal series* operates on a revolutionary invention, the tiered publishing system, initially addressing specific communities of scholars, and gradually climbing up to broader public understanding, thus serving the interests of the lay society, too.

Dedication to quality

Each Frontiers article is a landmark of the highest quality, thanks to genuinely collaborative interactions between authors and review editors, who include some of the world's best academicians. Research must be certified by peers before entering a stream of knowledge that may eventually reach the public - and shape society; therefore, Frontiers only applies the most rigorous and unbiased reviews. Frontiers revolutionizes research publishing by freely delivering the most outstanding research, evaluated with no bias from both the academic and social point of view. By applying the most advanced information technologies, Frontiers is catapulting scholarly publishing into a new generation.

What are Frontiers Research Topics?

Frontiers Research Topics are very popular trademarks of the *Frontiers journals series*: they are collections of at least ten articles, all centered on a particular subject. With their unique mix of varied contributions from Original Research to Review Articles, Frontiers Research Topics unify the most influential researchers, the latest key findings and historical advances in a hot research area.

Find out more on how to host your own Frontiers Research Topic or contribute to one as an author by contacting the Frontiers editorial office: frontiersin.org/about/contact

Metabolic estimates during glucose challenge tests and continuous glucose monitoring – innovative and broad approaches to assessing glucose and insulin metabolism in diverse populations

Topic editors

Joon Ha — Howard University Washington, United States
Stephanie Therese Chung — National Institutes of Health (NIH), United States
Melanie Cree-Green — University of Colorado, United States
Cecilia Diniz Behn — Colorado School of Mines, United States

Citation

Ha, J., Chung, S. T., Cree-Green, M., Behn, C. D., eds. (2023). *Metabolic estimates during glucose challenge tests and continuous glucose monitoring – innovative and broad approaches to assessing glucose and insulin metabolism in diverse populations*. Lausanne: Frontiers Media SA. doi: 10.3389/978-2-83251-214-2

Table of contents

frontiers | Frontiers in Physiology

TYPE Editorial
PUBLISHED 16 December 2022
DOI 10.3389/fphys.2022.1112502

OPEN ACCESS

EDITED AND REVIEWED BY
Johannes Van Lieshout,
University of Amsterdam, Netherlands

*CORRESPONDENCE
Joon Ha,
joon.ha@howard.edu
Melanie Cree-Green,
melanie.green@childrenscolorado.org
Stephanie Therese Chung,
stephanie.chung@nih.gov
Cecilia Diniz Behn,
cdinizbe@mines.edu

SPECIALTY SECTION
This article was submitted to Clinical and Translational Physiology, a section of the journal Frontiers in Physiology

RECEIVED 30 November 2022
ACCEPTED 06 December 2022
PUBLISHED 16 December 2022

CITATION
Ha J, Cree-Green M, Chung ST and Diniz Behn C (2022), Editorial: Metabolic estimates during glucose challenge tests and continuous glucose monitoring—Innovative and broad approaches to assessing glucose and insulin metabolism in diverse populations.
Front. Physiol. 13:1112502.
doi: 10.3389/fphys.2022.1112502

Editorial: Metabolic estimates during glucose challenge tests and continuous glucose monitoring—Innovative and broad approaches to assessing glucose and insulin metabolism in diverse populations

Joon Ha[1]*, Melanie Cree-Green[2]*, Stephanie Therese Chung[3]* and Cecilia Diniz Behn[4]*

[1]Department of Mathematics, Howard University, Washington, DC, United States, [2]Department of Pediatrics, University of Colorado Anschutz Medical Campus, Aurora, CO, United States, [3]National Institute of Diabetes and Digestive and Kidney Diseases (NIH), Bethesda, MD, United States, [4]Department of Applied Mathematics and Statistics, Colorado School of Mines, Golden, CO, United States

KEYWORDS

oral glucose tolerance test (OGTT), continuous glucose monitoring, beta-cell function, insulin sensitivity, glucose fluctuation

Editorial on the Research Topic
Metabolic estimates during glucose challenge tests and continuous glucose monitoring—Innovative and broad approaches to assessing glucose and insulin metabolism in diverse populations

Introduction

Identifying early signs of metabolic dysfunction is crucial for preventing and delaying type 2 diabetes (T2D). As such, glucose challenge tests that assess fasting and postprandial glucose and related hormonal factors (e.g., insulin/C-peptide, glucagon) provide critical information on pathophysiological mechanisms of type 2 diabetes (T2D). Glucose challenge tests range in complexity from intravenous glucose tolerance tests (IVGTT) that are technically challenging and require specialized metabolic testing centers to mixed meal and oral glucose tolerance tests (OGTT) that can be conducted in outpatient settings. While existing simple mathematical indices (e.g., insulinogenic index (IGI), oral disposition index, HOMA-IR, and

Matsuda index [1, 2] are widely used in clinical and epidemiological studies, more complex mathematical models of glucose challenge tests are emerging as sensitive and precise markers for beta-cell function and insulin sensitivity [3, 15, 16]. Recently, continuous glucose monitoring (CGM)-derived metabolic parameters, including mean amplitude of glycemic excursions (MAGE), offer pragmatic alternatives to assess metabolic risk and status [4].

The development of new measures for quantifying data from glucose challenge tests and CGM is necessary to support clinical practice and promote scientific understanding. This Research Topic sought to highlight new and emerging modeling approaches and markers based on data from glucose challenge tests and CGM with the potential for advancing the field of diabetes risk prediction and assessment especially in diverse populations. Given the variability in metabolic responses associated with age, sex, and race/ethnicity, mathematical models and diagnostic markers must be tested in a wide range of patient populations [10]. Moreover, the application of these approaches in varied populations often requires re-examination of the assumptions and application of mathematical models and diagnostic markers. In particular, several articles address the promising possibilities raised by analysis of CGM data. We provide an overview of the published articles below.

Novel modeling approaches

Minimal models have been widely used in mathematical modeling of metabolism [15]. However, in cases where more data are available, models that incorporate additional metabolites provide insights into specific aspects of metabolic dysregulation. Several articles in this Research Topic proposed novel mathematical models of the interacting dynamics of different metabolites. Subramanian et al. introduced a model of coupled glucose-insulin-glucagon dynamics during an isoglycemic intravenous glucose infusion (IIGI) experiment designed to mimic an OGTT. This model was used to identify several differences between participants with T2D relative to weight matched control participants without diabetes. Abohtyra et al. described a model-based method for inferring a parameterization of insulin secretion rate using glucose, insulin, and C-peptide data from an OGTT even when sampling of these data was sparse. Hampton et al. presented a mathematical model of glycerol-insulin dynamics that considered how the dynamics of glycerol suppression and recovery probe the function of adipose tissue and its response to insulin in adolescent girls. They found that the dynamics of glycerol differ from the dynamics of glucose in this population, thereby emphasizing the need to consider age/life-stage in metabolic assessments.

Markers for improving diabetes screening and treatment

There is much effort focused on improving T2D screening and understanding diabetes progression. Several papers in this Research Topic addressed this question while considering the modifying factors of demographics and genetics. Shi et al. investigated the prevalence and significance of low muscle mass and its relationship to glycemia. Low muscle mass was associated with glycemic excursions in males but not females. Richter et al. used a data assimilation approach to predict glycemic states in adolescents following bariatric surgery. They first estimated parameters in a mechanistic model using data assimilation on clinical OGTT data [11]; then they applied logistic regression models with variables including these parameters as well as clinical data from the electronic health record to predict post-surgical glycemic control. Vejrazkova et al. analyzed OGTT data and found that the G allele of the rs10830963 polymorphism is associated with impaired early phase of beta cell function. Interestingly, this impairment was present even in healthy individuals with normoglycemia. Karamched et al. described the concept of delay-induced uncertainty (DIU) and the implications of DIU for glucose fluctuations. They established that DIU was present in large regions of parameter space for an established model of glucose-insulin dynamics [13, 14], and they argued that DIU is pathogenic for obesity and type 2 diabetes. These theoretical models are important as they explore diagnostic screening tools as well as mechanisms for diabetes progressions. Additional experimental data are needed to evaluate these provocative model predictions.

Markers of glucose fluctuations

There has been much effort to find markers of glucose excursions [5, 6, 7, 12] to identify patients who are at high risk for progression to diabetes and its complications [8, 9]. In-line with one of the goals of this Research Topic, novel metabolic markers or model parameters of glucose challenge tests, the following two articles found novel markers of glucose fluctuations. Ha et al. showed that the discrepancy between glucose management indicator and HbA1c is a good predictor for intensive care unit (ICU) stay and mortality. Jagannathan et al. Identified that elevated 1-h glucose at the time of remission of T2D dysglycemia is a risk factor for T2D relapse among Black patients with obesity. However, large fluctuations in blood glucose concentrations are not the only indicators for high risk for worsened glycemia and diabetic complications: glucose variability may also play a role. New methods leveraging CGM hold much promise for the screening and monitoring of diabetes with a focus on glucose variability. Wang et al. used CGM data to relate glucose variability to

risk for nocturnal hypoglycemia in patients with T2D. Similarly, in another article, Wang et al. used CGM data to compare the effects of basal insulin *vs.* premixed insulin on glucose variability and hypoglycemia in T2D patients. However, Faerch et al. found that there was poor agreement between measurements from venous blood plasma and CGM during an OGTT. More work is needed to understand the relationship between CGM data and typical plasma-based measures of glucose dynamics.

Conclusion and future directions

In conclusion, the fields of method and model development to understand glucose and related hormone dynamics are active, with new emerging ideas. The articles in this Research Topic highlighted novel modeling approaches and markers based on data from glucose challenge tests and CGM that could improve T2D risk prediction, screening, and glucose control. The primary need for the future will be to determine how to translate the research based-methods presented here into simpler models with broadly clinically relevant endpoints. This will require additional studies of glucose metabolism in the postprandial state. Ideally, this would allow for more sophisticated risk assessments of dysglycemia and clinical methods for assessing beta-cell function relative to insulin sensitivity. Such methods could be translated to large epidemiologic studies and move us closer to clinical precision medicine.

Author contributions

JH, MC-G, SC, and CBD designed, wrote, and reviewed the final manuscript, and approved it for publication.

Conflict of interest

The authors declare that the research was conducted in the absence of any commercial or financial relationships that could be construed as a potential conflict of interest.

Publisher's note

frontiers in Endocrinology

ORIGINAL RESEARCH
published: 05 October 2021
doi: 10.3389/fendo.2021.753810

Discordance Between Glucose Levels Measured in Interstitial Fluid *vs* in Venous Plasma After Oral Glucose Administration: A *Post-Hoc* Analysis From the Randomised Controlled PRE-D Trial

Kristine Færch[1,2], Hanan Amadid[1], Lea Bruhn[1], Kim Katrine Bjerring Clemmensen[1], Adam Hulman[3], Mathias Ried-Larsen[4,5], Martin Bæk Blond[1,2], Marit Eika Jørgensen[1,6] and Dorte Vistisen[1,7]*

[1] Steno Diabetes Center Copenhagen, Gentofte, Denmark, [2] Department of Biomedical Sciences, University of Copenhagen, Copenhagen, Denmark, [3] Steno Diabetes Center Aarhus, Aarhus, Denmark, [4] Centre for Physical Activity Research, Rigshospitalet, Copenhagen, Denmark, [5] Institute of Sports and Clinical Biomechanics, University of Southern Denmark, Odense, Denmark, [6] University of Southern Denmark, Copenhagen, Denmark, [7] Department of Public Health, University of Copenhagen, Copenhagen, Denmark

OPEN ACCESS

Edited by:
Stephanie Therese Chung, National Institutes of Health (NIH), United States

Reviewed by:
David H. Wagner, University of Colorado Denver, United States
Yunting Zhou, Nanjing Medical University, China

***Correspondence:**
Kristine Færch
kristine.faerch@regionh.dk

Specialty section:
This article was submitted to Clinical Diabetes, a section of the journal Frontiers in Endocrinology

Received: 05 August 2021
Accepted: 15 September 2021
Published: 05 October 2021

Citation:
Færch K, Amadid H, Bruhn L, Clemmensen KKB, Hulman A, Ried-Larsen M, Blond MB, Jørgensen ME and Vistisen D (2021) Discordance Between Glucose Levels Measured in Interstitial Fluid vs in Venous Plasma After Oral Glucose Administration: A Post-Hoc Analysis From the Randomised Controlled PRE-D Trial. Front. Endocrinol. 12:753810. doi: 10.3389/fendo.2021.753810

Aims: The oral glucose tolerance test (OGTT) is together with haemoglobin A_{1c} (HbA_{1c}) gold standard for diagnosing prediabetes and diabetes. The objective of this study was to assess the concordance between glucose values obtained from venous plasma versus interstitial fluid after oral glucose administration in 120 individuals with prediabetes and overweight/obesity.

Methods: 120 adults with prediabetes defined by HbA_{1c} 39-47 mmol/mol and overweight or obesity who participated in the randomised controlled PRE-D trial were included in the study. Venous plasma glucose concentrations were measured at 0, 30, 60 and 120 minutes during a 75 g oral glucose tolerance test (OGTT) performed on three different occasions within a 26 weeks period. During the OGTT, the participants wore a CGM device (IPro2, Medtronic), which assessed glucose concentrations every five minutes.

Results: A total of 306 OGTTs with simultaneous CGM measurements were obtained. Except in fasting, the CGM glucose values were below the OGTT values throughout the OGTT period with mean (SD) differences of 0.2 (0.7) mmol/L at time 0 min, -1.1 (1.3) at 30 min, -1.4 (1.8) at 60 min, and -0.5 (1.1) at 120 min). For measurements at 0 and 120 min, there was a proportional bias with an increasing mean difference between CGM and OGTT values with increasing mean of the two measurements.

Conclusions: Due to poor agreement between the OGTT and CGM with wide 95% limits of agreement and proportional bias at 0 and 120 min, the potential for assessing glucose tolerance in prediabetes using CGM is questionable.

Keywords: oral glucose challenge test, continuous glucose monitor system, prediabetes, Bland-Altman, proportional bias

INTRODUCTION

The oral glucose tolerance test (OGTT) provides important information about fasting and post-challenge glucose metabolism and is together with haemoglobin A_{1c} (HbA_{1c}) gold standard for diagnosing prediabetes and diabetes (1). However, because the OGTT is inconvenient and time consuming it is seldom used in clinical practice. The use of HbA_{1c} for diagnosing diabetes and especially prediabetes is also challenging, as HbA_{1c} levels in the non-diabetic range is affected by several factors not related to glycaemia (e.g. genetics, iron-deficiency, anaemia, etc.) (2, 3).

In recent years, continuous glucose monitoring (CGM) has become widely used for clinical purposes, because it replaces self-monitoring of glucose among diabetes patients and gives detailed information on glucose excursions during free-living conditions. As such, glucose concentrations measured by a glucose sensor (CGM) placed in the subcutaneous tissue for several days may be more physiologically and clinically relevant for assessing glucose tolerance than a single OGTT. Glycaemic variability assessed by the CGM is associated with the development of diabetic complications even in people with well-controlled HbA_{1c} levels (4), which makes the CGM relevant as a monitor of cardiometabolic risk.

Because glucose concentrations during an OGTT are measured in venous blood and glucose concentrations using CGMs are measured in the interstitial fluid, differences in glucose concentrations between the two methods are expected, but knowledge on the magnitude of the difference and the time-lag between the measures are still limited, especially among people without diabetes. Studies have found the time-lag in glucose readings from CGMs compared to plasma glucose concentrations to be of approx. 5-10 min during hyperglycaemic excursions using data from 14 people with type 1 diabetes (5, 6). In another study of 15 healthy individuals subjected to OGTTs, the time-lag was on average 15 min (7). Also, using model simulations, it has been suggested that CGMs overestimate low glucose values, but underestimate high glucose values, leading to an underestimation of both hypo- and hyperglycaemic events in people with diabetes (6). In healthy non-diabetic individuals, CGMs also seem to underestimate plasma glucose levels during hyper-insulinemic conditions (8). Studies of the relationship between interstitial and plasma glucose concentrations during glucose stimulation in individuals with prediabetes are lacking. Thus, the objective of this study was to assess the concordance between glucose values obtained from venous plasma versus interstitial fluid after oral glucose administration in 120 individuals with prediabetes and overweight/obesity who had three repeated measures over 6 months. Specifically, we examined: 1) the time-lag in interstitial glucose compared with blood glucose during an OGTT and 2) the concordance between blood and interstitial glucose concentrations after taking the time-lag into account.

METHODS

Participants and Setting

We used data from a randomised, multi-arm, parallel, controlled trial, the PRE-D Trial (9, 10). Between February 2016 and July 2019, 120 men and women with BMI ≥25 and HbA_{1c} levels in the prediabetic range (5.7-6.4%/39-47 mmol/mol) were randomised to one of four interventions for 13 weeks: 1) dapagliflozin (10 mg once daily); 2) metformin (850 mg twice daily); 3) exercise (interval training, 30 min, 5 times per week); or 4) control (habitual living). The 13 weeks of intervention were followed by another period of 13 weeks where no interventions were provided. The PRE-D Trial is described in detail elsewhere (9, 10). The study was conducted in accordance with the Helsinki II declaration and Good Clinical Practice. The protocol was approved by the Ethics Committee of the Capital Region (H-15011398) and the Danish Medicines Agency (EudraCT number: 2015-001552-30). Approval for data storage was obtained from the Danish Data Protection Board (2012-58-0004). All participants provided written informed consent before taking part in the study.

Examinations

At baseline and at 13 and 26 weeks, the participants attended the research facility at Steno Diabetes Center Copenhagen, Gentofte, Denmark, for a clinical examination after an overnight fast of ≥8 hours. Upon arrival between 08:00-9:00 AM on the day of the clinical examination, the participants had a CGM attached (iPro2 CGM with Enlite sensor, Medtronic Denmark A/S, Copenhagen, Denmark), which was used to assess glucose concentrations every five minutes during the following six days. The CGM was calibrated after one and two hours. After the second calibration, 75 g glucose was administered orally and venous blood samples for assessment of plasma glucose concentrations were drawn at 0, 30, 60, and 120 min. Questionnaires on socio-economic factors, health, and disease were filled in during the OGTT. During the test day, measurements of height, body weight, waist and hip circumference, and blood pressure were also performed, and body composition was measured by Dual-Energy X-ray

Absorptiometry (Discovery DXA System, Hologic, Marlborough, Massachusetts, USA).

Following each test day (baseline, 13 weeks, 26 weeks), interstitial glucose levels were monitored for six consecutive days during free-living with the CGM system. The CGM provided glucose measurements every 5 min during the entire measurement period (both during the OGTT and free living). To calibrate the CGMs, the participants measured blood glucose levels at home four times a day (before breakfast, before lunch, before dinner, and before bedtime) for the following 6 days using a glucometer (Contour XT, Ascensia Diabetes Care Denmark ApS, Copenhagen, Denmark).

Biochemical Analysis

Samples for biochemical analysis of plasma glucose concentrations were put on ice immediately following sampling. Samples were centrifuged shortly after collection at 4000 rpm for 15 minutes (Sigma 4K15, Osterode Am Harz, Germany), except for samples used for analysis of HbA_{1c} and serum insulin concentrations. Samples for analysis of serum insulin concentration were centrifuged 30 minutes after collection. The samples were stored in a refrigerator for the remainder of the test day. Serum insulin was analysed using electro-chemiluminescence immunoassay (Cobas e411, Roche Diagnostics, Switzerland). HbA_{1c} was measured by High Performance Liquid Chromatography (Tosoh G8, Tosoh Corporation, Japan). Plasma glucose, total cholesterol, HDL cholesterol, and triglycerides were analysed by cholometric analysis (Vitros 5600, Ortho Clinical Diagnostics, USA). Plasma VLDL cholesterol was calculated as plasma triglycerides (mmol/l) divided by 2.2, and plasma LDL cholesterol was calculated based on the Friedewald equation (11). Estimated glomerular filtration rate (eGFR) was calculated using the CKD-epi formula (12).

Data Management, Calculations and Definitions

Raw data from the CGM and glucometer were downloaded from the online system CareLink™ (Medtronic MiniMed, Northridge, CA, USA). The mean amplitude of glycaemic excursions (MAGE), a measure of glycaemic variability, was calculated by taking the arithmetic mean of the blood glucose increases or decreases when both ascending and descending segments exceeded the value of one standard deviation of the blood glucose during a 24-hour measurement period. Data from the free-living measurement period was used for calculating MAGE.

Statistical Analysis

Linear mixed-effects analysis with a participant-specific random intercept was used to estimate population mean levels of plasma glucose at each CGM and OGTT time-point. For all participants, we matched each of their post-challenge OGTT values to their least deviating CGM value in the period 0-15 min after the OGTT sample was obtained. In **Figure 1**, this method is illustrated for one of the participants. Because the CGM provided glucose measurements every 5 min, the time of best match was at 0, 5, 10 or 15 min after the OGTT sample. For the best matching CGM value, the corresponding time-lag and observed difference in glucose level between the CGM and OGTT was recorded.

To examine the agreement between glucose concentrations obtained from subcutaneous tissue versus venous plasma, Bland-Altman plots (13) were performed for each time point during the OGTT using the best matching CGM value. Potential

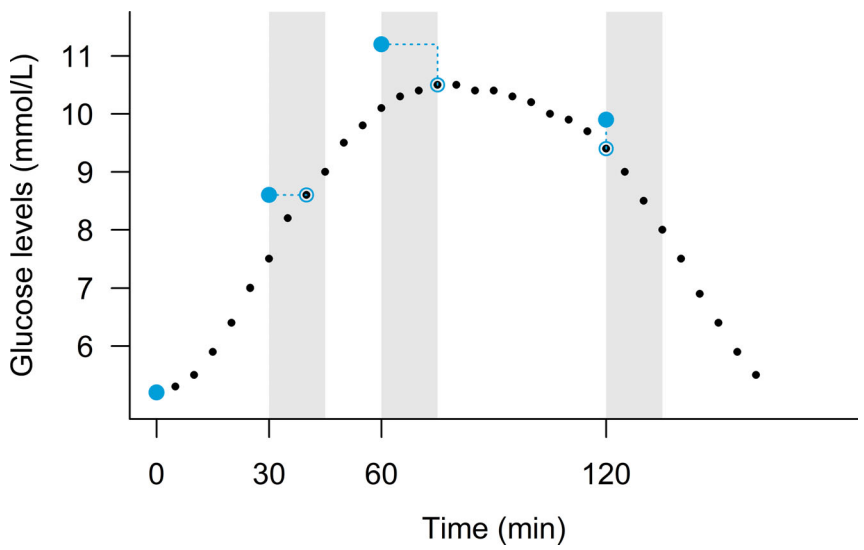

FIGURE 1 | An example of (plasma glucose levels) measured during the OGTT (large blue points) and simultaneously by the continuous glucose monitoring device (black points) in a person. The light grey areas indicate the 0-15 min period after the OGTT measurements, and the dotted blue lines point to the best CGM match within the 15 min period.

TABLE 1 | Characteristics of study participants at baseline (n = 120).

Age (years)	62.6 (54.0,68.0)
Men (n, %)	53 (44)
Current smoker (n, %)	13 (11)
Family history of diabetes (n, %)	64 (53)
Family history of CVD (n, %)	70 (58)
Antihypertensive medication (n, %)	32 (27)
Lipid-lowering medication (n, %)	28 (23)
Systolic blood pressure (mmHg)	131 (122,144)
Diastolic blood pressure (mmHg)	85 (79,90)
Body weight (kg)	91 (82,104)
BMI (kg/m^2)	30.8 (27.4,34.3)
Waist circumference (cm)	104 (98,113)
Body fat (%)	40 (31,44)
eGFR (ml/min/1.73 m^2)	88.5 (80.6,97.5)
Total cholesterol (mmol/l)	5.1 (4.3,5.9)
LDL cholesterol (mmol/l)	3.1 (2.4,3.7)
HDL cholesterol (mmol/l)	1.3 (1.1,1.5)
Triglycerides (mmol/l)	1.3 (0.9,1.8)
HbA_{1c}	
mmol/mol	41 (39,43)
%	5.9 (5.7,6.1)
Fasting plasma glucose (mmol/l)	5.6 (5.2,5.9)
Fasting serum insulin (pmol/l)	71.5 (48.0,98.5)
MAGE (mmol/l)	1.6 (1.4,2.2)

Data are medians (Q1;Q3) or numbers (%).

heteroscedasticity was assessed graphically. We estimated limits of agreement and tested for proportional bias using linear mixed-effects analysis with a participant-specific random intercept.

We assumed that the association between glucose levels measured by the OGTT and CGM was unaffected by the interventions. However, in a sensitivity analysis, we studied the potential confounding effect of the different interventions on the relationship between CGM and OGTT glucose data by repeating all analyses including only data from the baseline visit.

Statistical analyses were performed in R version 3.5.2 (The R Foundation for Statistical Computing).

RESULTS

Clinical Characteristics

The median (Q1; Q3) age of the study population was 63 (54; 68) years, BMI was 30.8 (27.4; 34.3) kg/m^2, and 44% were men. A total of 306 OGTTs with simultaneous valid CGM measurements were obtained. In **Table 1**, the characteristics of the study participants are shown.

Time-Lag Between CGM and OGTT

Figure 2 shows the distribution of possible time-lags (0, 5, 10 or 15 min) of the corresponding CGM measurement for each of the post-challenge OGTT glucose values. For the OGTT value at 30 min, there was a 15 min lag-time in CGM measurements for more than 60% of the participants. For the OGTT values at 60 and 120 min, the best match of CGM measurements was at the same time as the OGTT measurements for approximately half of the participants, but in 33% and 26% of the participants, a 15 min lag-time in CGM measurements at 60 and 120 min, respectively, was present.

Concordance Between Blood and Interstitial Glucose Concentrations

Figure 3 illustrates the population mean plasma glucose levels measured during the OGTT and simultaneously by the CGM device. Except in the fasting state, the mean CGM glucose values were on average below the mean OGTT values throughout the 120 min period, and this was especially pronounced at 60 min. The mean (SD) differences between observed CGM and OGTT glucose concentrations were 0.2 (0.7) mmol/L (equivalent to 3.2 (13.4)%) at time 0 min, -1.1 (1.3) mmol/L (-12.2 (15.4)%) at 30 min, -1.4 (1.8) mmol/L (-13.3 (18.2)%) at 60 min, and -0.5 (1.1) mmol/L (-3.9 (14.9)%) at 120 min.

The Bland-Altman analyses at time points 0, 30, 60 and 120 min are presented in **Figure 4**. For the measurements at 0

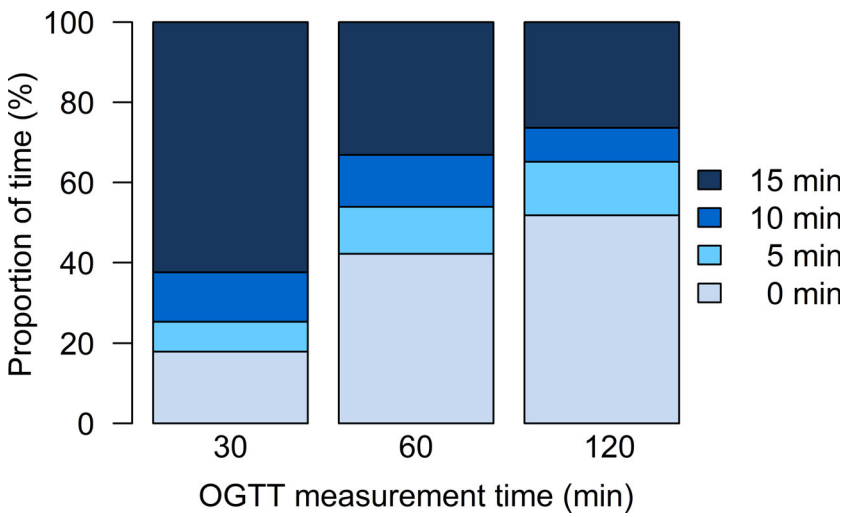

FIGURE 2 | Distribution of possible time-lags (0, 5, 10 or 15 min) of the corresponding CGM measurement for each of the post-challenge OGTT glucose values.

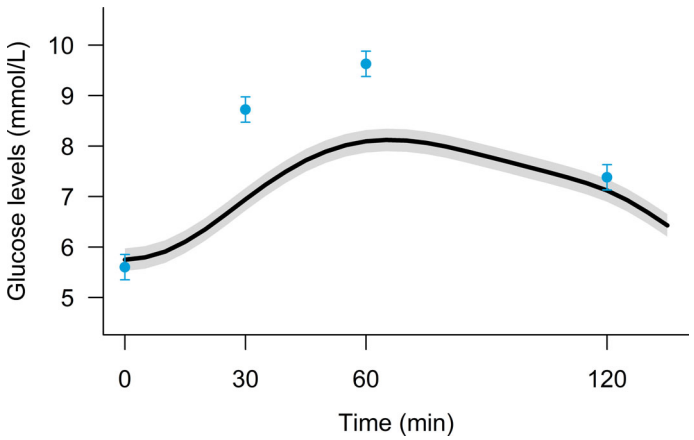

FIGURE 3 | Mean (95%-CI) plasma glucose levels measured during the OGTT (blue points) and simultaneously by the continuous glucose monitoring device (black curve) in 120 persons with prediabetes examined three times over 26 weeks.

and 120 min there was a proportional bias with an increasing or decreasing mean difference between CGM and OGTT values (y-axis) with increasing mean of the two measurements (x-axis) (0 min: P <0.001, 120 min: P <0.001). Hence, during fasting conditions, the CGM particularly overestimated glucose values for high mean values (slope 0.6 per mmol/L), and at 120 min the CGM greatly underestimated glucose at high mean values (slope -0.3 per mmol/L). There was no sign of heteroscedasticity with limits of agreement being overall parallel to the mean curve in any of the plots in **Figure 4**. The sensitivity analysis including only data from the baseline visit showed similar results (**Electronic Supplementary Material**).

DISCUSSION

The use of glucose sensors to inform diabetes management decisions has become part of most practices during recent years (14). In contrast, the potential usefulness of CGMs to guide diagnostic decisions has received less attention. In this analysis of 120 individuals with prediabetes and overweight or obesity, we show that glucose levels obtained by CGMs during an OGTT are on average 12-13% lower at 30 and 60 min and 4% lower at 120 min after oral glucose administration than those measured in venous plasma – even when taking individual time-lag in sensor glucose measurements into account.

Plasma and interstitial fluid are both part of the body's extracellular fluid, and interstitial fluid can be considered the ultrafiltrate of plasma, which transports nutrients, including glucose, from the blood stream to the cells and back. Therefore, using glucose concentrations determined from CGMs with real-time feedback seems highly relevant in evaluation of glucose tolerance in individuals at a high risk for diabetes (15). However, there is a lack of studies with concomitant analysis of OGTT and CGM data. Previous studies on CGM accuracy compared to blood glucose concentrations have included people with diabetes during a liquid meal test (5), insulin-induced hypoglycaemic conditions (16), or during a 24-hour hospital stay (16) (not OGTT). Also, one study of 11 young healthy adults found 15% lower interstitial glucose concentrations than plasma glucose concentrations concomitantly measured during a stepped euglycemic-hypoglycaemic-hyperglycaemic insulin clamp (8). Another study in 15 healthy overweight men subjected to an OGTT found that the time to peak of glucose was significantly delayed for the interstitial fluid measurement compared to the plasma glucose measurement and that body fat percentage was related to the time to peak (7). Using Bland-Altman plots, the study also suggested that the differences between the plasma glucose and interstitial fluid measures increased with increasing level of circulating glucose (7), which is in alignment with our findings. Together, our findings and findings from other studies underscore that interstitial glucose concentrations do not sufficiently capture plasma glucose when glucose levels are acutely changed. This is not surprising as several factors contribute to the concentration difference and time-lag between glucose measured in the venous plasma and the interstitial fluid, including the rate of glucose diffusion, the magnitude of concentration differences in various tissues, blood flow, blood vessel permeability to glucose, and acute changes in the release of insulin and glucagon (17, 18). Also, the fact that the OGTT was performed within the first 24 hours of the CGM measurement period may have contributed to the limited agreement between the two measures, because the accuracy of the CGM may be lower on the first day of measurement.

A strength of this analysis was the availability of up to three pairwise measures of CGM and OGTT data for 120 participants within 26 weeks, enabling us to study the difference between venous plasma glucose and interstitial glucose during a dynamic but standardised change of glucose concentration. The different interventions are not likely to affect the association between

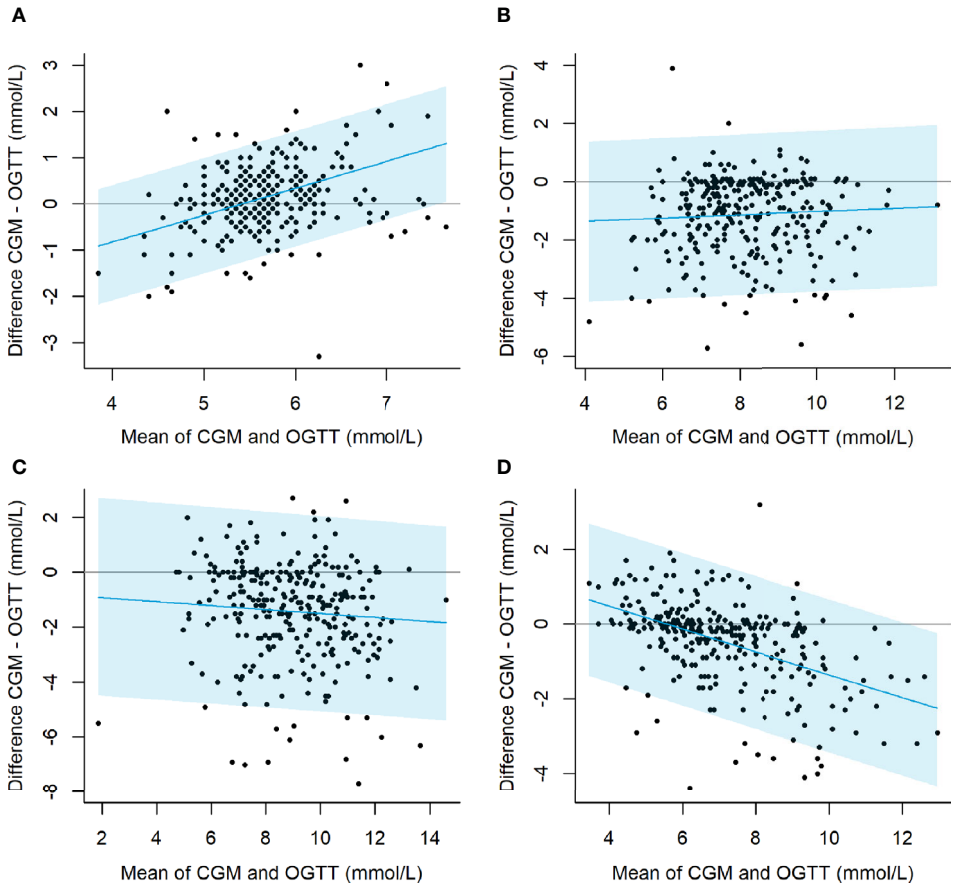

FIGURE 4 | Bland-Altman plots illustrating the agreement between the CGM and OGTT glucose measured during fasting **(A)**, and after 30 min **(B)**, 60 min **(C)**, and 120 min **(D)** after oral administration of 75 g glucose. Light blue areas indicate limits of agreement. Test of proportional bias: 0 min: P <0.001, 0 min: P = 0.306, 0 min: P = 0.196, 120 min: P <0.001.

glucose measured in venous plasma and in the interstitial fluid, and our sensitivity analysis showed that analysis of baseline data produced comparable results. A limitation of our study was that we only studied individuals with prediabetes and overweight or obesity. Accordingly, we were not able to test the potential of the CGM to distinguish between individuals with normoglycaemia and prediabetes – an aspect which has been addressed in previous studies with emphasis on the role of glycaemic variability (19–21). Another limitation is related to the type of CGM used in this study. Our findings may be specific to the iPro2 sensor and may not be generalised to other types of sensors, for instance the FreeStyle Libre Flash CGM system by Abbott, which is now more commonly used in clinical settings. The FreeStyle Libre Flash only assesses glucose concentrations every 15 min as compared to the IPro2 where glucose concentrations are assessed every 5 min, which is an additional challenge. Therefore, more studies using different types of CGMs together with the OGTT are warranted.

Not unexpectedly the CGM systematically underestimated the glucose level when compared to plasma samples with 13% discrepancy between observed OGTT and CGM levels. In general, there is a high intra-individual variation in fasting glucose (15%) and 2-hour glucose (46%) concentrations during an OGTT (22). We also found a large interindividual variation in the difference between the results for the two methods. However, more critically we found a proportional bias in the difference between OGTT and CGM levels and inter-individual differences in the time-lag, making it unlikely that the IPro2 can be used as a substitute for plasma samples when performing an OGTT. As such, crude CGM measures may not be accurate enough to assess glucose tolerance among individuals with prediabetes. Further investigations are needed to assess the link between CGM measures and long-term outcomes before CGMs can be used for diagnostic purposes.

DATA AVAILABILITY STATEMENT

Data described in the manuscript and analytic code will be made available upon request to the corresponding author pending application and approval.

ETHICS STATEMENT

The studies involving human participants were reviewed and approved by The Ethics Committee of the Capital Region, Region Hovedstaden, Blegdamsvej 60. 1. sal, 2100 København Ø. The patients/participants provided their written informed consent to participate in this study.

AUTHOR CONTRIBUTIONS

KF and DV conceived the idea and drafted the manuscript. KF is the sponsor and MJ is the principal investigator of the PRE-D Trial. HA, LB, and MR-L contributed to the design of the study. KF, HA, LB, KC, MB, and MJ were involved in the conduct of the trial and data collection. KC and DV performed statistical analyses. AH, MR-L, and MB provided statistical input. All authors critically revised the manuscript for important intellectual content and approved the final version of the manuscript. KF is the guarantor of this work and, as such, had full access to all the data in the study, takes responsibility for the integrity of the data and the accuracy of the data analysis, and had final responsibility for the decision to submit for publication. All authors contributed to the article and approved the submitted version.

FUNDING

The study was funded by the Novo Nordisk Foundation, AstraZeneca AB, the Danish Innovation Foundation, and University of Copenhagen. The funders had no role in study design, data collection, data analysis, interpretation, or writing of the report. The corresponding author had full access to all data in the study and had final responsibility for the decision to submit for publication.

ACKNOWLEDGMENTS

We are grateful to the study participants for their cooperation and willingness to participate. The laboratory technicians Hanne Vishof, Lars Sander Koch, Sara Sidenius, and Camilla Søs Nielsen at SDCC are thanked for their great dedication, skilled assistance, and coordination. Christian S. Hansen, Narges Safai, Nicklas J. Johansen, Johan I.B. Egholk, SDCC, are thanked for their assistance during the study.

SUPPLEMENTARY MATERIAL

The Supplementary Material for this article can be found online at: https://www.frontiersin.org/articles/10.3389/fendo.2021.753810/full#supplementary-material

REFERENCES

1. American Diabetes Association. Classification and Diagnosis of Diabetes. *Diabetes Care* (2017) 40(Supplement 1):S11–24. doi: 10.2337/dc17-S005
2. Coban E, Ozdogan M, Timuragaoglu A. Effect of Iron Deficiency Anemia on the Levels of Hemoglobin A1c in Nondiabetic Patients. *Acta Haematol* (2004) 112(3):126–8. doi: 10.1159/000079722
3. Færch K, Alssema M, Mela DJ, Borg R, Vistisen D. Relative Contributions of Preprandial and Postprandial Glucose Exposures, Glycemic Variability, and Non-Glycemic Factors to HbA 1c in Individuals With and Without Diabetes. *Nutr diabetes* (2018) 8(1):38. doi: 10.1038/s41387-018-0047-8
4. Tang X, Li S, Wang Y, Wang M, Yin Q, Mu P, et al. Glycemic Variability Evaluated by Continuous Glucose Monitoring System Is Associated With the 10-Y Cardiovascular Risk of Diabetic Patients With Well-Controlled HbA1c. *Clinica Chimica Acta; Int J Clin Chem* (2016) 461:146–50. doi: 10.1016/j.cca.2016.08.004
5. Boyne MS, Silver DM, Kaplan J, Saudek CD. Timing of Changes in Interstitial and Venous Blood Glucose Measured With a Continuous Subcutaneous Glucose Sensor. *Diabetes* (2003) 52(11):2790–4. doi: 10.2337/diabetes.52.11.2790
6. Rebrin K, Sheppard NFJr., Steil GM. Use of Subcutaneous Interstitial Fluid Glucose to Estimate Blood Glucose: Revisiting Delay and Sensor Offset. *J Diabetes Sci Technol* (2010) 4(5):1087–98. doi: 10.1177/193229681000400507
7. Dye L, Mansfield M, Lasikiewicz N, Mahawish L, Schnell R, Talbot D, et al. Correspondence of Continuous Interstitial Glucose Measurement Against Arterialised and Capillary Glucose Following an Oral Glucose Tolerance Test in Healthy Volunteers. *Br J Nutr* (2010) 103(1):134–40. doi: 10.1017/s0007114509991504
8. Monsod TP, Flanagan DE, Rife F, Saenz R, Caprio S, Sherwin RS, et al. Do Sensor Glucose Levels Accurately Predict Plasma Glucose Concentrations During Hypoglycemia and Hyperinsulinemia? *Diabetes Care* (2002) 25(5):889–93. doi: 10.2337/diacare.25.5.889
9. Færch KAH, Nielsen LB, Ried-Larsen M, Karstoft K, Persson F, Jørgensen ME. Protocol for a Randomised Controlled Trial of the Effect of Dapagliflozin, Metformin and Physical Activity on Glycaemic Variability, Body Composition and Cardiovascular Risk in Pre-Diabetes (The PRE-D Trial). Protocol. *BMJ Open* (2017) 6(7(5):e013802. doi: 10.1136/bmjopen-2016-013802
10. Færch K, Blond MB, Bruhn L, Amadid H, Vistisen D, Clemmensen KKB, et al. The Effects of Dapagliflozin, Metformin or Exercise on Glycaemic Variability in Overweight or Obese Individuals With Prediabetes (the PRE-D Trial): A Multi-Arm, Randomised, Controlled Trial. *Diabetologia* (2020). doi: 10.1007/s00125-020-05306-1
11. Friedewald WT, Levy RI, Fredrickson DS. Estimation of the Concentration of Low-Density Lipoprotein Cholesterol in Plasma, Without Use of the Preparative Ultracentrifuge. *Clin Chem* (1972) 18(6):499–502. doi: 10.1093/clinchem/18.6.499
12. Levey AS, Stevens LA. Estimating GFR Using the CKD Epidemiology Collaboration (CKD-EPI) Creatinine Equation: More Accurate GFR Estimates, Lower CKD Prevalence Estimates, and Better Risk Predictions. *Am J Kidney Dis* (2010) 55(4):622–7. doi: 10.1053/j.ajkd.2010.02.337
13. Bland JM, Altman DG. Agreement Between Methods of Measurement With Multiple Observations Per Individual. *J Biopharmaceutical Statistics* (2007) 17(4):571–82. doi: 10.1080/10543400701329422
14. Ceriello A, Monnier L, Owens D. Glycaemic Variability in Diabetes: Clinical and Therapeutic Implications. *Lancet Diabetes Endocrinol* (2019) 7(3):221–30. doi: 10.1016/s2213-8587(18)30136-0
15. Hegedus E, Salvy SJ, Wee CP, Naguib M, Raymond JK, Fox DS, et al. Use of Continuous Glucose Monitoring in Obesity Research: A Scoping Review. *Obes Res Clin Practice* (2021). doi: 10.1016/j.orcp.2021.08.006
16. Caplin NJ, O'Leary P, Bulsara M, Davis EA, Jones TW. Subcutaneous Glucose Sensor Values Closely Parallel Blood Glucose During Insulin-Induced Hypoglycaemia. *Diabetic Med J Br Diabetic Assoc* (2003) 20(3):238–41. doi: 10.1046/j.1464-5491.2003.00837.x
17. Michel CC, Curry FE. Microvascular Permeability. *Physiol Rev* (1999) 79(3):703–61. doi: 10.1152/physrev.1999.79.3.703
18. Pappenheimer JR. Passage of Molecules Through Capillary Wals. *Physiol Rev* (1953) 33(3):387–423. doi: 10.1152/physrev.1953.33.3.387

19. Acciaroli G, Sparacino G, Hakaste L, Facchinetti A, Di Nunzio GM, Palombit A, et al. Diabetes and Prediabetes Classification Using Glycemic Variability Indices From Continuous Glucose Monitoring Data. *J Diabetes Sci Technol* (2018) 12 (1):105–13. doi: 10.1177/1932296817710478
20. Ye L, Gu W, Chen Y, Li X, Shi J, Lv A, et al. The Impact of Shift Work on Glycemic Characteristics Assessed by CGM and Its Association With Metabolic Indices in Non-Diabetic Subjects. *Acta Diabetologica* (2020) 57 (1):53–61. doi: 10.1007/s00592-019-01372-z
21. Chakarova N, Dimova R, Grozeva G, Tankova T. Assessment of Glucose Variability in Subjects With Prediabetes. *Diabetes Res Clin Practice* (2019) 151:56–64. doi: 10.1016/j.diabres.2019.03.038
22. Mooy JM, Grootenhuis PA, de Vries H, Kostense PJ, Popp-Snijders C, Bouter LM, et al. Intra-Individual Variation of Glucose, Specific Insulin and Proinsulin Concentrations Measured by Two Oral Glucose Tolerance Tests in a General Caucasian Population: The Hoorn Study. *Diabetologia* (1996) 39 (3):298–305. doi: 10.1007/BF00418345

Conflict of Interest: KF, HA, LB, KC, MB, MJ, and DV are employed by Steno Diabetes Center Copenhagen, a research hospital working in the Danish National Health Service. Until 31 December 2016, Steno Diabetes Center was owned by Novo Nordisk A/S. KF, DV, KC, and MJ own shares in Novo Nordisk A/S. KF has received research support from AstraZeneca and Unilever, is member of the Board of Directors for ChemoMetec A/S. MR-L has received personal lecture fees from Novo Nordisk A/S. MJ has received research grants from Amgen, Sanofi Aventis, Boehringer Ingelheim, and Astra Zeneca. DV has received research grants from Boehringer Ingelheim and Bayer A/S.

The remaining author declares that the research was conducted in the absence of any commercial or financial relationships that could be construed as a potential conflict of interest.

Publisher's Note: All claims expressed in this article are solely those of the authors and do not necessarily represent those of their affiliated organizations, or those of the publisher, the editors and the reviewers. Any product that may be evaluated in this article, or claim that may be made by its manufacturer, is not guaranteed or endorsed by the publisher.

frontiers | Frontiers in Endocrinology

ORIGINAL RESEARCH
published: 14 April 2022
doi: 10.3389/fendo.2022.858912

Largest Amplitude of Glycemic Excursion Calculating from Self-Monitoring Blood Glucose Predicted the Episodes of Nocturnal Asymptomatic Hypoglycemia Detecting by Continuous Glucose Monitoring in Outpatients with Type 2 Diabetes

Shoubi Wang[1,2†], Zhenhua Tan[3†], Ting Wu[4], Qingbao Shen[1], Peiying Huang[1], Liying Wang[1], Wei Liu[1], Haiqu Song[1], Mingzhu Lin[1], Xiulin Shi[1] and Xuejun Li[1*]*

[1] Department of Endocrinology and Diabetes, Xiamen Diabetes Institute, Xiamen Clinical Medical Center for Endocrine and Metabolic Diseases, Xiamen Diabetes Prevention and Treatment Center, Fujian Key Laboratory of Diabetes Translational Medicine, The First Affiliated Hospital of Xiamen University, School of Medicine, Xiamen University, Xiamen, China, [2] Fujian Provincial Key Laboratory of Ophthalmology and Visual Science, Eye Institute of Xiamen University, School of Medicine, Xiamen University, Xiamen, China, [3] Xiahe Branch of the Zhongshan Hospital Affiliated to Xiamen University, Xiamen, China, [4] The School of Clinical of Medicine, Fujian Medical University, Fuzhou, China

Aims: Nocturnal asymptomatic hypoglycemia (NAH) is a serious complication of diabetes, but it is difficult to be detected clinically. This study was conducted to determine the largest amplitude of glycemic excursion (LAGE) to predict the episodes of NAH in outpatients with type 2 diabetes.

Methods: Data were obtained from 313 outpatients with type 2 diabetes. All subjects received continuous glucose monitoring (CGM) for consecutive 72 hours. The episodes of NAH and glycemic variability indices (glucose standard deviation [SD], mean amplitude of plasma glucose excursion [MAGE], mean blood glucose [MBG]) were accessed *via* CGM. LAGE was calculated from self-monitoring blood glucose (SMBG).

Results: A total of 76 people (24.3%) had NAH. Compared to patients without NAH, patients with NAH showed higher levels of glucose SD (2.4 ± 0.9 mmol/L vs 1.7 ± 0.9 mmol/L, p <0.001), MAGE (5.2 ± 2.1 mmol/L vs 3.7 ± 2.0, p<0.001) and LAGE (4.6 ± 2.3 mmol/L vs 3.8 ± 1.9 mmol/L, p=0.007), and lower level of MBG (7.5 ± 1.5 mmol/L vs 8.4 ± 2.2 mmol/L, p=0.002). LAGE was significantly associated with the incidence of NAH and time below rang (TBR) in model 1 [NAH: 1.189 (1.027-1.378), p=0.021; TBR: 0.008 (0.002-0.014), p=0.013] with adjustment for age, BMI, sex, work, hyperlipidemia, complication and medication, and in model 2 [NAH: 1.177 (1.013-1.367), p=0.033; TBR: 0.008 (0.002-0.014), p=0.012] after adjusting for diabetes duration based on

OPEN ACCESS

Edited by:
Melanie Cree-Green, University of Colorado, United States

Reviewed by:
Xiaoying Li, Fudan University, China
Qing Su, Shanghai Jiao Tong University, China

***Correspondence:**
Xuejun Li
xmlixuejun@163.com
Xiulin Shi
shixiulin2002@163.com

†These authors have contributed equally to this work

Specialty section:
This article was submitted to Clinical Diabetes, a section of the journal Frontiers in Endocrinology

Received: *20 January 2022*
Accepted: *15 March 2022*
Published: *14 April 2022*

Citation:
Wang S, Tan Z, Wu T, Shen Q, Huang P, Wang L, Liu W, Song H, Lin M, Shi X and Li X (2022) Largest Amplitude of Glycemic Excursion Calculating from Self-Monitoring Blood Glucose Predicted the Episodes of Nocturnal Asymptomatic Hypoglycemia Detecting by Continuous Glucose Monitoring in Outpatients with Type 2 Diabetes. Front. Endocrinol. 13:858912. doi: 10.3389/fendo.2022.858912

model 1, as well as in model 3 [NAH: 1.244 (1.057-1.464), p=0.009; TBR: 0.009 (0.002-0.016), p=0.007] with further adjustment for HbA1c based on model 2. In addition, no significant interactions were found between LAGE and sex, age, HbA1c, duration of diabetes, BMI and insulin therapy on the risk of NAH. The receiver operator characteristic (ROC) curve shows the ideal cutoff value of LAGE for the prediction of NAH was 3.48 mmol/L with 66.7% sensitivity, 50% specificity and 0.587 (95% CI: 0.509-0.665) of area under the ROC curve.

Conclusions: High glycemic variability is strongly associated with the risk of NAH. The LAGE based on SMBG could be an independent predictor of NAH for outpatients with type 2 diabetes, and LAGE greater than 3.48 mmol/L could act as a warning alarm for high risk of NAH in daily life.

Keywords: nocturnal asymptomatic hypoglycemia, largest amplitude of glycemic excursion, self-monitoring blood glucose, continuous glucose monitoring, outpatients with type 2 diabetes

INTRODUCTION

Hypoglycemia is a serious complication of diabetes mellitus, which could contribute to "dead in bed" syndrome, neurological damage (poorer cognitive function, spatial memory dysfunction, neuron damage, and epilepsy), and psychological impact (negative psychosocial consequences, undesirable compensatory behaviors, unforeseen anxiety, and poor sleep) (1). With the implementation of intensive glucose control over the years, the morbidity of hypoglycemia is relatively higher (2, 3). Accordingly, high rates of different degrees of hypoglycemia episodes, namely severe events [1.0~16.9% (4–8)], moderate severity events [17~46% (4–7)] and mild events [46~58% (5–7)] have been reported. Simultaneously, hypoglycemia was assigned as the cause of death in 4% (9), 7% (10), and 10% (11) in population-based registers. As almost 50% of all severe hypoglycemia episodes occur at nighttime during sleep with unawareness, nocturnal asymptomatic hypoglycemia (NAH) has been especially emphasized (12). Recurrent episodes of asymptomatic hypoglycemia can increase the risk of severe hypoglycemic episodes (13), contributing to life-threatening events, such as major macrovascular events, major microvascular events, death from cardiovascular disease, and death from any cause (14). Actually, the incidence of NAH is far more than these due to recall bias, missing detection, and underreporting. Especially for outpatients who manage blood glucose with the target of normal glycemic level, the risk of hypoglycemia will inevitably increase, which is less likely to be recognized and concerned without timely medical guidance. Hence, in view of its universality and perniciousness, predicting the episodes of NAH to minimize hypoglycemic events is significantly meaningful for better diabetes management.

Continuous glucose monitoring (CGM), which provides maximal information about glucose fluctuation levels throughout the day (15), provides an improved opportunity to capture NAH events. CMG has been proved to be superior to daily self-monitoring blood glucose (SMBG) in the detection of hypoglycemia. In hospitalized patients with type 2 diabetes, the detection rates of hypoglycemia by CMG ranges from 1.6-fold (16), 2.5-fold (17), 4-fold (18) than those by point-of-care capillary glucose testing (POC). Additionally, compared with SMBG, significantly higher percentages of hypoglycemic episodes [(3.8% vs 1.7%) (19); (4.35% vs 1.5%) (20); (90.4% vs 38.5%) (21); (52 vs. 3 events/patient-year) (22)] were detected by CGM, particularly in terms of asymptomatic and nocturnal hypoglycemia (19, 21, 22). Nonetheless, probably due to high cost and technical complexity (23), CGM is still underutilized in the real world. SMBG, on the other hand, remains the basic approach for glycemic management in daily life, which is widely used because of its familiarity, convenience and relatively low cost for long-term daily diabetes management (23). We propose that by combining the advantages of CGM and SMBG, that is, based on precisely capturing hypoglycemia by CGM, predicting the episodes of hypoglycemia through glycemic indicators monitored by SMBG may be possible to prevent hypoglycemia with accuracy and convenience.

Glycemic variability, characterized by extreme glucose excursions, is associated with the risk of overall symptomatic, nocturnal symptomatic and severe hypoglycemia in patients with diabetes (24), and different indices of glycemic fluctuations have been used to predict hypoglycemia (25–27). However, most of these predictors are obtained by CGM data, and the majority of subjects are hospitalized patients. Relatively few studies focus on outpatients, and efforts are needed to provide easily acquired indictors for outpatients to warn and prevent NAH. In this study, we used CGM device to continuously monitor blood glucose in outpatients with type 2 diabetes to access the episodes of NAH and glycemic variability indices, including glucose standard deviation (SD), mean amplitude of plasma glucose excursions (MAGE) and mean blood glucose (MBG). Simultaneously, the largest amplitude of glycemic excursion (LAGE) was acquired by SMBG without changing patients' lifestyle and medications. We aimed to clarify the associations of glucose fluctuations and NAH of outpatients with type 2 diabetes, and to explore whether LAGE could independently predict the episodes of NAH, providing a relatively convenient warning index for daily NAH prevention.

METHODS

Participants

In this study, 313 out-patients with type 2 diabetes who were admitted to the First Affiliated Hospital of Xiamen University from January 2018 to June 2021 were included. All participants wore CGM device at the outpatient clinic, during which medication use was not affected. Pregnant and perioperative patients were excluded. Body mass index (BMI) was calculated as the weight in kilograms divided by the square of height in meters. HbA1c and C-peptide were detected by the Laboratory Department of the First Affiliated Hospital of Xiamen University. This study was approved by the ethics committees of the First Affiliated Hospital of Xiamen University. Written informed consent was obtained from all subjects.

Continuous Glucose Monitoring

A iPro™2 CGM system (Medtronic, Minimed, Inc. Northridge, CA), which is extensively used in detecting low glucose levels with validated reproducibility and reliability (28), was used in this study to monitor glucose fluctuations. After wearing the CGM device, participants returned home and resumed normal activities for consecutive 72 hours. NAH was defined as hypoglycemia (<3.9mmol/L) occurring between 0 am and 6 am. We obtained glycemic variability indices from CGM, including glucose SD, MAGE, MBG, time in range (TIR; 3.9-10.0 mmol/L), time below range (TBR; <3.9 mmol/L).

Self-Monitoring Blood Glucose

The OneTouch UltraVue® (Johnson and Johnson K.K., Tokyo, Japan) device and ACCU-CHEK Performa (Roche, Switzerland) glucometer were used for SMBG. Each subject used the same glucometer during the 72-h study period. Participants were guided to conduct blood glucose self-monitoring four times daily - prior to meals and bedtime. The maximum range of daily blood glucose fluctuation was obtained by subtracting the minimum from the maximum value, and then the daily maximum ranges of the 72 hours were equilibrated to obtain the LAGE value.

Statistical Analyses

Data were expressed as mean ± standard deviation (SD) for normally distributed variables, median (25th percentile, 75th percentile) for non-normally distributed variables, and percentages for categorical variables. The significance of differences between the two groups was assessed using t test or Kruskal-Wallis test for quantitative data, and Chi-square test for categorical data. The associations between LAGE and the incidence of NAH and TBR were analyzed by a logistic regression model and a linear regression model, respectively. The interaction of LAGE and potential risk factors of NAH was performed by logistic regression analysis as well. We run receiver operating characteristic (ROC) curve analysis to demonstrate the sensitivity, specificity and optimal cut-off value of LAGE for predicting NAH. The predictive validity was quantified as areas under the ROC curve. A P<0.05 was considered to be statistically significant. All statistical analyses were conducted with SAS version 9.3.

RESULTS

Clinical Characteristics and Blood Glucose Monitoring Results

Table 1 shows the characteristics of total 313 outpatients with type 2 diabetes, including 76 patients with NAH and 237 patients without. There were no significant differences in age, duration of diabetes, BMI, HbA1c, concentration of C-peptide, and drug uses (metformin, dipeptidyl peptidase-4 inhibitor, alpha-glucosidase inhibitors, thiazolidinedione, glucagon-like peptide-1 receptor agonists, sulfonylurea, sodium–glucose cotransporter 2 inhibitors, long-acting insulin, premixed insulin, short-acting insulin) between the two groups. Further, we found that diabetic comorbidities (hypertension, hyperlipidemia, fatty liver, cardio-cerebral vascular disease) and diabetic complications (diabetic retinopathy, diabetic peripheral neuropathy, diabetic peripheral vascular disease, diabetic nephropathy, diabetic foot) were not statistically different. The glycemic variability indices, including glucose SD (2.4 ± 0.9 mmol/L vs 1.7 ± 0.9 mmol/L, p<0.001), MAGE (5.2 ± 2.1 mmol/L vs 3.7 ± 2.0 mmol/L, p <0.001) and LAGE (4.6 ± 2.3 mmol/L vs 3.8 ± 1.9 mmol/L, p=0.007), were higher in patients with NAH than those in patients without, while MBG (7.5 ± 1.5 mmol/L vs 8.4 ± 2.2 mmol/L, p=0.002) was lower. TIR [0.8 (0.7,0.9) vs 0.9 (0.7,1.0)] did not differ statistically in subjects with or without NAH.

Association Between LAGE and the Incidence of NAH and TBR

In **Table 2**, the associations of LAGE with the incidence of NAH and TBR were elucidated by a logistic regression model and a linear regression analysis, respectively. TBR is a key metric for evaluating the degree and severity of hypoglycemia (29), which is more relevant for capturing hypoglycemic events and quantifying their magnitude and duration (30). In model 1 with adjustment for age, BMI, sex, work, hyperlipidemia, complication and medication, LAGE was significantly associated with the increased risk of NAH, with the incidence of NAH [1.189 (1.027-1.378), p=0.021] and TBR [0.008 (0.002-0.014), p=0.013]. In model 2 after adjusting for diabetes duration based on model 1, the same significant result was seen, with the incidence of NAH [1.177 (1.013-1.367), p=0.033] and TBR [0.008 (0.002-0.014), p=0.012]. In model 3 with further adjustment for HbA1c based on model 2, the incidence of NAH increased 1.244-fold (95% CI: 1.057-1.464, p=0.009) and TBR increased 0.009 (95% CI: 0.002-0.016, p=0.007) for 1 mmol/L increase of LAGE.

Association Between LAGE and Potential Risk Factors on the Risk of NAH

In order to further determine whether LAGE was independently correlated with NAH, the logistic regression model was further performed according to potential risk factors. **Table 3** shows that no significant interactions were found between LAGE and sex (p for interaction= 0.732), age (p for interaction= 0.187), HbA1c (p for interaction= 0.877), duration of diabetes (p for interaction= 0.734), BMI (p for

TABLE 1 | Clinical characteristics and blood glucose monitoring results.

	Without NAH (n = 237)	With NAH (n = 76)	P value
Age (years)	55.4 ± 14.1	51.7 ± 15.5	0.058
Duration of diabetes (years)	6.0 (2.0,11.0)	5.0 (3.0,13.0)	0.445
BMI (kg/m^2)	23.2 ± 3.1	22.6 ± 3.2	0.217
HbA1c (%)	7.0 ± 1.5	7.0 ± 1.5	0.933
C-peptide (ng/mL)	1.5 (0.9,2.3)	0.9 (0.3,1.9)	5.691
Medication (%)			
Metformin	64 (28.2)	21 (29.2)	0.873
DPP-4i	34 (15)	11 (15.3)	0.951
α-GI	46 (20.3)	11 (15.3)	0.348
TZD	5 (2.2)	3 (4.2)	0.368
GLP-1RA	4 (1.8)	1 (1.4)	0.830
SU	49 (21.6)	18 (25)	0.545
SGLT-2i	8 (3.5)	2 (2.8)	0.759
Long-acting insulin	50 (22.0)	15 (20.8)	0.831
Premixed insulin	27 (11.9)	6 (8.3)	0.401
Short-acting insulin	38 (16.7)	11 (15.3)	0.770
Comorbidity (%)			
Hypertension	28 (12.3)	9 (12.5)	0.970
Hyperlipidemia	35 (15.4)	12 (16.7)	0.800
Fatty liver	11 (4.9)	5 (6.9)	0.491
CCVD	19 (8.4)	7 (9.7)	0.723
Complication (%)			
DR	31 (13.7)	13 (18.1)	0.359
DPN	31 (13.7)	9 (12.5)	0.802
DPVD	10 (4.4)	4 (18.1)	0.687
DN	11 (4.9)	4 (5.6)	0.810
DF	2 (0.9)	0 (0)	0.424
CGM data			
SD (mmol/L)	1.7 ± 0.9	2.4 ± 0.9	<0.001
MBG (mmol/L)	8.4 ± 2.2	7.5 ± 1.5	0.002
MAGE (mmol/L)	3.7 ± 2.0	5.2 ± 2.1	<0.001
TIR (%)	90 (70,100)	80 (70,90)	9.895
SMBG data			
LAGE (mmol/L)	3.8 ± 1.9	4.6 ± 2.3	0.007

NAH, nocturnal asymptomatic hypoglycemia; BMI, body mass index; HbA1c, glycated hemoglobin; DPP-4i, dipeptidyl peptidase-4 inhibitors; α-GI, alpha-glucosidase inhibitors; TZD, thiazolidinedione; GLP-1RA, glucagon-like peptide-1 receptor agonists; SU, sulfonylurea; SGLT-2i, sodium–glucose cotransporter 2 inhibitors; CCVD, cardio-cerebral vascular disease; DR, diabetic retinopathy; DPN, diabetic peripheral neuropathy; DPVD, diabetic peripheral vascular disease; DN, diabetic nephropathy; DF, diabetic foot; CGM, continuous glucose monitoring; SD, glucose standard deviation; MBG, mean blood glucose; MAGE, mean amplitude of plasma glucose excursion; TIR, time in range (3.9–10.0 mmol/L); SMBG, self-monitoring blood glucose; LAGE, largest amplitude of glycemic excursion. P < 0.05 was considered significant.

TABLE 2 | Associations between LAGE and the incidence of NAH and TBR.

	The incidence of nocturnal asymptomatic hypoglycemia		TBR	
	OR (95% CI)	P value	Estimateβ (95% CI)	P value
Model 1	1.189 (1.027-1.378)	0.021	0.008 (0.002-0.014)	0.013
Model 2	1.177 (1.013-1.367)	0.033	0.008 (0.002-0.014)	0.012
Model 3	1.244 (1.057-1.464)	0.009	0.009 (0.002-0.016)	0.007

TBR, time below range (<3.9 mmol/L); CI, confidence interval. P < 0.05 was considered significant. Model 1 was adjusted for age, BMI, sex, work, hyperlipidemia, complication and medication. Model 2 was further adjusted for diabetes duration based on model 1. Model 3 was further adjusted for HbA1c based on model 2.

interaction= 0.864) and insulin therapy (p for interaction= 0.474) on the risk of NAH.

ROC Curve of LAGE for the Prediction of NAH

The ideal cutoff value of LAGE for the prediction of NAH was 3.48 mmol/L with 66.7% sensitivity and 50% specificity. The area under the ROC curve (AUC) was 0.587 (95%CI: 0.509-0.665).

DISCUSSION

In this study, we clarified that higher levels of glucose SD, MAGE and LAGE and lower levels of MBG were strongly associated with NAH in outpatients with type 2 diabetes, and demonstrated that LAGE may be an independent predictor of NAH, irrespective of HbA1c level and other potential risk factors.

TABLE 3 | Association between LAGE and potential risk factors on the risk of NAH.

		With nocturnal asymptomatic hypoglycemia		
	Total	**OR (95% CI)**	**P value**	**Interaction**
Sex				0.732
Men	175	1.36 (1.04-1.77)	0.023	
Women	138	1.19 (0.95-1.48)	0.130	
Age(years)				0.187
<55	163	1.41 (1.09-1.82)	0.009	
≥55	150	1.13 (0.88-1.46)	0.357	
HbA1c (%)				0.877
≤7	217	1.35 (1.04-1.74)	0.025	
>7	96	1.27 (0.99-1.62)	0.059	
Duration of diabetes (years)				0.734
≤5	164	1.20 (0.90-1.61)	0.218	
>5	149	1.32 (1.06-1.64)	0.014	
BMI ($kg/m^{2)}$				0.864
<24	216	1.09 (0.86-1.39)	0.471	
≥24	97	1.38 (1.04-1.83)	0.024	
Insulin therapy				
With	96	1.39 (1.07-1.81)	0.123	0.474
Without	217	1.13 (0.89-1.44)	0.313	

It has been shown that frequent hypoglycemia often occurred with a greater level of glucose fluctuations (31). In addition, glycemic variability has been suggested to be a potential indicator of diabetes complications (32) and severe hypoglycemia (25). Through re-analyzing the Diabetes Control and Complications Trial (DCCT) data, Kilpatrick et al. found that MBG and glycemic variability each have an independent role in increased risk of hypoglycemia in type 1 diabetes. The incidence of time to first hypoglycemic event increased 1.05-fold for each 1 mmol/l decrease in MBG and 1.07-fold for every 1 mmol/l increase in glucose SD. After adjusting for HbA1c, a 1 mmol/l increase in SD was associated with a 1.09-fold increased risk of a first event (26). Saisho et al. reported that glucose SD and other glycemic variability indices were more strongly correlated with hypoglycemia compared with MBG, and the combination of MBG and glucose SD was useful for predicting hypoglycemia in diabetes patients (33). Service et al. suggested that a high MAGE was a vital characteristic of glucose instability, which was more accurate than other indexes of glycemic fluctuation (34). Another study of 5-day consecutive CGM showed that hypoglycemic patients had lower MBG and higher glucose SD compared to non-hypoglycemic patients, with no statistical difference of HbA1c (35), which is consistent with our research. In this study, patients with NAH manifested as higher levels of SD, MAGE and LAGE and lower level of MBG. After adjusting for possible interference factors, there were still significant associations of LAGE with NAH and TBR. Moreover, no significant interactions were observed between LAGE and potential risk factors, indicating that LAGE could be an independent predictor of NAH in patients with type 2 diabetes. According to the CGM data conducted by Zhou el al. in Shanghai, China, MAGE <3.9 mmol/L and SD <1.4 mmol/L were recommended as the normal reference ranges for glycemic variability in Chinese adults (36), and LAGE <5.7mmol/L was recommended in normal glucose tolerance people (37). To the best of our knowledge, the value of LAGE in determining the risk of NAH has not been reported. Here, we showed that LAGE greater than 3.48 mmol/L could act as a warning alarm for high risk of NAH in outpatients with type 2 diabetes.

Although the diabetes management has focused on HbA1c, as an index reflecting recent average blood glucose levels, HbA1c could not accurately portray the frequency of hypoglycemia and glucose fluctuations (35). HbA1c was reported to minimally contributes to hypoglycemia risk in type 2 diabetes and has no relation to hypoglycemia in type 1 diabetes, while the variability in glucose levels showed great promise as better predictors (38).In this study, HbA1c did not differ between the two groups, which was consistent with other researches (28, 35), confirming the ability of LAGE beyond HbA1c for predicting NAH.

Our research has the following strengths. Firstly, the subjects in this study are outpatients with type 2 diabetes, the diabetic condition of whom are generally considered to be in stable, so NAH is not seriously concerned among these individuals. In addition, as they usually aim for normal blood glucose level, NAH is more likely to occur and leads to serious complications without timely medical assistances. Therefore, the prediction and prevention of NAH is extremely meaningful in such a population. Secondly, in spite of some advantages of CGM, long-term wearing of CGM devices for outpatients is currently impractical. Nevertheless, LAGE based on SMBG is easily calculated and convenient to make a rapid assessment for NAH risk. Thirdly, all data were acquired without changing patients' lifestyle and medications, which reflects the true daily glucose fluctuations, improving the reliability of LAGE as an independent predictor of NAH.

Several limitations of this study should be noted. Firstly, the sample size included in this study is relatively small. A study with a larger sample size and longer duration is needed to further consolidate the results of this study. Secondly, subjects included in this study are patients with type 2 diabetes, thus our findings may not be applicable to all diabetes patients, especially patients

with type 1 diabetes. Thirdly, other factors that may affect glycemic variability, such as exercise, food intake and beta-cell function, were not investigated in the current study. In the near future, we will continue to study with a larger sample size and try to combine these factors for analysis to improve the specificity and sensitivity of the prediction of NAH. Finally, severe hypoglycemia (<3.0 mmol/L) is also critical. Because there were only 30 patients with severe hypoglycemia in this study, which may affect statistical power, there was no statistical difference between LAGE and severe hypoglycemia (data not shown). Our subsequent studies will also include more patients with blood glucose less than 3.0 mmol/L to clarify the association between LAGE and severe hypoglycemia.

CONCLUSIONS

In conclusion, our study showed that higher glycemic variability is strongly associated with higher risk of NAH, and proposed LAGE could be an independent predictor of NAH for outpatients with type 2 diabetes. LAGE greater than 3.48 mmol/L could act as a warning alarm for high risk of NAH. Taking the convenience and feasibility of SBMG into account, a real-time alarm based on LAGE may minimize NAH exposure to further achieve better diabetes management. We hope our research can serve as a reference that helps in hypoglycemia prevention.

DATA AVAILABILITY STATEMENT

The datasets generated during the current study are available from the corresponding author on reasonable request.

ETHICS STATEMENT

The studies involving human participants were reviewed and approved by The First Affiliated Hospital of Xiamen University. The patients/participants provided their written informed consent to participate in this study.

AUTHOR CONTRIBUTIONS

SW researched the data and wrote the manuscript. ZT researched the data and edited the manuscript. TW and QS integrated the data. PH, LW, and WL contributed to the discussion. HS and ML contributed to the introduction. XS analyzed the data. XL reviewed and edited the manuscript. All authors approved the manuscript.

FUNDING

This work was supported by the Natural Science Foundation of Fujian Province, China (No.2021J011363).

ACKNOWLEDGMENTS

The authors thank all patients and research staff who participated in this work.

REFERENCES

1. Abraham MB, Jones TW, Naranjo D, Karges B, Oduwole A, Tauschmann M, et al. Ispad Clinical Practice Consensus Guidelines 2018: Assessment and Management of Hypoglycemia in Children and Adolescents With Diabetes. *Pediatr Diabetes* (2018) 19 Suppl 27:178–92. doi: 10.1111/pedi.12698
2. Group AC, Patel A, MacMahon S, Chalmers J, Neal B, Billot L, et al. Intensive Blood Glucose Control and Vascular Outcomes in Patients With Type 2 Diabetes. *N Engl J Med* (2008) 358(24):2560–72. doi: 10.1056/NEJMoa0802987
3. Duckworth W, Abraira C, Moritz T, Reda D, Emanuele N, Reaven PD, et al. Glucose Control and Vascular Complications in Veterans With Type 2 Diabetes. *N Engl J Med* (2009) 360(2):129–39. doi: 10.1056/NEJMoa0808431
4. Pettersson B, Rosenqvist U, Deleskog A, Journath G, Wandell P. Self-Reported Experience of Hypoglycemia Among Adults With Type 2 Diabetes Mellitus (Exhype). *Diabetes Res Clin Pract* (2011) 92(1):19–25. doi: 10.1016/j.diabres.2010.12.005
5. Stargardt T, Gonder-Frederick L, Krobot KJ, Alexander CM. Fear of Hypoglycaemia: Defining a Minimum Clinically Important Difference in Patients With Type 2 Diabetes. *Health Qual Life Outcomes* (2009) 7:91. doi: 10.1186/1477-7525-7-91
6. Chan SP, Ji LN, Nitiyanant W, Baik SH, Sheu WH. Hypoglycemic Symptoms in Patients With Type 2 Diabetes in Asia-Pacific-Real-Life Effectiveness and Care Patterns of Diabetes Management: The Recap-Dm Study. *Diabetes Res Clin Pract* (2010) 89(2):e30–2. doi: 10.1016/j.diabres.2010.05.008
7. Marrett E, Radican L, Davies MJ, Zhang Q. Assessment of Severity and Frequency of Self-Reported Hypoglycemia on Quality of Life in Patients With Type 2 Diabetes Treated With Oral Antihyperglycemic Agents: A Survey Study. *BMC Res Notes* (2011) 4:251. doi: 10.1186/1756-0500-4-251
8. McCoy RG, Van Houten HK, Ziegenfuss JY, Shah ND, Wermers RA, Smith SA. Self-Report of Hypoglycemia and Health-Related Quality of Life in Patients With Type 1 and Type 2 Diabetes. *Endocr Pract* (2013) 19(5):792–9. doi: 10.4158/EP12382.OR
9. Patterson CC, Dahlquist G, Harjutsalo V, Joner G, Feltbower RG, Svensson J, et al. Early Mortality in Eurodiab Population-Based Cohorts of Type 1 Diabetes Diagnosed in Childhood Since 1989. *Diabetologia* (2007) 50 (12):2439–42. doi: 10.1007/s00125-007-0824-8
10. Feltbower RG, Bodansky HJ, Patterson CC, Parslow RC, Stephenson CR, Reynolds C, et al. Acute Complications and Drug Misuse Are Important Causes of Death for Children and Young Adults With Type 1 Diabetes: Results From the Yorkshire Register of Diabetes in Children and Young Adults. *Diabetes Care* (2008) 31(5):922–6. doi: 10.2337/dc07-2029
11. Skrivarhaug T, Bangstad HJ, Stene LC, Sandvik L, Hanssen KF, Joner G. Long-Term Mortality in a Nationwide Cohort of Childhood-Onset Type 1 Diabetic Patients in Norway. *Diabetologia* (2006) 49(2):298–305. doi: 10.1007/s00125-005-0082-6
12. Edelman SV, Blose JS. The Impact of Nocturnal Hypoglycemia on Clinical and Cost-Related Issues in Patients With Type 1 and Type 2 Diabetes. *Diabetes Educ* (2014) 40(3):269–79. doi: 10.1177/0145721714529608
13. Lamounier RN, Geloneze B, Leite SO, Montenegro RJr., Zajdenverg L, Fernandes M, et al. Hypoglycemia Incidence and Awareness Among Insulin-Treated Patients With Diabetes: The Hat Study in Brazil. *Diabetol Metab Syndr* (2018) 10:83. doi: 10.1186/s13098-018-0379-5
14. International Hypoglycaemia Study G. Hypoglycaemia, Cardiovascular Disease, and Mortality in Diabetes: Epidemiology, Pathogenesis, and Management. *Lancet Diabetes Endocrinol* (2019) 7(5):385–96. doi: 10.1016/S2213-8587(18)30315-2
15. Klonoff DC. Continuous Glucose Monitoring: Roadmap for 21st Century Diabetes Therapy. *Diabetes Care* (2005) 28(5):1231–9. doi: 10.2337/diacare.28.5.1231

16. Levitt DL, Spanakis EK, Ryan KA, Silver KD. Insulin Pump and Continuous Glucose Monitor Initiation in Hospitalized Patients With Type 2 Diabetes Mellitus. *Diabetes Technol Ther* (2018) 20(1):32–8. doi: 10.1089/dia.2017.0250
17. Gomez AM, Umpierrez GE, Munoz OM, Herrera F, Rubio C, Aschner P, et al. Continuous Glucose Monitoring Versus Capillary Point-Of-Care Testing for Inpatient Glycemic Control in Type 2 Diabetes Patients Hospitalized in the General Ward and Treated With a Basal Bolus Insulin Regimen. *J Diabetes Sci Technol* (2015) 10(2):325–9. doi: 10.1177/1932296815602905
18. Galindo RJ, Migdal AL, Davis GM, Urrutia MA, Albury B, Zambrano C, et al. Comparison of the Freestyle Libre Pro Flash Continuous Glucose Monitoring (Cgm) System and Point-Of-Care Capillary Glucose Testing in Hospitalized Patients With Type 2 Diabetes Treated With Basal-Bolus Insulin Regimen. *Diabetes Care* (2020) 43(11):2730–5. doi: 10.2337/dc19-2073
19. Pazos-Couselo M, Garcia-Lopez JM, Gonzalez-Rodriguez M, Gude F, Mayan-Santos JM, Rodriguez-Segade S, et al. High Incidence of Hypoglycemia in Stable Insulin-Treated Type 2 Diabetes Mellitus: Continuous Glucose Monitoring Vs. Self-Monitored Blood Glucose. Observational Prospective Study. *Can J Diabetes* (2015) 39(5):428–33. doi: 10.1016/j.jcjd.2015.05.007
20. Afandi B, Hassanein M, Roubi S, Nagelkerke N. The Value of Continuous Glucose Monitoring and Self-Monitoring of Blood Glucose in Patients With Gestational Diabetes Mellitus During Ramadan Fasting. *Diabetes Res Clin Pract* (2019) 151:260–4. doi: 10.1016/j.diabres.2019.01.036
21. Shivaprasad C, Gautham K, Shah K, Gupta S, Palani P, Anupam B. Continuous Glucose Monitoring for the Detection of Hypoglycemia in Patients With Diabetes of the Exocrine Pancreas. *J Diabetes Sci Technol* (2021) 15(6):1313–9. doi: 10.1177/1932296820974748
22. Agesen RM, Kristensen PL, Beck-Nielsen H, Norgaard K, Perrild H, Jensen T, et al. Effect of Insulin Analogs on Frequency of Non-Severe Hypoglycemia in Patients With Type 1 Diabetes Prone to Severe Hypoglycemia: Much Higher Rates Detected by Continuous Glucose Monitoring Than by Self-Monitoring of Blood Glucose-The Hypoana Trial. *Diabetes Technol Ther* (2018) 20 (3):247–56. doi: 10.1089/dia.2017.0372
23. Ajjan RA. How Can We Realize the Clinical Benefits of Continuous Glucose Monitoring? *Diabetes Technol Ther* (2017) 19(S2):S27–36. doi: 10.1089/dia.2017.0021
24. DeVries JH, Bailey TS, Bhargava A, Gerety G, Gumprecht J, Heller S, et al. Day-To-Day Fasting Self-Monitored Blood Glucose Variability Is Associated With Risk of Hypoglycaemia in Insulin-Treated Patients With Type 1 and Type 2 Diabetes: A *Post Hoc* Analysis of the Switch Trials. *Diabetes Obes Metab* (2019) 21(3):622–30. doi: 10.1111/dom.13565
25. Siegelaar SE, Holleman F, Hoekstra JB, DeVries JH. Glucose Variability; Does It Matter? *Endocr Rev* (2010) 31(2):171–82. doi: 10.1210/er.2009-0021
26. Kilpatrick ES, Rigby AS, Goode K, Atkin SL. Relating Mean Blood Glucose and Glucose Variability to the Risk of Multiple Episodes of Hypoglycaemia in Type 1 Diabetes. *Diabetologia* (2007) 50(12):2553–61. doi: 10.1007/s00125-007-0820-z
27. Klimontov VV, Myakina NE. Glucose Variability Indices Predict the Episodes of Nocturnal Hypoglycemia in Elderly Type 2 Diabetic Patients Treated With Insulin. *Diabetes Metab Syndr* (2017) 11(2):119–24. doi: 10.1016/j.dsx.2016.08.023
28. Woodward A, Weston P, Casson IF, Gill GV. Nocturnal Hypoglycaemia in Type 1 Diabetes–Frequency and Predictive Factors. *QJM* (2009) 102(9):603–7. doi: 10.1093/qjmed/hcp082
29. Advani A. Positioning Time in Range in Diabetes Management. *Diabetologia* (2020) 63(2):242–52. doi: 10.1007/s00125-019-05027-0
30. Monnier L, Colette C, Owens D. Application of Medium-Term Metrics for Assessing Glucose Homoeostasis: Usefulness, Strengths and Weaknesses. *Diabetes Metab* (2021) 47(2):101173. doi: 10.1016/j.diabet.2020.06.004
31. He H, Wang C, Chen DW, Xiao J, Yang XJ, Lu LF, et al. Characteristics of 72 H Glucose Profiles Detected by Continuous Glucose Monitoring System in Patients With Insulinoma. *Sichuan Da Xue Xue Bao Yi Xue Ban* (2014) 45 (4):623–7.
32. Nalysnyk L, Hernandez-Medina M, Krishnarajah G. Glycaemic Variability and Complications in Patients With Diabetes Mellitus: Evidence From a Systematic Review of the Literature. *Diabetes Obes Metab* (2010) 12(4):288–98. doi: 10.1111/j.1463-1326.2009.01160.x
33. Saisho Y, Tanaka C, Tanaka K, Roberts R, Abe T, Tanaka M, et al. Relationships Among Different Glycemic Variability Indices Obtained by Continuous Glucose Monitoring. *Prim Care Diabetes* (2015) 9(4):290–6. doi: 10.1016/j.pcd.2014.10.001
34. Service FJ, O'Brien PC, Rizza RA. Measurements of Glucose Control. *Diabetes Care* (1987) 10(2):225–37. doi: 10.2337/diacare.10.2.225
35. Uemura F, Okada Y, Torimoto K, Tanaka Y. Relation Between Hypoglycemia and Glycemic Variability in Type 2 Diabetes Patients With Insulin Therapy: A Study Based on Continuous Glucose Monitoring. *Diabetes Technol Ther* (2018) 20(2):140–6. doi: 10.1089/dia.2017.0306
36. Zhou J, Li H, Ran X, Yang W, Li Q, Peng Y, et al. Establishment of Normal Reference Ranges for Glycemic Variability in Chinese Subjects Using Continuous Glucose Monitoring. *Med Sci Monit* (2011) 17(1):CR9–13. doi: 10.12659/msm.881318
37. Zhou J, Jia WP, Yu M, Yu HY, Bao YQ, Ma XJ, et al. The Reference Values of Glycemic Parameters for Continuous Glucose Monitoring and Its Clinical Application. *Zhonghua Nei Ke Za Zhi* (2007) 46(3):189–92.
38. Rama Chandran S, Tay WL, Lye WK, Lim LL, Ratnasingam J, Tan ATB, et al. Beyond Hba1c: Comparing Glycemic Variability and Glycemic Indices in Predicting Hypoglycemia in Type 1 and Type 2 Diabetes. *Diabetes Technol Ther* (2018) 20(5):353–62. doi: 10.1089/dia.2017.0388

Conflict of Interest: The authors declare that the research was conducted in the absence of any commercial or financial relationships that could be construed as a potential conflict of interest.

Publisher's Note: All claims expressed in this article are solely those of the authors and do not necessarily represent those of their affiliated organizations, or those of the publisher, the editors and the reviewers. Any product that may be evaluated in this article, or claim that may be made by its manufacturer, is not guaranteed or endorsed by the publisher.

frontiers | Frontiers in Endocrinology

ORIGINAL RESEARCH
published: 27 April 2022
doi: 10.3389/fendo.2022.791439

Basal Insulin Reduces Glucose Variability and Hypoglycaemia Compared to Premixed Insulin in Type 2 Diabetes Patients: A Study Based on Continuous Glucose Monitoring Systems

Huiying Wang†, Yunting Zhou†, Yuming Wang, Tingting Cai, Yun Hu, Ting Jing, Bo Ding, Xiaofei Su, Huiqin Li and Jianhua Ma**

Department of Endocrinology, Nanjing First Hospital, Nanjing Medical University, Nanjing, China

OPEN ACCESS

Edited by:
Cecilia Diniz Behn, Colorado School of Mines, United States

Reviewed by:
Asimina Mitrakou-Fanariotou, National and Kapodistrian University of Athens, Greece
Benjamin C. T. Field, University of Surrey, United Kingdom

***Correspondence:**
Huiqin Li
lihuiqin496@126.com
Jianhua Ma
majianhua196503@126.com

†These authors have contributed equally to this work

Specialty section:
This article was submitted to Clinical Diabetes, a section of the journal Frontiers in Endocrinology

Received: *08 October 2021*
Accepted: *29 March 2022*
Published: *27 April 2022*

Citation:
Wang H, Zhou Y, Wang Y, Cai T, Hu Y, Jing T, Ding B, Su X, Li H and Ma J (2022) Basal Insulin Reduces Glucose Variability and Hypoglycaemia Compared to Premixed Insulin in Type 2 Diabetes Patients: A Study Based on Continuous Glucose Monitoring Systems. Front. Endocrinol. 13:791439. doi: 10.3389/fendo.2022.791439

Aims: To examine the glycaemic variability and safety of basal and premixed insulin by using continuous glucose monitoring (CGM) systems.

Methods: 393 patients with type 2 diabetes mellitus (T2DM) treated with basal or premixed insulin for more than 3 months were enrolled. Patients were classified into a basal insulin group or premixed insulin group according to their insulin regimens. CGMs were used for 72 h with their previous hypoglycaemic regimen unchanged. The following glycaemic parameters were calculated for each 24 h using CGM data.

Results: Despite similar HbA1c and fasting C-peptide concentrations, glycaemic variability (GV), including the mean amplitude of glycaemic excursion (MAGE), standard deviation (SD) and coefficient of variation (CV), and the time below range (TBR) were significantly lower in the basal insulin group than these in the premixed insulin group. Night-time hypoglycaemia was lower in the basal insulin group than that in the premixed insulin group ($p<0.01$). Among participants with haemoglobin A1c (HbA1c) < 7%, the GV and TBR were higher in the premixed insulin group than that in the basal insulin group.

Conclusion: Compared with basal insulin, the patients who use premixed insulin had higher GV, smaller TIR and an increased incidence of hypoglycaemia. For patients who use premixed insulin and with HbA1c < 7%, more attention needs to be given to hypoglycaemic events and asymptomatic hypoglycaemia.

Clinical Trial Registration: ClinicalTrials.gov, identifier NCT03566472.

Keywords: basal insulin, premixed insulin, continuous glucose monitoring, glycaemic variability, T2DM, hypoglycaemia

INTRODUCTION

Type 2 diabetes mellitus (T2DM), characterized by insulin resistance and insulin secretion deficiency (1), is rising at an alarming rate. The prevalence of diabetes in China has increased from 0.67% in 1980 to 12.8% in 2017 (2). In China, all diabetes care is provided by hospital specialists. The current treatment paradigm of T2DM is gradual regimens intensification (3). When lifestyle modification and oral antidiabetic drugs fail to achieve adequate glycaemic control, many patients eventually require and benefit from insulin therapy (4).

Guidelines recommend that insulin therapy should be initiated timely in patients with a long duration of diabetes, use of oral hypoglycaemic drugs that fail to achieve goals and poor islet function. It is known that Chinese diets are carbohydrate-heavy, and β-cell function is generally poorer in Chinese individuals (5). Depending on the patient's illness and the physician's practice, premixed insulin therapy and basal insulin therapy are both recommended for initiation for initial insulin therapy to maintain their blood glucose concentrations in the target range in China (6, 7). Due to its lower price than basal insulin, premixed insulins are more widely used as the starting insulin therapy in clinical practice (8, 9).

In an attempt to reach glycaemic targets, patients who are treated with premixed insulin usually require an increased number of injections. Unfortunately, researchers found that a high proportion of patients still did not achieve the goal that HbA1c levels are lower than 7%, and this treatment regimen might be associated with a higher risk of hypoglycaemic episodes and weight gain (10). A randomized clinical trial reported that T2DM patients who were treated with premixed insulin had glycaemic control similar to that of patients treated with a basal insulin regimen but had a significantly higher frequency of hypoglycaemia (11).

Continuous glucose monitoring (CGM) systems have been recognized as an ideal method of monitoring glycaemic control in diabetic patients (12). The data of rigorous 24 h glucose profiles from CGM allowed the calculation of glycaemic variations, detection of asymptomatic hypoglycaemia (Without typical symptoms of hypoglycaemia but plasma glucose measurements ≤ 3.9 mmol/L) and accurately depict the characteristics of blood glucose fluctuations (13). At present, few studies have reported the use of CGM to observe the effects of basal insulin and premixed insulin on the glycaemic profile in T2DM patients. Thus, this study was conducted to investigate the differences in glycaemic variability and hypoglycaemia between basal insulin and premixed insulin by using CGM.

PATIENTS AND METHODS

Participants

In this cross-sectional observation study, 393 outpatients with T2DM who had been treated with basal insulin or premixed insulin were enrolled at Nanjing First Hospital from July 2019 to December 2020.

The inclusion criteria were as follows (1): patients diagnosed with T2DM as defined by the World Health Organization in 1999; (2) patients aged ≥ 18 years; (3) body mass index (BMI) between 19 and 35 kg/m^2; (4) patients using basal insulin or premixed insulin (daily dose > 0.2 IU/kg/day) for more than 3 months; (5) patients with relatively consistent diet and exercise habits during the study period.

The following patients were excluded: (1) patients with type 1 diabetes mellitus; (2) patients with serious acute and/or chronic complications, including ketoacidosis, hyperosmolar state, end-stage renal disease, and severe cardiovascular diseases; (3) patients with severe infectious diseases; (4) patients with known cancers; (5) patients with cognitive disorders, drug abuse, or alcoholism.

Study Design

Written informed consent has signed by each participant. The study protocol was conducted in accordance with the 1964 Helsinki Declaration and its later amendments or comparable ethical standards. General information (such as age, sex, duration of T2DM, types and dosage of oral hypoglycaemic medication, insulin type and insulin dose) of the patients was collected by trained doctors (**Figure 1**).

393 patients who used basal insulin or premixed insulin for more than 3 months were classified into the basal insulin group (199 cases) or premixed insulin group (194 cases) according to their insulin regimen. The basal insulin used in this study is insulin glargine, including Basalin and Lantus, both of which are insulin analogues. Insulin types of premixed insulin group were Mixed Protamine Zinc Recombinant Human Insulin Injection, Biosynthetic Human Insulin Injection, Insulin Aspart 30 Injection, Mixed Protamine Zinc Recombinant Human Insulin Lispro Injection (50R), Mixed Protamine Zinc Recombinant Human Insulin Lispro Injection (25R) respectively. Blood samples from all patients were collected after fasting more than 10 h overnight. HbA1c was measured using a high-performance liquid chromatography assay (Bio-Rad Laboratories, Inc. CA, USA), C-peptide was assessed by ECLIA immunoassay analyzer Elecsys170 (Roche, Germany). Each sample for insulin antibodies measurement was run in duplicate, and optical density (OD) by ECLIA semi-quantitative assay. An index identified as COI was calculated based on the average of the results of each sample for Ins-Ab: COI = OD/CO (OD of test sample)/(OD of average absorbance of negative control) using a previously described method with some modification (14). The reference range of normal values for antibody is <1 COI.

The CGM in this study were retrospective CGM (Medtronic Mini Med), which were worn for 72 h. All patients were educated and provided with the CGM device by endocrine specialist nurses. Glucose values of peripheral blood were entered into CGM to calibrate device four times a day. The data of CGM was blinded to all the subjects. The patients maintained consistent diet and exercise habits, and recorded any incidences of hypoglycaemia (blood glucose level < 3.9 mmol/L), allergic reactions, and other abnormalities during the study period. Patients were advised to eat if they experienced asymptomatic hypoglycaemia or symptomatic hypoglycaemia (Typical symptoms of hypoglycaemia with plasma glucose concentration ≤ 3.9 mmol/L). If severe hypoglycaemia (Require help from others to administer glucose, inject glucagon, or take any other

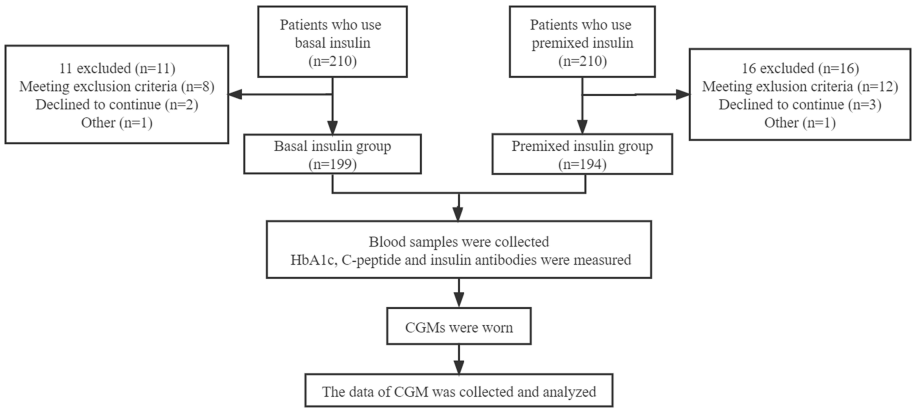

FIGURE 1 | Flow chart.

corrective action) occurred, the researchers would adjust the insulin dose of the participants.

To improve statistical power, we combined all patients and divided all patients (both the basal insulin group and premixed insulin group) into three groups according to the level of HbA1c, namely as HbA1c < 7%, 7% ≤ HbA1c ≤ 9%, HbA1c > 9%. At last, we sub-divided patients according to HbA1c within the basal insulin group (HbA1c < 7% and HbA1c ≥ 7%) and premixed insulin group (HbA1c < 7% and HbA1c ≥ 7%).

CGM

Data was collected from 00:00 to 24:00 on the second day of CGM. The following parameters were calculated: 1) 24-h mean blood glucose (MBG); 2) the mean fluctuation amplitude value from peak to valley every 24 h (24-h MAGE); 3) Standard deviation of blood glucose (24-h SDBG); 4) Percentage of time in the range of 3.9–10 mmol/L: time in range (TIR); 5) Percentage of time < 3.9 mmol/L or < 3.0 mmol/L: time below range (TBR); 6) Percentage of time > 13.9 mmol/L: time above range (TAR).

Statistical Analysis

Data were analysed using SPSS software (version 21.0, SPSS, Inc, Chicago, USA). All data were recorded and exported from the CGM 3.0 software analysis system (Medtronic Mini Med, USA). Normally distributed and continuous variables are presented as the mean (standard deviation, SD). Nonnormally distributed variables are presented as medians (interquartile ranges). An independent samples t-test and a rank sum test were used to compare difference between the groups for normally and non-normally distributed data, respectively. P values were two tailed with a significance level of 5%.

RESULTS

Baseline Characteristics

The mean age of patients in the basal insulin group was 59.40 ± 11.88 years, and that of the premixed insulin group was 63.14 ± 9.51 years. The percentage of achieving HbA1c <7% in the basal insulin group was 35.1% and that in the premixed insulin group was 34.7%. The clinical and demographic characteristics of both groups were similar, except for the duration of insulin, insulin dose and insulin antibody level, which were all increased in the premixed insulin group (**Table 1**). Patients who were treated with insulin combined with oral agents are shown in **Table 2**.

TABLE 1 | Baseline characteristics of patients.

Group	Basal Insulin Group (N=199)	Premixed Insulin Group (N=194)	p value
Sex (M/F)	125/74	113/81	0.83
Age (years)	59.40 ± 11.88	63.14 ± 9.51	0.68
HbA1c (%)	7.90 ± 1.69	7.69 ± 1.43	0.33
BMI (kg/m2)	24.92 ± 4.56	24.82 ± 3.10	0.61
Duration of T2DM (years)	15.0 (10.00, 16.50)	13.00 (9.00, 20.00)	0.51
Duration of insulin (years)	5.23 (3.00, 7.71)	6.42 (5.57, 11.00)	<0.01**
Insulin dose (IU/kg/day)	0.30 ± 0.10	0.53 ± 0.17	<0.01**
Fasting C-peptide (ng/ml)	1.20 ± 1.00	1.38 ± 0.99	0.07
Ins-Ab (COI)	4.69 (1.91, 10.02)	10.57 (3.95, 28.07)	<0.01**

*Data was shown as mean ± SD or median (first quartile, third quartile). M, male; F, female; HbA1c, glycated haemoglobin; BMI, body mass index; **p < 0.01. Ins-Ab, insulin antibody; COI, OD/CO; OD, absorbance; CO, average absorbance of negative control; The reference range of normal values for antibody is <1 COI.*

TABLE 2 | Drugs used in addition to insulin.

Group	Basal Insulin Group (N=199)	Premixed Insulin Group (N=194)	p value
Metformin (%)	59.3%	63.9%	0.58
α-glucosidase inhibitor (%)	73.4%	71.1%	0.61
Insulin secretagogues (%)	40.9%	7.8%	<0.01**
DPP-4 inhibitor (%)	9.5%	6.7%	0.48

***p < 0.01.*

There is a significantly greater frequency of use of insulin secretagogues in the basal insulin group than in the premixed insulin group.

The Glucose Profiles

The MBG of the basal insulin group was 9.27 ± 2.38 mmol/L, and that of the premixed insulin group was 8.92 ± 2.74 mmol/L; there was no significant difference between the two groups. The 24-h glucose profiles recorded by CGM during the use of basal insulin and premixed insulin are shown in **Figure 2**.

Glycaemic Variability

The glycaemic variability, including value of MAGE, SD and CV, was significantly lower in the basal insulin group than these in the premixed insulin group (p<0.01) (**Figure 3A** and **Table 3**).

Time in Range

The TIR (3.9–10.0 mmol/L) was significantly higher in the basal insulin group compared to the premixed insulin group (64.9% ± 29.3% *vs* 59.8% ± 23.8%, p=0.01) (**Figure 3B** and **Table 3**). The frequency of achieving TIR > 70% had significantly increased in the basal insulin group compared to the premixed insulin group (51.8% *vs* 40.2%, p<0.01).

Time Below Range

There were no severe hypoglycaemic events reported or dose adjustment issues occurred during the whole study. TBR < 3.9 mmol/L and < 3.0 mmol/L were significantly lower in the basal insulin participants compared to the premixed insulin participants, especially at night (0:00–05:59 h) (p<0.01) (**Figure 3C** and **Table 3**).

Time Above Range

TAR>13.9 mmol/L was significantly higher in the premixed insulin group (3.82 (0.00, 16.15) *vs* 0.00 (0.00, 15.97), p=0.01) compared to the basal insulin group (**Figure 3D** and **Table 3**).

Intergroup Clinical Characteristics of Patients With Different HbA1c Values

For the subgroups with HbA1c <7%, the value of MAGE was decreased in basal insulin group compared to premixed insulin group (4.72 ± 2.53 and *vs* 5.36 ± 2.09, p<0.01). TBR<3.9mmol/L in basal insulin group was lower compared to premixed insulin group (0.00 (0.00,0.35) *vs* 9.38 (1.04, 18.06), p < 0.01). For the subgroups with 7% ≤ HbA1c ≤ 9%, the GV and TBR of the premixed insulin group showed a significant increase than those in the basal insulin group (p<0.05), as well as the insulin antibody level. For the subgroups with HbA1c > 9%, there was no significant difference in CGM parameters between the two groups (**Table 4**).

Intragroup Clinical Characteristics of Patients With Different HbA1c Levels

In the basal insulin group and premixed insulin group, there was no significant difference in clinical characteristics between patients with HbA1c < 7% and patients with HbA1c ≥ 7% (**Tables 5**, **6**).

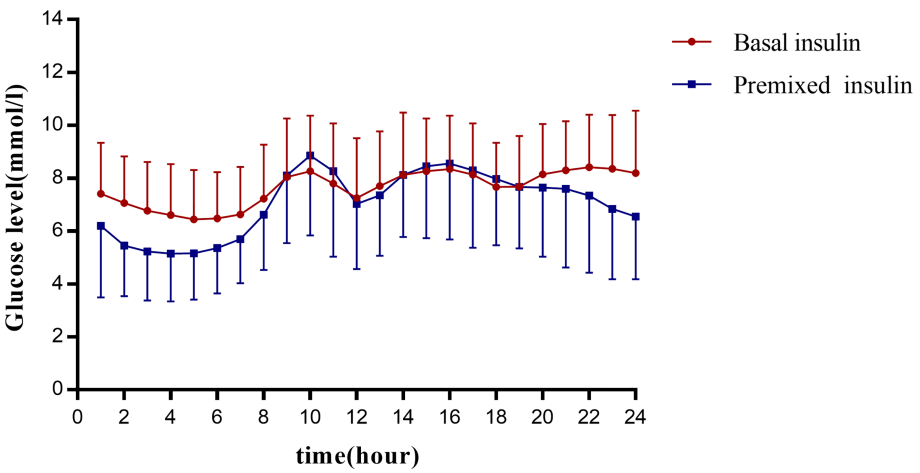

FIGURE 2 | Graph presents the glucose profiles of basal insulin and premixed insulin. The vertical coordinates show the mean glucose ± SD per hour for all patients in each group. The 24 points in each group are connecting to visualize the 24-hour glucose fluctuations in this group of patients. The horizontal coordinates are spaced at 2-hour intervals for each point.

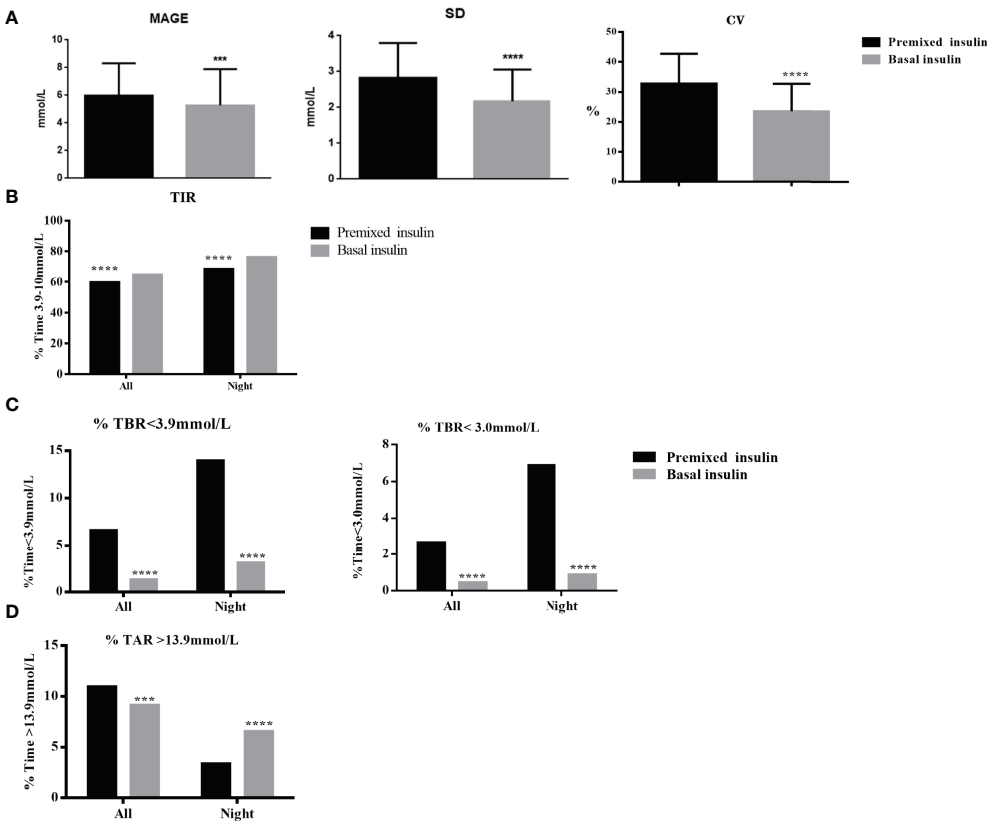

FIGURE 3 | **(A)** GV (MAGE, SD, CV) of the basal insulin group and the premixed insulin group within the full 24-hrs. **(B)** Percentage of TIR (3.0~10 mmol/L) of the basal insulin group and the premixed insulin group within the full 24-hrs and nighttime (00:00–05:59) periods. **(C)** TBR (<3.9 and <3.0 mmol/L) of the basal insulin group and the premixed insulin group within the full 24-hrs and nighttime (00:00–05:59) periods. **(D)** TAR (>13.9 mmol/L) of the basal insulin group and the premixed insulin group within the full 24-hrs and nighttime (00:00–05:59) periods. ***p < 0.001, ****p < 0.0001.

TABLE 3 | CGM index between two groups.

Group		Basal Insulin Group (N=199)	Premixed Insulin Group (N=194)	p value
MBG (mmol/L)		9.27 ± 2.38	8.92 ± 2.74	0.078
GV	MAGE (mmol/L)	4.72 ± 2.53	5.36 ± 2.09	0.035*
	SD (mmol/L)	1.82 ± 0.78	2.54 ± 0.77	<0.01**
	CV (%)	22.87 ± 9.03	36.08 ± 9.77	<0.01**
TIR (%) (3.9-10mmol/L)		64.9 ± 29.3	59.8 ± 23.8	<0.01**
TAR (%) >13.9mmol/L		0.00 (0.00, 0.00)	0.00 (0.00, 5.12)	<0.01**
TBR (%) <3.9mmol/L		0.00 (0.00, 0.35)	9.38 (1.04, 18.06)	<0.01**
TBR (%) <3.0mmol/L		0.00 (0.00, 0.00)	1.74 (0.00, 7.38)	<0.01**

**p < 0.05, **p < 0.01. Data was shown as mean ± SD or median (first quartile, third quartile). MBG, 24-hour mean blood glucose; GV, Glycaemic variability; MAGE, 24-hour mean amplitude of glycaemic excursion; SD, Standard deviation of blood glucose; CV, coefficient of variation; TIR, time in range (3.9-10 mmol/L); TAR, time above target range (>13.9 mmol/L); TBR, time-below-target ranges (<3.9 mmol/L or <3.0 mmol/L).*

DISCUSSION

In this cross-sectional study, our results showed although there was not a gap of actual HbA1c between the two groups, TIR in the basal insulin group was greater than that in the premixed insulin group. Although the MBG of both groups were similar, the basal insulin group had lower GV, overall hypoglycaemia and nocturnal hypoglycaemia than the premixed insulin group.

In the present study we found that the basal insulin group had similar levels of C-peptide as the premixed insulin group. C-peptide is produced with an equal amount of insulin and is the

TABLE 4 | Clinical characteristics of patients with different HbA1c levels.

Group	HbA1c<7%			7%≤HbA1c≤9%			HbA1c>9%		
	Basal Insulin (N=69)	Premixed Insulin (N=68)	P value	Basal Insulin (N=80)	Premixed Insulin (N=93)	P value	Basal Insulin (N=50)	Premixed Insulin (N=33)	P value
MBG (mmol/L)	7.54±1.57	7.15±1.51	<0.01**	9.62±2.40	9.28±2.21	0.412	10.53±2.43	11.58±3.50	0.211
MAGE (mmol/L)	4.72±2.53	5.36±2.09	0.035*	5.43±2.48	6.33±2.13	0.011*	5.78±2.88	6.28±3.10	0.389
SD (mmol/L)	1.82±0.78	2.54±0.77	<0.01**	2.28±0.84	3.04±0.95	<0.01**	2.46±0.98	2.85±1.22	0.182
CV (%)	22.87 ±9.03	36.08±9.77	<0.01**	24.25±9.61	33.35±8.70	<0.01**	23.43±8.59	24.62±9.18	0.612
TIR (%)	86.46 (72.05, 96.35)	73.96 (61.28, 80.90)	<0.01**	64.76 (36.63, 86.72	60.76 (43.58, 75.87)	0.287	48.78 (19.53, 74.83)	37.84 (19.44, 59.20)	0.235
TBR <3.9 mmol/L (%)	0.00 (0.00, 0.35)	9.38 (1.04, 18.06)	<0.01**	0.00 (0.00, 0.00)	1.04 (0.00, 7.29)	<0.01**	0.00 (0.00, 0.00)	0.00 (0.00, 0.00)	0.508
TBR <3.0 mmol/L (%)	0.00 (0.00, 0.00)	1.74 (0.00, 7.38)	<0.01**	0.00 (0.00, 0.00)	0.00 (0.00, 2.43)	<0.01**	0.00 (0.00, 0.00)	0.00 (0.00, 0.00)	0.321
C-Peptide (ng/ml)	1.22±0.83	1.32±0.73	0.53	1.36±0.38	1.47±1.13	0.58	1.05±1.82	1.32±1.22	0.27
Ins-Ab (COI)	3.10 (1.13, 11.06)	9.25 (2.89, 29.74)	<0.01**	5.06 (2.37, 10.09)	13.43 (5.53, 30.31)	<0.01**	4.31 (1.98, 9.14)	8.42 (2.68, 13.98)	0.13

*Data was shown as mean ± SD or median (first quartile, third quartile). *p < 0.05, **p < 0.01. HbA1c, glycated haemoglobin; MBG, 24-hour mean blood glucose; GV, Glycaemic variability; MAGE, 24-hour mean amplitude of glycaemic excursion; SD, Standard deviation of blood glucose; CV, coefficient of variation; TIR, time in range (3.9-10 mmol/L); TAR, time above target range (>13.9 mmol/L); TBR, time-below-target ranges (<3.9 mmol/L or <3.0 mmol/L); Ins-Ab, insulin antibody; COI, OD/CO; OD, absorbance; CO, average absorbance of negative control; The reference range of normal values for antibody is <1 COI.*

TABLE 5 | Clinical characteristics of patients with subdivided basal insulin group.

Basal Insulin	HbA1c<7% (N=69)	HbA1c≥7% (N=130)	p value
Age (years)	59.64 ± 10.22	59.28 ± 12.71	0.83
Fasting C-peptide (ng/ml)	1.20 ± 0.08	1.20 ± 0.10	0.98
Ins-Ab (COI)	7.7 ± 0.99	9.12 ± 1.32	0.39
Duration of T2DM (years)	14.24 ± 6.02	13.21 ± 6.13	0.25
Duration of insulin (years)	5.76 ± 3.12	5.20 ± 3.18	0.22
Insulin dose (IU/kg/day)	0.28 ± 0.08	0.32 ± 0.13	0.12

Data was shown as mean ± SD. HbA1c, glycated haemoglobin; Ins-Ab, insulin antibody; COI, OD/CO; OD, absorbance; CO, average absorbance of negative control; The reference range of normal values for antibody is <1 COI.

TABLE 6 | Clinical characteristics of patients with subdivided premixed insulin group.

Premixed Insulin	HbA1c<7% (N=68)	HbA1c≥7% (N=126)	p value
Age (years)	63.09 ± 9.32	63.15 ± 9.09	0.86
Fasting C-peptide (ng/ml)	1.32 ± 0.09	1.43 ± 0.10	0.48
Ins-Ab (COI)	17.01 ± 2.27	18.36 ± 1.73	0.64
Duration of T2DM (years)	12.75 ± 6.92	14.07 ± 6.82	0.20
Duration of insulin (years)	7.91 ± 6.78	7.59 ± 5.95	0.73
Insulin dose (IU/kg/day)	0.49 ± 0.02	0.47 ± 0.02	0.63

Data was shown as mean ± SD. HbA1c, glycated haemoglobin; Ins-Ab, insulin antibody; COI, OD/CO; OD, absorbance; CO, average absorbance of negative control; The reference range of normal values for antibody is <1 COI.

best measure of endogenous insulin secretion in patients with diabetes (15). The key current clinical role of C-peptide is to assist classification and management of insulin-treated patients. C-peptide is inversely associated with glycaemic variability and post-meal glucose rise in both Type 1 and Type 2 diabetes (16) and is inversely associated with response to prandial insulin in experimental conditions in a mixed population with diabetes. Given that low C-peptide is associated with higher glucose variability, the absence of statistically significant difference in C-peptide between basal insulin and premixed insulin groups suggests that residual beta-cell function was not responsible for the CGM differences observed in this study.

Severe hypoglycaemia causes patients to show signs of an insufficient energy supply to the central nervous system, such as drowsiness, disturbance of consciousness, nonsense, and even coma and death (17). It was reported that 80% of diabetes specialists feel they are unable to proactively treat the disease because of the risk of hypoglycaemia (18); thus, treatment that does not result in hypoglycaemia is very important for diabetic patients. Basal insulin treatment has a lower risk of hypoglycaemia, which enables more aggressive treatment and is easier to use with less variation (19). In this study, symptomatic hypoglycaemia and severe hypoglycaemia did not occur, but the TBR < 3.9 mmol/L and TBR < 3.0 mmol/L were significantly higher in the premixed insulin group than in the basal insulin group. More importantly, nocturnal hypoglycaemia also causes severe damage to patients if it recurs and is undetectable, and even mild asymptomatic episodes can lead to further impairment and defective counterregulatory responses to

subsequent events (20). In addition to an increased risk for future episodes, the effects of nocturnal hypoglycaemia that occur during the day, such as fatigue, impaired mood and higher calorie intake and weight gain, considerably lower quality of life (21). Our study found the TBR < 3.9 mmol/L and TBR < 3.0 mmol/L in the premixed insulin group at night were both higher than those in the basal insulin group.

In addition, in this study, we divided patients according to the level of HbA1c across the two groups. For the subgroups with HbA1c <7%, the GV, TBR < 3.9 mmol/L and TBR < 3.0 mmol/L of the premixed insulin group were higher than those in the basal insulin group. Patients in the premixed insulin group do not have lower C-peptide levels compared to the basal insulin group and have elevated insulin antibody (IA), as well as a higher incidence of hypoglycaemia. Longer duration of insulin use which made possible exposure to more types of insulin are potential causes for significantly greater insulin antibody levels in the premixed insulin group. Administration of exogenous animal insulin for the treatment of diabetes often induces the production of IA (22). In recent years, the usage of recombinant human insulin preparations and human insulin analogues has significantly reduced but not entirely suppressed the incidence of IA development. These antibodies might affect a patient's glycaemic control due to their tendency to bind and/or release insulin in an unpredictable fashion. The higher circulating IA was associated with increased MAGE in T2DM patients (23), thus greater GV may be due to greater IA levels in the premixed insulin group potentially, which indicate that those patients with elevated IA levels should receive GV assessment and individualized treatment. For the subgroups with HbA1c <7% and 7% ≤ HbA1c ≤ 9%, patients who use premixed insulin have a higher IA level, the TIR was not higher than patients in the basal insulin group, however the incidence of hypoglycaemia and GV were both higher in premixed insulin group. For the subgroups with HbA1c > 9%, the MBG and TIR of patients in both groups did not meet the standard, and the C-peptide levels of patients who use basal insulin were not high.

C-peptide measurement is critical in insulin selection for it can reflect islet function of patients, the regimen for patients who use premixed insulin could be considered to use basal insulin if they present higher incidence of hypoglycaemia, greater GV and better islet function. CGM is an important device on detection of asymptomatic hypoglycaemia and hypoglycaemia, and should be fully considered when choosing an insulin regimen. Although the lower price of premixed insulin is one of the reasons for Chinese patients and physicians tend to use premixed insulin. It is still important not to be price oriented when making the choice of insulin type, as the above mentioned, islet function, frequency of hypoglycaemia, and GV are all factors to be considered.

Limitations should also be addressed. Firstly, findings using a larger sample size may be more convincing. Secondly, the differential use of insulin secretagogues, insulin dosing, and duration of insulin use between the two groups could partly contribute to result bias. Thirdly, the cross-sectional study design is insufficiently to answer persistent effects on the glycaemic control process of the same individual with premixed insulin or basal insulin therapy. Finally, our study was limited to a single centre, which should be expanded. We hope to follow up these subjects and expand the sample in the future.

CONCLUSIONS

In summary, compared with basal insulin, the patients who currently use premixed insulin had more severe GV, a smaller TIR and a higher incidence of hypoglycaemia. Among people who use premixed insulin and have an HbA1c < 7%, more attention needs to be paid on hypoglycaemic events and asymptomatic hypoglycaemia. If necessary, the insulin regimen should be adjusted.

DATA AVAILABILITY STATEMENT

The raw data supporting the conclusions of this article will be made available by the authors, without undue reservation.

ETHICS STATEMENT

The studies involving human participants were reviewed and approved by Ethics Committee of Nanjing First Hospital. The patients/participants provided their written informed consent to participate in this study.

AUTHOR CONTRIBUTIONS

HW and YZ analyzed data and wrote the manuscript. YW, TC, and YH organized data. TJ, BD, and XS modified the manuscript. HL and JM conceived, and directed the study. All authors contributed to the article and approved the submitted version.

FUNDING

This study was partly supported by the National Key R&D Program of China (No. 2018YFC1314103), the Xinghuo Talent Program of Nanjing First Hospital (To YZ), and Jiangsu Innovative and Entrepreneurial Talent Programme (No.JSSCBS20211546).

ACKNOWLEDGMENTS

This trial is registered at ClinicalTrials.gov (ClinicalTrials.gov identifier: NCT03566472). We thank the members of Endocrinology department of Nanjing First hospital for their support.

REFERENCES

1. Ding B, Su X, Li H, Ma J. Classification and Diagnosis of Diabetes. *Diabetes Care* (2015) 38 (Suppl):S8–8S16. doi: 10.2337/dc15-S005
2. Li Y, Teng D, Shi X, Qin G, Qin Y, Quan H, et al. Prevalence of Diabetes Recorded in Mainland China Using 2018 Diagnostic Criteria From the American Diabetes Association: National Cross Sectional Study. *BMJ* (2020) 369:m997. doi: 10.1136/bmj.m997
3. Giugliano D, Tracz M, Shah S, Calle-Pascual A, Mistodie C, Duarte R, et al. Initiation and Gradual Intensification of Premixed Insulin Lispro Therapy Versus Basal {+/-} Mealtime Insulin in Patients With Type 2 Diabetes Eating Light Breakfasts. *Diabetes Care* (2014) 37:372–80. doi: 10.2337/dc12-2704
4. Jellinger PS, Handelsman Y, Rosenblit PD, Bloomgarden ZT, Fonseca VA, Garber AJ, et al. American Association of Clinical Endocrinologists and American College of Endocrinology Guidelines For Management of Dyslipidemia and Prevention of Cardiovascular Disease. *Endocr Pract* (2017) 23:1–87. doi: 10.4158/EP171764.APPGL
5. Gao Z, Yan W, Fang Z, Zhang Z, Yuan L, Wang X, et al. Annual Decline in β-Cell Function in Patients With Type 2 Diabetes in China. *Diabetes Metab Res Rev* (2021) 37:e3364. doi: 10.1002/dmrr.3364
6. Aschner P. Insulin Therapy in Type 2 Diabetes. *Am J Ther* (2020) 27:e79–79e90. doi: 10.1097/MJT.0000000000001088
7. Ilag LL, Kerr L, Malone JK, Tan MH. Prandial Premixed Insulin Analogue Regimens Versus Basal Insulin Analogue Regimens in the Management of Type 2 Diabetes: An Evidence-Based Comparison. *Clin Ther* (2007) 29:1254–70. doi: 10.1016/j.clinthera.2007.07.003
8. Jean-Baptiste E, Larco P, von Oettingen J, Ogle GD, Moïse K, Fleury-Milfort E, et al. Efficacy of a New Protocol of Premixed 70/30 Human Insulin in Haitian Youth With Diabetes. *Diabetes Ther* (2021) 12:2545–56. doi: 10.1007/s13300-021-01130-x
9. Sheu WH, Ji L, Lee WJ, Jabbar A, Han JH, Lew T. Efficacy and Safety of Premixed Insulin Analogs in Asian Patients With Type 2 Diabetes: A Systematic Review. *J Diabetes Investig* (2017) 8:518–34. doi: 10.1111/jdi.12605
10. Qayyum R, Bolen S, Maruthur N, Feldman L, Wilson LM, Marinopoulos SS, et al. Systematic Review: Comparative Effectiveness and Safety of Premixed Insulin Analogues in Type 2 Diabetes. *Ann Intern Med* (2008) 149:549–59. doi: 10.7326/0003-4819-149-8-200810210-00242
11. Holman RR, Farmer AJ, Davies MJ, Levy JC, Darbyshire JL, Keenan JF, et al. Three-Year Efficacy of Complex Insulin Regimens in Type 2 Diabetes. *N Engl J Med* (2009) 361:1736–47. doi: 10.1056/NEJMoa0905479
12. Lee I, Probst D, Klonoff D, Sode K. Continuous Glucose Monitoring Systems - Current Status and Future Perspectives of the Flagship Technologies in Biosensor Research. *Biosens Bioelectron* (2021) 181:113054. doi: 10.1016/j.bios.2021.113054
13. Wei W, Zhao S, Fu SL, Yi L, Mao H, Tan Q, et al. The Association of Hypoglycemia Assessed by Continuous Glucose Monitoring With Cardiovascular Outcomes and Mortality in Patients With Type 2 Diabetes. *Front Endocrinol (Lausanne)* (2019) 10:536. doi: 10.3389/fendo.2019.00536
14. Quan H, Tan H, Li Q, Li J, Li S. Immunological Hypoglycemia Associated With Insulin Antibodies Induced by Exogenous Insulin in 11 Chinese Patients With Diabetes. *J Diabetes Res* (2015) 2015:746271. doi: 10.1155/2015/746271
15. Ferrannini E, Gastaldelli A, Miyazaki Y, Matsuda M, Mari A, DeFronzo RA. Beta-Cell Function in Subjects Spanning the Range From Normal Glucose Tolerance to Overt Diabetes: A New Analysis. *J Clin Endocrinol Metab* (2005) 90:493–500. doi: 10.1210/jc.2004-1133
16. Kohnert KD, Augstein P, Zander E, Heinke P, Peterson K, Freyse EJ, et al. Glycemic Variability Correlates Strongly With Postprandial Beta-Cell Dysfunction in a Segment of Type 2 Diabetic Patients Using Oral Hypoglycemic Agents. *Diabetes Care* (2009) 32:1058–62. doi: 10.2337/dc08-1956
17. Frier BM. Hypoglycaemia in Diabetes Mellitus: Epidemiology and Clinical Implications. *Nat Rev Endocrinol* (2014) 10:711–22. doi: 10.1038/nrendo.2014.170
18. Peyrot M, Barnett AH, Meneghini LF, Schumm-Draeger PM. Insulin Adherence Behaviours and Barriers in the Multinational Global Attitudes of Patients and Physicians in Insulin Therapy Study. *Diabetes Med* (2012) 29:682–9. doi: 10.1111/j.1464-5491.2012.03605.x
19. Raccah D. Basal Insulin Treatment Intensification in Patients With Type 2 Diabetes Mellitus: A Comprehensive Systematic Review of Current Options. *Diabetes Metab* (2017) 43:110–24. doi: 10.1016/j.diabet.2016.11.007
20. Graveling AJ, Frier BM. The Risks of Nocturnal Hypoglycaemia in Insulin-Treated Diabetes. *Diabetes Res Clin Pract* (2017) 133:30–9. doi: 10.1016/j.diabres.2017.08.012
21. Jauch-Chara K, Schultes B. Sleep and the Response to Hypoglycaemia. *Best Pract Res Clin Endocrinol Metab* (2010) 24:801–15. doi: 10.1016/j.beem.2010.07.006
22. Oak S, Phan TH, Gilliam LK, Hirsch IB, Hampe CS. Animal Insulin Therapy Induces a Biased Insulin Antibody Response That Persists for Years After Introduction of Human Insulin. *Acta Diabetol* (2010) 47:131–5. doi: 10.1007/s00592-009-0135-2
23. Zhu J, Yuan L, Ni WJ, Luo Y, Ma JH. Association of Higher Circulating Insulin Antibody With Increased Mean Amplitude Glycemic Excursion in Patients With Type 2 Diabetes Mellitus: A Cross-Sectional, Retrospective Case-Control Study. *J Diabetes Res* (2019) 2019:7304140. doi: 10.1155/2019/7304140

Conflict of Interest: The authors declare that the research was conducted in the absence of any commercial or financial relationships that could be construed as a potential conflict of interest.

frontiers | Frontiers in Endocrinology

ORIGINAL RESEARCH
published: 04 May 2022
doi: 10.3389/fendo.2022.869451

Novel Glycemic Index Based on Continuous Glucose Monitoring to Predict Poor Clinical Outcomes in Critically Ill Patients: A Pilot Study

Eun Yeong Ha[1†], Seung Min Chung[1†], Il Rae Park[1], Yin Young Lee[2], Eun Young Choi[3] and Jun Sung Moon[1]*

[1] Division of Endocrinology and Metabolism, Department of Internal Medicine, College of Medicine, Yeungnam University, Daegu, South Korea, [2] Division of Endocrinology and Metabolism, Department of Internal Medicine, Veterans Health Service Medical Center, Daegu, South Korea, [3] Division of Pulmonology and Allergy, Department of Internal Medicine, Respiratory Center, Yeungnam University Medical Center, College of Medicine, Yeungnam University, Daegu, South Korea

OPEN ACCESS

Edited by:
Joon Ha,
Howard University, United States

Reviewed by:
Sangsoo Kim,
Pusan National University Hospital, South Korea
Claudia Piona,
University City Hospital of Verona, Italy
Christine Chan,
University of Colorado, United States

***Correspondence:**
Jun Sung Moon
mjs7912@yu.ac.kr

[†]These authors have contributed equally to this work and share first authorship

Specialty section:
This article was submitted to Clinical Diabetes, a section of the journal Frontiers in Endocrinology

Received: *04 February 2022*
Accepted: *05 April 2022*
Published: *04 May 2022*

Citation:
Ha EY, Chung SM, Park IR, Lee YY, Choi EY and Moon JS (2022) Novel Glycemic Index Based on Continuous Glucose Monitoring to Predict Poor Clinical Outcomes in Critically Ill Patients: A Pilot Study. Front. Endocrinol. 13:869451. doi: 10.3389/fendo.2022.869451

Aim: We explored the prospective relationship between continuous glucose monitoring (CGM) metrics and clinical outcomes in patients admitted to the intensive care unit (ICU).

Materials and Methods: We enrolled critically ill patients admitted to the medical ICU. Patients with an Acute Physiology and Chronic Health Evaluation (APACHE) score ≤9 or ICU stay ≤48 h were excluded. CGM was performed for five days, and standardized CGM metrics were analyzed. The duration of ICU stay and 28-day mortality rate were evaluated as outcomes.

Results: A total of 36 patients were included in this study (age [range], 49–88 years; men, 55.6%). The average APACHE score was 25.4 ± 8.3; 33 (91.7%) patients required ventilator support, and 16 (44.4%) patients had diabetes. The duration of ICU stay showed a positive correlation with the average blood glucose level, glucose management indicator (GMI), time above range, and GMI minus (-) glycated hemoglobin (HbA1c). Eight (22.2%) patients died within 28 days, and their average blood glucose levels, GMI, and GMI-HbA1c were significantly higher than those of survivors ($p<0.05$). After adjustments for age, sex, presence of diabetes, APACHE score, and dose of steroid administered, the GMI-HbA1c was associated with the risk of longer ICU stay (coefficient=2.34, 95% CI 0.54-4.14, p=0.017) and higher 28-day mortality rate (HR=2.42, 95% CI 1.01-5.76, p=0.046).

Conclusion: The acute glycemic gap, assessed as GMI-HbA1c, is an independent risk factor for longer ICU stay and 28-day mortality rate. In the ICU setting, CGM of critically ill patients might be beneficial, irrespective of the presence of diabetes.

Keywords: blood glucose, diabetes mellitus, glucose, hospitals, intensive care units, technology

INTRODUCTION

Acute hyperglycemia is commonly encountered in critically ill patients admitted to the intensive care unit (ICU), regardless of the presence of diabetes mellitus (DM) (1). Hyperglycemia is induced by acute stress and is also associated with the prognosis of severely ill patients (2). In addition, these patients are vulnerable to hypoglycemia, both iatrogenic and idiopathic, and several studies have suggested that hypoglycemia is an independent risk factor for mortality. Recent guidelines recommend that the goal of glycemic control in the ICU is 140–180 mg/dL, although there are controversies about the appropriate target range. These findings emphasize the importance of glucose monitoring and management in critically ill patients. However, point-of-care (POC) blood glucose monitoring has limitations in ICU settings, such as missing or not being able to predict hypoglycemia or hyperglycemia. In addition, though glycated hemoglobin (HbA1c) is an important indicator of the condition of diabetic patients and the risk of long-term diabetic complications (3), this may be insufficient to optimally induce personalized treatment changes, especially in patients using insulin, as the degree or timing of hypoglycemia, and the presence of clinically significant glucose variability or hyperglycemic patterns are unknown. Previous studies have demonstrated glucose variability with mean amplitude of glucose excursion (MAGE), continuous overall net glycemic action (CONGA), and M-values (4–6). However, these require the use of a special calculation program and are difficult to calculate and apply immediately in ICU patients. On the other hand, continuous glucose monitoring (CGM) is a great help in evaluating blood glucose variability as it can easily obtain sufficient data (7).

CGM is a powerful tool with the potential to transform the management of individuals with diabetes. In real time, CGM can show trends in hypoglycemia, hyperglycemia, and glucose variability, some of which warrant immediate therapeutic action (8, 9). In other words, CGM helps individuals with diabetes and clinicians optimize diabetes management strategies. CGM is strongly recommended in clinical situations requiring intensive glucose monitoring, such as patients receiving multiple insulin injections (10–12). The benefits of CGM include the prediction and prevention of rapid glycemic changes, which cannot be recognized with POC, HbA1c, glycated albumin, or fructosamine, and this technology will be accepted in various situations including in-hospital care (13, 14).

CGM has also been highlighted as an attractive alternative to hourly POC in the ICU and shows high accuracy and reliability in patients admitted to cardiac, surgical, and medical ICUs, as well as patients with coronavirus disease 2019 (15–18). The use of CGM metrics for remote blood glucose monitoring in the ICU has been approved due to the recent coronavirus disease 2019 pandemic (19, 20). However, little is known about the clinical usefulness or implications of CGM metrics in ICU settings. Therefore, we aimed to investigate the correlation of CGM metrics with clinical outcomes in critically ill patients admitted to the medical ICU. In addition, we attempted to devise a novel index based on conventional CGM metrics to predict the prognosis of patients admitted to the ICU.

MATERIALS AND METHODS

Study Design and Patient Selection

This prospective observational study enrolled critically ill patients admitted to the medical ICU of Yeungnam University Hospital, Daegu, South Korea, between June 2020 and February 2021. The study was conducted after the patient or legal representative provided written informed consent. We initially selected 52 patients and examined their eligibility. The inclusion criteria were as follows: 1) patients aged >45 years and 2) critically ill patients who were admitted due to pneumonia, septic shock, or acute respiratory distress syndrome (ARDS). The exclusion criteria were as follows: 1) patients whose expected the duration of ICU stay was ≤48 h, 2) patients with an Acute Physiology and Chronic Health Evaluation (APACHE) II score ≤9, 3) patients with chronic disease who were less likely to be resuscitated, and 4) patients with a high risk of bleeding during CGM (platelet count < 50,000/μL). A total of 36 patients were included in the final analysis. The study protocol adhered to the tenets of the Declaration of Helsinki and was reviewed and approved by the Institutional Review Board of Yeungnam University Hospital (approval no. 2019-07-043).

Clinical and Biochemical Measurements

Disease severity was assessed using the APACHE II score (21). Higher scores (range, 0–71) are closely correlated with the subsequent risk of in-hospital death: an APACHE II score ≥10 reflects an estimated in-hospital mortality of >15%. ARDS was diagnosed according to the Berlin definition (22). Septic shock was defined according to the Third International Consensus Definitions for Sepsis and Septic Shock (Sepsis-3) (23). Data on ventilator support and administration of steroids or insulin during ICU care were collected.

Waist circumference and blood pressure were measured by trained staff members. All laboratory parameters were evaluated at the central laboratory of Yeungnam University Hospital. The white blood cell and platelet counts, and hemoglobin (Hb), C-reactive protein (CRP), procalcitonin, glycated hemoglobin (HbA1c), fasting glucose, fasting insulin, total cholesterol, triglyceride, high-density lipoprotein cholesterol, and creatinine levels were measured.

The diagnostic criteria for DM were as follows: 1) previous diagnosis by a doctor or 2) satisfying the following conditions: fasting plasma glucose ≥ 126 mg/dL and HbA1c ≥ 6.5% (24).

CGM and Initiation of Insulin Infusion

For glucose monitoring, a CGM system (Dexcom G5, Dexcom, San Diego, USA) was attached for 5 days immediately after the admission, and calibration was performed using the same self-monitoring glucometers at least twice a day to increase the accuracy of the data. Venous blood glucose levels were checked to ensure that the CGM system was functioning properly. The transmitter was removed during radiography or computed tomography.

Irrespective of the presence of DM, patients with two or more instances of blood glucose levels > 180 mg/dL were initiated on the Yale ICU insulin infusion protocol (25). The target blood glucose range was 140–180 mg/dL. Based on the International Consensus statement, the following key CGM metrics were collected (26): average blood glucose level, glucose management indicator (GMI), coefficient of variation (CV), time in range (TIR, 70–180 mg/dL), time above range (TAR, > 180 mg/dL), and time below range (TBR, < 70 mg/dL). In addition, we analyzed the difference between GMI and HbA1c levels (GMI-HbA1c) (8). We also calculated other CGM-derived metrics such as MAGE, CONGA, and M-values using EasyGV software (www.phc.ox.ac.uk/research/resources/easygv).

Outcomes

The outcomes evaluated were the duration of ICU stay and 28-day mortality rate. *Post-hoc* power was calculated using previously published data (27) as known population, and the *post-hoc* power of our study was 50.7%.

Statistical Analysis

All statistical tests were performed using R software (version 3.6.3, R Foundation, Vienna, Austria). Baseline characteristics are expressed as mean ± standard deviation for continuous variables and as numbers and percentages for categorical variables. Differences between groups were assessed using the Mann–Whitney U test for continuous variables and chi-square tests for categorical variables. Spearman's correlation analysis was used to assess the correlation between CGM metrics and duration of ICU stay. Linear regression analysis was used to assess the effects of CGM metrics on the duration of ICU stay. Cox regression analysis was used to assess the effects of CGM metrics on 28-day mortality rate. Hazard ratios (HRs) were reported with 95% confidence intervals (CIs). Statistical significance was set at $P < 0.05$.

RESULTS

Baseline Characteristics

Baseline characteristics and their comparisons between patients with and without diabetes are presented in **Table 1**.

The mean age was 71.0 ± 9.9 years (range, 49–88 years), and the male-to-female ratio was 1.25:1. The most common diagnosis at the time of admission was pneumonia (58.3%), followed by septic shock (22.2%) and ARDS (19.4%). The mean APACHE score was 25.4 ± 8.3. The CGM system was attached for 5.5 ± 0.8 days and activated for 98.5% ± 3.1% of time. Thirty-three patients (91.7%) required ventilator support. Steroids were administered to 75% of patients, and insulin was administered to 66.7% of patients. The average duration of ICU stay was 10.8 ± 7.6 days, and 8 patient (22.2%) died within 28 days.

Among all patients, 16 (44.4%) had DM. Thirteen patients were previously diagnosed by a doctor; however, 10 of them did not receive anti-hyperglycemic treatment. Three patients were newly diagnosed at the time of admission. Age, sex, diagnosis, and disease severity at the time of admission were not different between patients with and without DM. The white blood cell count and levels of CRP and procalcitonin were increased in patients with and without DM without statistically significant differences. The average HbA1c level of patients with DM was 8.0%, and that of patients without DM was 5.9% (p<0.001). Compared to patients with DM, the average blood glucose level (150 mg/dL vs. 177 mg/dL, p=0.030), GMI (6.9% vs. 7.8%, p=0.033), CV (25.1% vs. 32.0%, p=0.028), and TAR (22.5% vs. 38.8%, p=0.030) were significantly lower, and the TIR (76.5% vs. 60.0%, p=0.039) and GMI-HbA1c (1.0% vs. -0.2%, p=0.020) were significantly higher in non-diabetic patients. Treatment, including ventilator support, steroids, and insulin, and clinical outcomes (ICU stay and 28-day mortality rate) did not differ significantly between patients with and without DM.

Association Between CGM Metrics and Duration of ICU Stay

The correlation analysis for CGM metrics and ICU stay is presented in **Table 2**. The average blood glucose level (r=0.532, p<0.001), GMI (r=0.545, p<0.001), TAR (r=0.457, p=0.005), and GMI-HbA1c (r=0.533, p<0.001) were positively associated, and TIR (r=-0.435, p=0.008) was negatively associated with the duration of ICU stay. GMI-HbA1c was positively correlated with duration of ICU stay in both patients without DM (r=0.66, p=0.002) and patients with DM (r=0.59, p=0.016; **Figure 1**). However, the correlation between duration of ICU stay and CV or TBR was not significant. Other CGM-derived parameters, such as MAGE, CONGA, and M-value, were also not correlated to ICU stay length (**Supplementary Table 1**).

Association Between CGM Metrics and 28-Day Mortality Rate

Clinical characteristics of the survivors and non-survivors at 28 days are presented in **Table 3**. Eight patients died within 28 days. There were no differences in age, sex, presence of DM, and APACHE scores between survivors and non-survivors. In non-survivors, the prevalence of ARDS was significantly higher (75% vs. 3.6%, p=0.001), and a higher dose of steroid was administered (61.7 mg/day vs. 25.6 mg/day, p=0.007) than in survivors. Among CGM metrics, the average blood glucose level (188.8 ± 35.6 vs. 154.6 ± 42.7, p=0.021), GMI (8.2 ± 1.3 vs. 7.0 ± 1.5, p=0.024), and GMI-HbA1c (2.0 ± 1.3 vs. 0.0 ± 1.6, p<0.001) were significantly higher in non-survivors than in survivors. The GMI-HbA1c was significantly higher in non-survivors than in survivors in both patients without DM (2.3 ± 1.6 vs. 0.6 ± 0.9, p=0.025) and patients with DM (1.6 ± 0.7 vs. -0.7 ± 2.0, p=0.008; **Figure 2**). M-value was also marginally higher in the non-survivor group (p=0.059), but MAGE was not different between group (**Supplementary Table 1**).

The Effect of CGM Metrics on Clinical Outcomes

The effects of HbA1c, fasting glucose, and CGM metrics on the duration of ICU stay and 28-day mortality rate were analyzed

TABLE 1 | Comparison of baseline characteristics between patients with and without diabetes.

	Overall (n=36)	non-DM (n=20)	DM (n=16)	p-value
Age, years	71.0 ± 9.9	69.5 ± 11.0	72.9 ± 8.1	0.305
Men, n (%)	20 (55.6)	11 (55.0)	9 (56.2)	
Diagnosis at ICU admission				
Pneumonia, n (%)	21 (58.3)	11 (55.0)	10 (37.0)	0.711
Septic shock, n (%)	8 (22.2)	4 (20.0)	4 (14.8)	
ARDS, n (%)	7 (19.4)	5 (25.0)	2 (7.4)	
Disease severity at ICU admission				
APACHE	25.4 ± 8.3	25.1 ± 8.8	25.8 ± 7.9	0.765
Laboratory data				
Waist circumference, cm	89.5 ± 11.2	89.3 ± 10.7	89.9 ± 12.2	0.959
Systolic BP, mmHg	118.7 ± 25.8	118.2 ± 27.1	119.4 ± 25.0	0.694
Diastolic BP, mmHg	86.8 ± 91.4	97.6 ± 121.7	73.2 ± 19.4	0.962
WBC, $x10^9$/L	12.3 ± 5.8	12.3 ± 6.2	12.2 ± 5.5	0.814
Hb, g/dL	11.2 ± 1.9	11.5 ± 1.9	10.8 ± 2.0	0.237
Platelet, $x10^9$/L	241.1 ± 93.9	252.2 ± 86.2	227.2 ± 103.9	0.626
CRP, mg/dL	16.9 ± 11.9	16.1 ± 12.3	18.0 ± 11.8	0.604
Procalcitonin, mg/dL	5.8 ± 12.9	4.9 ± 11.9	6.8 ± 14.4	0.249
HbA1c, %	6.8 ± 1.7	5.9 ± 0.5	8.0 ± 2.0	<0.001
Fasting glucose, mg/dL	194.2 ± 85.4	194.8 ± 85.2	193.4 ± 88.4	0.987
Fasting insulin, uIU/mL	37.1 ± 52.3	39.7 ± 55.4	33.9 ± 49.7	0.178
Total cholesterol, mg/dL	116.9 ± 53.8	128.4 ± 64.6	102.5 ± 32.8	0.305
Triglyceride, mg/dL	129.8 ± 82.8	138.1 ± 100.9	119.4 ± 53.8	0.838
HDL cholesterol, mg/dL	29.1 ± 13.7	32.1 ± 15.7	25.3 ± 10.0	0.149
Creatinine, mg/dL	1.4 ± 1.2	1.1 ± 0.8	1.8 ± 1.6	0.095
CGM metrics				
Days CGM worn, days	5.5 ± 0.8	5.5 ± 0.8	5.4 ± 0.8	0.369
Time CGM is Active, %	98.5 ± 3.1	98.4 ± 2.3	98.6 ± 3.9	0.479
Average glucose, mg/dL	162.2 ± 43.2	150.2 ± 40.6	177.2 ± 42.8	0.030
GMI, %	7.3 ± 1.5	6.9 ± 1.4	7.8 ± 1.5	0.033
CV, %	28.2 ± 9.1	25.1 ± 7.3	32.0 ± 9.9	0.028
TAR, %	29.8 ± 26.5	22.5 ± 25.9	38.8 ± 25.0	0.030
TIR, %	69.2 ± 26.2	76.5 ± 25.5	60.0 ± 24.8	0.039
TBR, %	1.1 ± 2.3	1.0 ± 2.2	1.2 ± 2.5	0.814
GMI-HbA1c, %	0.4 ± 1.7	1.0 ± 1.3	-0.2 ± 2.0	0.020
Treatment				
Ventilator care, n (%)	33 (91.7)	19 (95.0)	14 (87.5)	0.574
Steroid, n (%)	27 (75.0)	14 (70.0)	13 (81.2)	0.7
Insulin, n (%)	24 (66.7)	11 (55.0)	13 (81.2)	0.192
Outcome				
ICU stay, days	10.8 ± 7.6	10.2 ± 6.5	11.6 ± 8.9	0.789
28-day mortality rate, n (%)	8 (22.2)	5 (25.0)	3 (18.8)	0.709

APACHE, Acute Physiology and Chronic Health Evaluation; ARDS, acute respiratory distress syndrome; BP, blood pressure; CGM, continuous glucose monitoring; CRP, C-reactive protein; CV, coefficient of variation; DM, diabetes mellitus; GMI, glucose management indicator; HbA1c, glycated hemoglobin; HDL, high-density lipoprotein; ICU, intensive care unit; TAR, time above range; TBR, time below range; TIR, time in range; WBC, white blood cell.

TABLE 2 | Correlation between CGM metrics and ICU stay.

	Correlation coefficients	p
Average glucose, mg/dL	0.532	<0.001
GMI, %	0.545	<0.001
CV, %	0.051	0.767
TAR, %	0.457	0.005
TIR, %	-0.435	0.008
TBR, %	-0.213	0.212
GMI-HbA1c, %	0.533	<0.001

The correlation coefficients are presented as Spearman r.

CV, coefficient of variation; DM, diabetes mellitus; GMI, glucose management indicator; HbA1c, glycated hemoglobin; TAR, time above range; TBR, time below range; TIR, time in range.

using linear regression analysis and Cox regression analysis, respectively. Age, sex, presence of DM, APACHE score, and dose of steroid administered were considered as covariates.

Before adjustments, HbA1c, average glucose level, GMI, TAR, TIR, and GMI-HbA1c were significant risk factors for ICU stay (all $p<0.05$). After adjustments for covariates, GMI-HbA1c

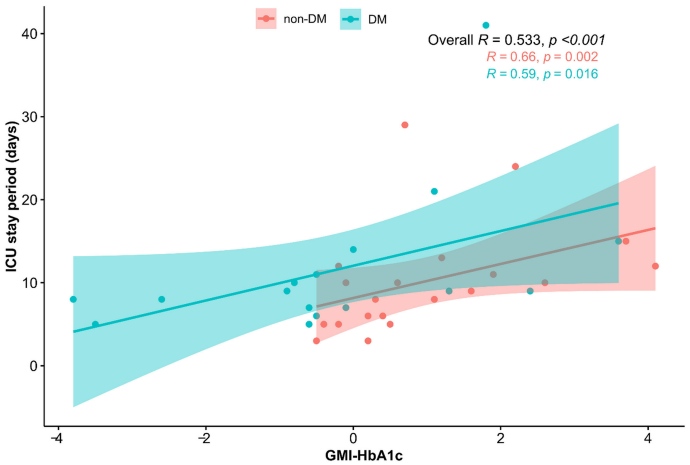

FIGURE 1 | Scatter plot of the relationship between GMI-HbA1c and ICU stay. The correlation coefficients are presented as Spearman's r.

TABLE 3 | Comparison of characteristics according to mortality within 28 days.

	Survivor (n=28)	Non-survivor (n=8)	p-value
Age, years	70.9 ± 10.1	71.2 ± 9.7	0.537
Men, n(%)	16 (57.1)	4 (50.0)	1
DM, n(%)	13 (46.4)	3 (37.5)	0.709
Diagnosis at ICU admission			
Pneumonia, n (%)	20 (71.4)	1 (12.5)	0.001
Septic shock, n (%)	7 (25.0)	1 (12.5)	
ARDS, n (%)	1 (3.6)	6 (75.0)	
Disease severity at ICU admission			
APACHE	25.2 ± 8.5	26.2 ± 8.1	0.668
HbA1c, %	7.0 ± 1.9	6.2 ± 0.5	0.236
Fasting glucose, mg/dL	183.6 ± 77.5	231.2 ± 106.2	0.339
Fasting insulin, uIU/mL	32.4 ± 42.8	53.6 ± 78.7	0.668
CGM metrics			
Average glucose, mg/dL	154.6 ± 42.7	188.8 ± 35.6	0.021
GMI, %	7.0 ± 1.5	8.2 ± 1.3	0.024
CV, %	27.6 ± 9.6	30.2 ± 7.1	0.339
TAR, %	25.5 ± 26.2	44.6 ± 22.8	0.099
TIR, %	73.2 ± 26.0	55.1 ± 22.8	0.099
TBR, %	1.3 ± 2.6	0.3 ± 0.5	0.466
GMI-HbA1c, %	0.0 ± 1.6	2.0 ± 1.3	<0.001
Treatment			
Ventilator care, n (%)	25 (89.3)	8 (100.0)	1
Steroid, n (%)	21 (75.0)	6 (75.0)	1
Steroid dose, mg/day*	25.6 ± 24.8	61.7 ± 25.8	0.007
Insulin, n (%)	17 (60.7)	7 (87.5)	0.224
Insulin dose, IU/day	50.8 ± 61.2	71.7 ± 62.2	0.383

Converted to methylprednisolone.

APACHE, Acute Physiology and Chronic Health Evaluation; ARDS, acute respiratory distress syndrome; CGM, continuous glucose monitoring; CV, coefficient of variation; DM, diabetes mellitus; GMI, glucose management indicator; HbA1c, glycated hemoglobin; HDL, high-density lipoprotein; ICU, intensive care unit; TAR, time above range; TBR, time below range; TIR, time in range.

(adjusted coefficient = 2.34; 95% CI 0.54–4.14; p=0.017) remained as an independent risk factor for ICU stay (**Table 4**).

In the aspect of 28-day mortality, before adjustments, GMI-HbA1c was an only significant risk factor (p=0.003). After adjustments for covariates, HbA1c (adjusted HR=0.13; 95% CI 0.02-0.99; p=0.049) and GMI-HbA1c (adjusted HR=2.42; 95% CI 1.01–5.76; p=0.046) were significant risk factors for 28-day mortality rate (**Table 5**).

DISCUSSION

We demonstrated that poor CGM metrics were associated with longer ICU stay and higher 28-day mortality rate. In particular, GMI-HbA1c, which indicates the acute glycemic gap (8), was associated with prolonged ICU stay and was higher in non-survivors than in survivors in both patients without DM (0.6 vs. 2.3%, p=0.025) and with DM (-0.7 vs. 1.6, p=0.008). For every 1%

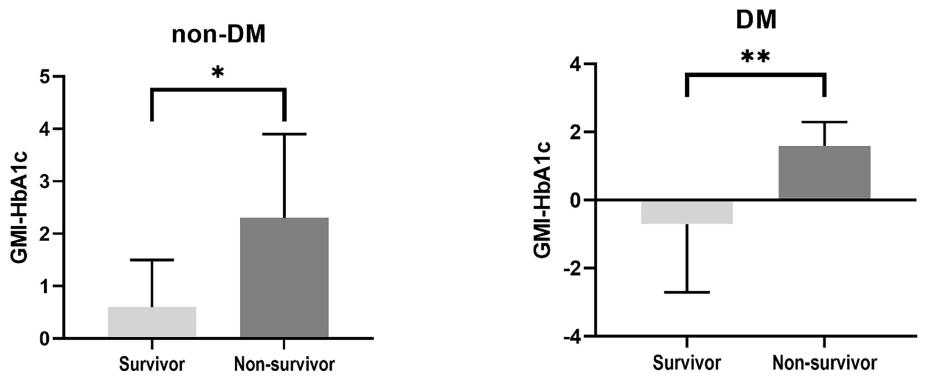

FIGURE 2 | Difference in GMI-HbA1c between survivors and non-survivors. *p < 0.05, **p < 0.01.

TABLE 4 | Effect of CGM metrics on ICU stay.

	Crude coeff. (95%CI)	CrudeP value	Adjusted coeff. (95%CI)	adjusted P value
HbA1c	0.03 (0, 0.06)	0.049	-0.79 (-2.9, 1.31)	0.466
Fasting glucose	-0.36 (-1.81, 1.09)	0.63	0.03 (-0.01, 0.07)	0.11
Average glucose	0.06 (0.01,0.12)	0.04	0.06 (-0.01, 0.13)	0.089
GMI	1.76 (0.18,3.34)	0.036	1.84 (-0.16, 3.85)	0.082
CV	0.04 (-0.24, 0.32)	0.774	-0.04 (-0.39, 0.31)	0.83
TAR	0.10 (0.01, 0.19)	0.034	0.11 (-0.01, 0.22)	0.071
TIR	-0.10 (-0.19, -0.01)	0.041	-0.1 (-0.22, 0.01)	0.086
TBR	-0.64 (-1.72, 0.44)	0.255	-0.67 (-1.87, 0.52)	0.664
GMI-HbA1c	1.68 (0.33, 3.02)	0.02	2.34 (0.54, 4.14)	0.017

Linear regression analysis was performed. In the adjusted model, age, sex, presence of DM, APACHE score, and steroid dose (mg/day) were adjusted for each metrics.
CGM, continuous glucose monitoring; CI, confidence interval; CV, coefficient of variation; DM, diabetes mellitus; GMI, glucose management indicator; HbA1c, glycated hemoglobin; TAR, time above range; TBR, time below range; TIR, time in range.

TABLE 5 | Effect of CGM metrics on 28-day mortality rate.

	Crude HR (95%CI)	CrudeP value	Adjusted HR (95%CI)	adjusted P value
HbA1c	0.65 (0.31, 1.34)	0.245	0.13 (0.02, 0.99)	0.049
Fasting glucose	1.01 (1, 1.01)	0.13	1 (0.99, 1.01)	0.922
Average glucose	1.01 (1.00,1.03)	0.052	1.01 (0.99, 1.03)	0.451
GMI	1.46 (1.00,2.15)	0.053	1.25 (0.7, 2.24)	0.453
CV	1.03 (0.96,1.10)	0.430	1.02 (0.93, 1.13)	0.656
TAR	1.02 (1.00,1.05)	0.076	1.01 (0.98, 1.05)	0.386
TIR	0.98 (0.95,1.00)	0.088	0.99 (0.95, 1.02)	0.429
TBR	0.69 (0.30,1.54)	0.363	0.67 (0.25, 1.77)	0.418
GMI-HbA1c	1.92 (1.25,2.96)	0.003	2.42 (1.01, 5.76)	0.046

A Cox regression analysis was performed. In the adjusted model, age, sex, presence of DM, APACHE score, and steroid dose (mg/day) were adjusted for each metrics.
CGM, continuous glucose monitoring; CV, coefficient of variation; DM, diabetes mellitus; GMI, glucose management indicator; Hba1c, glycated hemoglobin; HDL, high-density lipoprotein; HR, hazard ratio; TAR, time above range; TBR, time below range; TIR, time in range.

increase in GMI-HbA1c, the duration of ICU stay was prolonged by 2.3 times and the 28-day mortality rate was increased 2.4 times, irrespective of age, sex, presence of DM, APACHE score, and dose of steroid administered.

Traditional POC glucose measurements are considered to be accurate and reliable and have the advantage of providing quick results compared to central laboratory measurements (28). CGM in critically ill patients is not only as effective as POC, but also reduces hypoglycemic events (29, 30) and nursing workload, and is cost effective (31, 32). It may be argued that placing a subcutaneous CGM can be disadvantageous in some clinical scenarios that may occur in the ICU setting, such as hypoperfusion. In fact, an intravascular microdialysis CGM showed superior accuracy compared to the subcutaneous CGM in cardiac surgery (33). Recently, however, the results of subcutaneous CGM are reported to be consistent irrespective of the use of vasopressors, mechanical ventilation, high-dose glucocorticoids, renal replacement therapy, and anasarca and even after surgery (34, 35). In respect of accuracy, the mean absolute relative difference (MARD) in this study was 15.5%

(data not shown), which was higher than the recommended cut-off (9%) in general population, but consistent to the previously reported MARDs in ICU setting: 13.9% in Dexcom G6 (Dexcom, San Diego, USA) (36), 7.0% to 30.5% in FreeStyle Navigator or FreeStyle Libre (Abbott Diabetes, Alameda, USA) (37), and 14.0% to 23.7% in Guardian REAL-Time (Medtronic, Californea, USA) (37). In April 2020, the US FDA exercised enforcement discretion for the temporary use of inpatient CGM during the pandemic, and a recent report suggested an acceptable accuracy of CGM in critical care setting (36). Therefore, CGM can be an accurate, reliable, and practical method for glucose monitoring in an ICU setting (38–40).

A recent study using CGM technology concluded that 10–14 days of CGM data provide a good estimate of CGM metrics for a 3-month period (41). In this study, we only attached CGM for 5.5 ± 0.8 days, which was insufficient to determine long term glycemic control. However, we presented a new indicator, GMI-HbA1c, and its potential as a key clinical prognostic factor in acutely ill phase. Critically ill patients admitted to the medical ICU had high levels of inflammatory markers; accordingly, their blood glucose levels were also high. In addition, the use of high-dose steroid might have induced acute glycemic gap. Even after adjusting for these confounders, our results suggested that favorable outcomes can be achieved by reducing acute glycemic gap derived from GMI-HbA1c. GMI is an estimated A1c, which is calculated from a formula derived from the regression line computed from a plot of mean glucose concentration points on the x-axis and contemporaneously measured A1C values on the y-axis (8). Indeed, 22% of subjects showed discordance between GMI and HbA1c of >1% (3). Contrary to our expectations, there was no difference in HbA1c between survivors and non-survivors (7.0 ± 1.9 vs. 6.2 ± 0.5, p>0.05). Rather, the GMI-HbA1c was revealed to be a more reliable predictor for 28-day mortality. Therefore, understanding the differences between CGM-derived GMI and laboratory HbA1c may aid in safe and effective clinical management (42). GMI-HbA1c is easy to calculate, can assess acute or dramatic changes in blood glucose levels, and can be used as an index for personalized glucose management (8). Stringent glucose control is required if GMI is higher than HbA1c, to minimize excessive hyperglycemia. Conversely, if GMI is lower than HbA1c, less stringent glucose control may be needed to avoid hypoglycemic events (43). One thing to note is that the GMI-HbA1c should be interpretated considering various physical and biological factors. The GMI formula was derived from a cohort of adult patients mainly affected by Type 1 diabetes (8), and the hemoglobin glycosylation and red blood cell survival alter in the critically ill phase. Therefore, further clinical studies assessing GMI-HbA1c in various patient groups might reveal the effect of acute hypo- or hyperglycemic gaps on clinical outcomes.

We demonstrated that acute hyperglycemia and larger glycemic gap reflected by CGM metrices increased ICU stay and 28-day mortality rate in patients with and without DM. Newly diagnosed hyperglycemia affects in-hospital mortality and functional outcomes, regardless of a history of DM (44). In a study of patients with DM who underwent ICU care, the glycemic gap (mean blood glucose level during the first 7 days after admission to ICU minus the HbA1c-derived average blood glucose level) was an independent risk factor for 28-day mortality rate (27). Another study of patient without DM who underwent percutaneous coronary intervention, glycemic variability, based on the MAGE, increased the risk of 3-month major adverse cardiovascular events and mortality (45). Taken all, glucose monitoring using CGM metrics, and its appropriate management are required for critically ill patients, even those without DM.

The main strength of this study is that it documents the effect of the acute glycemic gap (GMI-HbA1c) on the risk of ICU stay and 28-day mortality rate, which has been less explored. In addition, this study showed the clinical implications of CGM in non-diabetic patients in the ICU setting. Despite these strengths, this study had several limitations. First, the number of patients was relatively small, and the patients enrolled were limited to those with medical conditions (especially respiratory disease); thus, selection bias may exist. Second, the recruited patients were infected, and hypoglycemic events did not occur; the TBR of all patients was approximately 1%. Third, since GMI is meant to represent the recent 10-14 days average glucose levels, it is required for the acquisition of CGM data for at least 10 days. However, we wanted to employ early phase 'GMI' within the first 3-days following admission to provide additional information for acutely ill patients - even if this did not mean the 'average glucose' indicator for a couple of weeks, as it intends to be used. Previous studies also consistently demonstrated the usefulness of the first 3- 5 days CGMS metrics in acute-ill patients (13, 29, 31). Further large and prospective studies using CGMS are warranted whether tight glycemic control is beneficial or not, or novel metrics for predicting mortality in medical or surgical ICU settings.

In conclusion, the acute glycemic gap (GMI-HbA1c) increased the risk of ICU stay and 28-day mortality rate irrespective of the presence of DM. CGM of critically ill patients in ICU settings is useful, and CGM metrics need to be studied in more detail.

DATA AVAILABILITY STATEMENT

The raw data supporting the conclusions of this article will be made available by the authors, without undue reservation.

AUTHOR CONTRIBUTIONS

JSM conceived the idea. SMC, EYC, and JSM designed the study. EYH, IRP, and YYL collected the data. EYH and SMC analyzed and interpreted the data and drafted the manuscript. JSM critically revised the manuscript. All authors gave final

approval and agreed to be accountable for all aspects of the work, ensuring integrity and accuracy.

FUNDING

This study was supported by a research grant funded by the Korean Diabetes Association (2019F-5 to SMC) and by a National Research Foundation of Korea grant funded by the Korean government (grant no. NRF-2019M3E5D1A02068242 to JSM).

ACKNOWLEDGMENTS

The authors thank Nr. Su Ji Hong for contributing to this study.

SUPPLEMENTARY MATERIAL

The Supplementary Material for this article can be found online at: https://www.frontiersin.org/articles/10.3389/fendo.2022.869451/full#supplementary-material

REFERENCES

1. Gunst J, De Bruyn A, Van den Berghe G. Glucose Control in the ICU. *Curr Opin Anaesthesiol* (2019) 32(2):156–62. doi: 10.1097/ACO.0000000000000706
2. Chang MC, Hwang JM, Jeon JH, Kwak SG, Park D, Moon JS. Fasting Plasma Glucose Level Independently Predicts the Mortality of Patients With Coronavirus Disease 2019 Infection: A Multicenter, Retrospective Cohort Study. *Endocrinol Metab (Seoul)* (2020) 35(3):595–601. doi: 10.3803/EnM.2020.719
3. Perlman JE, Gooley TA, McNulty B, Meyers J, Hirsch IB. HbA1c and Glucose Management Indicator Discordance: A Real-World Analysis. *Diabetes Technol Ther* (2021) 23(4):253–8. doi: 10.1089/dia.2020.0501
4. Service FJ, Molnar GD, Rosevear JW, Ackerman E, Gatewood LC, Taylor WF. Mean Amplitude of Glycemic Excursions, a Measure of Diabetic Instability. *Diabetes* (1970) 19(9):644–55. doi: 10.2337/diab.19.9.644
5. McDonnell CM, Donath SM, Vidmar SI, Werther GA, Cameron FJ. A Novel Approach to Continuous Glucose Analysis Utilizing Glycemic Variation. *Diabetes Technol Ther* (2005) 7(2):253–63. doi: 10.1089/dia.2005.7.253
6. Wójcicki JM. Mathematical Descriptions of the Glucose Control in Diabetes Therapy. Analysis of the Schlichtkrull "M"-Value. *Horm Metab Res* (1995) 27 (1):1–5. doi: 10.1055/s-2007-979895
7. Sunghwan Suh JHK. Glucose Variability. *J Korean Diabetes* (2014) 15(4):6. doi: 10.4093/jkd.2014.15.4.196
8. Bergenstal RM, Beck RW, Close KL, Grunberger G, Sacks DB, Kowalski A, et al. Glucose Management Indicator (GMI): A New Term for Estimating A1C From Continuous Glucose Monitoring. *Diabetes Care* (2018) 41 (11):2275–80. doi: 10.2337/dc18-1581
9. Moon SJ, Jung I, Park CY. Current Advances of Artificial Pancreas Systems: A Comprehensive Review of the Clinical Evidence. *Diabetes Metab J* (2021) 45 (6):813–39. doi: 10.4093/dmj.2021.0177
10. Cappon G, Vettoretti M, Sparacino G, Facchinetti A. Continuous Glucose Monitoring Sensors for Diabetes Management: A Review of Technologies and Applications. *Diabetes Metab J* (2019) 43(4):383–97. doi: 10.4093/dmj.2019.0121
11. Hur KY, Moon MK, Park JS, Kim SK, Lee SH, Yun JS, et al. 2021 Clinical Practice Guidelines for Diabetes Mellitus of the Korean Diabetes Association. *Diabetes Metab J* (2021) 45(4):461–81. doi: 10.4093/dmj.2021.0156
12. Li L, Sun J, Ruan L, Song Q. Time-Series Analysis of Continuous Glucose Monitoring Data to Predict Treatment Efficacy in Patients With T2DM. *J Clin Endocrinol Metab* (2021) 106(8):2187–97. doi: 10.1210/clinem/dgab356
13. Rodríguez-Quintanilla KA, Lavalle-González FJ, Mancillas-Adame LG, Zapata-Garrido AJ, Villarreal-Pérez JZ, Tamez-Pérez HE. Continuous Glucose Monitoring in Acute Coronary Syndrome. *Arch Cardiol Mex* (2013) 83(4):237–43. doi: 10.1016/j.acmx.2013.08.001
14. Goldberg PA, Siegel MD, Russell RR, Sherwin RS, Halickman JI, Cooper DA, et al. Experience With the Continuous Glucose Monitoring System in a Medical Intensive Care Unit. *Diabetes Technol Ther* (2004) 6(3):339–47. doi: 10.1089/152091504774198034
15. Perez-Guzman MC, Shang T, Zhang JY, Jornsay D, Klonoff DC. Continuous Glucose Monitoring in the Hospital. *Endocrinol Metab (Seoul)* (2021) 36 (2):240–55. doi: 10.3803/EnM.2021.201
16. Schuster KM, Barre K, Inzucchi SE, Udelsman R, Davis KA. Continuous Glucose Monitoring in the Surgical Intensive Care Unit: Concordance With Capillary Glucose. *J Trauma Acute Care Surg* (2014) 76(3):798–803. doi: 10.1097/TA.0000000000000127
17. Ballesteros D, Martínez Ó, Blancas Gómez-Casero R, Martín Parra C, López Matamala B, Estébanez B, et al. Continuous Tissue Glucose Monitoring Correlates With Measurement of Intermittent Capillary Glucose in Patients With Distributive Shock. *Med Intensiva* (2015) 39(7):405–11. doi: 10.1016/j.medin.2014.09.004
18. Chung SM, Lee YY, Ha E, Yoon JS, Won KC, Lee HW, et al. The Risk of Diabetes on Clinical Outcomes in Patients With Coronavirus Disease 2019: A Retrospective Cohort Study. *Diabetes Metab J* (2020) 44(3):405–13. doi: 10.4093/dmj.2020.0105
19. US Food & Drug Administration (2020). *Using Home Use Blood Glucose Meters in Hospitals During the COVID-19 Pandemic*. Available at: https://www.fda.gov/medical-devices/coronavirus-covid-19-and-medical-devices/using-home-use-blood-glucose-meters-hospitals-during-covid-19-pandemic
20. Yoo JH, Kim JH. Time in Range From Continuous Glucose Monitoring: A Novel Metric for Glycemic Control. *Diabetes Metab J* (2020) 44(6):828–39. doi: 10.4093/dmj.2020.0257
21. Knaus WA, Draper EA, Wagner DP, Zimmerman JE. APACHE II: A Severity of Disease Classification System. *Crit Care Med* (1985) 13(10):818–29. doi: 10.1097/00003246-198510000-00009
22. Force ADT, Ranieri VM, Rubenfeld GD, Thompson BT, Ferguson ND, Caldwell E, et al. Acute Respiratory Distress Syndrome: The Berlin Definition. *JAMA* (2012) 307(23):2526–33. doi: 10.1001/jama.2012.5669
23. Singer M, Deutschman CS, Seymour CW, Shankar-Hari M, Annane D, Bauer M, et al. The Third International Consensus Definitions for Sepsis and Septic Shock (Sepsis-3). *JAMA* (2016) 315(8):801–10. doi: 10.1001/jama.2016.0287
24. Kim MK, Ko SH, Kim BY, Kang ES, Noh J, Kim SK, et al. 2019 Clinical Practice Guidelines for Type 2 Diabetes Mellitus in Korea. *Diabetes Metab J* (2019) 43(4):398–406. doi: 10.4093/dmj.2019.0137
25. Shetty S, Inzucchi SE, Goldberg PA, Cooper D, Siegel MD, Honiden S. Adapting to the New Consensus Guidelines for Managing Hyperglycemia During Critical Illness: The Updated Yale Insulin Infusion Protocol. *Endocr Pract* (2012) 18(3):363–70. doi: 10.4158/EP11260.OR
26. Battelino T, Danne T, Bergenstal RM, Amiel SA, Beck R, Biester T, et al. Clinical Targets for Continuous Glucose Monitoring Data Interpretation: Recommendations From the International Consensus on Time in Range. *Diabetes Care* (2019) 42(8):1593–603. doi: 10.2337/dci19-0028
27. Lou R, Jiang L, Zhu B. Effect of Glycemic Gap Upon Mortality in Critically Ill Patients With Diabetes. *J Diabetes Investig* (2021) 12(12):2212–20. doi: 10.1111/jdi.13606
28. Rice MJ, Smith JL, Coursin DB. Glucose Measurement in the ICU: Regulatory Intersects Reality. *Crit Care Med* (2017) 45(4):741–3. doi: 10.1097/CCM.0000000000002274
29. Holzinger U, Warszawska J, Kitzberger R, Wewalka M, Miehsler W, Herkner H, et al. Real-Time Continuous Glucose Monitoring in Critically Ill Patients: A Prospective Randomized Trial. *Diabetes Care* (2010) 33(3):467–72. doi: 10.2337/dc09-1352
30. Galindo RJ, Migdal AL, Davis GM, Urrutia MA, Albury B, Zambrano C, et al. Comparison of the FreeStyle Libre Pro Flash Continuous Glucose Monitoring (CGM) System and Point-of-Care Capillary Glucose Testing in Hospitalized Patients With Type 2 Diabetes Treated With Basal-Bolus Insulin Regimen. *Diabetes Care* (2020) 43(11):2730–5. doi: 10.2337/dc19-2073
31. Boom DT, Sechterberger MK, Rijkenberg S, Kreder S, Bosman RJ, Wester JP, et al. Insulin Treatment Guided by Subcutaneous Continuous Glucose Monitoring Compared to Frequent Point-of-Care Measurement in Critically

Ill Patients: A Randomized Controlled Trial. *Crit Care* (2014) 18(4):453. doi: 10.1186/s13054-014-0453-9
32. Chow KW, Kelly DJ, Rieff MC, Skala PA, Kravets I, Charitou MM, et al. Outcomes and Healthcare Provider Perceptions of Real-Time Continuous Glucose Monitoring (rtCGM) in Patients With Diabetes and COVID-19 Admitted to the ICU. *J Diabetes Sci Technol* (2021) 15(3):607–14. doi: 10.1177/1932296820985263
33. Schierenbeck F, Franco-Cereceda A, Liska J. Accuracy of 2 Different Continuous Glucose Monitoring Systems in Patients Undergoing Cardiac Surgery. *J Diabetes Sci Technol* (2017) 11(1):108–16. doi: 10.1177/1932296816651632
34. Agarwal S, Mathew J, Davis GM, Shephardson A, Levine A, Louard R, et al. Continuous Glucose Monitoring in the Intensive Care Unit During the COVID-19 Pandemic. *Diabetes Care* (2021) 44(3):847–9. doi: 10.2337/dc20-2219
35. Perez-Guzman MC, Duggan E, Gibanica S, Cardona S, Corujo-Rodriguez A, Faloye A, et al. Continuous Glucose Monitoring in the Operating Room and Cardiac Intensive Care Unit. *Diabetes Care* (2021) 44(3):e50–e2. doi: 10.2337/dc20-2386
36. Longo RR, Elias H, Khan M, Seley JJ. Use and Accuracy of Inpatient CGM During the COVID-19 Pandemic: An Observational Study of General Medicine and ICU Patients. *J Diabetes Sci Technol* (2021), 19322968211008446. doi: 10.1177/19322968211008446
37. Van Steen SC, Rijkenberg S, Limpens J, Van der Voort PH, Hermanides J, DeVries JH. The Clinical Benefits and Accuracy of Continuous Glucose Monitoring Systems in Critically Ill Patients-A Systematic Scoping Review. *Sensors (Basel)* (2017) 17(1):146. doi: 10.3390/s17010146
38. Rijkenberg S, Van Steen SC, DeVries JH, Van der Voort PHJ. Accuracy and Reliability of a Subcutaneous Continuous Glucose Monitoring Device in Critically Ill Patients. *J Clin Monit Comput* (2018) 32(5):953–64. doi: 10.1007/s10877-017-0086-z
39. Van Hooijdonk RT, Leopold JH, Winters T, Binnekade JM, Juffermans NP, Horn J, et al. Point Accuracy and Reliability of an Interstitial Continuous Glucose-Monitoring Device in Critically Ill Patients: A Prospective Study. *Crit Care* (2015) 19:34. doi: 10.1186/s13054-015-0757-4
40. Wollersheim T, Engelhardt LJ, Pachulla J, Moergeli R, Koch S, Spies C, et al. Accuracy, Reliability, Feasibility and Nurse Acceptance of a Subcutaneous Continuous Glucose Management System in Critically Ill Patients: A Prospective Clinical Trial. *Ann Intensive Care* (2016) 6(1):70. doi: 10.1186/s13613-016-0167-z
41. Riddlesworth TD, Beck RW, Gal RL, Connor CG, Bergenstal RM, Lee S, et al. Optimal Sampling Duration for Continuous Glucose Monitoring to Determine Long-Term Glycemic Control. *Diabetes Technol Ther* (2018) 20 (4):314–6. doi: 10.1089/dia.2017.0455
42. Danne T, Nimri R, Battelino T, Bergenstal RM, Close KL, DeVries JH, et al. International Consensus on Use of Continuous Glucose Monitoring. *Diabetes Care* (2017) 40(12):1631–40. doi: 10.2337/dc17-1600
43. Chehregosha H, Khamseh ME, Malek M, Hosseinpanah F, Ismail-Beigi F. A View Beyond HbA1c: Role of Continuous Glucose Monitoring. *Diabetes Ther* (2019) 10(3):853–63. doi: 10.1007/s13300-019-0619-1
44. Umpierrez GE, Isaacs SD, Bazargan N, You X, Thaler LM, Kitabchi AE. Hyperglycemia: An Independent Marker of in-Hospital Mortality in Patients With Undiagnosed Diabetes. *J Clin Endocrinol Metab* (2002) 87(3):978–82. doi: 10.1210/jcem.87.3.8341
45. Mi SH, Su G, Yang HX, Zhou Y, Tian L, Zhang T, et al. Comparison of in-Hospital Glycemic Variability and Admission Blood Glucose in Predicting Short-Term Outcomes in Non-Diabetes Patients With ST Elevation Myocardial Infarction Underwent Percutaneous Coronary Intervention. *Diabetol Metab Syndr* (2017) 9:20. doi: 10.1186/s13098-017-0217-1

Conflict of Interest: The authors declare that the research was conducted in the absence of any commercial or financial relationships that could be construed as a potential conflict of interest.

Publisher's Note: All claims expressed in this article are solely those of the authors and do not necessarily represent those of their affiliated organizations, or those of the publisher, the editors and the reviewers. Any product that may be evaluated in this article, or claim that may be made by its manufacturer, is not guaranteed or endorsed by the publisher.

frontiers | Frontiers in Endocrinology

ORIGINAL RESEARCH
published: 02 June 2022
doi: 10.3389/fendo.2022.871965

1-h Glucose During Oral Glucose Tolerance Test Predicts Hyperglycemia Relapse-Free Survival in Obese Black Patients With Hyperglycemic Crises

*Ram Jagannathan[1], Darko Stefanovski[2], Dawn D. Smiley[3], Omolade Oladejo[3], Lucia F. Cotten[3], Guillermo Umpierrez[3] and Priyathama Vellanki[3]**

[1] Division of Hospital Medicine, Emory University School of Medicine, Atlanta GA, United States, [2] Department of Biostatistics, University of Pennsylvania School of Veterinary Medicine, Kennett Square, PA, United States, [3] Division of Endocrinology, Metabolism and Lipids, Emory University School of Medicine, Atlanta, GA, United States

OPEN ACCESS

Edited by:
Joon Ha,
Howard University, United States

Reviewed by:
Jan Brož,
Charles University, Czechia
Micaela Morettini,
Marche Polytechnic University, Italy

***Correspondence:**
Priyathama Vellanki
pvellan@emory.edu

Specialty section:
This article was submitted to Clinical Diabetes, a section of the journal Frontiers in Endocrinology

Received: 08 February 2022
Accepted: 04 April 2022
Published: 02 June 2022

Citation:
Jagannathan R, Stefanovski D, Smiley DD, Oladejo O, Cotten LF, Umpierrez G and Vellanki P (2022) 1-h Glucose During Oral Glucose Tolerance Test Predicts Hyperglycemia Relapse-Free Survival in Obese Black Patients With Hyperglycemic Crises. Front. Endocrinol. 13:871965. doi: 10.3389/fendo.2022.871965

Objective: Approximately 50% of obese Black patients with unprovoked diabetic ketoacidosis (DKA) or severe hyperglycemia (SH) at new-onset diabetes achieve near-normoglycemia remission with intensive insulin treatment. Despite the initial near-normoglycemia remission, most DKA/SH individuals develop hyperglycemia relapse after insulin discontinuation. Traditional biomarkers such as normal glucose tolerance at the time of remission were not predictive of hyperglycemia relapse. We tested whether 1-h plasma glucose (1-h PG) at remission predicts hyperglycemia relapse in Black patients with DKA/SH.

Methods: Secondary analysis was performed of two prospective randomized controlled trials in 73 patients with DKA/SH at the safety net hospital with a median follow-up of 408 days. Patients with DKA/SH underwent a 5-point, 2-h 75-g oral glucose tolerance test after hyperglycemia remission. Hyperglycemia relapse is defined by fasting blood glucose (FBG) > 130 mg/dl, random blood glucose (BG) >180 mg/dl, or HbA1c > 7%.

Results: During the median 408 (interquartile range: 110–602) days of follow-up, hyperglycemia relapse occurred in 28 (38.4%) participants. One-hour PG value ≥199 mg/dl discriminates hyperglycemia relapse (sensitivity: 64%; specificity: 71%). Elevated levels of 1-h PG (≥199 mg/dl) were independently associated with hyperglycemia relapse (adjusted hazard ratio: 2.40 [95% CI: 1.04, 5.56]). In a multivariable model with FBG, adding 1-h PG level enhanced the prediction of hyperglycemia relapse, with significant improvements in C-index (Δ: +0.05; p = 0.04), net reclassification improvement (NRI: 48.7%; p = 0.04), and integrated discrimination improvement (IDI: 7.8%; p = 0.02) as compared with the addition of 2-h PG (NRI: 20.2%; p = 0.42; IDI: 1.32%; p = 0.41) or HbA1c (NRI: 35.2%; p = 0.143; IDI: 5.8%; p = 0.04).

Conclusion: One-hour PG at the time of remission is a better predictor of hyperglycemia relapse than traditional glycemic markers among obese Black patients presenting with

DKA/SH. Testing 1-h PG at insulin discontinuation identifies individuals at high risk of developing hyperglycemia relapse.

Keywords: diabetic ketoacidosis, 1-h and 2-h glucose values, stress hyperglycemia, oral glucose tolerance, net reclassification improvement, ROC (receiver operating characteristic curve)

INTRODUCTION

Approximately 50% of obese Black patients with new-onset, unprovoked diabetic ketoacidosis (DKA) or severe hyperglycemia (SH) achieve near-normoglycemia remission (defined as fasting blood glucose [FBG] <130 mg/dl, random blood glucose (BG) <180 mg/dl, and HbA1c < 7% while off insulin for at least 1 week) with aggressive insulin treatment (1). These patients exhibit clinical, metabolic, genetic, and autoimmune features consistent with type 2 diabetes. Although exact pathophysiologic mechanisms are unknown, near-normoglycemia remission is achieved in this patient population due to improved pancreatic beta (β)-cell function and insulin sensitivity (2–4). Glycemic control after near-normoglycemia remission is variable. Over the long-term, most patients experience pancreatic β-cell function failure resulting in the need for antidiabetic medications (4–6), while less than 10% of patients are able to maintain remission without medication over ~8 years (3). Despite the initiation of antidiabetic medications, 73% experience hyperglycemia relapse, and even DKA (4). Therefore, predictors of glycemic failure at the time of near-normoglycemia remission are needed to see which patients should have more aggressive treatment. We and others have shown that glycemic control consistent with glucose levels at near-normoglycemia remission can be maintained with monotherapy up to a median of 480 days (2, 6).

At near-normoglycemia remission, the clinical presentation and oral glucose tolerance test (OGTT) are heterogeneous, with 12%–17% having normal glucose tolerance (3, 7). However, normal glucose tolerance did not predict time in glycemic control (3, 7). Accumulating longitudinal evidence from epidemiological studies shows that a 1-h plasma glucose load (1-h PG) level >155 mg/dl during OGTT is a better predictor of type 2 diabetes and cardiovascular disease mortality than fasting glucose 2-h PG load or HbA1c (8–10). In addition, an elevated 1-h PG level is associated with decreased insulin secretion and sensitivity (11), impaired hepatic enzymes (12), and increased accentuation of reactive oxygen species generation (13, 14). However, the association of 1-h PG with hyperglycemia relapse in patients with DKA and SH at new-onset diabetes was never studied. In this study, we evaluated the association of the 1-h PG with the incident hyperglycemia relapse in obese Black patients presenting DKA and SH at new-onset diabetes over a mean follow-up period of 3 years. We also evaluated whether adding 1-h PG significantly improves the prediction of hyperglycemia relapse compared to glucose levels at other time points during the OGTT and HbA1c levels at the time of insulin discontinuation.

MATERIALS AND METHODS

Participants

This study combined participants from two randomized controlled studies (NCT01099618 and NCT00426413) conducted between 2007 and 2014. The study design inclusion/exclusion criteria are detailed elsewhere (6, 7). Briefly, for both studies, participants with no prior history of diabetes presenting with DKA as defined by the American Diabetes Association (ADA) and SH (blood glucose >400 mg/dl without ketoacidosis) have consented during hospital admission. All subjects had glutamic decarboxylase-65 antibody measured to exclude autoimmune diabetes.

Study Protocol

The Institutional Review Board at Emory University approved the combined analysis for both studies. After acute resolution of DKA or SH, all participants were treated intensively with subcutaneous insulin to a target fasting and pre-meal BG between 70 and 130 mg/dl (3.9–7.2 mmol/L). Insulin was titrated to achieve near-normoglycemia remission defined as FBG < 130 mg/dl (7.2 mmol/L) and random BG <180 mg/dl (10 mmol/L) and HbA1c < 7% (53 mmol/L) while off insulin therapy for at least 1 week. All participants then received a 75-g 120-min OGTT. After the OGTT, in one study (NCT01099618), participants were randomized into three groups: sitagliptin 100 mg daily (n = 16), metformin 1,000 mg daily (n = 17), or placebo (n = 15) (6). In the second study (NCT00426413), participants were randomized into two groups, pioglitazone 30 mg daily (n = 22) or placebo (n = 22), and followed up till hyperglycemia relapse (defined as FBG > 130 mg/dl (7.2 mmol/L), random BG >180 mg/dl (10 mmol/L) for a period of two consecutive days, or HbA1c ≥ 7% (53 mmol/L)). All participants were followed up until hyperglycemia relapsed or till the end of the study duration (~3 years) (2, 7).

Study Measurements

Patient demographics and clinical characteristics were obtained from the electronic medical record and medical history during study visits. OGTTs were performed after at least an 8-h overnight fast. After fasting insulin and glucose levels were measured, 75 g of anhydrous glucose was ingested within 1 min. Glucose and insulin levels were then measured at 15, 30, 60, 90, and 120 min. Analyses of post-load glucose levels were focused on measurements at 1 h.

Outcomes and Calculations

Hyperglycemia relapse was defined as FBG > 130 mg/dl, random BG >180 mg/dl on at least 2 consecutive days, or HbA1c > 7%.

Glucose and insulin levels were used to calculate insulin sensitivity and secretion. Insulin sensitivity (Si) was calculated using oral minimal model analysis (6). Insulin secretion was calculated as the incremental area under the curve (AUCi) from insulin levels during the OGTT (6). The disposition index was calculated as the product of Si and AUCi.

Statistical Analysis

Baseline characteristics of participants were expressed as means with SD or medians with interquartile ranges (IQRs) for continuous variables and numbers (proportions) with percentages for categorical variables. Since previous studies did not find a significant difference in insulin secretion and sensitivity after insulin discontinuation (6, 7), the data for this study were combined. Because this *post-hoc* analysis's primary objective was to assess the predictive power of 1-h PG on incident hyperglycemia relapse, both control (placebo) and intervention groups (metformin, sitagliptin, or pioglitazone) were examined as a single cohort. For the time-to-event analysis, the follow-up length was calculated as the time from near-normoglycemia remission to the date of the first occurrence of hyperglycemia relapse or the last follow-up with the last censoring date of February 2014. To evaluate the optimal threshold of 1-h PG levels to predict hyperglycemia relapse, the 1-h PG levels were identified for the maximum of Youden's Index, a summary statistic of the receiver operating characteristic (ROC) curve defined as (sensitivity + specificity − 1) (15). To minimize overfitting and to quantify optimism, specificity and sensitivity of the thresholds given were computed with 1,000 stratified bootstrap replicates with a 95% CI. The cutoff value of 1-h PG was appraised according to the least distance from the upper-left corner of the ROC curve. The Kaplan–Meier curves were generated to estimate the cumulative incidence of hyperglycemia relapse by the identified 1-h PG categories at the time of insulin discontinuation; a log-rank test was computed to compare survival distributions. For each subject, Cox proportional hazards models were used to estimate hazard ratios (HRs) and corresponding 95% CIs for incident hyperglycemia relapse associated with the baseline levels of 1-h PG levels. Proportionality hazard assumption in Cox models for all predictors and covariates in a fully adjusted multivariable model was assessed using the Schoenfeld residuals regressed against follow-up time; no violation of proportionality was observed. The biologically relevant or statistically significant variables in univariate analysis for the multivariable-adjusted models were chosen.

The incremental benefit of 1-h PG, 2-h PG, or HbA1c above and beyond the traditional risk factors (age, sex, body mass index (BMI), treatment allocation, and FBG) for predicting the risk of hyperglycemia relapse in patients with DKA/SH were assessed using a model fit, calibration, discrimination, and reclassification. Model fit was determined using the deviance analysis, with lower deviance, which means better model fit. Model calibration was determined using the Hosmer–Lemeshow goodness-of-fit test, with larger p-values (>0.05) indicating good agreement between observed and predicted outcomes. The AUC of the ROC was used to compute model discrimination. Improvement in AUC after adding the 1-h PG, 2-h PG, or HbA1c was estimated using the method of DeLong et al. (16, 17) Finally, continuous/category-free net reclassification improvement (NRI > 0) and absolute integrated discrimination improvement (IDI) was assessed to ascertain the enhanced predictability of glucose biomarkers on the hyperglycemia relapse outcomes (18).

A two-sided p-value of less than 0.05 was considered significant. Statistical analyses were performed using the survminer (version 0.4.7) (19), survival (version 3.2-3) (20), optimal cut points, PredictABEL (version 0.1), and tableone (version 0.10.0) packages in R (version 3.3.1).

RESULTS

Cohort Description

Seventy-three participants with DKA (n = 40) and SH (n = 33) with near-normoglycemia remission who had OGTTs performed after insulin discontinuation were included in the analysis. The mean age was 46.9 ± 10.3 years, 26 (35.6%) were women, and the mean BMI was 36.1 ± 9.5 kg/m^2. Based on the fasting and 2-h PG levels, 9 (12.1%) had normal glucose tolerance, 34 (45.9%) had prediabetes, and 30 (41.2%) had diabetes as defined by the ADA guidelines (21).

Association of 1-h Plasma Glucose Levels With Incident Hyperglycemic Relapse

During the median 408 (IQR: 110–602) days of follow-up, hyperglycemia relapse occurred in 28 (38.4%) participants. The cumulative incidence of hyperglycemia relapse was lower in those who received oral antidiabetic agents [pioglitazone, metformin, or sitagliptin; 14 (28.0%)] than in controls [placebo; n = 14 (60.9%)]. There was no significant difference in age, BMI, and the proportion of smokers and family history of diabetes between those who did and did not have hyperglycemia relapse. Participants who progressed to hyperglycemia relapse outcome had higher baseline values of FBG and 15-min, 1-h, and 2-h PG. In the crude model, the unadjusted HR per 1 SD change in plasma 1-h PG was 1.88 [95% CI: 1.25, 2.82] (**Table 1**) for hyperglycemia relapse. In the fully adjusted model including age, sex, randomization group (placebo vs. treated), BMI, and baseline diagnosis (DKA vs. SH), the independent association between 1-h PG and incident hyperglycemia relapse remained significant [adjusted HR (aHR): 1.98 (95% CI: 1.27, 3.09)].

1-h Plasma Glucose Optimal Cut Point to Predict Hyperglycemia Relapse

Based on Youden's analysis, a 1-h PG cutoff of 11.0 mmol/L (199 mg/dl) was found to differentiate the individuals with/without the development of hyperglycemia relapse. The sensitivity and specificity of the optimal cutoff value [11.0 mmol/L (199 mg/dl)] were 64% and 71%, respectively. Then, we dichotomize the 1-h PG values and estimated the association of 1-h PG categories [1-h PG_{High} ≥11.0 mmol/L [≥199 mg/dl); 1-h PG_{Normal} <11.0 mmol/L (<199 mg/dl)] on the risk of developing hyperglycemia

TABLE 1 | Hazard ratio for 1-h PG levels and hyperglycemia relapse.

Model	1-h PG as a continuous variable (per SD change)	1-h PG (≥199 vs. <199 mg/dl)
1	1.88 [1.25, 2.82]	2.50 [1.15, 5.43]
2	1.97 [1.27, 3.05]	2.43 [1.05, 5.62]
3	2.02 [1.29, 3.15]	2.42 [1.04, 5.61]
4	1.98 [1.27, 3.09]	2.40 [1.04, 5.56]

Data are expressed as hazard ratio (HR) (95% CI). The given HR is for 1 SD change in 1-h PG or 1-h PG categories (≥199 vs. <199 mg/dl) and continuous covariates in multivariable Cox regression analysis. Model 1, crude model; model 2, adjusted for age, sex, and intervention group; model 3, further adjusted for BMI; and model 4, further adjusted for baseline diagnosis (severe hyperglycemia vs. diabetic ketoacidosis).
PG, plasma glucose; BMI, body mass index.

relapse (**Table 1**). The aHR shows a 2.5-fold incidence of hyperglycemia relapse with a 1-h PG_{High} compared to 1-h PG_{Normal}. Characteristics of participants according to the 1-h PG cut point are shown in **Table 2**. Participants who were in the 1-h PG_{High} category were significantly older and had higher FBG and 15-min, 30-min, and 2-h PG levels. Furthermore, the levels of Si were 76.8% (1.42 vs. 0.33), and DI was 70.0% (0.63 vs. 0.19) lower in individuals with 1-h PG_{High} than in those with 1-h PG_{Normal}. We did not observe any significant differences in other variables between the 1-h PG_{High} and 1-h PG_{Normal} groups.

Hazard Risk

The Kaplan–Meier plot shows the unadjusted hyperglycemia relapse-free survival stratified based on 1-h PG levels (**Figure 1**). Individuals with 1-h PG_{Normal} (<199 mg/dl) had ~3 months of delayed median time to onset of hyperglycemia relapse than those with 1-h PG_{High} (≥199 mg/dl; log-rank test p = 0.02). Congruent with the above, both crude [HR: 2.50 (95% CI: 1.15,5.43)] and aHRs for the development of hyperglycemia relapse were significantly greater in the 1-h PG_{High} group [aHR: 2.40 (95% CI: 1.04, 5.56)] versus the 1-h PG_{Normal} (<199 mg/dl) group.

Discriminative Ability

The results of five multivariate prognostic models [traditional (model 1) and traditional+1-h PG (model 2), traditional+2-h PG (model 3), traditional+HbA1c (model 4), and traditional+1-h PG+2-h PG (model 5)] are shown in **Table 3**. The addition of the 1-h PG to the traditional model containing age, sex, BMI, gender, treatment group, baseline diagnosis, and FBG improved model fit (Δ deviance: −5.60, p = 0.018), calibration (Hosmer–Lemeshow test, p > 0.05; **Supplementary Figure 1**), discrimination (AUC increase from 0.84 to 0.89, ΔC: +0.05; p = 0.039; **Table 3**), and risk classification (**Supplementary Figure 2**). On the contrary, adding 2-h PG did not improve the model fit (traditional+2-h PG; Δ deviance: −1.31; p = 0.25; ΔC: +0.01). The addition of HbA1c marginally improved the model fit (traditional +HbA1c; Δ deviance: −4.17; p = 0.041; ΔC: +0.04). The addition of both 1-h and 2-h PG did not improve the predictive utility. Furthermore, 1-h PG improved risk classification when added to the traditional model [overall NRI 48.7 (1.2; 96.2); IDI 7.8 (1.4; 14.1)]. However, the addition of HbA1c did not improve the other metrics, and only marginal improvement was observed in IDI, whereas 2-h PG did not improve the discriminative ability appreciably in predicting hyperglycemia relapse in this patient population.

TABLE 2 | Baseline characteristics of the study population, stratified according to 1-h plasma glucose challenge 199 mg/dl.

	1-h plasma glucose challenge	
	Normal (<199 m/dl, 11.0 mmol/L) n = 42	High (≥199 mg/dl, 11.0 mmol/L) n = 31
Age, years	44.43 (11.44)	50.23 (7.59)
Gender, male, n (%)	25 (59.5)	22 (71.0)
BMI, kg/m^2	36.81 (10.65)	35.06 (7.62)
Family history of diabetes, n (%)	35 (83.3)	26 (83.9)
Baseline diagnosis, n (%)		
Severe hyperglycemia	22 (52.4)	18 (58.1)
Diabetic ketoacidosis	20 (47.6)	13 (41.9)
Treatment with an oral antidiabetic agent, n (%)		
No (placebo)	11 (26.2)	12 (38.7)
Yes (sitagliptin, pioglitazone, or metformin)	31 (73.8)	19 (61.3)
Glucose, mg/dl (mmol/L)		
Fasting	98 ± 15.41 (5.4 ± 0.8)	117 ± 18 (6.5 ± 1.0)
15 min	110 ± 20 (6.1 ± 1.1)	131 ± 33 (7.3 ± 1.8)
30 min	135 ± 29 (7.5 ± 1.6)	174 ± 41 (9.7 ± 2.3)
120 min	163 ± 42 (9.0 ± 2.3)	222 ± 55 (12.3 ± 3.1)
AUCi	5416.50 [2538.30, 7845.19]	4384.50 [2868.00, 6132.38]
Si	1.42 [0.56, 3.49]	0.33 [0.00, 0.84]
Di	0.63 [0.36, 1.43]	0.19 [0.00, 0.38]
Hyperglycemia relapse during follow-up, n (%)	10 (23.8)	18 (58.1)
The median time to hyperglycemia relapse, days (IQR)	427.50 [102.75, 598.75]	336.00 [116.00, 580.00]

Continuous variables are shown as mean ± SD or medians (IQR). Data for the categorical variables (gender, active smoking, family history of diabetes, and baseline diagnosis) are presented as counts and corresponding percentages.
IQR, interquartile range; BMI, body mass index; AUCi, area under the curve of insulin; Si, insulin sensitivity from the minimal model; and Di, disposition index.

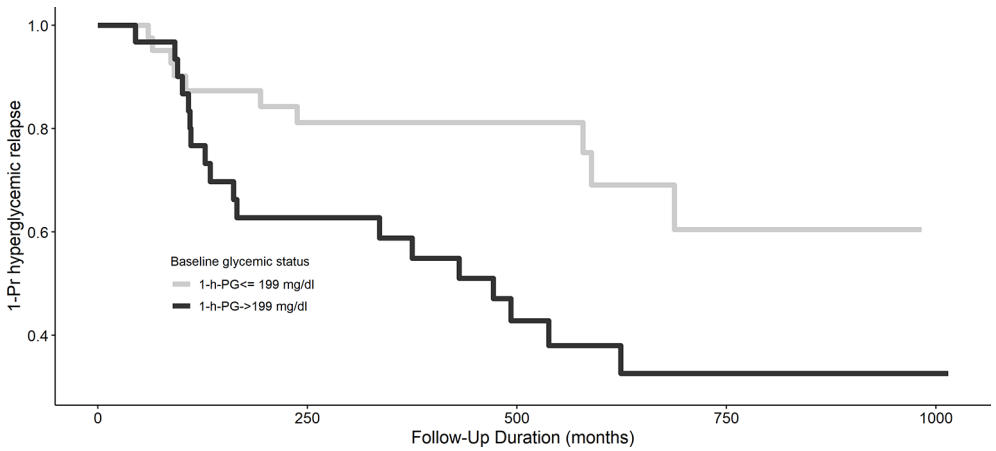

FIGURE 1 | Kaplan–Meier curve of hyperglycemia relapse based on 1-h plasma glucose challenge categories. A 1-h plasma glucose challenge level ≥199 mg/dl is associated with longer hyperglycemia relapse-free survival, p = 0.02.

DISCUSSION

This is the first study to determine the association of 1-h PG with the incidence of hyperglycemia relapse among obese Black patients presenting with DKA/SH who achieve near-normoglycemia remission. We showed that 1-PG was an independent predictor of hyperglycemia relapse in this patient population. Specifically, 1-h PG ≥199 mg/dl at the time of insulin discontinuation, even after adjustment for age, BMI, gender, presentation with DKA or SH, and HbA1c levels, was independently associated with hyperglycemia relapse. Overall, 1-h PG levels were able to predict the incidence of hyperglycemia relapse or glycemic failure better than traditionally used glucose markers such as fasting or 2-h PG levels or HbA1c.

In our analysis, 1-h PG was an independent predictor of hyperglycemia relapse even after adjusting for treatment with an oral antidiabetic agent after insulin discontinuation. Prior studies in our population of patients with DKA and SH showed that normal glucose tolerance status as defined by the ADA was not a predictor of prolonged remission (3, 7). Despite the differences in the initial presentation, the long-term clinical course between DKA and SH does not seem to differ in our previous studies (3, 6, 22). In this current study, despite adjustment for DKA and SH, a high 1-PG was predictive of hyperglycemia relapse. In our previous publication, we found that intervention with oral antidiabetic medication at the time of insulin discontinuation or near-normoglycemia remission predicted longer hyperglycemia relapse-free survival. However, this current study showed that 1-h glucose was predictive of future hyperglycemia relapse independent of having an intervention with an antidiabetic agent. Use of only fasting and 2-h glucose levels in this population may miss abnormalities detected by 1-h PG levels. Insulin secretory abnormalities are present with an abnormal 1-h PG even with normal 2-h PG levels in several different populations (23–25). A recent study showed that the rate of oral glucose absorption is one of the precipitating factors of 1-h PG excursions (26). Oral glucose absorption can be decreased by increased gastric emptying time (27), and gastric emptying time can be reduced by incretin mimetics such as glucagon-like peptide-1 receptor agonists (27, 28). While the oral glucose absorption rate has not been determined in this population, it is possible that people with the higher 1-h PG may be optimally treated with a glucagon-like peptide-1 receptor agonist (GLP-1RA).

The 1-h PG is both practical and cost-effective. The national average time for visits is 84 min (29), which lends that this testing method could potentially be implemented during a routine visit without any increase in appointment duration. As a potential

TABLE 3 | Prognostic performance of 1-h PG levels for hyperglycemia relapse.

	C index	ΔC index	Net reclassification index		Integrated discrimination improvement	
			% (95% CI)	p	% (95% CI)	p
Traditional model	0.84	–	–	–	–	–
+1-h PG	0.89	0.05	48.7 [1.2; 96.2]	0.04437	7.8[1.4; 14.1]	0.01616
+2-h PG	0.85	0.01	20.2 [–28.0; 68.7]	0.41584	1.32 [–1.8; 4.4]	0.40757
+ HbA1c	0.88	0.04	35.2 [–11.9; 82.2]	0.14311	5.8 [0.3; 11.4]	0.03992
+1-h PG and 2-h PG	0.89	0.05	39.2 [–8.8; 87.2]	0.10961	7.7 [1.3; 14.1]	0.01761

*The traditional model refers to age, sex, randomization group, BMI, and baseline diagnosis (HG vs. DKA) (model 4 in **Table 2**) + fasting plasma glucose.*
PG, plasma glucose; DKA, diabetic ketoacidosis; BMI, body mass index.

method, a 75-g glucose drink could be administered by clinic staff after patient check-in, followed by the collection of the glucose level 1 h later (30). Additionally, glucose challenge testing with 1-h PG is cost-effective compared to the 2-h OGTT as a gold standard for hyperglycemia screening (31). Since there is no standard of care for optimal follow-up and treatment in our current population after insulin discontinuation, the 1-h PG could be used to determine which patients may need more intensive follow-up and earlier addition of intensification of antidiabetic therapy.

A 1-h PG >155 mg/dl has been proposed as the cutoff associated with metabolic abnormalities in several studies. However, a majority (~70%) of the participants in our study had a 1-h PG >155 mg/dl. Therefore, we performed ROC analysis to predict which 1-h PG level predicted hyperglycemia relapse with a 64% sensitivity for BG > 199 mg/day. This glucose level is potentially too high, and 1 h PG >155 mg/dl leads to metabolic abnormalities. However, 155 mg/dl was validated in patients without diabetes, and therefore, patients with diabetes may need different targets for 1-h glucose levels. Further, our definition of near-normoglycemia remission was chosen to reflect glycemic goals for people with diabetes. The definition of near-normoglycemia remission is variable depending on the study, with some studies in patients with DKA and SH using the definition of HbA1c < 6.3% and off medications for 3 months (4, 22). It is possible that a more stringent definition of near-normoglycemia remission in our study could have resulted in more participants with a 1-h PG <155 mg/dl.

The ADA published a consensus statement in 2021 defining remission as HbA1c < 6.5% and off medications for >3 months (32). We were unable to assess remission as per the ADA definition, as this study was a *post-hoc* analysis of 2 randomized controlled studies that randomized subjects to a drug or a placebo. Therefore, we used hyperglycemia relapse-free survival in this study. However, even a more rigorous HbA1c cutoff for initial remission showed that most people had dysglycemia on OGTT based on fasting and 2-h PG levels (3, 4). Further, we found that having normal glucose tolerance during OGTT does not predict time in remission while an intervention did (7). The findings from our study highlight that traditional markers used to define remission are not sufficient to predict future hyperglycemia relapse.

In conclusion, 1-h PG of ≥199 mg/dl was independently associated with hyperglycemia relapse in obese Black patients presenting with DKA/SH at the time of diagnosis of diabetes. In clinical use, adopting a 1-h PG check within 1 to 2 weeks after insulin discontinuation may offer a more effective strategy to determine which patients need an aggressive antidiabetic treatment regimen. Future studies in this population will need to be performed where the definition of remission is more stringent and includes 1-h PG and whether treatments targeted to reduce 1-h PG levels will prevent hyperglycemia relapse.

DATA AVAILABILITY STATEMENT

After reviewing the study hypothesis and detailed statistical analysis plan, the de-identified, individual participant-level data that underlie the results will be shared based on the reasonable request. All submissions should be addressed to the senior author (priyathama.vellanki@emory.edu). The applicants will be asked to sign a data access agreement before transferring the de-identified data and requested to get an IRB waiver.

ETHICS STATEMENT

The studies involving human participants were reviewed and approved by Emory University. The patients/participants provided their written informed consent to participate in this study.

AUTHOR CONTRIBUTIONS

RJ conceived the study, performed the data analysis, wrote the first draft, and critically reviewed and edited it. DS critically reviewed the manuscript and made critical contributions to data analyses. DDS and GU collected data from the original two studies and critically reviewed and edited the manuscript. OO and LC critically reviewed and edited the manuscript. PV conceived the study, directed the data analysis, wrote the first draft, and critically reviewed and edited the manuscript. PV had access to all the data and is the guarantor of the work. All authors listed have made a substantial, direct, and intellectual contribution to the work and approved it for publication.

FUNDING

PV is funded in part by NIH/NIDDK K23 DK 11324-01A1. This study was funded by NIH K08 DK083036 to DDS. GU is partly supported by research grants from the NIH/NATS UL1 TR002378 from the Clinical and Translational Science Award program and 1P30DK111024-01 from NIH and National Center for Research Resources.

SUPPLEMENTARY MATERIAL

The Supplementary Material for this article can be found online at: https://www.frontiersin.org/articles/10.3389/fendo.2022.871965/full#supplementary-material

Supplementary Figure 1 | Predictive performance of five different models for hyperglycemia relapse. The different curves represent the different goodness of fit of the traditional model (age, sex, BMI, treatment allocation, and FBG) along with plasma glucose time at various time points of the oral glucose tolerance test, or HbA1c. The model containing 1-h PG showed increased discriminatory ability in predicting hyperglycemia relapse than the other biomarkers.

Supplementary Figure 2 | Calibration plots of the proportion of hyperglycemia relapse within each tenth (identified using deciles) of predicted risk between traditional model and the model including 1-h PG- Hosmer-Lemeshow test.

REFERENCES

1. Umpierrez GE, Smiley D, Kitabchi AE. Narrative Review: Ketosis-Prone Type 2 Diabetes Mellitus. *Ann Internal Med* (2006) 144:350–7. doi: 10.7326/0003-4819-144-5-200603070-00011
2. Umpierrez GE, Clark WS, Steen MT. Sulfonylurea Treatment Prevents Recurrence of Hyperglycemia in Obese African-American Patients With a History of Hyperglycemic Crises. *Diabetes Care* (1997) 20:479–83. doi: 10.2337/diacare.20.4.479
3. Banerji MA, Chaiken RL, Lebovitz HE. Long-Term Normoglycemic Remission in Black Newly Diagnosed NIDDM Subjects. *Diabetes* (1996) 45:337–41. doi: 10.2337/diabetes.45.3.337
4. Mauvais-Jarvis F, Sobngwi E, Porcher R, Riveline JP, Kevorkian JP, Vaisse C, et al. Ketosis-Prone Type 2 Diabetes in Patients of Sub-Saharan African Origin: Clinical Pathophysiology and Natural History of Beta-Cell Dysfunction and Insulin Resistance. *Diabetes* (2004) 53:645–53. doi: 10.2337/diabetes.53.3.645
5. Choukem SP, Sobngwi E, Fetita LS, Boudou P, De Kerviler E, Boirie Y, et al. Multitissue Insulin Resistance Despite Near-Normoglycemic Remission in Africans With Ketosis-Prone Diabetes. *Diabetes Care* (2008) 31:2332–7. doi: 10.2337/dc08-0914
6. Vellanki P, Smiley DD, Stefanovski D, Anzola I, Duan W, Hudson M, et al. Randomized Controlled Study of Metformin and Sitagliptin on Long-Term Normoglycemia Remission in African American Patients With Hyperglycemic Crises. *Diabetes Care* (2016) 39:1948–55. doi: 10.2337/dc16-0406
7. Vellanki P, Stefanovski D, Anzola II, Smiley DD, Peng L, Umpierrez GE. Long-Term Changes in Carbohydrate Tolerance, Insulin Secretion and Action in African-American Patients With Obesity and History of Hyperglycemic Crises. *BMJ Open Diabetes Res Care* (2020) 8:1–7. doi: 10.1136/bmjdrc-2019-001062
8. Bergman M, Manco M, Sesti G, Dankner R, Pareek M, Jagannathan R, et al. Petition to Replace Current OGTT Criteria for Diagnosing Prediabetes With the 1-Hour Post-Load Plasma Glucose≥ 155 Mg/Dl (8.6 Mmol/L). *Diabetes Res Clin Pract* (2018) 146:18–33. doi: 10.1016/j.diabres.2018.09.017
9. Pareek M, Bhatt DL, Nielsen ML, Jagannathan R, Eriksson K-F, Nilsson PM, et al. Enhanced Predictive Capability of a 1-Hour Oral Glucose Tolerance Test: A Prospective Population-Based Cohort Study. *Diabetes Care* (2018) 41:171–7. doi: 10.2337/dc17-1351
10. Bianchi C, Miccoli R, Trombetta M, Giorgino F, Frontoni S, Faloia E, et al. Elevated 1-Hour Postload Plasma Glucose Levels Identify Subjects With Normal Glucose Tolerance But Impaired β-Cell Function, Insulin Resistance, and Worse Cardiovascular Risk Profile: The GENFIEV Study. *J Clin Endocrinol Metab* (2013) 98:2100–5. doi: 10.1210/jc.2012-3971
11. Bergman M, Abdul-Ghani M, DeFronzo RA, Manco M, Sesti G, Fiorentino TV, et al. Review of Methods for Detecting Glycemic Disorders. *Diabetes Res Clin Pract* (2020) 165:108233. doi: 10.1016/j.diabres.2020.108233
12. Succurro E, Arturi F, Grembiale A, Iorio F, Fiorentino TV, Andreozzi F, et al. One-Hour Post-Load Plasma Glucose Levels Are Associated With Elevated Liver Enzymes. *Nutr Metab Cardiovasc Dis* (2011) 21:713–8. doi: 10.1016/j.numecd.2011.02.002
13. Maessen DE, Hanssen NM, Scheijen JL, van der Kallen CJ, van Greevenbroek MM, Stehouwer CD, et al. Post-Glucose Load Plasma α-Dicarbonyl Concentrations Are Increased in Individuals With Impaired Glucose Metabolism and Type 2 Diabetes: The CODAM Study. *Diabetes Care* (2015) 38:913–20. doi: 10.2337/dc14-2605
14. Mah E, Noh SK, Ballard KD, Matos ME, Volek JS, Bruno RS. Postprandial Hyperglycemia Impairs Vascular Endothelial Function in Healthy Men by Inducing Lipid Peroxidation and Increasing Asymmetric Dimethylarginine: Arginine. *J Nutr* (2011) 141:1961–8. doi: 10.3945/jn.111.144592
15. American Diabetes Association. 2. Classification and Diagnosis of Diabetes: Standards of Medical Care in Diabetes—2021. *Diabetes Care* (2021) 44:S15–33. doi: 10.2337/dc21-S002
16. Harrell FE Jr. Package 'Hmisc'. (2019). Available at: https://cran.r-project.org/web/packages/Hmisc/index.html.
17. DeLong ER, DeLong DM, Clarke-Pearson DL. Comparing the Areas Under Two or More Correlated Receiver Operating Characteristic Curves: A Nonparametric Approach. *Biometrics* (1988) 44:837–45. doi: 10.2307/2531595
18. Cook NR. Quantifying the Added Value of New Biomarkers: How and How Not. *Diagn Prognostic Res* (2018) 2:14. doi: 10.1186/s41512-018-0037-2
19. Kassambara A, Kosinski M, Biecek P. Package 'Survminer'. (2017). Available at: https://cran.r-project.org/web/packages/survminer/index.html
20. Therneau TM, Lumley T. Package 'Survival'. (2022). Available at: https://cran.r-project.org/web/packages/survival/index.html.
21. American Diabetes Association. 2. Classification and Diagnosis of Diabetes: Standards of Medical Care in Diabetes—2018. *Diabetes Care* (2018) 41:S13–27. doi: 10.2337/dc18-S002
22. Banerji MA, Chaiken RL, Lebovitz HE. Prolongation of Near-Normoglycemic Remission in Black NIDDM Subjects With Chronic Low-Dose Sulfonylurea Treatment. *Diabetes* (1995) 44:466–70. doi: 10.2337/diabetes.44.4.466
23. Nyirjesy SC, Sheikh S, Hadjiliadis D, De Leon DD, Peleckis AJ, Eiel JN, et al. Beta-Cell Secretory Defects are Present in Pancreatic Insufficient Cystic Fibrosis With 1-Hour Oral Glucose Tolerance Test Glucose >/=155 Mg/Dl. *Pediatr Diabetes* (2018) 19:1173–82. doi: 10.1111/pedi.12700
24. Bianchi C, Miccoli R, Trombetta M, Giorgino F, Frontoni S, Faloia E, et al. Elevated 1-Hour Postload Plasma Glucose Levels Identify Subjects With Normal Glucose Tolerance But Impaired Beta-Cell Function, Insulin Resistance, and Worse Cardiovascular Risk Profile: The GENFIEV Study. *J Clin Endocrinol Metab* (2013) 98:2100–5. doi: 10.1210/jc.2012-3971
25. Briker SM, Hormenu T, DuBose CW, Mabundo LS, Chung ST, Ha J, et al. Metabolic Characteristics of Africans With Normal Glucose Tolerance and Elevated 1-Hour Glucose: Insight From the Africans in America Study. *BMJ Open Diabetes Res Care* (2020) 8(1). doi: 10.1136/bmjdrc-2019-000837
26. Tricò D, Mengozzi A, Frascerra S, Scozzaro MT, Mari A, Natali A. Intestinal Glucose Absorption Is a Key Determinant of 1-Hour Postload Plasma Glucose Levels in Nondiabetic Subjects. *J Clin Endocrinol Metab* (2019) 104:2131–9. doi: 10.1210/jc.2018-02166
27. Trahair LG, Horowitz M, Marathe CS, Lange K, Standfield S, Rayner CK and Jones KL. Impact of Gastric Emptying to the Glycemic and Insulinemic Responses to a 75-G Oral Glucose Load in Older Subjects With Normal and Impaired Glucose Tolerance. *Physiol Rep* (2014) 2:e12204. doi: 10.14814/phy2.12204
28. Marathe CS, Rayner CK, Jones KL and Horowitz M. Relationships Between Gastric Emptying, Postprandial Glycemia, and Incretin Hormones. *Diabetes Care* (2013) 36:1396–405. doi: 10.2337/dc12-1609
29. Ray KN, Chari AV, Engberg J, Bertolet M and Mehrotra A. Opportunity Costs of Ambulatory Medical Care in the United States. *Am J Manag Care* (2015) 21:567–74.
30. Jagannathan R, Neves JS, Dorcely B, Chung ST, Tamura K, Rhee M and Bergman M. The Oral Glucose Tolerance Test: 100 Years Later. *Diabetes Metab Syndr Obes* (2020) 13:3787–805. doi: 10.2147/DMSO.S246062
31. Jackson SL, Safo SE, Staimez LR, Olson DE, Narayan KMV, Long Q, et al. Glucose Challenge Test Screening for Prediabetes and Early Diabetes. *Diabet Med* (2017) 34:716–24. doi: 10.1111/dme.13270
32. Riddle MC, Cefalu WT, Evans PH, Gerstein HC, Nauck MA, Oh WK, et al. Consensus Report: Definition and Interpretation of Remission in Type 2 Diabetes. *J Clin Endocrinol Metab* (2021) 107:1–9. doi: 10.1210/clinem/dgab585

Conflict of Interest: DDS was Speaker Bureau and Ad hoc consultant of: Novo Nordisk and Bayer. GU has received unrestricted research support for research studies (to Emory University) from Merck, Novo Nordisk, and Dexcom Inc.

The remaining authors declare that the research was conducted in the absence of any commercial or financial relationships that could be construed as a potential conflict of interest.

frontiers | Frontiers in Endocrinology

ORIGINAL RESEARCH
published: 06 June 2022
doi: 10.3389/fendo.2022.868364

The rs10830963 Polymorphism of the MTNR1B Gene: Association With Abnormal Glucose, Insulin and C-peptide Kinetics

Daniela Vejrazkova[1*], *Marketa Vankova*[1], *Josef Vcelak*[1], *Hana Krejci*[2], *Katerina Anderlova*[2], *Andrea Tura*[3], *Giovanni Pacini*[3], *Alena Sumova*[4], *Martin Sladek*[4] *and Bela Bendlova*[1]

[1] Department of Molecular Endocrinology, Institute of Endocrinology, Prague, Czechia, [2] Department of Obstetrics and Gynecology, 1st Faculty of Medicine, Charles University and General University Hospital in Prague, Prague, Czechia, [3] Metabolic Unit, Institute of Neuroscience, National Research Council, Padova, Italy, [4] Laboratory of Biological Rhythms, Institute of Physiology of the Czech Academy of Sciences, Prague, Czechia

OPEN ACCESS

Edited by:
Melanie Cree-Green, University of Colorado, United States

Reviewed by:
Sinan Tanyolac, Istanbul University, Turkey
Bo Ding, Nanjing First Hospital, China
Yun Hu, Wuxi People's Hospital, China

***Correspondence:**
Daniela Vejrazkova
dvejrazkova@endo.cz

Specialty section:
This article was submitted to Clinical Diabetes, a section of the journal Frontiers in Endocrinology

Received: *03 February 2022*
Accepted: *25 April 2022*
Published: *06 June 2022*

Citation:
Vejrazkova D, Vankova M, Vcelak J, Krejci H, Anderlova K, Tura A, Pacini G, Sumova A, Sladek M and Bendlova B (2022) The rs10830963 Polymorphism of the MTNR1B Gene: Association With Abnormal Glucose, Insulin and C-peptide Kinetics. Front. Endocrinol. 13:868364. doi: 10.3389/fendo.2022.868364

Background: The *MTNR1B* gene encodes a receptor for melatonin, a hormone regulating biorhythms. Disruptions in biorhythms contribute to the development of type 2 diabetes mellitus (T2DM). Genetic studies suggest that variability in the *MTNR1B* gene affects T2DM development. Our aim was to compare the distribution of the genetic variant rs10830963 between persons differing in glucose tolerance in a sample of the Czech population (N=1206). We also evaluated possible associations of the polymorphism with insulin sensitivity, beta cell function, with the shape of glucose, insulin and C-peptide trajectories measured 7 times during a 3-hour oral glucose tolerance test (OGTT) and with glucagon response. In a subgroup of 268 volunteers we also evaluated sleep patterns and biorhythm.

Results: 13 persons were diagnosed with T2DM, 119 had impaired fasting blood glucose (IFG) and/or impaired glucose tolerance (IGT). 1074 participants showed normal results and formed a control group. A higher frequency of minor allele G was found in the IFG/IGT group in comparison with controls. The GG constellation was present in 23% of diabetics, in 17% of IFG/IGT probands and in 11% of controls. Compared to CC and CG genotypes, GG homozygotes showed higher stimulated glycemia levels during the OGTT. Homozygous as well as heterozygous carriers of the G allele showed lower very early phase of insulin and C-peptide secretion with unchanged insulin sensitivity. These differences remained significant after excluding diabetics and the IFG/IGT group from the analysis. No associations of the genotype with the shape of OGTT-based trajectories, with glucagon or with chronobiological patterns were observed. However, the shape of the trajectories differed significantly between men and women.

Conclusion: In a representative sample of the Czech population, the G allele of the rs10830963 polymorphism is associated with impaired early phase of beta cell function, and this is evident even in healthy individuals.

Keywords: type 2 daibetes mellitus, insulin sensitivity, beta cell function, *MTNR1B* gene, rs10830963, OGTT trajectories, glucose tolerance

INTRODUCTION

The *MTNR1B* (melatonin receptor 1B) gene encodes a receptor for melatonin, a hormone that controls biorhythms. The gene is expressed primarily in the brain, but its expression has also been described in pancreatic cells (1). Genetic studies suggest that variability in the *MTNR1B* gene is one of the factors influencing the pathophysiology of type 2 diabetes mellitus (T2DM), with the single nucleotide polymorphism rs10830963 showing the strongest association (2–4).

It has been well documented that melatonin inhibits insulin secretion (5). This inhibition is more pronounced in carriers of the minor variant G of the rs10830963 C/G polymorphism. The reason is that minor variant G confers increased expression of the melatonin receptor in the human pancreas and leads to increased melatonin signaling (5). This poses a higher risk of T2DM in these individuals. The mechanism by which this intronic variant affects enhancer binding, thereby significantly altering gene expression, has already been explained (6). In addition, it has been found that acute melatonin administration leads to impaired glucose tolerance in certain circumstances, depending on the time of administration. Melatonin administered in the morning increased the area under the glycemic curve (AUC) during the OGTT by 186% and maximal glucose concentration during the OGTT by 21% in comparison with placebo administration, while melatonin administered in the evening increased AUC by 54% and maximal glucose concentration by 27% compared to placebo (7). Moreover, this impairment of glucose tolerance was exacerbated in carriers of the minor allele G of the rs10830963 polymorphism. As regards morning administration, the effect of melatonin was six times higher in G allele carriers. In the evening, the effect of melatonin did not differ significantly between G allele carriers and non-carriers (8).

Based on these findings, our aim was to build on our work of 2014 (9) and compare the distribution of the genetic variant rs10830963 between persons differing in glucose tolerance. Subjects with impaired fasting blood glucose (IFG) and/or impaired glucose tolerance (IGT) during a 3-hour oral glucose tolerance test (OGTT) were compared with healthy controls. The genotypes were then assessed in terms of insulin sensitivity (IS), beta cell function, glucagon response, hepatic extraction and other characteristics of glucose metabolism. The novelty of the study lay in the evaluation of possible associations of the polymorphism with the shape of glucose, insulin and C-peptide trajectories (monophasic, biphasic, triphasic, or more complex) formed on the basis of seven measurements during the OGTT, and also with glucagon dynamics (four measurements during the test). There are several current approaches for assessing glucose tolerance, IS and beta cell function *in vivo*. Of these, OGTT and the derived equations (IS and insulin secretion indices) is generally considered the most suitable approach for epidemiological studies. As OGTT provides diagnostic information limited to specific time points, a novel method of monitoring the entire curve has begun to be used to reflect an individual´s metabolic information, such as abnormal IS and impaired insulin secretion. This new method is based on evaluations of the shape of the glucose curve after a fixed oral dose of glucose (10). Glycemia is measured in 30 min intervals during the standard 2-hour OGTT or during the prolonged 3-hour OGTT. In this study, 3-hour trajectories of glucose and also of insulin and C-peptide were monitored with sampling at 0, 30, 60, 90, 120, 150 and 180 min of the test.

It has been postulated that melatonin might influence insulin secretion through a paracrine effect of glucagon (1). Therefore, glucagon was sampled four times at 60 min intervals (0, 60, 120 and 180 min) during the 3-hour OGTT in order to gain a deeper insight into the glucose metabolism of the subjects.

As low first-pass insulin extraction by the liver is considered a risk factor for insulin resistance (11), hepatic extraction was also included in the calculations and analyzed in relation to the variability of the MTNR1B gene.

Melatonin is a hormone that controls sleep and biorhythms and disruption of its natural secretory rhythmicity is considered to be one of the causes of impaired glucose metabolism. Therefore, a pilot study evaluating a possible association of melatonin receptor polymorphism with sleep and chronotype was performed in a subgroup of 268 volunteers.

The whole study was performed on a cohort of the Czech population, for which the rs10830963 polymorphism has not yet been evaluated in detail. Unlike many other European countries, the genographic variability of the Czech population is considerable, because as a country in the middle of Europe it has been affected by many different human migrations that have passed through Europe over time. The highest proportion of Czech people have Slavic origin (approximately 45%), followed by those with Germanic origin (25%) and then Scandinavian and Mediterranean (represented by 7 and 6%, resp.). In short, all study participants represent a combination of Eastern and Western Europeans of Caucasian descent.

MATERIALS AND METHODS

Study Subjects

In the years 2001–2020, adult volunteers with varying degrees of glucose tolerance were continuously examined at the Institute of Endocrinology in Prague. Examinations were based on genetic, anthropometric and biochemical characterization, including the 3-hour OGTT with 75g of glucose load. Exclusion criteria were the presence of serious diseases where passing a glucose test would pose a health risk, and pregnancy, as it is associated with specific changes in glucose metabolism. We also did not include people previously diagnosed with T2DM. Over the 20 years of assembling this cohort, we have used the same protocol and the same or very comparable methods. A total of 1206 volunteers were examined in the study: 985 women (mean age ± SD=32.8 ± 9.35 years, mean BMI ± SD=24.5 ± 5.21 kg/m^2) and 221 men (mean age ± SD=34.2 ± 11.88 years, mean BMI ± SD=25.1 ± 4.09 kg/m^2).

Ethics Approval Statement

The study protocol was in accordance with the institutional ethics committee (Ethics committee of the Institute od

Endocrinology EK_EÚ_10062019) and national legislation complying with the principles laid down in the Declaration of Helsinki. Written consent to participate in the study was obtained from all participants.

Genotyping

DNA was extracted from peripheral leukocytes (QIAamp DNA Blood Kit, QIAGEN, Germany). Genotyping of rs10830963 in the MTNR1B gene was performed using ABI TaqMan SNP Genotyping Assays (LightCycler 480 System, Roche).

Clinical and Biochemical Characterization

Basic anthropometric characteristics were determined to calculate the body mass index (BMI), waist to hip ratio (WHR), and the body adiposity index (BAI) estimating the amount of total body fat (12).

Venous blood samples were taken at 8 a.m. after overnight fasting. During the 3-hour OGTT (75g of glucose in 250 ml of water), 7 samples were collected in 30 min intervals and blood glucose (enzymatic reference method with hexokinase, Roche), C-peptide (ECLIA, Roche) and insulin concentrations (ECLIA, Roche) were measured. Glucagon (EURIA glucagon radioimmunoassay, EuroDiagnostica AB, Sweden) was measured four times in 60 min intervals (at 0, 60, 120 and 180 min) during the OGTT. The areas under the glycemic (AUC_{Glc}), insulin (AUC_{Ins}) and C-peptide ($AUC_{C\text{-}pep}$) curves were calculated with the trapezoidal rule. Trajectories of blood glucose, insulin and C-peptide were analyzed according to Tura et al. (10). Fasting IS was assessed by HOMA-R and QUICKI, while dynamic IS was evaluated by ISIcomp also known as the Matsuda index, OGIS and PREDIM (13, 14). Beta cell function was evaluated by HOMA-B at fasting state and by the insulinogenic index IGI in dynamics (15). Further indices of beta cell function (in relation to IS) are the disposition index DI (16) computed as OGIS × AUC_{Ins} and the adaptation index AI (17) computed as OGIS × $AUC_{C\text{-}pep}$. Hepatic insulin extraction was evaluated according to Tura et al. (18).

Classification of Glycemic, Insulin and C-peptide Curves During the OGTT

The 3-hour glucose, insulin and C-peptide trajectories were monitored in 30 min intervals (at 0, 30, 60, 90, 120, 150 and 180 min) of the OGTT. The shape of the glucose curve was classified as monophasic when glycemia simply increased and then gradually decreased (one peak). The curve was biphasic when glycemia showed a further increase following the decrease. A three-phase shape was characterized by two complete peaks. In the prolonged 3-hour OGTT, much more complex and heterogeneous curve shapes were observed. In some people, there were also four- and five-phase curves with 3 and 4 complete peaks, respectively. These were classified together as multiphasic glycemic curves. Glucose variations were considered significant if the difference was at least 2% (this criterion was necessary to avoid the detection of false minima and maxima in the glucose curve). For the curves of insulin and C-peptide, criteria with higher requirements for significant variability (5%) were used.

Chronotype Assessment

Sleep patterns and biorhythms in a pilot subgroup of 268 volunteers were assessed using questions from Munich ChronoType Questionnaire (19) translated into the Czech language. The chronotype was calculated from the mid-sleep phase corrected for sleep debt accumulated during working days, adjusted for age and gender (20). Apart from using sleep phase, circadian preferences were also determined on the basis of self-assessment, asking the subjects to indicate the interval during which they experience the highest cognitive alertness (maximum activity/performance), from which we calculated its midpoint.

Statistical Analysis

To assess deviations from the Hardy-Weinberg equilibrium of genotype frequencies, the Chi-square test was used. Allele/genotype frequencies were compared between groups by the Chi-square test. Odds ratios and 95% Confidence Intervals were calculated in MedCalc Software. Differences in biochemical and anthropometric data between groups were tested by the non-parametric Mann-Whitney test owing to the non-normal data distribution. The Kruskal-Wallis Z-Value Test with Bonferroni correction was used for multiple comparisons. The power analysis was conducted using the NCSS2020/PASS software. The p-values <0.05 (two tailed) were considered significant.

RESULTS

Glucose Metabolism

According to the results of the 3-hour OGTT, participants were divided into three groups: 13 persons were newly diagnosed with T2DM (fasting glycemia ≥7 mmol/l or/and glycemia at 120 min of the test ≥11.1 mmol/l) and formed a T2DM group (21). 119 persons had IFG (fasting glycemia ≥5.6 mmol/l) or IGT (glycemia at 120 min of the test ≥7.8 mmol/l) or these probands met both of the criteria and together they formed an IFG/IGT group. 1074 participants showed normal results (fasting glycemia <5.6 mmol/l and at the same time plasma glucose at 120 min of the test did not rise to 7.8 mmol/l or above) and formed the control group.

Genotypic Frequencies

The distribution of *MTNR1B* rs10830963 genotypic frequencies did not deviate from Hardy-Weinberg equilibrium ($Chi^2 = 0.825$, p=0.36). The frequency of the minor allele G in the whole cohort was 33.2%. A higher frequency of minor allele G was found in the IFG/IGT group compared to controls (40.7% vs. 32.4%, p=0.01), OR=1.57, CI 95% [1.06; 2.33], p_{OR}=0.03). The GG constellation was present in 23% of diabetics, in 17% of the IFG/IGT probands and in 11% of controls ($Chi^2 = 11.2$. p=0.02).

Raw genotype data and complete genotypic and allelic frequencies of our cohort of 1206 participants were published in public repository Figshare.com (22), item. "The rs10830963 SNP of the MTNR1B gene in the Czech cohort" with DOI for public link: 10.6084/m9.figshare.16586039.

Comparisons of Biochemical Parameters Between the Genotypes

Anthropometric characteristics of the compared genotypic groups are shown in **Table 1**. The female to male ratio was comparable in all genotypic groups. Furthermore, no clinically significant differences between the groups were observed in age, BMI or in body adiposity measured by BAI, or in body fat distribution monitored by WHR. These observations fulfill an important condition for comparing biochemical data.

Parameters of glucose metabolism depending on the *MTNR1B* rs10830963 genotype are listed in **Table 2** and **Figure 1**. The GG genotype showed slightly higher basal glycemia compared to the CC genotype. GG homozygotes also showed higher stimulated glycemia (AUC_{Glc}) during the OGTT in comparison with CC homozygotes and with heterozygotes (**Figure 1A**). The time points showing the most significant differences were at 30 min (CC vs. GG: $p=5x10^{-5}$, CC vs. CG: p=0.004) and at 60 min (CC vs. GG: $p=6x10^{-5}$, CC vs. CG: $p=6x10^{-4}$), weaker but still highly significant differences were at 90 min of the test ($p<0.01$ for both comparisons). Insulin sensitivity indices (fasting and dynamic) were not different between the genotype groups (**Table 2** and **Figure 1B**). Homozygous as well as heterozygous carriers of the G allele showed lower HOMA-B and IGI indices of beta cell function in comparison with wild-type CC homozygotes (**Figures 1C, D**), signifying reduced insulin secretion since the hepatic extraction did not differ between the three genotypes (**Table 2**). This assumption strongly supports the observation of the significantly reduced secretion of both insulin and C-peptide at 30 min of the OGTT in G allele carriers compared to the CC genotype (p=0.03 and 0.02, resp.), although the overall 3-hour insulinemia and C-peptidemia measured by AUC_{Ins} and $AUC_{C\text{-}pep}$ did not mirror impaired beta cell response. This indicates that the very early phase of insulin secretion is attenuated or delayed in G allele carriers, which then translates into higher blood glucose during the first two hours of the test.

The differences observed between the genotypes in AUC_{Glc} and in the indices of beta cell function (HOMA-B, IGI) remained statistically significant after excluding diabetics from the analysis. Moreover, all the described differences remained fully preserved even after the exclusion of the IFG/IGT group, which indicates the effect of the G allele in completely healthy individuals in terms of glucose control. Within the IFG/IGT group alone, the effect of the allele was systematically evident, but as this group was less numerous compared to controls, the differences were not significant.

Evaluations of the relationship between the polymorphism and glucagon levels showed no association with either fasting glucagon or post-glucose glucagon response at 60, 120 or 180 min of the OGTT. In addition, no association of the genotype with hepatic extraction was observed in either the overall cohort or in any of the subgroups.

Comparisons of Glycemic, Insulin and C-peptide Curves Between the Genotypes

Analysis of the *MTNR1B* rs10830963 in relation with trajectories of glucose, insulin and C-peptide showed that the three genotypes are distributed equally within the four different types of curves (monophasic, biphasic, triphasic, or more complex), **Table 3**.

However, a different distribution of men and women was observed in the particular categories of glycemic curves, **Table 4**. Significantly more men had a biphasic curve (the percentage of men showing biphasic glucose response was double that of women), and significantly more women had a triphasic curve. This finding was independent of genotype, the difference between the genders was significant within all three genotypes, as shown in **Table 5**.

Graphs and tables showing medians of glucose, insulin, C-peptide as well as glucagon dynamics at all time points measured during the OGTT for each genotype are available in the **Supplementary Material A**.

Comparisons of Sleep Regime and Chronotype Between the Genotypes

In the subcohort of 268 volunteers who completed the questionnaire data for this pilot study, minor variant G was present in a heterozygous constellation in 124 participants (46%) and in a homozygous constellation in 26 (10%) with an allelic frequency of 33%. The remaining 118 individuals (44%) were homozygous in the common variant C. The average age and the ratio of women/men did not differ significantly between the compared genotype groups. The average duration of sleep on weekdays and days off did not differ between the genotypes, nor

TABLE 1 | Anthropometric characteristics depending on the *MTNR1B* rs10830963 genotype.

	CC (n=545)	CG (n=521)	GG (n=140)	p-level<0.05
Males proportion	103 (19%)	96 (18%)	22 (16%)	ns
Age (years)	32.0 [30.8; 32.5]	32.0 [30.8; 32.5]	31.1 [29.3; 32.9]	ns
Body Weight (kg)	69.3 [67.8; 71.3]	67.3 [64.9; 69.0]	67.9 [63.7; 70.6]	ns
Body Heigh (cm)	170 [169; 171]	169 [168.1; 170]	168.6 [167.6; 170.5]	ns
Waist circumference (cm)	77.7 [76.2; 79.0]	75.6 [74.5; 76.6]	74.9 [73.5; 79.0]	ns
Abdominal circumference (cm)	85.4 [84.2; 86.9]	84.0 [82.3; 85.4]	84.5 [81.5; 87.5]	ns
Hip circumference (cm)	100 [99.1; 101.0]	98.5 [98.0; 99.7]	99 [97.5; 101.0]	CCxCG p=0.01
BMI (kg/m^2)	23.8 [23.4; 24.4]	23.2 [22.7; 23.6]	23.5 [22.2; 24.6]	ns
WHR	0.78 [0.77; 0.79]	0.77 [0.77; 0.78]	0.77 [0.76; 0.79]	ns
BAI (%)	26.8 [26.3; 27.1]	26.7 [26.3; 27.1]	26.9 [25.5; 28.2]	ns

Data are given as medians [95% LCL; 95% UCL], p-level according to Kruskal-Wallis Z-Value Test with Bonferroni correction.
ns, not significant.

TABLE 2 | Parameters of glucose metabolism depending on the *MTNR1B* rs10830963 genotype.

	CC (n=545)	CG (n=521)	GG (n=140)	p-level<0.05
Basal glycemia (mM/l)	4.7 [4.6; 4.7]	4.7 [4.7; 4.8]	4.8 [4.7; 4.9]	CCxGG p=0.01
Basal insulinemia (mIU/l)	6.3 [5.9; 6.5]	5.9 [5.5; 6.2]	5.65 [4.9; 6.4]	ns
AUC_{Ins} (pM x min/l)	33201 [31464; 34893]	31248 [30267; 33489]	35752.5 [31977; 39870]	CGxGG p=0.04
Basal C-peptide (nM/l)	0.61 [0.59; 0.63]	0.57 [0.55; 0.60]	0.57 [0.54; 0.62]	ns
$AUC_{C\text{-}pep}$ (pM x min/l)	$3.7x10^5$ [$3.5x10^5$, $3.8x10^5$]	$3.5x10^5$ [$3.4x10^5$; $3.7x10^5$]	$3.9x10^5$ [$3.5x10^5$; $4.2x10^5$]	CGxGG p=0.01
HOMA-R (mIU x mM/l^2)	1.30 [1.23; 1.36]	1.25 [1.18; 1.32]	1.24 [1.04; 1.36]	ns
HOMA_B (mIU/mM)	112.5 [106.7; 118.2]	98.8 [94.7; 106.2]	93.8 [80.0; 106.7]	CCxCG p=0.002 CCxGG p=0.003
QUICKI	0.37 [0.36; 0.37]	0.37 [0.37; 0.37]	0.37 [0.36; 0.38]	ns
$OGIS_{180min}$ (ml/min/m^2)	506.3 [497.9; 511.9]	511.1 [503.7; 517.9]	519.3 [495.5; 534.2]	ns
ISI_{COMP} ([(mg/dl)^2(µU/ml)^2]$^{-1/2}$)	8.78 [8.24; 9.20]	8.89 [8.55; 9.35]	8.76 [7.72; 9.48]	ns
Ins_{0min}/Glc_{0min} (pM/mM)	8.09 [7.63; 8.50]	7.47 [7.00; 7.96]	7.13 [6.24; 7.60]	CCxCG p=0.04 CCxGG p=0.02
Disposition Index DI	$1.7x10^7$ [$1.6x10^7$; $1.8x10^7$]	$1.6x10^7$ [$1.5x10^7$; $1.7x10^7$]	$1.8x10^7$ [$1.6x10^7$; $2.0x10^7$]	CGxGG p=0.04
Adaptation Index AI	$1.9x10^8$ [$1.8x10^8$; $1.9x10^8$]	$1.8x10^8$ [$1.8x10^8$; $1.9x10^8$]	$1.9x10^8$ [$1.9x10^8$; $2.1x10^8$]	CGxGG p=0.01
Hepatic insulin extraction (%)	69.2 [68.2; 69.8]	70.1 [69.2; 70.9]	69.5 [67.1; 70.9]	ns
Basal glucagonemia (pM/l)	36.5 [35.2; 37.5]	37.05 [36.5; 37.9]	37.5 [34.8; 40.2]	ns

Data are given as medians [95% LCL; 95% UCL], p-level according to Mann-Whitney test.
ns, not significant.

did the mid-sleep phase on weekdays and days off. The chronotype calculated from the mid-sleep phase corrected for sleep debt accumulated during working days and adjusted for age and gender was also comparable. The time of subjective maximum daily activity and performance (best alertness midpoint) was similar in all three genotype groups, with a median at 11 a.m. The social jet lag resulting from the discrepancy between the natural biorhythm and work/social duties averaged 0.85 ± 0.698 h regardless of genotype. Graphs showing medians of sleep and biorhythm patterns for each genotype of the MTNR1B rs10830963 SNP are available in the **Supplementary Material B**.

DISCUSSION

Meta analyses have indicated relationships between the rs10830963 minor allele G and T2DM, with the G allele associated with higher fasting blood glucose levels in Cuacasians and Asians (23–27). However, limited cross-ethnicity has been observed as regards the effect of the allele on insulin sensitivity, beta cell function (28–31), or whether a minor allele dose effect is apparent. A dose effect of the G allele on the ability of beta cells to maintain blood glucose levels was described in a recent study conducted on almost 190 thousand participants of European descent, and each additional risk allele was associated with 10% higher odds of T2DM (32). A genome-wide

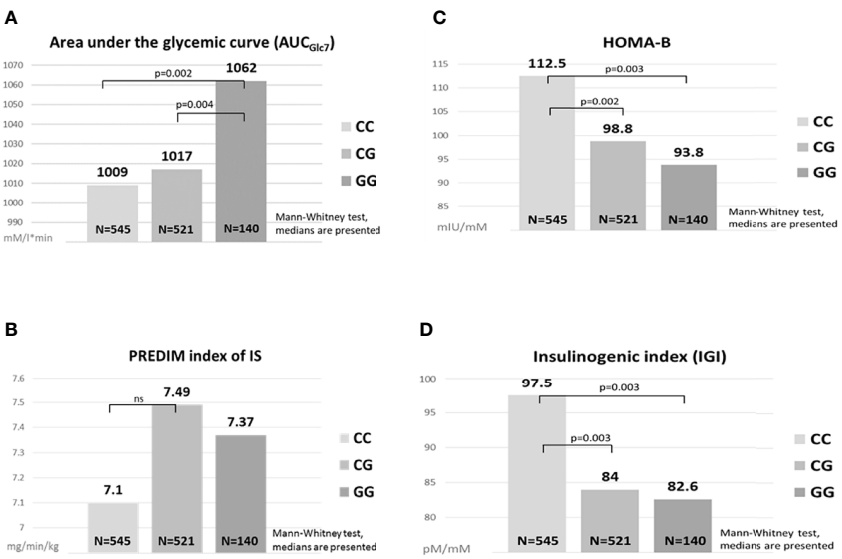

FIGURE 1 | Comparisons of glucose metabolism between the *MTNR1B* genotypes. Area under the glycemic curve **(A)**, HOMA-B **(C)**, PREDIM index of IS **(B)**, Insulinogenic index **(D)**. ns, not significant.

TABLE 3 | Proportions of the *MTNR1B* rs10830963 genotype depending on the shape of glycemic, insulinemic and C-peptide curves.

	MTNR1B genotype (%)			STATISTICS
Glycemic curve	**CC**	**CG**	**GG**	
monophasic	48	45.5	56	Chi^2 = 5.9
biphasic	21	22.5	16.5	power=0.40
triphasic	26	26	21.5	p-level=0.43
multiphasic	5	6	6	
Insulinemic curve	**CC**	**CG**	**GG**	
monophasic	69.5	67	72	Chi^2 = 1.85
biphasic	6.5	6.5	6	power=0.14
triphasic	22	24.5	20	p-level=0.93
multiphasic	2	2	2	
C-peptide curve	**CC**	**CG**	**GG**	
monophasic	80	77	81	Chi^2 = 5.11
biphasic	1	2	1	power=0.34
triphasic	18	20	18	p-level=0.53
multiphasic	1	1	0	

association study evaluating IVGTT-based measures of first-phase insulin secretion revealed a strong association of the G allele with a lower first-phase insulin response and also with insulin secretion rate in several different ethnic groups (29). Also, previous data from the OGTT-based Botnia Study showed that the G variant of *MTNR1B* has the strongest effect on beta cell function in nondiabetic participants from the Botnia region of western Finland (30). Accordingly, our data demonstrate lower beta cell function assessed by HOMA-B and IGI indices in homozygous and heterozygous carriers of the G allele. This impairment was not detected by overall 3-hour AUC_{Ins} or $AUC_{C\text{-}pep}$, as only data at 30 min directly demonstrated that carriers of the G allele show a reduced secretion of both insulin and C-peptide. During the rest of the OGTT, this effect was no longer noticeable. On the contrary, increasing glycemia led to a gradual compensatory increase in insulin secretion starting with the second hour of the test. It can only be assumed that even more significant differences in insulin secretion between the genotypes would be detected at 15 min. Thus, the early phase of the pancreatic beta cell response to a glucose stimulus, which is attenuated or delayed in G allele carriers, is likely crucial for understanding and interpreting our results. To this end, we are currently adjusting the examination protocol, to evaluate glycemia, insulinemia and C-peptide levels at the 15 min of the OGTT.

The dominant effect of the G allele observed in beta cell function was not apparent in insulin sensitivity. Based on values of the PREDIM index, considered a valuable index due to the close correlation with the clamp method, IS was not reduced in homozygous or heterozygous G allele carriers. In general, beta cell function is the actual discriminant between the genotype groups, as demonstrated by the HOMA-B, IGI, DI and AI indices. This leads to a conclusion useful for clinical practice, supported by the results of previous studies (33, 34). Individuals carrying the G allele could benefit greatly from adjusting their lifestyle so that they are not forced to have breakfast early in the morning, when their melatonin levels are still high, due to work and social responsibilities. These people have a delayed morning drop in melatonin (34). High levels of melatonin disrupt insulin secretion. In addition, G allele carriers are significantly more vulnerable due to increased melatonin signaling (5) and impaired early insulin secretion capacity, and the long-term regular need for insulin secretion due to early morning food intake could expose this group to a greater risk of developing glucose tolerance disorders. The already mentioned shift in melatonin secretion towards a later rise in the evening and a slower decline in the morning in G allele carriers led us to the idea of testing whether the sleep regime and the setting of the entire chronotype are not shifted as well. The results of the pilot study do not yet indicate this, which may be due to the relatively small number of individuals involved. We will continue to test this hypothesis on larger groups.

TABLE 4 | Gender proportions depending on the shape of glycemic curves.

Gender proportion (%)			Statistics
Glycemic curve	**Females**	**Males**	
monophasic	49	41	Chi^2 = 63.4
biphasic	17	40	power=1.00
triphasic	28	14	**p-level<0.000001**
multiphasic	6	5	

Statistically significant results are in bold.

One of the main benefits of this study is the original data from the Czech population analyzed in a representative cohort that is unique in its size and in the detailed biochemical examinations in the Czech Republic. We comprehensively assessed relationships between the genetic variant in the melatonin receptor and glucose metabolism using both standard and novel indices of inulin sensitivity and beta cell function, as well as by C-peptide and glucagon dynamics during a prolonged OGTT. All the conclusions are based on robust non-parametric evaluations. Innovative is the evaluation of the genetic variant in relation to the shapes of the glucose, insulin and C-peptide trajectories based on sampling before the glucose load and then at 30, 60, 90, 120, 150 and 180 min after it, as studies based on a two-hour OGTT have limited potential to evaluate the shape of the curves. Nevertheless, despite thorough analysis, no effect of the SNP on the shape of the trajectories was apparent. Interestingly, however, we found that twice the percentage of men had a biphasic glycemic curve during the 3-hour OGTT, while a triphasic

TABLE 5 | Gender proportions depending on the *MTNR1B* rs10830963 genotype and on the shape of glycemic curves.

Gender proportions			STATISTICS
Gender proportion in CC homozygotes (%)			
Glycemic curve	**Females**	**Males**	
monophasic	49	42	Chi^2 = 39.8
biphasic	16	43	power=1.00
triphasic	29	12	**p-level=<0.000001**
multiphasic	6	3	
Gender proportion in CG heterozygotes (%)			
Glycemic curve	**Females**	**Males**	
monophasic	47	39	Chi^2 = 18.8
biphasic	18	39	power=0.97
triphasic	28	18	**p-level=0.0003**
multiphasic	7	4	
Gender proportion in GG homozygotes (%)			
Glycemic curve	**Females**	**Males**	
monophasic	59	36	Chi^2 = 10.9
biphasic	13	36	power=0.80
triphasic	23	14	**p-level=0.01**
multiphasic	5	14	

Statistically significant results are in bold.

curve was significantly more common in women. This clearly shows that gender should always be taken into account when evaluating the shapes of glucose trajectories and other related parameters during the OGTT. In this context, the question arises as to whether the blood glucose levels at 120 min of the OGTT represent the optimal criterion for impaired glucose tolerance (21) for both genders, as the different shape of the glycemic trajectory in women and men may require a distinct approach. This issue has not been elaborated in detail in the literature and will be the subject of our research in the future.

One disadvantage of our study was the significantly lower number of individuals with impaired glycemic control compared to healthy controls. The relatively low average age of the participants also contributes to this disparity. However, while maintaining the current longitudinal character of our research, which has been going on for over 20 years, it will be possible to verify existing data on significantly older participants, in whom the proportion of people with glucose metabolism disorders will be significantly higher. Furthermore, a lower proportion of men compared to women can also be considered a weakness. Although we addressed a similar number of men as women, their willingness to participate in clinical trials was significantly lower. However, the gender ratio did not differ in the compared genotype groups, so the impact of this imbalance on the study results is minimized.

In a representative sample of the Czech population, we demonstrated the association of the minor allele G of the rs10830963 polymorphism in the *MTNR1B* gene with glucose metabolism. The G allele was more frequent in people with impaired glucoregulation. Homozygous carriers of this allele showed higher blood glucose levels during the OGTT. Since there were no differences in insulin sensitivity between the genotypes, the higher glycemia was due to lower beta cell function, especially early insulin secretion, observed in homozygous as well as in heterozygous G allele carriers. This association with impaired early pancreatic function was significant even in individuals with healthy glucose processing. As such, the G allele is a factor that may, under certain circumstances, promote higher glucose levels and contribute to the development of glucose intolerance.

DATA AVAILABILITY STATEMENT

The datasets presented in this study can be found in online repositories. The names of the repository/repositories and accession number(s) can be found in the article/**Supplementary Material**.

ETHICS STATEMENT

The studies involving human participants were reviewed and approved by Ethics committee of the Institute of Endocrinology EK_EÚ_10062019. The patients/participants provided their written informed consent to participate in this study.

AUTHOR CONTRIBUTIONS

Conceptualization and design of the work, formal analysis, project administration, original draft preparation and writing: DV. Review & editing, statistical analysis: MV. Methodology of genetic analyzes: JV. Significant data completion: HK, KA. Data curation, indices calculation: GP, AT. Final approval of the work: BB. Processing of chronotype questionnaires: AS, MS. All authors contributed to the article and approved the submitted version.

FUNDING

The study was supported by Ministry of Health of the Czech Republic, grant NU20-01-00308. All rights reserved.

ACKNOWLEDGMENTS

The authors would like to thank all the nurses and physicians of the Institute of Endocrinology for their excellent assistance.

SUPPLEMENTARY MATERIAL

The Supplementary Material for this article can be found online at: https://www.frontiersin.org/articles/10.3389/fendo.2022.868364/full#supplementary-material

REFERENCES

1. Ramracheya RD, Muller DS, Squires PE, Brereton H, Sugden D, Huang GC, et al. Function and Expression of Melatonin Receptors on Human Pancreatic Islets. *J Pineal Res* (2008) 44:273–9. doi: 10.1111/j.1600-079X.2007.00523.x
2. Lyssenko V, Nagorny CL, Erdos MR, Wierup N, Jonsson A, Spégel P, et al. Common Variant in MTNR1B Associated With Increased Risk of Type 2 Diabetes and Impaired Early Insulin Secretion. *Nat Genet* (2009) 41:82–8. doi: 10.1038/ng.288
3. Xia Q, Chen ZX, Wang YC, Ma YS, Zhang F, Che W, et al. Association Between the Melatonin Receptor 1B Gene Polymorphism on the Risk of Type 2 Diabetes, Impaired Glucose Regulation: A Meta-Analysis. *PLos One* (2012) 7:e50107. doi: 10.1371/journal.pone.0050107
4. Mahajan A, Taliun D, Thurner M, Robertson NR, Torres JM, Rayner NW, et al. Fine-Mapping Type 2 Diabetes Loci to Single-Variant Resolution Using High-Density Imputation and Islet-Specific Epigenome Maps. *Nat Genet* (2018) 50:1505–13. doi: 10.1038/s41588-018-0241-6
5. Tuomi T, Nagorny CLF, Singh P, Bennet H, Yu Q, Alenkvist I, et al. Increased Melatonin Signaling Is a Risk Factor for Type 2 Diabetes. *Cell Metab* (2016) 23:1067–77. doi: 10.1016/j.cmet.2016.04.009
6. Gaulton KJ, Ferreira T, Lee Y, Raimondo A, Mägi R, Reschen ME, et al. DIAbetes Genetics Replication And Meta-Analysis (DIAGRAM) Consortium. Genetic Fine Mapping and Genomic Annotation Defines Causal Mechanisms at Type 2 Diabetes Susceptibility Loci. *Nat Genet* (2015) 47:1415–25. doi: 10.1038/ng.3437
7. Rubio-Sastre P, Scheer FA, Gómez-Abellán P, Madrid JA, Garaulet M. Acute Melatonin Administration in Humans Impairs Glucose Tolerance in Both the Morning and Evening. *Sleep* (2014) 37:1715–9. doi: 10.5665/sleep.4088
8. Garaulet M, Gómez-Abellán P, Rubio-Sastre P, Madrid JA, Saxena R, Scheer FA. Common Type 2 Diabetes Risk Variant in MTNR1B Worsens the Deleterious Effect of Melatonin on Glucose Tolerance in Humans. *Metabolism* (2015) 64:1650–7. doi: 10.1016/j.metabol.2015.08.003
9. Vejrazkova D, Lukasova P, Vankova M, Vcelak J, Bradnova O, Cirmanova V, et al. MTNR1B Genetic Variability Is Associated With Gestational Diabetes in Czech Women. *Int J Endocrinol* (2014) 2014:508923. doi: 10.1155/2014/508923
10. Tura A, Morbiducci U, Sbrignadello S, Winhofer Y, Pacini G, Kautzky-Willer A. Shape of Glucose, Insulin, C-Peptide Curves During a 3-H Oral Glucose Tolerance Test: Any Relationship With the Degree of Glucose Tolerance? *Am J Physiol Regul Integr Comp Physiol* (2011) 300:R941–8. doi: 10.1152/ajpregu.00650.2010
11. Asare-Bediako I, Paszkiewicz RL, Kim SP, Woolcott OO, Kolka CM, Burch MA, et al. Variability of Directly Measured First-Pass Hepatic Insulin Extraction and Its Association With Insulin Sensitivity and Plasma Insulin. *Diabetes* (2018) 67:1495–503. doi: 10.2337/db17-1520
12. Bergman RN, Stefanovski D, Buchanan TA, Sumner AE, Reynolds JC, Sebring NG, et al. A Better Index of Body Adiposity. *Obes (Silver Spring)* (2011) 19:1083–9. doi: 10.1038/oby.2011.38
13. Pacini G, Mari A. Methods for Clinical Assessment of Insulin Sensitivity and Beta-Cell Function. *Best Pract Res Clin Endocrinol Metab* (2003) 17:30522. doi: 10.1016/s1521-690x(03)00042-3
14. Tura A, Chemello G, Szendroedi J, Göbl C, Færch K, Vrbíková J, et al. Prediction of Clamp-Derived Insulin Sensitivity From the Oral Glucose Insulin Sensitivity Index. *Diabetologia* (2018) 61:1135–41. doi: 10.1007/s00125-018-4568-4
15. Tura A, Kautzky-Willer A, Pacini G. Insulinogenic Indices From Insulin and C-Peptide: Comparison of Beta-Cell Function From OGTT and IVGTT. *Diabetes Res Clin Pract* (2006) 72:298–301. doi: 10.1016/j.diabres.2005.10.005
16. Ahrén B, Pacini G. Islet Adaptation to Insulin Resistance: Mechanisms and Implications for Intervention. *Diabetes Obes Metab* (2005) 7:2–8. doi: 10.1111/j.1463-1326.2004.00361.x
17. Ahrén B, Pacini G. Impaired Adaptation of First-Phase Insulin Secretion in Postmenopausal Women With Glucose Intolerance. *Am J Physiol* (1997) 273: E701–7. doi: 10.1152/ajpendo.1997.273.4.E701
18. Tura A, Ludvik B, Nolan JJ, Pacini G, Thomaseth K. Insulin and C-Peptide Secretion and Kinetics in Humans: Direct and Model-Based Measurements During OGTT. *Am J Physiol Endocrinol Metab* (2001) 281:E966–74. doi: 10.1152/ajpendo.2001.281.5.E966
19. Roenneberg T, Wirz-Justice A, Merrow M. Life Between Clocks: Daily Temporal Patterns of Human Chronotypes. *J Biol Rhythms* (2003) 18:80–90. doi: 10.1177/0748730402239679
20. Sládek M, Kudrnáčová Röschová M, Adámková V, Hamplová D, Sumová A. Chronotype Assessment *via* a Large Scale Socio-Demographic Survey Favours Yearlong Standard Time Over Daylight Saving Time in Central Europe. *Sci Rep* (2020) 10:1419. doi: 10.1038/s41598-020-58413-9
21. American Diabetes Association. Report of the Expert Committee on the Diagnosis and Classification of Diabetes Mellitus. *Diabetes Care* (1997) 20:1183–97. doi: 10.2337/diacare.20.7.1183
22. *Figshare Data Repository*. Available at: https://figshare.com (Accessed 8. 9. 2021).
23. Prokopenko I, Langenberg C, Florez JC, Saxena R, Soranzo N, Thorleifsson G, et al. Variants in MTNR1B Influence Fasting Glucose Levels. *Nat Genet* (2009) 41:77–81. doi: 10.1038/ng.290
24. Langenberg C, Pascoe L, Mari A, Tura A, Laakso M, Frayling TM, et al. Common Genetic Variation in the Melatonin Receptor 1B Gene (MTNR1B) is Associated With Decreased Early-Phase Insulin Response. *Diabetologia* (2009) 52:1537–42. doi: 10.1007/s00125-009-1392-x
25. Bouatia-Naji N, Bonnefond A, Cavalcanti-Proença C, Sparsø T, Holmkvist J, Marchand M, et al. A Variant Near MTNR1B Is Associated With Increased Fasting Plasma Glucose Levels and Type 2 Diabetes Risk. *Nat Genet* (2009) 41:89–94. doi: 10.1038/ng.277
26. Tam CH, Ho JS, Wang Y, Lee HM, Lam VK, Germer S, et al. Common Polymorphisms in MTNR1B, G6PC2 and GCK are Associated With Increased Fasting Plasma Glucose and Impaired Beta-Cell Function in Chinese Subjects. *PLos One* (2010) 5:e11428. doi: 10.1371/journal.pone.0011428
27. Wang H, Liu L, Zhao J, Cui G, Chen C, Ding H, et al. Large Scale Meta-Analyses of Fasting Plasma Glucose Raising Variants in GCK, GCKR, MTNR1B and G6PC2 and Their Impacts on Type 2 Diabetes Mellitus Risk. *PLos One* (2013) 8:e67665. doi: 10.1371/journal.pone.0067665
28. Scott RA, Scott LJ, Mägi R, Marullo L, Gaulton KJ, Kaakinen M, et al. An Expanded Genome-Wide Association Study of Type 2 Diabetes in Europeans. *Diabetes* (2017) 66:2888–902. doi: 10.2337/db16-1253
29. Wood AR, Jonsson A, Jackson AU, Wang N, van Leewen N, Palmer ND, et al. A Genome-Wide Association Study of IVGTT-Based Measures of First-Phase Insulin Secretion Refines the Underlying Physiology of Type 2 Diabetes Variants. *Diabetes* (2017) 66:2296–309. doi: 10.2337/db16-1452
30. Jonsson A, Ladenvall C, Ahluwalia TS, Kravic J, Krus U, Taneera J, et al. Effects of Common Genetic Variants Associated With Type 2 Diabetes and Glycemic Traits on α- and β-Cell Function and Insulin Action in Humans. *Diabetes* (2013) 62:2978–83. doi: 10.2337/db12-1627
31. Shen LL, Jin Y. Effects of MTNR1B Genetic Variants on the Risk of Type 2 Diabetes Mellitus: A Meta-Analysis. *Mol Genet Genomic Med* (2019) 7:e611. doi: 10.1002/mgg3.611
32. Dashti HS, Vetter C, Lane JM, Smith MC, Wood AR, Weedon MN, et al. Assessment of *MTNR1B* Type 2 Diabetes Genetic Risk Modification by Shift

Work and Morningness-Eveningness Preference in the UK Biobank. *Diabetes* (2020) 69:259–66. doi: 10.2337/db19-0606
33. Burgess HJ, Eastman CI. Early Versus Late Bedtimes Phase Shift the Human Dim Light Melatonin Rhythm Despite a Fixed Morning Lights on Time. *Neurosci Lett* (2004) 356:115–8. doi: 10.1016/j.neulet.2003.11.032
34. Lane JM, Chang AM, Bjonnes AC, Aeschbach D, Anderson C, Cade BE, et al. Impact of Common Diabetes Risk Variant in MTNR1B on Sleep, Circadian, and Melatonin Physiology. *Diabetes* (2016) 65:1741–51. doi: 10.2337/db15-0999

Conflict of Interest: The authors declare that the research was conducted in the absence of any commercial or financial relationships that could be construed as a potential conflict of interest.

Publisher's Note: All claims expressed in this article are solely those of the authors and do not necessarily represent those of their affiliated organizations, or those of the publisher, the editors and the reviewers. Any product that may be evaluated in this article, or claim that may be made by its manufacturer, is not guaranteed or endorsed by the publisher.

frontiers | Frontiers in Endocrinology

ORIGINAL RESEARCH
published: 13 July 2022
doi: 10.3389/fendo.2022.913207

Sex-Specific Associations Between Low Muscle Mass and Glucose Fluctuations in Patients With Type 2 Diabetes Mellitus

Xiulin Shi[1,2†], Wenjuan Liu[3†], Lulu Zhang[1], Fangsen Xiao[1], Peiying Huang[1], Bing Yan[1], Yiping Zhang[2], Weijuan Su[1], Qiuhui Jiang[2], Mingzhu Lin[1], Wei Liu[1] and Xuejun Li[1,2*]*

[1] Department of Endocrinology and Diabetes, Xiamen Diabetes Institute, Fujian Province Key Laboratory of Translational Research for Diabetes, The First Affiliated Hospital of Xiamen University, School of Medicine, Xiamen University, Xiamen, China, [2] The School of Clinical Medicine, Fujian Medical University, Fouzhou, China, [3] Department of Endocrine, Zhangzhou Hospital of Traditional Chinese Medicine, Zhangzhou, China

OPEN ACCESS

Edited by:
Joon Ha,
Howard University, United States

Reviewed by:
Sangsoo Kim,
Pusan National University Hospital, South Korea
Guangda Xiang,
General Hospital of Central Theater Command, China

***Correspondence:**
Xuejun Li
lixuejun@xmu.edu.cn
Wei Liu
sissi_liu@163.com

†These authors have contributed equally to this work

Specialty section:
This article was submitted to Clinical Diabetes, a section of the journal Frontiers in Endocrinology

Received: 05 April 2022
Accepted: 16 June 2022
Published: 13 July 2022

Citation:
Shi X, Liu W, Zhang L, Xiao F, Huang P, Yan B, Zhang Y, Su W, Jiang Q, Lin M, Liu W and Li X (2022) Sex-Specific Associations Between Low Muscle Mass and Glucose Fluctuations in Patients With Type 2 Diabetes Mellitus. Front. Endocrinol. 13:913207. doi: 10.3389/fendo.2022.913207

Objective: Studies have shown that sex differences in lean mass, concentrations of sex hormones, and lifestyles influence cle health and glucose metabolism. We evaluated the sex-specific association between low muscle mass and glucose fluctuations in hospitalized patients with type 2 diabetes mellitus (T2DM) receiving continuous subcutaneous insulin infusion (CSII) therapy.

Methods: A total of 1084 participants were included. Body composition was determined by dual-energy X-ray absorptiometry. Intraday blood glucose fluctuation was estimated by the Largest amplitude of glycemic excursions (LAGE) and standard deviation of blood glucose (SDBG).

Results: The prevalence of low muscle mass was higher in males than in females ($p<0.001$). There was a significant sex-specific interaction between the status of low muscle mass and glucose fluctuations (LAGE and SDBG) (p for interaction=0.025 and 0.036 for SDBG and LAGE, respectively). Among males, low muscle mass was significantly associated with a higher LAGE and SDBG (difference in LAGE: 2.26 [95% CI: 1.01 to 3.51], $p < 0.001$; difference in SDBG: 0.45 [95% CI: 0.25 to 0.65], $p < 0.001$) after adjustment for HbA1c, diabetes duration, hyperlipidemia, diabetic peripheral neuropathy, diabetic nephropathy, and cardiovascular disease. These associations remained significant after further adjustment for age and C-peptide. Among females, low muscle mass was not associated with LAGE or SDBG after adjustment for all covariates.

Conclusion: The prevalence of low muscle mass was higher in males than in females. Low muscle mass was significantly associated with higher LAGE and SDBG among males, but not females.

Keywords: low muscle mass, glucose fluctuations, sex-specific, type 2 diabetes mellitus, continuous subcutaneous insulin infusion

INTRODUCTION

Diabetes is a major public health challenge in the world due to its high and increasing prevalence and related risk of chronic complications and mortality. Accumulating evidence indicates that glucose fluctuations are more harmful in the occurrence and development of diabetic chronic complications compared to constant hyperglycemia (1–3). Generalized and progressive skeletal muscle function disorder is the definition of sarcopenia, which includes progressive loss of muscle mass and function leading to adverse outcomes such as functional decline, frailty, falls, and mortality (4). The prevalence of sarcopenia is significantly higher in type 2 diabetes mellitus (T2DM) than in non-diabetic individuals (5–7). Sarcopenia has been implicated as both a cause and consequence of T2DM (8, 9). The progressive loss of the skeletal muscle might lead to diminished insulin-mediated glucose disposal and exacerbated insulin resistance, resulting in severe glucose abnormalities (10). It has been demonstrated that not only the glycosylated hemoglobin A1c (HbA1c) level but also glucose fluctuations were significantly related to sarcopenia (11).

Lean mass, body fat composition and distribution, hormone concentrations, and lifestyles showed a difference between males and females, which influenced muscle health and glucose metabolism (12). Lean mass, which is generally greater in men, may play an important role in mediating the regulation of glucose metabolism by skeletal muscle. However, to the best of our knowledge, no study focusing on the potential impact of sex differences on the relationship between low muscle mass and glucose fluctuations has been reported.

In this study, we aimed to assess the sex-specific relationship between low muscle mass and glucose fluctuations in hospitalized patients with T2DM undergoing continuous subcutaneous insulin infusion (CSII) treatments.

MATERIALS AND METHODS

Study Design and Participants

The study was performed following the rules of the Declaration of Helsinki, and the protocol was approved by the ethics committee of the First Affiliated Hospital of Xiamen University. All participants provided written informed consent before participating in the study. We included 1084 hospitalized patients for hyperglycemia in the Department of Endocrinology and Diabetes, First Affiliated Hospital, Xiamen University, Xiamen, China from 2017 to 2019. The included criteria for patients were as follows: patients aged 35 years or older with T2DM which was defined as having either fasting plasma glucose (FPG)≥7.0mmol/l or 2-h PG ≥11.1 mmol/l according to the World Health Organization definition. The exclusion criteria were as follows (1): serious health conditions, such as diabetic ketoacidosis, severe hepatic insufficiency, moderate to severe renal insufficiency, cardiac insufficiency, or stroke affected daily activities (2); cognitive disability or an inability to cooperate with the examination (3); pregnant or contemplating pregnancy.

All patients were managed according to established protocols for performing CSII with a length of 7 days, glucose monitoring, and dual-energy X-ray absorptiometry. Diabetes-associated chronic complications were evaluated for the coexistence of neuropathy, retinopathy, and nephropathy.

Glucose Control

On the first day of hospitalization, oral hypoglycemic agents used were stopped, then Humalog rapid-acting insulin (insulin lispro; Eli Lilly, Indianapolis, IN, USA) with the insulin pump (MiniMed Paradigm 722, Medtronic, Northridge, CA, USA) was used among all patients used. The initial insulin dosage was 0.7 unit × body weight (kg) and total daily doses were divided into 50% of basal and 50% of bolus injections. The dawn phenomenon and nocturnal hypoglycemia were taken into account, and the basal rate was fixed depending on the period: basal insulin dose/24 × 0.8 between 2200 and 0300 hours; basal insulin dose/24 × 1.2 between 0300 and 0700 hours; basal insulin dose/24 × 1.0 between 0700 and 2200 hours. The basal and bolus doses of insulin infusion were tailored every 2 days by one doctor by 0.3 unit/h and 3 units, respectively, according to the capillary blood glucose (BG) level to achieve the glycemic target (fasting BG<7.0 mmol/L and average postprandial BG <10.0 mmol/L). All patients received the same education for lifestyle management, and they were fed by the hospital nutrition canteen during the hospitalization.

BG was monitored 7 times per day (before and 2 h after each meal and at bedtime) by a trained nurse using a unified glucometer (Johnson & Johnson, New Brunswick, NJ, USA). Hypoglycemia was defined as a glucose level less than 3.9 mmol/L, and the presence or absence of hypoglycemic symptoms was recorded at every BG measurement point.

Date Collection

Data were collected from electronic health records in the hospital. The clinical condition and medical history of all participants were obtained, including smoking, alcohol consumption habit, medical history (cardiovascular disease, hypertension, diabetic neuropathy, diabetic retinopathy, and diabetic nephropathy), previous hospitalizations, as well as regular antidiabetic drugs, *etc.* Blood and urine samples were taken the day following admission after overnight fasting. The following biochemical parameters were obtained: HbA1c, C-peptide, triglyceride (TG), total cholesterol (TC), high-density lipoprotein cholesterol (HDL-c), and low-density lipoprotein cholesterol (LDL-c), serum albumin, alanine aminotransferase (ALT), aspartate aminotransferase (AST), and urinary albumin.

Anthropometric and Body Composition Measurements

Height and weight were measured by trained nurses according to the standard protocol and body mass index (BMI) was calculated as weight (kilograms) divided by height (meters) squared. BMI was further categorized into four groups:<18.5, 18.5–23.9, 24.0–27.9, and ≥28.0 kg/m^2, according to the Chinese BMI cut-offs (13). Blood pressure was measured with a standard electronic sphygmomanometer on the right arm 5 minutes after sitting for rest. Body composition was determined by dual-energy X-ray absorptiometry (HOLOGIC Discovery A) on the first day of the

hospitalization. The appendicular skeletal muscle mass index (ASMI) was calculated by dividing the appendicular skeletal muscle mass by the height squared (kg/m^2).

Evaluation of Low Muscle Mass, Glucose Fluctuation, and Pancreatic β-Cell Function

The Asian specific cutoff point for diagnosis of low muscle mass was according to the recommendation of the Asian Working Group for Sarcopenia (AWGS) in 2014 (14). Participants with an ASMI less than 7.0 Kg/m^2 for men or 5.4 Kg/m^2 for women were considered to have low muscle mass. The largest amplitude of glycemic excursions (LAGE), mean blood glucose (MBG), the standard deviation of blood glucose (SDBG), postprandial glucose excursion (PPGE) and were indicators for estimating intraday blood glucose fluctuations (3, 14). The MBG was the average glucose for 7 days. SDBG was calculated as the square root of the variance of the daily blood glucose for a whole day during the 7 days of hospitalization, respectively (15). LAGE was determined based on the mean of the diurnal range from minimum glucose levels to maximum glucose levels of BG for 7 days. PPGE was calculated based on the mean of the difference between pre-prandial and 2-h postprandial glucose. C-peptide was a more accurate marker of endogenous insulin secretion than insulin (16, 17). Fasting plasma C-peptide was measured to represent an index of pancreatic β-cell function.

Statistical Analysis

To assess our hypothesis that the sex-specific association between low muscle mass and glucose fluctuations in hospitalized patients with T2DM with CSII therapy, several analyses were performed. Data were summarized using frequencies and counts for categorical variables and means and standard deviations for continuous variables. Student's *t*-tests or the Mann-Whitney *U* test for continuous variables and Chi-square (χ^2) test for categorical variables were performed to compare the difference in baseline characteristics between diabetic patients with low muscle mass and diabetic patients with non-low muscle mass. An *a priori* sex-specific association between glucose fluctuations and sarcopenia was examined. We used multiple linear regression models to examine the association between low muscle mass and glucose fluctuations (SDBG and LAGE), after adjustment for HbA1c, diabetes duration, hyperlipidemia, diabetic peripheral neuropathy, diabetic nephropathy, and cardiovascular disease in Model 1. We further adjusted for age in Model 2. To further explore whether the relationship was independent of C-peptide, we additionally controlled for diabetes duration in Model 3.

Potential modification effects were assessed through a stratified analysis by the following factors: age (<65 or ≥65), BMI (<18.5, 18.5-23.9, 24.0-27.9, ≥28.0), diabetes duration (<5, 5-9.9, ≥10), diabetic peripheral nephropathy (yes or no), diabetic neuropathy (yes or no), and cardiovascular disease (yes or no). We evaluated the potential effect of modification by modeling the cross-product term of the stratifying variable with low muscle mass.

Two-tailed p-value < 0.05 was considered statistically significant. The data analysis for this article was conducted using SAS version 9.4.

RESULTS

Overall, the prevalence of low muscle mass was 31.2% in all diabetic participants. The prevalence of low muscle mass was higher in males than in females (39.9% vs 18.0%, $p<0.001$) (**Figure 1**). The characteristics of participants were shown in **Table 1** according to the status of low muscle mass and sex of patients. For males, participants with low muscle mass were older, and more likely to have a lower BMI, lower SBP and DBP, longer diabetes duration, higher LDL-c, LAGE, MBG, SDBG, and PPGE, lower TG and C-peptide, and higher prevalence of diabetic neuropathy and hypoglycemia compared with patients without low muscle mass. For females, BMI, SBP, DBP, C-peptide, TG, ALT, and AST were lower in patients with low muscle mass than in those without low muscle mass.

We observed a significant and sex-specific interaction between the status of low muscle mass and glucose fluctuations (LAGE and SDBG) (p for interaction=0.025 and 0.036 for SDBG and LAGE, respectively). In **Table 2**, Among males, low muscle mass was significantly associated with a higher LAGE and SDBG (difference in LAGE: 2.26 [95% CI: 1.01 to 3.51], $p < 0.001$; difference in SDBG: 0.45 [95% CI: 0.25 to 0.65], $p < 0.001$) after adjustment for HbA1c, diabetes duration, hyperlipidemia, diabetic peripheral neuropathy, diabetic nephropathy, and cardiovascular disease (Model 1). These associations remained significant after further adjustment for age (difference in LAGE: 2.17 [95% CI: 0.92 to 3.41], $p < 0.001$; difference in SDBG: 0.41 [95% CI: 0.21 to 0.61], $p < 0.001$ in Model 2), and C-peptide (difference in LAGE: 1.18 [95% CI: 0.51 to 3.11], $p = 0.006$; difference in SDBG: 0.31 [95% CI: 0.11 to 0.52], $p = 0.003$ in Model 3) (**Table 2**). However, among females, no significant association between low muscle mass and LAGE, or SDBG was observed after adjustment for all covariates.

In the stratified analysis (**Table 3**), the associations between low muscle mass and LAGE and SDBG were not modified by risk factors in both males and females, including age, BMI, diabetes duration, diabetic nephropathy, diabetic peripheral neuropathy, or cardiovascular disease.

DISCUSSION

In the present study, based on the included 1084 hospitalized patients with T2DM receiving CSII therapy, we found the prevalence of low muscle mass was higher in males than in females and a significant sex-specific association between low muscle mass and glucose fluctuations (LAGE and SDBG). Low muscle mass was significantly associated with a higher LAGE and SDBG for males after adjustment for HbA1c, diabetes duration, hyperlipidemia, diabetic peripheral neuropathy, diabetic

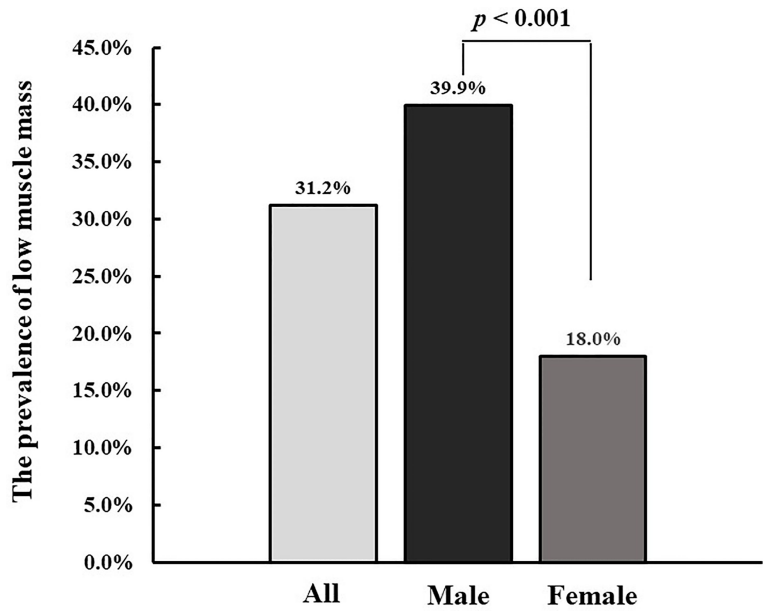

FIGURE 1 | The prevalence of low muscle mass among all patients, male and female, male vs female:

nephropathy, cardiovascular disease, age, and C-peptide, but not for females.

Our findings were in line with a previous study that showed that glucose fluctuations were related to low muscle mass. In the study of 69 T2DM patients diagnosed with or without cognitive impairment, glucose fluctuations were found to be independently associated with sarcopenia, even after adjusting for HbA1c levels and associated factors among patients with cognitive impairment (11).

TABLE 1 | Characteristics of the T2DM participants in the Low muscle mass group and non- Low muscle mass group stratified by sex.

	Female			Male		
	Non- Low muscle mass	Low muscle mass	*p* value	Non- Low muscle mass	Low muscle mass	*p* value
N	355	78		391	260	
Age, mean (SD), y	56.1 (11.5)	57.4 (14.5)	0.369	50.7 (11.7)	53.2 (13.6)	0.014
BMI, mean (SD), kg/m2	25.0 (3.9)	19.8 (2.1)	<0.001	26.2 (3.2)	21.6 (2.5)	<0.001
Systolic BP, mean (SD), mmHg	134.4 (20.7)	123.6 (19.0)	<0.001	130.3 (16.9)	126.4 (18.0)	0.006
Diastolic BP, mean (SD), mmHg	80.6 (10.3)	73.7 (9.0)	<0.001	81.9 (9.8)	78.1 (10.6)	<0.001
Diabetes duration, mean (SD), y	8.5 (2.3)	8.5 (2.8)	0.552	8.1 (2.4)	8.5 (3.0)	0.045
HbA1c, mean (SD), %	9.6 (2.3)	9.8 (2.6)	0.589	9.7 (2.4)	10.2 (9.8)	0.053
C-peptide	1.4 (1.0 to 2.0)	1.0 (0.7 to 1.7)	<0.001	1.5 (1.0 to 2.1)	0.9 (0.5 to 1.5)	<0.001
Total cholesterol, mean (SD), mmol/L	5.2 (1.3)	5.2 (1.5)	0.983	5.1 (1.4)	5.0 (1.4)	0.700
HDL cholesterol, mean (SD), mmol/L	1.3 (0.3)	1.3 (0.4)	0.115	1.2 (0.4)	1.2 (0.3)	0.703
LDL cholesterol, mean (SD), mmol/L	3.0 (1.1)	3.2 (1.2)	0.166	2.7 (2.3)	3.1 (1.1)	0.008
ALT, mean (SD), U/L	25.6 (18.2)	17.9 (14.6)	0.001	33.4 (38.4)	28.1 (29.3)	0.087
AST, mean (SD), U/L	22.0 (12.2)	17.5 (7.8)	0.003	24.1 (19.5)	22.8 (20.0)	0.454
Triglycerides, median (IQR), mmol/L	1.6 (1.2 to 2.4)	1.1 (0.9 to 1.7)	<0.001	1.6 (1.1 to 2.6)	1.1 (0.8 to 1.6)	<0.001
Heart failure, n (%)	14 (3.9)	2 (2.6)	0.559	14 (3.6)	11 (4.2)	0.672
Coronary heart disease, n (%)	97 (27.3)	22 (28.2)	0.875	114 (29.2)	92 (35.40	0.094
Diabetic nephropathy, n (%)	89 (25.1)	13 (16.7)	0.113	83 (21.2)	49 (18.9)	0.46
Diabetic retinopathy, n (%)	174 (49.0)	42 (53.9)	0.44	164 (42.0)	125 (48.1)	0.123
Diabetic peripheral neuropathy, n (%)	97 (27.3)	20 (25.6)	0.762	99 (25.3)	87 (33.5)	0.024
Hypoglycemia, n (%)	41 (11.6)	11 (14.1)	0.530	36 (9.2)	39 (15.0)	0.023
MBG, mean (SD), mmol/L	10.2 (1.9)	10.2 (2.0)	0.865	9.9 (1.7)	10.3 (1.7)	0.003
PPGE, mean (SD), mmol/L	2.8 (0.9)	2.9 (0.7)	0.135	2.9 (1.0)	3.2 (1.0)	0.002
LAGE, mean (SD), mmol/L	13.1(3.4)	13.0 (3.7)	0.816	12.9 (3.2)	14.2 (3.1)	<0.001
SDBG, mean (SD), mmol/L	3.0 (0.9)	3.1(1.0)	0.620	3.1 (0.9)	3.4(0.9)	<0.001
Insulin dosage (units per day per kg)	0.73 (0.2)	0.72 (0.3)	0.312	0.73 (0.2)	0.72 (0.3)	0.398

Values are mean (SD), or median [IQR] for continuous variables, and N (%) for categorical variables. BMI, body mass index; MBG, mean blood glucose; PPGE, postprandial glucose excursion; LAGE, large amplitude of glycemic excursions; SDBG, standard deviation of MBG.

TABLE 2 | Association of low muscle mass with glucose fluctuations (LAGE and SDBG) among participants with type 2 diabetes receiving CSII therapy.

	Model 1 Estimate β (95%CI)	*p* value	Model 2 Estimate β (95%CI)	*p* value	Model 3 Estimate β (95%CI)	*p* value
Female						
LAGE	-0.83 (-3.96 to 2.30)	0.603	-1.18 (-4.35 to 1.99)	0.465	-1.37 (-4.74 to 2.00)	0.426
SDBG	-0.08 (-0.52 to 0.36)	0.724	-0.07 (-0.51 to 0.38)	0.775	-0.13 (-0.60 to 0.34)	0.593
Male						
LAGE	**2.26 (1.01 to 3.51)**	**<0.001**	**2.17 (0.92 to 3.41)**	**<0.001**	**1.18 (0.51 to 3.11)**	**0.006**
SDBG	**0.45 (0.25 to 0.65)**	**<0.001**	**0.41 (0.21 to 0.61)**	**<0.001**	**0.31 (0.11 to 0.52)**	**0.003**

Model 1: adjusted for HbA1c, diabetes duration, hyperlipidemia, diabetic peripheral neuropathy, diabetic nephropathy, and cardiovascular disease;
Model 2: adjusted for covariates in Model 1 + age;
Model 3: adjusted for covariates in Model 2+ C-peptide.
Reference: non- Low muscle mass.
P interaction for between the status of low muscle mass and sex of patients on glucose fluctuations for (LAGE and SDBG) (p for interaction=0.021 and 0.029 for SDBG and LAGE, respectively).
CSII, continuous subcutaneous insulin infusion.
The bold values indicates the significant associations (P < 0.05).

However, the study was based on small sample size and whether the association of glucose fluctuations with sarcopenia among diabetes patients with cognitive impairment was modified by sex was unclear. In addition, previous studies have shown that poor glycemic control was associated with poor lower-limb muscle quality, physical performance, and knee extensor strength (18, 19).

To the best of our knowledge, there was no study performed to explore the role of sex-dependent differences in the relationship between low muscle mass and glucose fluctuations. In our study including 1084 hospitalized patients with T2DM receiving CSII therapy, we found that the association between low muscle mass and glucose fluctuations was sex-specific. Low muscle mass was significantly associated with a higher LAGE and SDBG for males after adjustment for HbA1c, diabetes duration, hyperlipidemia, diabetic peripheral neuropathy, diabetic nephropathy, and cardiovascular disease. A significant relationship has been repeatedly reported for association between sarcopenia and age in T2DM individuals (7, 20). Pancreatic β-cell function is an established risk factor for glucose fluctuations (3, 21, 22). To assess the association between low muscle mass and glucose fluctuations, we adjusted age and C-peptide further. Those associations were also significant after adjustment for age and C-peptide. Those associations were also significant after adjustment for age and C-peptide. But among females, low muscle mass was not associated with LAGE or SDBG after adjustment for all covariates. Low muscle mass is the key component of sarcopenia. There are interactions between T2DM and sarcopenia, and the existence of one disease may increase the risk of developing the other (8, 9). T2DM can negatively affect muscle health through insulin resistance (23, 24), advanced glycation end-products (AGEs) accumulation (25), inflammation (26, 27), oxidative stress (25), impaired protein metabolism (19, 28), vascular mitochondrial dysfunction, and cell death (9). In addition, glucose fluctuation is a greater trigger of oxidative stress and inflammation than sustained hyperglycemia (3, 29, 30) and may be involved in the development and progression of low muscle mass. Low muscle mass induced altered glucose disposal (10) and inter and intramuscular adipose tissue accumulation increased local inflammation (31), furthermore, sarcopenia may result in deterioration for the development and progression of T2DM.

In our study, the prevalence of low muscle mass was higher in males than in females. Low muscle mass was significantly associated with a higher LAGE and SDBG for males, but not for females. Previous researchers have revealed a sex gap in metabolic regulation, diabetes susceptibility and risks for sarcopenia amongst community-dwelling older adults, according to which, males were more likely to be diabetes and sarcopenic (32, 33). The underlying mechanism for such sex difference in the association between low muscle mass and fluctuations is unclear, whereas several potential biological mechanisms may contribute. Firstly, sex hormones play diverse roles in maintaining skeletal muscle homeostasis. Testosterone could exert an anabolic effect on skeletal muscle and estrogens have a protective effect on skeletal muscle. Age-induced sex hormone changes contribute to muscle wasting (34). During the aging process, levels of testosterone and insulin-like growth factor-1 could significantly decrease in males that leading to a rapid loss of muscle mass and strength, which significantly increase the risk of sarcopenia (35). As the largest organ responsible for insulin-induced glucose disposal in humans, the rapid loss of the skeletal muscle in males might lead to diminished insulin-induced glucose disposal and exacerbated insulin resistance, resulting in severe glucose abnormalities (36). Secondly, there are sex differences in metabolic adaption and diabetes susceptibility. Males are more likely to develop obesity, insulin resistance, and hyperglycemia than females in response to nutritional challenges (12). Besides, future studies are required to explore how sex differences contribute to the special association between low muscle mass and glucose fluctuations, further investigations could explore other mechanisms.

A major strength of this study is a large sample of hospitalized T2DM patients receiving CSII therapy was included and the monitoring of capillary blood glucose and tailoring of insulin dosage was conducted following the standard protocol by trained doctors and nurses. There are several limitations in our study. Firstly, due to the limitation of observational studies, they could not control factors that might affect the results of the study, and therefore, we could not identify a causal relationship between low muscle mass and glucose fluctuations in males. Secondly, some

TABLE 3 | Subgroup analyses of associations of low muscle mass with glucose fluctuations (LAGE and SDBG) among participants with type 2 diabetes receiving CSII therapy.

	Female				Male			
	N	Estimate β (95%CI)	*p* value	$p_{interaction}$	N	Estimate β (95%CI)	*p* value	$p_{interaction}$
LAGE								
Age				0.566				0.160
<65	326	-0.27 (-4.17 to 3.62)	0.890		546	1.07 (0.06 to 2.08)	0.017	
≥65	107	-2.79 (-9.82 to 4.25)	0.438		105	5.09 (-0.70 to 10.90)	0.085	
SDBG								
Age				0.434				0.173
<65	326	0.08 (-0.52 to 0.69)	0.793		546	0.22 (0.03 to 0.41)	0.023	
≥65	107	-0.46(-1.28 to 0.36)	0.270		105	0.83 (0.05 to 1.61)	0.037	
LAGE								
BMI				0.214				0.664
<18.5	39	1.11 (-0.95 to 3.18)	0.291		61	11.29 (-1.06 to 22.98)	0.073	
18.5-23.9	209	-0.445 (-1.62 to 0.73)	0.459		278	-0.25 (-1.01 to 0.51)	0.523	
24.0-27.9	127	-3.96 (-9.27 to 1.35)	0.143		218	5.70 (2.35 to 9.05)	<0.001	
≥28.0	58	-3.99 (-10.10 to 1.70)	0.312		94	2.71 (-3.34 to 8.76)	0.390	
SDBG								
BMI								0.674
<18.5	39	0.30 (-0.09 to 0.69)	0.131	0.188	61	1.62 (0.10 to 3.16)	0.037	
18.5-23.9	209	0.01 (-0.29 to 0.31)	0.960		278	-0.04 (-0.25 to 0.31)	0.709	
24.0-27.9	127	-1.05 (-2.47 to 0.36)	0.146		218	0.62 (0.13 to 1.10)	0.012	
≥28.0	58	-1.01 (-2.65 to 0.69)	0.204		94	0.59 (-0.99 to 2.18)	0.562	
LAGE								
Diabetes duration				0.946				0.441
<5	20	5.84 (4.64 to 7.04)	<0.001		20	4.07 (1.13 to 7.01)	0.007	
5-9.9	280	-1.51 (-5.62 to 2.59)	0.469		485	1.96 (0.32 to 3.59)	0.019	
≥10	133	-1.67 (-8.53 to 5.20)	0.634		146	1.65 (-0.47 to 0.45)	0.141	
SDBG								
Diabetes duration				0.967				0.491
<5	20	1.64 (0.90 to 2.31)	<0.001		20	-2.81 (-2.87 to -2.75)	<0.001	
5-9.9	280	-0.26 (-0.89 to 0.37)	0.419		485	0.36 (0.10 to 0.62)	0.006	
≥10	133	-0.09 (-0.92 to 0.74)	0.824		146	0.33 (-0.04 to 0.71)	0.083	
LAGE								
Diabetic nephropathy				0.483				0.228
No	331	-0.77 (-3.93 to 2.37)	0.628		519	2.15 (0.49 to 3.82)	0.011	
Yes	102	-2.48 (-13.59 to 9.80)	0.661		132	0.22 (-0.91 to 1.45)	0.724	
SDBG								
Diabetic nephropathy				0.340				0.283
No	331	-0.03 (-0.52 to 0.46)	0.906		519	0.35 (0.10 to 0.60)	<0.001	
Yes	102	-0.36 (-1.78 to 1.06)	0.620		132	0.09 (-0.25 to 0.42)	0.615	
LAGE								
Diabetic peripheral neuropathy				0.308				0.562
No	316	-0.89 (-3.85 to 2.07)	0.555		465	0.84(-0.61 to 2.29)	0.257	
Yes	117	-0.76(-1.81 to 1.49)	0.467		186	0.85 (-0.60 to 2.29)	0.253	
SDBG								
Diabetic peripheral neuropathy				0.647				0.820
No	316	0.17 (-0.04 to 0.38)	0.120		465	0.32 (0.08 to 0.56)	0.009	
Yes	117	0.17 (-0.04 to 0.38)	0.116		186	0.33 (-0.04 to 0.08)	0.100	
LAGE								
Cardiovascular disease				0.232				0.567
No	314	-0.09 (-3.67 to 3.50)	0.962		445	1.89 (0.06 to 3.72)	0.043	
Yes	119	-2.25 (-10.46 to 5.95)	0.591		206	1.49 (0.02 to 2.96)	0.046	
SDBG								
Cardiovascular disease				0.153				0.606
No	314	0.10 (-0.46 to 0.65)	0.734		445	0.34 (0.05 to 0.62)	0.019	
Yes	119	-0.45 (-1.42 to 0.53)	0.370		206	0.26 (-0.003 to 0.52)	0.052	

Adjusted for HbA1c, diabetes duration, hyperlipidemia, diabetic peripheral neuropathy, diabetic nephropathy, cardiovascular disease, age, and C-peptide.
CSII, continuous subcutaneous insulin infusion.
Reference: non- Low muscle mass.

detailed information, such as physical activity and low muscle strength which may impact glucose control, was not available in this study. Thirdly, standard capillary blood glucose monitoring was applied to evaluate glucose levels, while continuous glucose monitoring (CGM) might represent a more accurate glucose profile. However, the cost of CGM is too high to apply in routine clinical practice in China. Self-monitoring of blood glucose is still commonly used to determine glycemic variability indices,

especially in developing countries (37–39). We measured glucose levels 7 times per day by a trained nurse using a unified glucometer on 7 separate days during the in-hospital period, our data could reflect the characteristics of glucose profiles over this period. Finally, major participants were Chinese, further study should be generalized to other populations.

CONCLUSION

In the present study based on hospitalized patients with T2DM receiving CSII therapy, we found the prevalence of low muscle mass was higher in males than in females and a significant sex-specific association between low muscle mass and glucose fluctuations (LAGE and SDBG). Low muscle mass was significantly associated with a higher LAGE and SDBG for males, but not for females. The findings suggest that we should pay more attention to glucose fluctuations in male T2DM patients with low muscle mass when using medication to control glucose in clinical practice.

DATA AVAILABILITY STATEMENT

The raw data supporting the conclusions of this article will be made available by the authors, without undue reservation.

ETHICS STATEMENT

The studies involving human participants were reviewed and approved by The ethics committee of the First Affiliated Hospital of Xiamen University. The patients/participants provided their written informed consent to participate in this study.

AUTHOR CONTRIBUTIONS

XLS, WJL, WL, and XJL were involved in the design of the study. XLS conducted the data analysis. All authors were involved in the recruitment of participants and blood sample collection. XLS and WJL completed the first draft of the manuscript. All authors were involved in the critical revision of the manuscript. All authors read and approved the final manuscript. XLS, WJL, WL, and XJL guarantee this work and take responsibility for the integrity of the data. All authors contributed to the article and approved the submitted version.

FUNDING

This work was supported by the Natural Science Foundation of Fujian Province, China (No. 2021J011344) and Medical and Health Project of Xiamen (No. 3502Z20214ZD1025).

REFERENCES

1. Ceriello A, Kilpatrick ES. Glycemic Variability: Both Sides of the Story. *Diabetes Care* (2013) 36 (Suppl 2):S272–5. doi: 10.2337/dcS13-2030
2. Škrha J, Šoupal J, Škrha J Jr, Prázný M. Glucose Variability, HbA1c and Microvascular Complications. *Rev endocr Metab Disord* (2016) 17(1):103–10. doi: 10.1007/s11154-016-9347-2
3. Zhang ZY, Miao LF, Qian LL, Wang N, Qi MM, Zhang YM, et al. Molecular Mechanisms of Glucose Fluctuations on Diabetic Complications. *Front Endocrinol* (2019) 10:640. doi: 10.3389/fendo.2019.00640
4. Cruz-Jentoft AJ, Bahat G, Bauer J, Boirie Y, Bruyère O, Cederholm T, et al. Sarcopenia: Revised European Consensus on Definition and Diagnosis. *Age Ageing* (2019) 48(1):16–31. doi: 10.1093/ageing/afy169
5. Anagnostis P, Gkekas NK, Achilla C, Pananastasiou G, Taouxidou P, Mitsiou M, et al. Type 2 Diabetes Mellitus Is Associated With Increased Risk of Sarcopenia: A Systematic Review and Meta-Analysis. *Calcified Tissue Int* (2020) 107(5):453–63. doi: 10.1007/s00223-020-00742-y
6. Veronese N, Stubbs B, Punzi L, Soysal P, Incalzi RA, Saller A, et al. Effect of Nutritional Supplementations on Physical Performance and Muscle Strength Parameters in Older People: A Systematic Review and Meta-Analysis. *Ageing Res Rev* (2019) 51:48–54. doi: 10.1016/j.arr.2019.02.005
7. Izzo A, Massimino E, Riccardi G, Della Pepa G. A Narrative Review on Sarcopenia in Type 2 Diabetes Mellitus: Prevalence and Associated Factors. *Nutrients* (2021) 13(1):183. doi: 10.3390/nu13010183
8. Liccini A, Malmstrom TK. Frailty and Sarcopenia as Predictors of Adverse Health Outcomes in Persons With Diabetes Mellitus. *J Am Med Directors Assoc* (2016) 17(9):846–51. doi: 10.1016/j.jamda.2016.07.007
9. Mesinovic J, Zengin A, De Courten B, Ebeling PR, Scott D. Sarcopenia and Type 2 Diabetes Mellitus: A Bidirectional Relationship. *Diabetes Metab syndrome obesity: Targets Ther* (2019) 12:1057–72. doi: 10.2147/dmso.S186600
10. Scott D, de Courten B, Ebeling PR. Sarcopenia: A Potential Cause and Consequence of Type 2 Diabetes in Australia's Ageing Population? *Med J Aust* (2016) 205(7):329–33. doi: 10.5694/mja16.00446
11. Ogama N, Sakurai T, Kawashima S, Tanikawa T, Tokuda H, Satake S, et al. Association of Glucose Fluctuations With Sarcopenia in Older Adults With Type 2 Diabetes Mellitus. *J Clin Med* (2019) 8(3):319. doi: 10.3390/jcm8030319
12. Tramunt B, Smati S, Grandgeorge N, Lenfant F, Arnal JF, Montagner A, et al. Sex Differences in Metabolic Regulation and Diabetes Susceptibility. *Diabetologia* (2020) 63(3):453–61. doi: 10.1007/s00125-019-05040-3
13. Zhou B. [Predictive Values of Body Mass Index and Waist Circumference to Risk Factors of Related Diseases in Chinese Adult Population]. *Zhonghua liu xing bing xue za zhi = Zhonghua liuxingbingxue zazhi* (2002) 23(1):5–10.
14. Chen LK, Liu LK, Woo J, Assantachai P, Auyeung TW, Bahyah KS, et al. Sarcopenia in Asia: Consensus Report of the Asian Working Group for Sarcopenia. *J Am Med Directors Assoc* (2014) 15(2):95–101. doi: 10.1016/j.jamda.2013.11.025
15. Chen L, Sun W, Liu Y, Zhang L, Lv Y, Wang Q, et al. Association of Early-Phase In-Hospital Glycemic Fluctuation With Mortality in Adult Patients With Coronavirus Disease 2019. *Diabetes Care* (2021) 44(4):865–73. doi: 10.2337/dc20-0780
16. Sokooti S, Kieneker LM, Borst MH, Muller Kobold A, Kootstra-Ros JE, Gloerich J, et al. Plasma C-Peptide and Risk of Developing Type 2 Diabetes in the General Population. *J Clin Med* (2020) 9(9):3001. doi: 10.3390/jcm9093001
17. Jeyam A, Colhoun H, McGurnaghan S, Blackbourn L, McDonald TJ, Palmer CNA, et al. Clinical Impact of Residual C-Peptide Secretion in Type 1 Diabetes

on Glycemia and Microvascular Complications. *Diabetes Care* (2021) 44 (2):390–8. doi: 10.2337/dc20-0567
18. Yoon JW, Ha YC, Kim KM, Moon JH, Choi SH, Lim S, et al. Hyperglycemia Is Associated With Impaired Muscle Quality in Older Men With Diabetes: The Korean Longitudinal Study on Health and Aging. *Diabetes Metab J* (2016) 40 (2):140–6. doi: 10.4093/dmj.2016.40.2.140
19. Kalyani RR, Metter EJ, Egan J, Golden SH, Ferrucci L. Hyperglycemia Predicts Persistently Lower Muscle Strength With Aging. *Diabetes Care* (2015) 38 (1):82–90. doi: 10.2337/dc14-1166
20. Murata Y, Kadoya Y, Yamada S, Sanke T. Sarcopenia in Elderly Patients With Type 2 Diabetes Mellitus: Prevalence and Related Clinical Factors. *Diabetol Int* (2018) 9(2):136–42. doi: 10.1007/s13340-017-0339-6
21. Shao C, Gu J, Meng X, Zheng H, Wang D. Systematic Investigation Into the Role of Intermittent High Glucose in Pancreatic Beta-Cells. *Int J Clin Exp Med* (2015) 8(4):5462–9.
22. Murata M, Adachi H, Oshima S, Kurabayashi M. Glucose Fluctuation and the Resultant Endothelial Injury are Correlated With Pancreatic β Cell Dysfunction in Patients With Coronary Artery Disease. *Diabetes Res Clin Pract* (2017) 131:107–15. doi: 10.1016/j.diabres.2017.07.007
23. Kuo CK, Lin LY, Yu YH, Wu KH, Kuo HK. Inverse Association Between Insulin Resistance and Gait Speed in Nondiabetic Older Men: Results From the U.S. National Health and Nutrition Examination Survey (NHANES) 1999-2002. *BMC geriatrics* (2009) 9:49. doi: 10.1186/1471-2318-9-49
24. Lee CG, Boyko EJ, Strotmeyer ES, Lewis CE, Cawthon PM, Hoffman AR, et al. Association Between Insulin Resistance and Lean Mass Loss and Fat Mass Gain in Older Men Without Diabetes Mellitus. *J Am Geriatrics Soc* (2011) 59 (7):1217–24. doi: 10.1111/j.1532-5415.2011.03472.x
25. Aragno M, Mastrocola R, Catalano MG, Brignardello E, Danni O, Boccuzzi G. Oxidative Stress Impairs Skeletal Muscle Repair in Diabetic Rats. *Diabetes* (2004) 53(4):1082–8. doi: 10.2337/diabetes.53.4.1082
26. Park SW, Goodpaster BH, Strotmeyer ES, Kuller LH, Broudeau R, Kammerer C, et al. Accelerated Loss of Skeletal Muscle Strength in Older Adults With Type 2 Diabetes: The Health, Aging, and Body Composition Study. *Diabetes Care* (2007) 30(6):1507–12. doi: 10.2337/dc06-2537
27. Payette H, Roubenoff R, Jacques PF, Dinarello CA, Wilson PW, Abad LW, et al. Insulin-Like Growth Factor-1 and Interleukin 6 Predict Sarcopenia in Very Old Community-Living Men and Women: The Framingham Heart Study. *J Am Geriatrics Soc* (2003) 51(9):1237–43. doi: 10.1046/j.1532-5415.2003.51407.x
28. Russell ST, Rajani S, Dhadda RS, Tisdale MJ. Mechanism of Induction of Muscle Protein Loss by Hyperglycaemia. *Exp Cell Res* (2009) 315(1):16–25. doi: 10.1016/j.yexcr.2008.10.002
29. Ceriello A, Esposito K, Piconi L, Ihnat MA, Thorpe JE, Testa R, et al. Oscillating Glucose Is More Deleterious to Endothelial Function and Oxidative Stress Than Mean Glucose in Normal and Type 2 Diabetic Patients. *Diabetes* (2008) 57(5):1349–54. doi: 10.2337/db08-0063
30. Ohara M, Nagaike H, Goto S, Fukase A, Tanabe Y, Tomoyasu M, et al. Improvements of Ambient Hyperglycemia and Glycemic Variability Are Associated With Reduction in Oxidative Stress for Patients With Type 2 Diabetes. *Diabetes Res Clin Pract* (2018) 139:253–61. doi: 10.1016/j.diabres.2018.02.017
31. Marcus RL, Addison O, Dibble LE, Foreman KB, Morrell G, Lastayo P. Intramuscular Adipose Tissue, Sarcopenia, and Mobility Function in Older Individuals. *J Aging Res* (2012) 2012:629637. doi: 10.1155/2012/629637
32. Tay L, Ding YY, Leung BP, Ismail NH, Yeo A, Yew S, et al. Sex-Specific Differences in Risk Factors for Sarcopenia Amongst Community-Dwelling Older Adults. *Age (Dordrecht Netherlands)* (2015) 37(6):121. doi: 10.1007/s11357-015-9860-3
33. Du Y, Wang X, Xie H, Zheng S, Wu X, Zhu X, et al. Sex Differences in the Prevalence and Adverse Outcomes of Sarcopenia and Sarcopenic Obesity in Community Dwelling Elderly in East China Using the AWGS Criteria. *BMC endocr Disord* (2019) 19(1):109. doi: 10.1186/s12902-019-0432-x
34. Anderson LJ, Liu H, Garcia JM. Sex Differences in Muscle Wasting. *Adv Exp Med Biol* (2017) 1043:153–97. doi: 10.1007/978-3-319-70178-3_9
35. Kim KM, Jang HC, Lim S. Differences Among Skeletal Muscle Mass Indices Derived From Height-, Weight-, and Body Mass Index-Adjusted Models in Assessing Sarcopenia. *Korean J Internal Med* (2016) 31(4):643–50. doi: 10.3904/kjim.2016.015
36. NCD Risk Factor Collaboration (NCD-RisC) Abarca-Gómez L, Abdeen ZA, Abdul Hamid Z, Abu-Rmeileh NM, Acosta-Cazares B, Acuin C, et al. Worldwide Trends in Body-Mass Index, Underweight, Overweight, and Obesity From 1975 to 2016: A Pooled Analysis of 2416 Population-Based Measurement Studies in 128.9 Million Children, Adolescents, and Adults. *Lancet (London England)* (2017) 390(10113):2627–42. doi: 10.1016/s0140-6736(17)32129-3
37. Klatman EL, Jenkins AJ, Ahmedani MY, Ogle GD. Blood Glucose Meters and Test Strips: Global Market and Challenges to Access in Low-Resource Settings. *Lancet Diabetes Endocrinol* (2019) 7(2):150–60. doi: 10.1016/s2213-8587(18)30074-3
38. Weinstock RS, Braffett BH, McGuigan P, Larkin ME, Grover NB, Walders-Abramson N, et al. Self-Monitoring of Blood Glucose in Youth-Onset Type 2 Diabetes: Results From the TODAY Study. *Diabetes Care* (2019) 42(5):903–9. doi: 10.2337/dc18-1854
39. Zhang Y, Dai J, Han X, Zhao Y, Zhang H, Liu X, et al. Glycemic Variability Indices Determined by Self-Monitoring of Blood Glucose Are Associated With β-Cell Function in Chinese Patients With Type 2 Diabetes. *Diabetes Res Clin Pract* (2020) 164:108152. doi: 10.1016/j.diabres.2020.108152

Conflict of Interest: The authors declare that the research was conducted in the absence of any commercial or financial relationships that could be construed as a potential conflict of interest.

Publisher's Note: All claims expressed in this article are solely those of the authors and do not necessarily represent those of their affiliated organizations, or those of the publisher, the editors and the reviewers. Any product that may be evaluated in this article, or claim that may be made by its manufacturer, is not guaranteed or endorsed by the publisher.

frontiers | Frontiers in Physiology

ORIGINAL RESEARCH
published: 03 August 2022
doi: 10.3389/fphys.2022.893862

Inferring Insulin Secretion Rate from Sparse Patient Glucose and Insulin Measures

Rammah M. Abohtyra[1,2], *Christine L. Chan*[3], *David J. Albers*[4] *and Bruce J. Gluckman*[1,2,5,6]*

[1]Center for Neural Engineering, The Pennsylvania State University, University Park, PA, United States, [2]Department of Engineering Science and Mechanics, The Pennsylvania State University, University Park, PA, United States, [3]Section of Pediatric Endocrinology, University of Colorado School of Medicine, Aurora, CO, United States, [4]Department of Bioengineering, University of Colorado School of Medicine, Aurora, CO, United States, [5]Department of Neurosurgery, College of Medicine, The Pennsylvania State University, University Park, PA, United States, [6]Department of Biomedical Engineering, The Pennsylvania State University, University Park, PA, United States

The insulin secretion rate (ISR) contains information that can provide a personal, quantitative understanding of endocrine function. If the ISR can be reliably inferred from measurements, it could be used for understanding and clinically diagnosing problems with the glucose regulation system.

Objective: This study aims to develop a model-based method for inferring a parametrization of the ISR and related physiological information among people with different glycemic conditions in a robust manner. The developed algorithm is applicable for both dense or sparsely sampled plasma glucose/insulin measurements, where sparseness is defined in terms of sampling time with respect to the fastest time scale of the dynamics.

Methods: An algorithm for parametrizing and validating a functional form of the ISR for different compartmental models with unknown but estimable ISR function and absorption/decay rates describing the dynamics of insulin accumulation was developed. The method and modeling applies equally to c-peptide secretion rate (CSR) when c-peptide is measured. Accuracy of fit is reliant on reconstruction error of the measured trajectories, and when c-peptide is measured the relationship between CSR and ISR. The algorithm was applied to data from 17 subjects with normal glucose regulatory systems and 9 subjects with cystic fibrosis related diabetes (CFRD) in which glucose, insulin and c-peptide were measured in course of oral glucose tolerance tests (OGTT).

Results: This model-based algorithm inferred parametrization of the ISR and CSR functional with relatively low reconstruction error for 12 of 17 control and 7 of 9 CFRD subjects. We demonstrate that when there are suspect measurements points, the validity of excluding them may be interrogated with this method.

Significance: A new estimation method is available to infer the ISR and CSR functional profile along with plasma insulin and c-peptide absorption rates from sparse measurements of insulin, c-peptide, and plasma glucose concentrations. We propose

OPEN ACCESS

Edited by:
Stephanie Therese Chung, National Institutes of Health (NIH), United States

Reviewed by:
Ram Jagannathan, Emory University, United States
Pranay Goel, Indian Institute of Science Education and Research, India

***Correspondence:**
Bruce J. Gluckman
BruceGluckman@pus.edu

Specialty section:
This article was submitted to Clinical and Translational Physiology, a section of the journal Frontiers in Physiology

Received: *10 March 2022*
Accepted: *21 June 2022*
Published: *03 August 2022*

Citation:
Abohtyra RM, Chan CL, Albers DJ and Gluckman BJ (2022) Inferring Insulin Secretion Rate from Sparse Patient Glucose and Insulin Measures. Front. Physiol. 13:893862. doi: 10.3389/fphys.2022.893862

a method to interrogate and exclude potentially erroneous OGTT measurement points based on reconstruction errors.

Keywords: estimation algorithm, ISR function, compartment models, insulin and C-peptide, OGTT, and CSR/ISR molar ratio

1 INTRODUCTION

Insulin is the essential hormone that regulates cellular energy supply and the intracellular transport of glucose into muscle and adipose tissues (Wilcox, 2005). The endogenous insulin secretion rate (ISR) quantifies the amount of insulin the body is able to produce as a function of glucose concentration in the blood, providing important information for understanding how an individual's endocrine system is able to use insulin to regulate glucose regulation. The primary physiological stimulation for insulin secretion from beta-cell is elevated blood glucose levels following nutrition intake and glucose bolus (Ahrén and Pacini, 2004).

The objective of this work is to provide a methodology to infer the *functional form* of the ISR from insulin and glucose measurements at a personalized level that is robust to outliers.

Our motivation for this objective is threefold: First, from a clinical diagnostic standpoint, the ISR is a measure of the input/output function of a segment of the glucose regulation system - the pancreatic beta cells - and therefore would allow monitoring of their health or disease progression; second, accurate parametrization of the functional performance of the beta cells will allow more accurate modeling of the glucose regulation system and therefore understanding of normal and abnormal glucose regulation; and third, personalized ISR estimation combined with better modeling will allow for better interpretation of aberrant dynamics observed in standard glucose monitoring protocols.

In addition, glucose tolerance tests are intrusive and burdensome for subjects and have a relatively high rate of error due to outliers which limits their usefulness at a population scale. The development of an ISR estimation method that is robust to outliers, or able to identify and exclude outliers, increases the practical applicability of such tests.

Computational models of glucose regulation do already exist and have embedded in them model components for beta-cell function. But different models invoke significantly different functions for the ISR, as illustrated in the **Figure 1A** for the studies in (Tolić et al., 2000; Liu et al., 2009; Ha et al., 2016). These different ISR functions lead to significantly different glucose dynamics if used interchangeably within the same glucose regulation model for the same system input, as illustrated in the **Figures 1B,C**. Note that the functional forms change both the height and time course of the blood glucose response.

The most common methods to estimate ISR utilize plasma insulin and c-peptide concentration measurements. C-peptide (connecting peptide) is an amino acid polypeptide that is released, along with insulin, from the pancreatic beta cells when proinsulin is split into insulin and c-peptide (Steiner et al., 1967; Rigler et al., 1999), at a molar release ratio of 1:1 (ISR to c-peptide secretaoin rate CSR) (Lebowitz and Blumenthal, 1993). C-peptide is often used to distinguish insulin produced by the body from injected insulin to estimate ISR, to determine insulin resistance, and to indicate a differential diagnosis of fasting hypoglycemia with hyperinsulinism. Pancreatic beta cells release both insulin and c-peptide directly into the blood stream in the portal vein, which then passes through the liver and then combines with the rest of the circulating blood. Insulin is sensed by hypatocrytes, and signals them to start glucose uptake, and inhibit gluconeogenesis, glycogenolysis, and ketogenesis (Brundin, 1999), and at high levels to activate carcino-embryonic antigen-related cell adhesion molecule 1 (CEACAM1) to increase hypatic insulin clearance (Najjar and Perdomo, 2019). In contrast to insulin, c-peptide is primarily degraded by the kidneys (Jones and Hattersley, 2013). Insulin is degraded within 15–30 min in the bloodstream (Farris et al., 2003), while c-peptide degradation is longer (Leighton et al., 2017).

Glucose tolerance, insulin resistence, and insulin secretion in a clinical setting are generally measured with various types of glucose tolerance tests. These tests include the intravenous glucose tolerance test (IVGTT) (Bergman et al., 1981), fasting glucose assessment (Matthews et al., 1985; Pacini and Mari, 2003), and the oral glucose tolerance test (OGTT) (Ferrannini and Mari, 2004). IVGTT are less frequently performed because they are invasive and challenging to endure to the patient and expensive to achieve (Lotz et al., 2009) because of the frequent sampling protocols of the c-peptide up to every minute during an IVGTT. The more commonly used OGTT requires fasting patients to ingest a drink with a fixed amount of glucose followed by glucose measurements every 15–30 min over the subsequent two to 4 hours (Reaven et al., 1993).

Several model-based estimation methods have been developed to estimate ISR in the sense of the time course of insulin production. One approach is to estimate from insulin and c-peptide measurements (Watanabe et al., 1998; Watanabe and Bergman, 2000; Kjems et al., 2001; Venugopal et al., 2021). These multiple compartment methods treat ISR as an unknown time trajectory either without *a priori* knowledge of its secretion rate function or with different functions to describe the secretion rate. For example, in (Kjems et al., 2001), the deconvolution method is used to estimated ISR by modeling ISR with two exponential functions (biexponential model) with unknown parameters. Another approach that has both one-compartment model (Watanabe et al., 1998) and two-compartment model (Watanabe and Bergman, 2000) forms is used to estimate the time traces of ISR using a smoothed c-peptide profile generated by cubic spline interpolation. More recently, Venugopal et al. (2021) developed a method to estimate ISR using the Oral c-peptide Minimal Model (OCMM). This method describes

the ISR function by two rates proportional linearly with the c-peptide and glucose concentrations. Another recent estimation approach based on OGTT measurements of insulin and c-peptide has been developed to estimate the ISR time traces using two different models, for insulin and c-peptide (Schiavon et al., 2021).

To this end, we develop a new estimation algorithm to infer the ISR from glucose/insulin measurements such as OGTT data. Using a compartmental model for the accumulation/degradation of insulin similar to (Tolić et al., 2000; Liu et al., 2009; Ha et al., 2016), this new method begins with a parametrization of the form of the ISR function that takes glucose concentration as an input and then estimates the parametrization parameters by minimizing the difference between the model output and insulin measurements. The same accumulation/degradation model and inference method can be used to independently infer the c-peptide secretion rate from glucose/c-peptide data when available.

We note that the method we derive is not reliant on the experimental protocol being an OGTT, nor that all the data are measured densely with respect to the fastest time scale of the glucose or insulin dynamics. This time is estimated in the literature to be on the order of 8–20 min for circulating glucose/insulin dynamics, and faster if one is trying to resolve the pulsitivity of insulin production. In this sense it works with sparsely sampled data. This definition is in contrast to terms in the literature that refer to OGTTs with less than 7, and as little as 3, measurement points as 'sparse OGTTs'.

When both insulin and c-peptide are available, because the ISR and CSR functionals are independently inferred, we can use the expected 1:1 M ratio to validate the estimates and to identify data-related errors.

Our approach provides physiological insights into beta-cell secretion rates for people with different ISR health conditions. We validate the performance of the approach using OGTT clinical data for control and CFRD subjects.

2 MATERIALS AND METHODS

The proposed algorithm uses parametric models including a single and a two-compartment model, and ISR and CSR function forms with physiological parameters. The parameters of these models and ISR/CSR functions are assumed unknown, but can be inferred from patient data, including plasma glucose, insulin, and c-peptide measurements. We test the performance of this algorithm using OGTT clinical data collected from control and CFRD subjects.

2.1 Human Oral Glucose Tolerance Test Data

Data used is a subset of data collected under the GlycEmic Monitoring in CF (GEM-CF, NCT02211235), a study of early glucose abnormalities in youth with cystic fibrosis. The study was approved by the Colorado Multiple Institutional Review Board (Aurora, CO), and informed consent and assent obtained. Collection details have been previously published in (Tommerdahl et al., 2021; Chan et al., 2022).

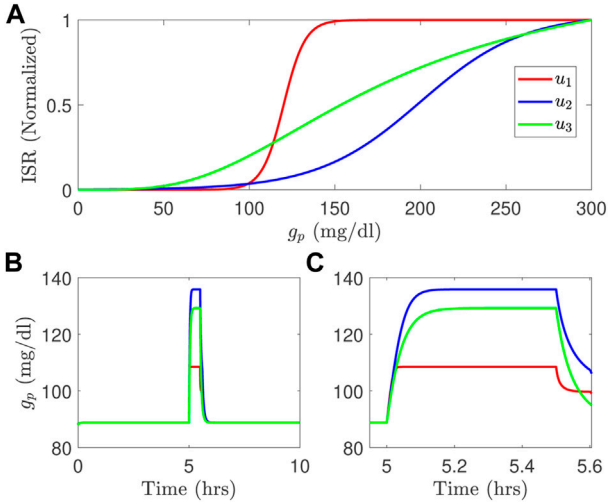

FIGURE 1 | Three different ISR functions **(A)** generate blood glucose variations, in long time course **(B)** and short time course **(C)** simulated using the model developed by Topp et al. (2000) with a meal; u_1 is the ISR function adopted from Liu et al. (2009); u_2 is the ISR used in Tolić et al. (2000), and u_3 is the ISR function used in the model of Ha et al. (2016).

In short, inclusion criteria for participants with CFRD included a confirmed diagnosis of CFRD by newborn screen, sweat chloride testing, or genetic testing. Exclusion criteria for participants with CFRD included known Type 1 or Type 2 diabetes, use of medications affecting glucose (eg, insulin, systemic steroids) in the prior 3 months, hospitalization in the prior 6 weeks, or pregnancy. For this report, n = 9 youth with CFRD were included. N = 3 (33%) were male. CFRD individuals were an average age of 14.6 ± 3.2 years with a mean BMI of 19.0 ± 2.7 kg/m^2 and BMI z-score of - 0.28 ± 0.53. Glucose tolerance categories by OGTT were as follows—6 CFRD patients had CFRD based on 2 h OGTT glucose > 200 mg/dl and 3 were classified as NGT. The CF cohort had an average A1C of 5.7 ± 0.2%.

Healthy controls without CFRD were identified using recruitment flyers and emails at the University of Colorado Anschutz Medical Campus. Exclusion criteria for healthy controls (HCs) included diagnoses of diabetes or prediabetes, overweight (defined as BMI ≥85th% by the Centers for Disease Control and Prevention BMI growth charts in youth), chronic disease, acute illness, or pregnancy. A total of n = 17 HCs were included of which n = 9 (53%) were male. HCs had an average age of 13.3 ± 3.6 years, BMI of 18.5 ± 2.9 kg/m^2, and BMI z-score of −0.20 ± 0.68. The HCs had an average A1C of 5.3 ± 0.2%.

Subjects underwent a standard OGTT protocol, with blood drawn at times.$t_i \in \{-10, 0, 20, 30, 60, 90, 120, 150, 180\}$ min, and assayed for plasma glucose, insulin, and c-peptide concentrations.

2.2 Insulin and C-peptide Models

The two models, described in **Figure 2**, are used in the algorithm to reconstruct ISR and CSR. These models, include a single and a two-compartment model both of which use the same ISR and CSR function but with different parameters to describe the time evolution of plasma insulin and c-peptide. The single

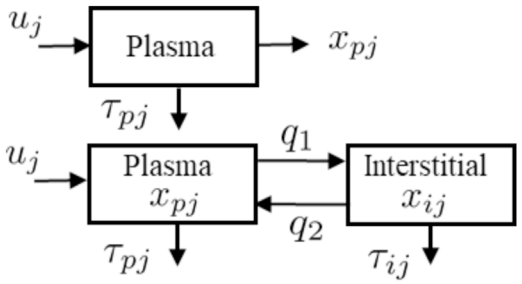

FIGURE 2 | Schematic representations for the single-compartment model (Top) used to describe plasma insulin and c-peptide, and two-compartment model (Bottom) used to describe both plasma and interstitial insulin and c-peptide.

compartment model consists of a single plasma pool with a degradation time for plasma insulin and c-peptide. On the other hand, the two-compartment model tracks insulin and c-peptide concentrations in both plasma and interstitial compartments.

2.2.1 Single Compartment Model

The detail of the single model (**Figure 2** Top) is parameterized as follows. The pancreatic beta-cell, which has a nonlinear output secretion function, is denoted by u_j, the subscript j is an index that takes I for insulin and $Cpep$ for c-peptide, and releases insulin and c-peptide using various physiological parameters. The subscript p denotes plasma, τ_{pI} and τ_{Cpep} denote the degradation time for the plasma insulin and c-peptide, respectively. The single compartment model is given by the equation:

$$\dot{x}_{pj} = u_j(t) - x_{pj} \Big/ \tau_{pj} \tag{1}$$

where x_{pj} is plasma insulin or c-peptide, and τ_{pj} is the associated degradation time.

Following (Tolić et al., 2000; Liu et al., 2009), we use a sigmodal function, which is glucose dependent, for both ISR (u_{pI}) and CSR (u_{pC}) are given by

$$u_j\big(g_p(t)\big) = \frac{K_m}{1 + e^{\left(\alpha\left(C_0 - g_p(t)\right)\right)}}. \tag{2}$$

Here, $g_p(t)$ (mg/dl) is the plasma glucose concentration at a given time t (min), K_m represents a maximum production rate for insulin (μU/ml/min) or c-peptide (ng/ml/min), C_0 refers to a glucose mid-point (mg/dl), and α represents 1/width (dl/mg) of the sigmoid curve.

We combine the unknown parameters of the single compartment model in this vector Θ_s:

$$\boldsymbol{\Theta}_s = \left[\tau_{pj}, K_m, C_0, \alpha\right]^T. \tag{3}$$

2.2.2 Two Compartment Model

The two compartmental model, as shown in **Figure 2** (Bottom), is comprised of two equations:

$$\dot{x}_{pj} = u_j + q_2 x_{ij} - \left(q_1 + 1\big/\tau_{pj}\right)x_{pj} \tag{4a}$$

$$\dot{x}_{ij} = q_1 x_{pj} - \left(q_2 + 1\big/\tau_{ij}\right)x_{ij} \tag{4b}$$

where x_{pj} and x_{ij} represent the insulin (or c-peptide) concentrations in the plasma (p) and interstitial (i) compartments; q_1 and q_2 represent the mass transport between these two compartments; τ_{pj} and τ_{ij} refer to the degradation time for insulin or c-peptide in the plasma and interstitial spaces. The values of $q_1 = 0.0473$ (min^{-1}) and $q_2 = 0.0348$ (min^{-1}) are adopted from the transport model of (Eaton et al., 1980). Alternatives to this model include the diffusive transport used, for example, in the ultradian model (Tolić et al., 2000). We combine the unknown parameters of the two compartment model in this vector Θ_m:

$$\boldsymbol{\Theta}_m = \left[\tau_{pj}, \tau_{ij}, K_m, C_0, \alpha\right]^T \tag{5}$$

Finally, we provide a summary for the two models given in **Eq. 1** and **Eq. 4**, as follows:

- The accumulation dynamics of the insulin and c-peptide use the same compartment models but with different parameters.
- u uses the same function for both ISR and CSR, and this function depends only on the blood glucose values.
- The function of $u(\bar{g})$ is given by a sigmoid **Eq. 2** as a function of interpolated (at 1 min) blood glucose values $\bar{g}$, described in the next section.
- The parameters of u (K_m, C_0, α), along with degradation time (τ_{pj}, τ_{ij}), are unknown and estimated independently from insulin and c-peptide measurements.

2.2.3 Compact Form Model

It is convenient and, as we'll show, computationally efficient to express these compartmental models in a compact state-space model form:

$$\dot{x} = A(\boldsymbol{\Theta})x + Bu\big(\boldsymbol{\Theta}, g_p\big) \tag{6a}$$

$$y = Cx \tag{6b}$$

where x, A, B, C, and $\boldsymbol{\Theta}$ are specific model state and parameters. For the single compartment model (2), we have $x = x_{pj}$, $A = 1/\tau_{pj}$, $B = 1$, $C = 1$, and $\boldsymbol{\Theta} = \boldsymbol{\Theta}_s$, which is defined in **Eq. 3**. For the two compartment model (4), we have $x = [x_{pj}, x_{ij}]^T$,

$$A = \begin{bmatrix} -\left(q_1 + 1\big/\tau_{pj}\right) & q_2 \\ q_1 & -\left(q_2 + 1\big/\tau_{ij}\right) \end{bmatrix} \tag{7}$$

$B = [1,0]^T$, $C = [1, 0]$, and $\boldsymbol{\Theta} = \boldsymbol{\Theta}_m$ defined in **Eq. 5**.

Since we use discrete-time data, the state space model, (6), is discretized at a sampling rate of $T_s = 0.1$ min and then given by

$$x_{k+1} = \Phi(\boldsymbol{\Theta})x_k + \Gamma(\boldsymbol{\Theta})u_k\big(\boldsymbol{\Theta}, \bar{g}\big) \tag{8a}$$

$$y_k = Cx_k \tag{8b}$$

where $\Phi = e^{AT}$ and $\Gamma = \int_0^T e^{ATs} ds B$. The input u_k is the ISR or CSR, which is a function of both $\boldsymbol{\Theta}$ and the interpolated glucose values $\bar{g}$ generated from cubic interpolation method.

3 RESULTS

The main contribution of this paper is the development of a new estimation approach to infer the ISR from data. The uncertainty in the estimation is studied based on random initial conditions used with the proposed approach to optimize the unknown parameters.

3.1 The Estimation Algorithm

Our new estimation method utilizes the above state space model, (8), and is based on the nonlinear least square method (Hansen et al., 2013) to optimize parameters that provide the best fit between the model's output (blood insulin or c-peptide) and data. The proposed algorithm uses interpolated blood glucose values as an input to the algorithm.

In practice, the time intervals of the measured blood glucose varies between 10 and 30 min, and are assumed to sufficiently cover shape of the glucose dynamics. This allows us to interpolate the glucose dynamics in order to resample the glucose values with sufficient time resolution to integrate the insulin or c-peptide dynamics, for which these measured time intervals are too long (sparse). We use cubic interpolation to resample the blood glucose values between the actual measurements to generate an interpolated glucose trajectory ($\bar{g}$) with a time step $T = 1$ min. This input glucose trajectory is used within the ISR or CSR function $u(\Theta, \bar{g})$ to integrate the model forward generating a model insulin or c-peptide trajectory $y(\mathbf{\Theta}, t)$. We take values from this trajectory at t_k, which are the times of the actual insulin or c-peptide measurements, and use them in the algorithm to optimize the parameters.

For given measurements of glucose and blood insulin or c-peptide: z (1), z (2), ..., $z(n)$, we minimize following least squares objective function $J(\mathbf{\Theta})$ to obtain $\hat{\Theta}$:

$$J(\mathbf{\Theta}) = \sum_{k=0}^{N} \left(z(k) - y(\mathbf{\Theta}, t_k)\right)^2 \tag{9}$$

where $y(\mathbf{\Theta}, t_k)$ is the model output (blood insulin or c-peptide) generated by $\bar{g}$, and $z(k)$ is a measured insulin or c-peptide value. Note that insulin and c-peptide are optimized independently. In **Figure 3**, we provide a schematic representation for our **Algorithm 1**. The algorithm consists of two nested loops: the outer one loops over a random set of initial conditions $\{\mathbf{\Theta}_{n,0}\}$, and the inner loop is based on the Levenberg-Marquardt method where the value Θ_n is updated on the ith cycle by $\Theta_{n,i+1} = \Theta_{n,i} - \nabla_{n,i}$ where $\nabla_{n,i}$ uses the steepest descent method (Marquadt, 1963; Levenberg, 1944). We use the MATLAB function 'lsqcurvefit' to implement this inner loop.

3.1.1 Uncertainty Quantification

The method as described is a nonlinear optimization process. It is not known or proven that for this process there is either a global minimum, or only one local minimum, of the objective function (**Eq. 9**). Therefore there is potential sensitivity to the initial conditions (initial guess for $\mathbf{\Theta}$). To address this, and to provide uncertainty quantification for the inferred parameterization, we adopt a bootstrap method.

We therefore explore the distribution of inferred parameters $\hat{\mathbf{\Theta}}$ from a large (1,000) randomly sampled initial conditions drawn from a range of allowed parameters defined within physiologically plausible ranges. In this analysis, $\tau_{px} \in [10, 180]$ min, $C_0 \in [200, 1{,}500]$ mg/L, $K_m \in [1, 350]$ mU/l/min, and $\alpha \in [0.015, 0.045]$ L/mg.

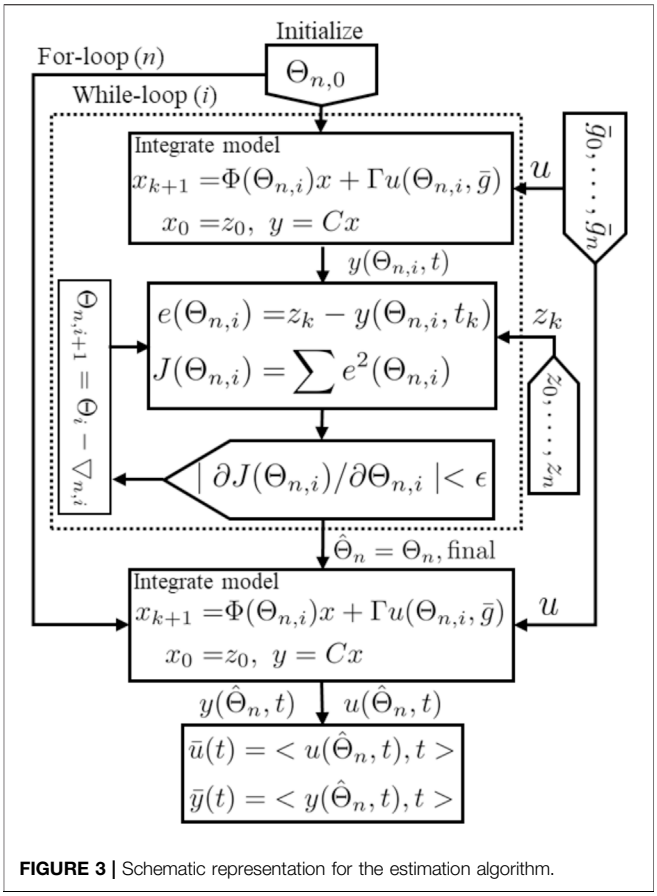

FIGURE 3 | Schematic representation for the estimation algorithm.

For each initial parameter $\mathbf{\Theta_0}$ the algorithm seeks a final parameter $\mathbf{\Theta}_f$ that minimizes J (**Eq. 9**) within the boundaries. If the minimization process reaches the allowed boundaries, the result is excluded.

Each solution in $\mathbf{\Theta}_f$ is used within the ISR/CSR function to simulate ISR and CSR trajectories and then generate plasma insulin and c-peptide trajectories by integrating the model, (8), forward using the interpolated glucose values as an input. Finally, we use these trajectories to compute the average and standard deviation (Mean ± SD). These steps are illustrated in **Algorithm 1**.

1. For over n
2. Initialize $\Theta_{n,0}$
3. While i ($| \partial J(\Theta_{n,i})/\partial \Theta_{n,i} | < \epsilon$ & $\Theta_{n,i} \in$ allowed range)
4. Integrate model (8) to get $y(\Theta_{n,i}, t)$
5. Compute: $J(\Theta_{n,i}) = \sum (z_k - y(\Theta_{n,i}, t_k))^2$
6. $\Theta_{n,i+1} = \Theta_{n,i} - \nabla_{n,i}$($\nabla_{n,i}$ steepest descent)
7. $\hat{\Theta}_n = \Theta_{n,\text{final}}$
8. Integrate model (8) to get $y(\hat{\Theta}_n, t)$
9. Average over $\hat{\Theta}_n$ in allowed range

$\bar{y}(t) = \langle y(\hat{\Theta}_n, t), t \rangle$, $\bar{u}(t) = \langle u(\hat{\Theta}_n, t), t \rangle$

3.2 Computational Method Validation

We validate the inference method by applying the algorithm to model-generated data sets. We then compare the inferred ISR

parametrization, and decay constant, to the model parameters used to generate the data.

Data sets were generated with the model described in Liu et al. (2009), with the published parameters unless otherwise noted. The ISR used matched the functional form in **Eq. 2**, with parameters K_m = 0.6 (mU/l/min), C_0 = 1,000 (mg/L), α = 0.01 (L/min). Data sets were generated for each of the following insulin degradation rates $\tau_{pI} \in \{10, 15, 30, 60, 90, 120\}$ min. The model was driven with an OGGT type feeding function, glucose and insulin values sampled at discrete times $T_i \in \{-10, 0, 10, 20, 30, 60, 90, 120, 150, 180\}$ min, and 20% random noise was added.

The inferred values of τ_{pI} matched the ideal (generating) values within 1.8% (i.e., $|\tau_{pI,i} - \tau_{pI}|/\tau_{pI} < 1.8\%$), and the other parameters (K_m, C_0, α) within a roughly average error of 1.2% of the generating parameter value.

We note that we achieved a very high level of accuracy in inference of these parameters almost independent of how sparsely the data was sampled with respect to the insulin dynamics (τ_{pI}, and robust to the presence of significant (20%) added measurement noise.

3.3 Application to Oral Glucose Tolerance Test Data

We use this method with clinically measured OGTT data, including plasma glucose, insulin, and c-peptide measurements, to parametrize the ISR/CSR functions ($\hat{\mathbf{\Theta}}$).

These measurements are taken from normal and CFRD subjects at times $t_i = \{-10, 0, 20, 30, 60, 90, 120, 150, 180\}$ min. The glucose values are interpolated at 1 min intervals using cubic interpolation and then used as an input for estimation, and as described $\hat{\mathbf{\Theta}}$ is the mean parameters over minimizations of the cost function $J(\mathbf{\Theta})$ (**Eq. 9**).

Given that insulin and c-peptide are secreted in a 1:1 M ratio (Lebowitz and Blumenthal, 1993), we expect that the parametrized functionals ISR and CSR should follow a similar linear relationship. Note that in the presented units for ISR (μ U/ml-min) and CSR (ng/ml-min), a 1:1 M ratio corresponds to 0.056 = ng/μ U. We therefore also fit the relation between CSR and ISR with a linear fit to get $\widetilde{CSR}(ISR)$.

Shown in **Figure 4** are stereotypical results for control (upper group) and CFRD subjects (lower panels). The actual glucose measurements (blue circles) and interpolated glucose (magenta), used as an input to the algorithm, are shown in the **Figure 4A**. Also, the measured c-peptide (red circles) and estimated c-peptide (magenta with standard deviation (±SD) black, green) are presented in the **Figure 4B**. Histograms of the inferred degradation times are shown for both c-peptide (**Figure 4C**) and insulin (**Figure 4D**). Measured insulin (red circles) and estimated insulin (magenta) are shown (with ±SD black, green) in the **Figure 4E**. Estimated ISR and CSR are presented with ±SD (black, green) are shown in the **Figures 4F,G** for the time points at which data was taken.

In both examples, the relationship between CSR and ISR closely matches a linear fit, with slope of order the expected value of 0.056 = ng/μU.

3.3.1 Quantification of Goodness of Fit

We quantify the goodness of fit of three different features of these fits the measured values; how well the trajectory of the modeled insulin ($I(t|\mathbf{\Theta})$) fits the measured values, how well the trajectory of the modeled c-peptide ($C(t|\mathbf{\Theta})$ fits the measured c-peptide values; and goodness of the linear fit between the CSR and ISR, $\widetilde{CSR}(ISR)$. In each of these cases, we use normalized root-mean-square (RMS) errors:

$$RMS_{I_k} = \frac{1}{\bar{I}_k}\sqrt{\sum_k I_k - I\left(t_k|\hat{\mathbf{\Theta}}\right)^2} \tag{10a}$$

$$RMS_{C_k} = \frac{1}{\bar{C}_k}\sqrt{\sum_k C_k - C\left(t_k|\hat{\mathbf{\Theta}}\right)^2} \tag{10b}$$

$$RMS_{CSR(ISR)} = \frac{1}{CSR_{k,max}}\sqrt{\sum_k CSR(t_k) - \widetilde{CSR}(ISR(t_k))^2} \tag{10c}$$

where $\bar{I}_k$ is the mean of the measured insulin values, $\bar{C}_k$ is the mean of the measured c-peptide values, and $CSR_{k,\max}$ is the maximum CSR value.

Estimation results are obtained and evaluated for all control and CFDR subjects. Based on the goodness of fit values (**Eq. 10**), our algorithm achieved relatively good estimates of ISR and CSR for 12 of 17 (71%) control subjects and 7 of 9 (78%) CFRD subjects. Error estimates are shown in **Figure 5** plotted for the output for each of the control subjects (filled circles). As can be seen in the left panel, four subjects had very high RMS error in reconstruction of both insulin trajectories (red). In addition, at least one subject's fit had especially poor linear relationship between CSR and ISR (blue).

3.3.2 Identification of Potential Outlier Data Points

We hypothesize that for these data sets, approximately 30% of the subjects' data have at least one outlier data point that is sufficient to corrupt the inference. Such outliers would also interfere with clinical diagnostics, and therefore the ability to identify and correct for these outliers would be a substantial gain.

In the five poorly estimated control subjects, we observed glucose values that had rather severe dip at 60 min, and then a recovery to a middle value, as illustrated in **Figure 6A**, which we suspect may be in error.

To test our interpretation for poor estimates, we consider one control subject with an uncertain glucose measurement that dropped at 60 min, from 140 mg/dl to 85 mg/dl. We then removed this 60 min glucose value and the associated insulin and c-peptide measurements. Since we use glucose interpolation as an input to the model, the gap between the glucose values between 30 and 90 min is filled by the interpolated glucose values, as shown in **Figures 6A,B**. Without the value at 60min, the insulin and c-peptide measurements are used to re-estimate the parameters. As shown in (D, F), the computed insulin and c-peptide trajectories better match the residual measured values, and the relationship between CSR and ISR is better fit by a line (H).

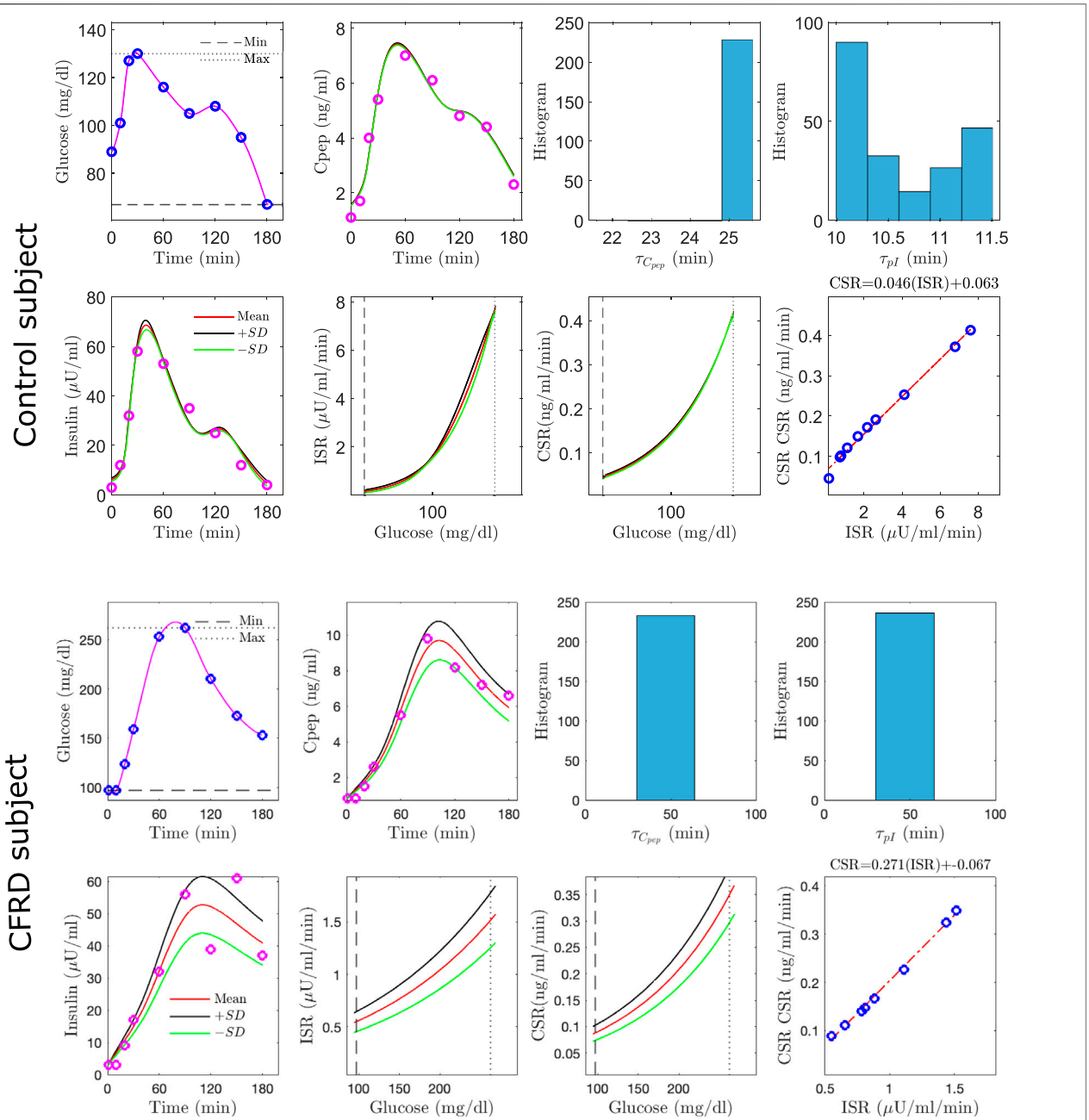

FIGURE 4 | Estimation results, using the algorithm with the single compartment model, for a single control (Top) and a single CFDR (Bottom) subject. Each composite includes **(A)** glucose measurements (blue circles) and the interpolated glucose (magenta line) used as model input **(B)** measured c-peptide (circles) and model-generated mean c-peptide (magenta line) and ±standard deviation (black, green lines); histograms of inferred degradation time for c-peptide **(C)** and insulin **(D)**; **(E)** measured insulin (red circles) and estimated insulin trajectory (magenta with ±SD black, green); mean inferred ISR **(F)** and CSR **(G)** (red with SD black, green); and **(H)** CSR/ISR relationship.

Quantitatively, all three of the RMS errors improved for this subject, as did the errors for all five subjects whose fits were previously identified as having high error. The improvement is illustrated by the green diamonds in **Figure 5**. The green lines link the improved error values with the error values prior to this analysis.

In contrast, for all other subjects, if the same 60 min time point was left out the errors did not significantly degrade.

Note that the objective function (**Eq. 9**) that is minimized with the optimization is only sensitive to the model reconstructed values at the measured times. The model dynamics (insulin or c-peptide accumulation) are substantially only sensitive to the ISR or CSR within approximately one degradation time constant (τ_x), which for controls is of order 15 min. Therefore the optimization is primarily sensitive to the interpolated glucose trajectory ($\bar{g}$)

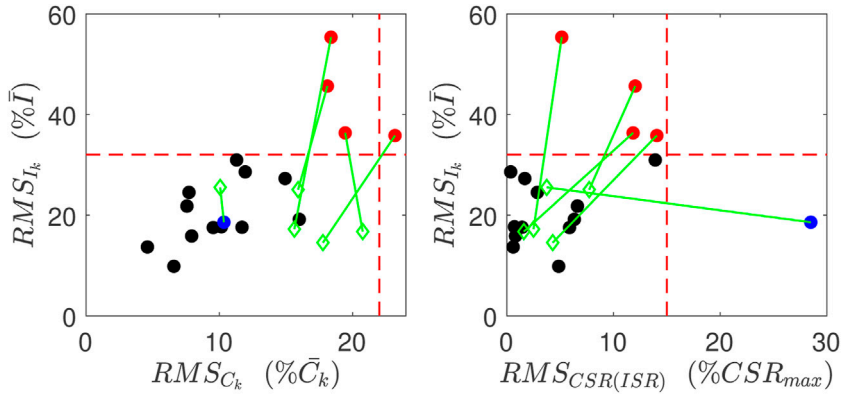

FIGURE 5 | Goodness of Fits for normal subjects. Red points indicate have relatively poor reconstruction of insulin measurements, and the blue point has relatively poor linear relation between CSR and ISR. These metrics for these poor reconstructions are all improved (green points) when the data point at 60 min is left out.

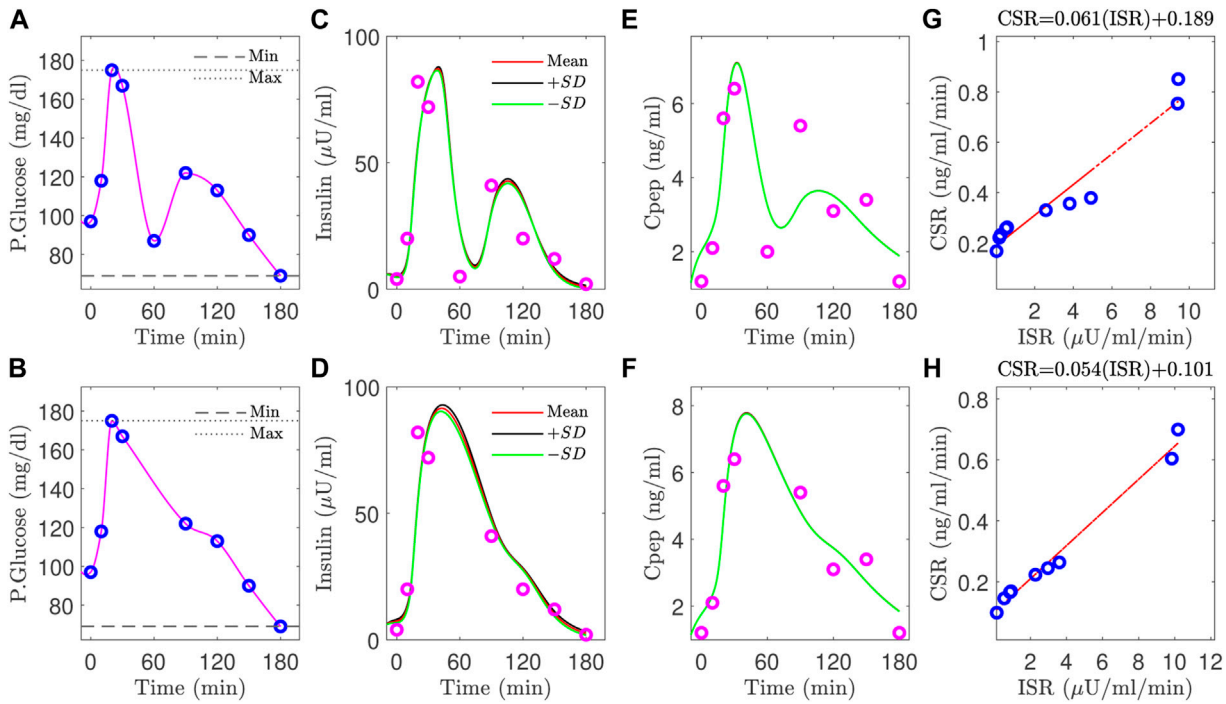

FIGURE 6 | Improvement for the estimation results of plasma insulin (**(D)** versus **(C)**), c-peptide (**(F)** versus **(E)**), and slope (**(H)** versus **(G)**) by removing the uncertain blood glucose value at 60 min **(A)**, and using the interpolated glucose values in the gap between the glucose values at 30, 90 min **(B)**.

over approximately τ_x ahead of measured data points. This means that as long as the measurements sufficiently sample the glucose dynamics, this method should be robust to dropping out individual data points.

This suggests that the poor estimate comes from the data, not the method.

In contrast, for in the two poorly estimated CFRD subjects, the glucose value dramatically increased to greater than 250 mg/dl within 40 min. This sharp increase in glucose level reduces the amount of time at intermediate glucose levels. As a consequence, it makes estimating ISR difficult at those intermediate values.

3.3.3 Inferred Parameters

In **Table 1**, we provide a summary for the 12 normal and 7 CFRD subjects who were estimated well, including the ISR average values of the estimated parameters presented by the mean and 95% confident interval, slope, and the ISR evaluated at the glucose

TABLE 1 | A summary for the normal and CFRD subjects, including the ISR average values of the estimated parameters, presented by the mean and 95% confident interval, slope, and the ISR evaluated at the glucose value of 140 mg/dl.

Parameter	τ_{PI}	K_m	C_0	α	Slope	ISR(140 mg/dl)
Control Subject	15 ± 5	123 ± 57	209 ± 39	0.06 ± 0.02	0.06 ± 0.01	128 ± 57
CFDR Subject	28 ± 12	75 ± 60	600 ± 240	0.014 ± 0.01	0.14 ± 0.06	73 ± 60

value of 140 mg/dl. Note that only 9 of 13 control subjects have peak glucose values that reached 140 mg/dl, whereas all of the 7 CFRD had blood glucose of 140 mg/dl or greater.

As a final external validation of the method, we were able to differentiate CFRD from normal patients in two ways. First, as shown in **Table 1**, the ISR at a glucose of 140 mg/dl is higher for the control subjects than the CFRD subjects. This result indicates the ability of the beta-cells for healthy subjects to produce more insulin to mitigate the increased glucose level. Second, the estimated τ_{pI} for CFRD subjects is larger than the control subjects, as shown in **Table 1**. This result reflects physiological insights for CFRD that insulin takes a longer time to accumulate and reach a high value than in the control subjects, due to Lower production in beta cells and lower peripheral degradation rate. Therefore, the increased glucose values in CFRD subjects provide better dynamics for estimation that allows the algorithm to estimate τ_{pI} more precisely.

The peak of the ISR can be estimated if the glucose range is wide, e.g., 100–350 mg/dl. However, in a short glucose range of 100–140 mg/dl, accurate estimation of the peak is not guaranteed. This observation means it is more likely for CFRD subjects to capture the ISR peak than the control subjects due to the high glucose range in these individuals. We found that two CFRD subjects from among the CFRD group had a glucose range that allowed us to estimate the ISR peak and hence the full ISR functional shape. In these two CFRD subjects, the blood glucose range is between 100–400 mg/dl. On the other hand, the blood glucose range for control subjects is between 95–140 mg/dl, which makes estimating the ISR peak hard to achieve. However, we found only one control subject that the ISR peak was nearly estimated. The glucose range in this control subject is between 95–180 mg/dl. Therefore, we conclude that the peak of the ISR can be better estimated for CFRD subjects, in which the range of blood glucose is wide.

To compare the normal and CFRD subjects, we evaluated the estimated ISR at the glucose value of 140 mg/dl for subjects with good estimation in the two groups. After removing the poorly fitted subjects and the control subjects that had not reached the glucose value of 140 mg/dl, we obtained 12 control subjects and 7 CFRD subjects out of 17 and 9 subjects, respectively. The results are presented using the empirical cumulative distribution function (ECDF), in **Figures 7A,B**. Therefore, we found that the ISR values of the normal subjects were with 50% that the ISR exceeds the rate of 100 μU/ml/min. Whereas, the CFRD subjects were with 50% that the associated ISR value around 15 μU/ml/min. These results indicate that the pancreatic beta-cell of the CFRD cannot produce enough insulin due to the dysfunction of these beta-cells. On the other hand, these beta-cells can produce more insulin at the value of glucose (140 mg/dl) in normal subjects.

The estimated slope between the estimated ISR and CSR was also used to characterize these two groups. The slope (CSR/ISR) between the estimated CSR and ISR for both normal and CFRD subjects was plotted in **Figures 7C,D**, as ECDF. In both control and CFRD subjects we observed a straight line describing the physiological relationship between ISR and CSR. The slope is in the unit of ng/μU. When both units are converted to moles, the expected conversion factor is 0.056. In **Figures 7C,D**, we plotted this value (0.056) as a vertical (dashed-red) line to illustrate how these slopes, which are predictions of the expected value 0.056, are close to this expected value. As shown in **Figure 7C**, the predicted slope of the control subjects was around the expected value of 0.056. On the other hand, the wide glucose range in the CFRD subjects used to estimate both ISR and CSR, which gives more information to estimate ISR and CSR trajectories (e.g., ISR secretion and peak regions), increased the uncertainty in the estimated slope, as shown in **Figure 7D**.

3.3.4 Two-Compartment Model

Note that the above fits and figures were obtained using the single-compartment model. However, comparable results can be obtained when incorporating the two-compartment model with the algorithm. But, it is a significant to note that, when the single model cannot estimate the patient's ISR and CSR, adding a second compartment is not helpful. For a comparison between the two models, the ISR was evaluated at the glucose value of 140 mg/dl, and the slope between ISR and CSR was estimated, for control subjects, using our algorithm incorporating the two models. Therefore, shifting to the two-compartment model, the control subjects' data gives a fraction difference of absolute mean error for the ISR at glucose value of 140 mg/dl provided by (Mean ± SD) 0.32 ± 0.2. In contrast, the fraction difference of the absolute average error of the slope is given by 0.14 ± 0.15. These results indicate that adding more compartments and unknown parameters is unnecessary to estimate reliable ISR. Instead, a simple model can be incorporated with our method to estimate ISR for people with different beta-cell functions.

4 DISCUSSION

We developed a new estimation approach for inferring the ISR from plasma insulin and c-peptide measurements. We validated this method with synthetic data and nominal physiological parameters and were able to reconstruct these values from generated ground truth data with 20% noise is added to each data point for both plasma glucose and insulin. Then the algorithm was applied to OGTT clinical data for both control and CFRD subjects. We use the estimated slope between ISR and

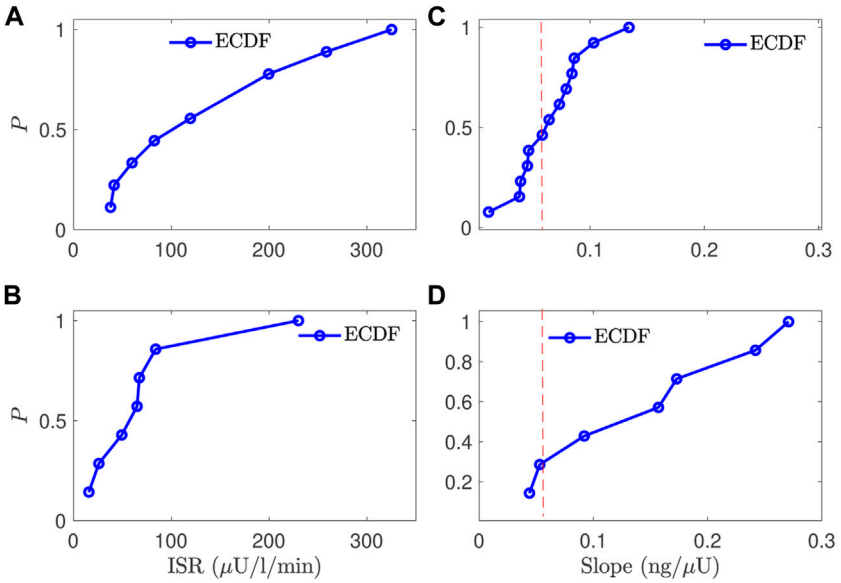

FIGURE 7 | A comparison between the normal and CFRD subjects, using the probability of empirical cumulative distribution function (ECDF), for the ISR value **(A,B)** evaluated at the glucose value of 140 mg/dl (horizontal) and the slope between ISR and CSR **(C,D)**, the vertical axis is the probability (ECDF); the expected value is 0.056 for the slope (red line **(C,D)**).

CSR to evaluate the estimation for both normal and CFRD groups, as well as the RMS between the observations and the model-estimated values.

We hypothesize that to estimate ISR, it is not necessary to use an OGTT, IVGTT, or other glucose tolerance test. Instead, it can be estimated by knowing glucose values and a nonlinear function of the secretion rate with unknown parameters. Therefore, we specifically implemented a sigmoid function to model the ISR and CSR and then estimate them independently from insulin and c-peptide data. The ISR peak can be estimated, using this function, if the glucose value is high enough to capture the peak. Using our method, we expect to estimate the baseline of the secretion rates if we have more sampled data, especially at the beginning of the test.

4.1 Validation

Our validation test uses the equal molar ratio between plasma insulin and c-peptide secretion rates. Even though the CFRD and control subjects have different physiology and the ISR and CSR have various physiological parameters and nonlinear relations with plasma glucose concentration, our algorithm recovers the linear relationship between ISR and CSR for both groups. This result indicates the accuracy of the estimation of the algorithm. Another test uses the normalized root-mean-square (RMS) error between the estimation and the measured values. We showed that the estimation, in the two groups, in which the relationship between ISR and CSR is linear, the RMS error between modeled insulin or c-peptide and estimated ones is small. This observation reflects the consistency in our results showed by these two validation tests used in our method.

4.2 Phenotype

We were able to differentiate the normal and CFRD diabetes phenotypes. We show that the ISR for individuals with CFRD is statistically significantly lower than the ISR for individuals' normal glucose regulatory systems (see **Table 1**). However, the ISR peak for the two groups did not differentiate them because the peak ISR was often not observable or computable for normal patients. In addition, due to the high glucose dynamics and slow insulin accumulation in the CFRD subjects, which reveals more information about the insulin degradation time (τ_{pI}), the estimated τ_{pI} was larger in this group than the control subjects.

4.3 Identifying Potentially Erroneous Data Points and Improving Reliability

As shown in **Section 3.3.2**, this inference method may be able to identify erroneous data points. In the example shown (**Figure 6**, and green point in **Figure 5**), such identification leverages three separate components: the goodness of fit of the insulin trajectory, the goodness of fit of c-peptide trajectory, and the linear relationship between ISR and CSR. Because both ISR and CSR are inferred independently, these three are independent measures.

The inference relies on the physiological knowledge that ISR is primarily a function of plasma glucose concentration, and the linear relation embodies the physiological fact that c-peptide and insulin are released in a 1:1 molecular ratio. Such use of external knowledge - that ISR is primarily a function of plasma glucose, and that CSR is proportional to ISR - is a simple and principled pathway to identifying data errors.

We note also that because the underlying model for plasma insulin or c-peptide accumulation includes a degradation time that appears to be in the range of τ_I 5–15 min, the model is in effect only dependent on the interpolated glucose values within τ_I or τ_C ahead of each data point, and for the distally separated points residual after removal of the point at 60 min, this time is relatively small.

If proven reliable in future studies, we anticipate that such analysis - and removal of erroneous points - could make clinical testing more reliable by increasing the amount of diagnostic information that can be extracted from a single diagnostic test, and decrease the need for multiple diagnostic tests using model-based inference. Currently, the ADA recommends four pathways for diagnosing pre-diabetes and type-2 diabetes, one of which includes an OGTT (Davidson et al., 2021b). Similarly, the recommendation to diagnose gestational diabetes is via a GTT or OGTT (Davidson et al., 2021a). In both cases, a diagnosis requires two tests. By using inference paired with the information in the dynamics of the OGTT rather than a single value, we suspect it would be possible, as we show in this work (**Figure 6**), to remove inaccurate outliers and accurately estimate ISR and other diagnostic quantities. If corroborated with further studies, this should motivate quantification of *both insulin and c-peptide* from blood draws during such clinical measures.

4.4 Inferring Pancreatic Health

Additionally, the model provides a platform for extracting additional information. For example, here we estimate the entire ISR curve, increasing accuracy and explainability of the context of the patient state, leading to quantified information regarding how much of the ISR was observed for observed glucose levels and how much excess capacity for insulin production the patient may have, leading to more accurate diagnosis of the patient's endocrine state.

Considering the above results and discussion, we now have a suitable method with physiological insights about estimating ISR for subjects with different physiological conditions. Furthermore, we showed that using a simple model is good enough to estimate ISR rather than a more complex model with more compartments and unknown parameters. Moreover, we found that using the two compartment, when the single compartment failed to estimate the ISR and CSR correctly, is not useful. These results allow us to implement the estimated ISR function into glucose models with various fidelity and complicity to understand better the glucose regulation system for patients with different pancreatic beta-cell functions.

4.5 Hepatic Insulin Degradation

We note that in this modeling we have lumped all insulin and c-peptide degradation to a general degradation rate, and have not tried to differentiate hepatic degradation or its effects. In the ISR literature (i.e., Watanabe et al., 1998; Watanabe and Bergman, 2000), such efforts are motivated because the pancratic beta-cells secrete insulin and c-peptide into the portal vein blood stream. The portal vein then passes through the liver and some insulin (up to 80%) is immediately degraded by the hepatocrytes (Najjar and Perdomo, 2019). If this process were simply proportional to plasma insulin concentration, then the one-compartment model for insulin would be modified to:

$$\dot{x}_{pi} = u_{i,p}(t)(1-\alpha_h) - \left(\kappa_i + \beta_{port}\alpha_h\right)x_{pi} \tag{11}$$

Here $u_{i,p}$ is the ISR at the pancrease into the portal vein, α_h is the absorption proportionality $\alpha_h \in (0:1)$, and β_{port} is the ratio of the portal blood flow rate to the total blood volume, which for adult humans $\beta_{port} \in (0.15–0.4)$/s. Likewise, κ_i is the degradation proportionality due to other processes. The addition to the standard degradation rate comes because the liver cannot distinguish between freshly secreted insulin and circulating insulin.

For the work as described, the ISR inferred is effectively the rate of insulin secretion into the circulation system following transit through the liver, i.e., $u_{i,inferred} = u_{i,p}(t)\ (1-\alpha_h)$. Because c-peptide is not primarily degraded in the liver, this correction factor doesn't apply. Therefore in cases where both insulin and c-peptide are measured, the slope of the linear relation between parametrized CSR and ISR should be equal to $1/(1-\alpha_h)$ (after unit conversion to molar units). For normal subjects, the majority of subjects therefore had hepatic absorption ratios of $\alpha_h < 0.4$ (**Figure 7C**). But the CFRD subjects had wider range of slopes, consistent with values as high as $\alpha_h < 0.8$.

Because our inference method also estimates the insulin degradation rate for an individual, this model implies that $\beta_{port}\alpha_h < 1/\tau_{pI}$. The inferred fit for normal subjects, with degradation times are of order τ_{pI} are of order 10–15 min and α_h 0.1, are consistent with this inequality and reasonable values of β_{port}. But, for example, the CFRD subject whose data is shown in **Figure 4**, has an α_h 0.8 and τ_{pI} ~50 min, which is not consistent with normal portal blood flow values.

In future work with larger data sets we will investigate these observations as a function of subject health.

We further note that this linear model (11) for hepatic insulin degradation has limitations. In particular, the insulin-receptors on the hepatocytes then signal insulin endocytosis and degradation (Najjar and Perdomo, 2019). Therefore the rate of degradation is insulin dependent.

4.6 Study Limitations

This work represents a first attempt to apply this modeling approach to infer the parametrization of the ISR from clinical data. Here we have applied this approach to rather small data sets for both control and CFRD subjects. We anticipate that the distribution of normal and abnormal ISR functions will only be clear from much larger sets. We note that this effort fall short in terms of the aim of establishing functional shape for control subjects. This method can only infer the ISR function over the range expressed during the clinical measurement, and the maximum glucose level for control subjects represented here was well below 150mg/ld - and the inferred ISRs were far from saturated.

5 CONCLUSION

This study presents a new approach for estimating ISR using plasma insulin and c-peptide measurements. Our approach uses

simple insulin and c-peptide models and applies both insulin and c-peptide measures. This algorithm can infer ISR and CSR from OGTT data. Additionally, the method provides a deeper interpretation of the OGTT and a measure of the robustness and accuracy in both the inference and data.

We validate the estimation results in three ways. First, we validate the results by estimating the plasma insulin and c-peptide and comparing RMS between measurements and modeled responses of these variables. Second, we use the 1:1 M ratio between ISR and CSR to assess the estimation results. We showed that a linear relationship between ISR and CSR can be observed when they are estimated correctly. This result is confirmed in both CFRD and normal subjects. Third, we showed that our algorithm can differentiate between subjects with different beta-cell phenotype-related diseases. Moreover, we showed that the ISR level in CFDR subjects is lower than the ISR level in normal subjects. However, since the variation in blood glucose is high in CFRD patients, the peak of ISR and plasma degradation time of insulin and c-peptide are estimated more precisely. Further, we showed that the estimation of ISR utilizing the single-compartment model is very similar to the results using the two-compartment model. This indicates different models the robustness of our approach in estimating the ISR using different models' complicity and confirms that the ISR can be estimated precisely using only a simple model with less parameters. We also tested our model by treating uncertain measured values in the data. Finally, we provided a physiological interpretation that our method can handle the uncertainty in measured values and improve the estimation of ISR.

The immediate impact of this work is the development of a new approach for estimating ISR, which is now available for determining the beta-cell secretion rates for people with different conditions. This method is ready to implement into glucose models providing a better understanding of the glucose regulation system and monitoring people with diabetes.

CODE AVAILABILITY

Code for both fitting the ISRs, CSRs, and parametrizing the relationship between CSR and ISR, with examples to model-generated data, are available at (Inferring Insulin Secretion Rate From Sparse Patient Glucose and Insulin Measures (hyperlink = https://scholarsphere.psu.edu/resources/20d599c4-93fb-4a62-81d8-b69a88d58627) at doi: 10.26207/e8rf-e082).

DATA AVAILABILITY STATEMENT

The datasets presented in this article are not readily available because The request should be submitted to the Colorado Multiple Institutional Review Board (Aurora, CO). Requests to access the datasets should be directed to Name: CC, email: ChristineL.Chan@childrenscolorado.org.

ETHICS STATEMENT

The studies involving human participants were reviewed and approved by The study was approved by the Colorado Multiple Institutional Review Board (Aurora, CO), and informed consent and assent were obtained. The Title of the Study and NCT number are Glycemic Monitoring in Cystic Fibrosis, NCT02211235. Written informed consent for participation was not required for this study in accordance with the national legislation and the institutional requirements.

AUTHOR CONTRIBUTIONS

RA: is the corresponding author, developed and applied the method, calculated statistical analysis, and wrote the manuscript. BG: contributed to the conception and design of the method. DA: contributed to the conception and wrote one paragraph of the manuscript. CC: provided the clinical data. RA, BG, DA: contributed to manuscript revision, read, and approved the submitted version.

FUNDING

This work funded through NIH Grant 5R01LM012734.

REFERENCES

Ahrén, B., and Pacini, G. (2004). Importance of Quantifying Insulin Secretion in Relation to Insulin Sensitivity to Accurately Assess Beta Cell Function in Clinical Studies. *Eur. J. Endocrinol.* 150, 97–104. doi:10.1530/eje.0.1500097

Bergman, R. N., Phillips, L. S., and Cobelli, C. (1981). Physiologic Evaluation of Factors Controlling Glucose Tolerance in Man: Measurement of Insulin Sensitivity and Beta-Cell Glucose Sensitivity from the Response to Intravenous Glucose. *J. Clin. Investig.* 68, 1456–1467. doi:10.1172/jci110398

Brundin, T. (1999). Splanchnic and Extrasplanchnic Extraction of Insulin Following Oral and Intravenous Glucose Loads. *Clin. Sci.* 97, 429–436. doi:10.1042/cs0970429

Chan, C. L., Pyle, L., Vigers, T., Zeitler, P. S., and Nadeau, K. J. (2022). The Relationship between Continuous Glucose Monitoring and OGTT in Youth and Young Adults with Cystic Fibrosis. *J. Clin. Endocrinol. Metabolism* 107, E548–E560. doi:10.1210/clinem/dgab692

Davidson, K. W., Davidson, K. W., Barry, M. J., Mangione, C. M., Cabana, M., Caughey, A. B., et al. (2021b). Screening for Prediabetes and Type 2 Diabetes: Us Preventive Services Task Force Recommendation Statement. *Jama* 326, 736–743. doi:10.1001/jama.2021.12531

Davidson, K. W., Davidson, K. W., Barry, M. J., Mangione, C. M., Cabana, M., Caughey, A. B., et al. (2021a). Screening for Gestational Diabetes: Us Preventive Services Task Force Recommendation Statement. *JAMA* 326, 531–538. doi:10.1001/jama.2021.11922

Eaton, R. P., Allen, R. C., Schade, D. S., Erickson, K. M., and Standefer, J. (1980). Prehepatic Insulin Production in Man: Kinetic Analysis Using Peripheral Connecting Peptide Behavior*. *J. Clin. Endocrinol. Metabolism* 51, 520–528. doi:10.1210/jcem-51-3-520

Farris, W., Mansourian, S., Chang, Y., Lindsley, L., Eckman, E. A., Frosch, M. P., et al. (2003). Insulin-degrading Enzyme Regulates the Levels of Insulin, Amyloid β-protein, and the β-amyloid Precursor Protein Intracellular Domain *In Vivo*. *Proc. Natl. Acad. Sci. U.S.A.* 100, 4162–4167. doi:10.1073/pnas.0230450100

Ferrannini, E., and Mari, A. (2004). Beta Cell Function and its Relation to Insulin Action in Humans: a Critical Appraisal. *Diabetologia* 47, 943–956. doi:10.1007/s00125-004-1381-z

Ha, J., Satin, L. S., and Sherman, A. S. (2016). A Mathematical Model of the Pathogenesis, Prevention, and Reversal of Type 2 Diabetes. *Endocrinology* 157, 624–635. doi:10.1210/en.2015-1564

Hansen, P. C., Pereyra, V., and Scherer, G. (2013). *Least Squares Data Fitting with Applications*. Baltimore: JHU Press.

Jones, A. G., and Hattersley, A. T. (2013). The Clinical Utility of C-peptide Measurement in the Care of Patients with Diabetes. *Diabet. Med.* 30, 803–817. doi:10.1111/dme.12159

Kjems, L. L., Vølund, A., and Madsbad, S. (2001). Quantification of Beta-Cell Function during Ivgtt in Type Ii and Non-diabetic Subjects: Assessment of Insulin Secretion by Mathematical Methods. *Diabetologia* 44, 1339–1348. doi:10.1007/s001250100639

Lebowitz, M. R., and Blumenthal, S. A. (1993). The Molar Ratio of Insulin to C-Peptide. an Aid to The Diagnosis of Hypoglycemia Due to Surreptitious (Or Inadvertent) Insulin Administration. *Archives Intern. Med.* 153, 650–655. doi:10.1001/archinte.153.5.650

Leighton, E., Sainsbury, C. A., and Jones, G. C. (2017). A Practical Review of C-Peptide Testing in Diabetes. *Diabetes Ther.* 8, 475–487. doi:10.1007/s13300-017-0265-4

Levenberg, K. (1944). A Method for the Solution of Certain Non-Linear Problems in Least Squares. *Quart. Appl. Mathem.*, 2 (2), 164–168.

Liu, W., Hsin, C., and Tang, F. (2009). A Molecular Mathematical Model of Glucose Mobilization and Uptake. *Math. Biosci.* 221, 121–129. doi:10.1016/j.mbs.2009.07.005

Lotz, T., Göltenbott, U., Chase, J. G., Docherty, P., and Hann, C. E. (2009). A Minimal C-Peptide Sampling Method to Capture Peak and Total Prehepatic Insulin Secretion in Model-Based Experimental Insulin Sensitivity Studies. *J. Diabetes Sci. Technol.* 3, 875–886. doi:10.1177/193229680900300435

Marquadt, D. W. (1963). An Algorithm for Least-Squares Estimation of Nonlinear Parameters. *J. Soc. Ind. Appl. Math.* 11, 431

Matthews, D. R., Hosker, J. P., Rudenski, A. S., Naylor, B. A., Treacher, D. F., and Turner, R. C. (1985). Homeostasis Model Assessment: Insulin Resistance and ?-Cell Function From Fasting Plasma Glucose and Insulin Concentrations in Man. *Diabetologia* 28, 412–419. doi:10.1007/bf00280883

Najjar, S. M., and Perdomo, G. (2019). Hepatic Insulin Clearance: Mechanism and Physiology. *Physiology* 34, 198–215. doi:10.1152/physiol.00048.2018

Pacini, G., and Mari, A. (2003). Methods for Clinical Assessment of Insulin Sensitivity and B-Cell Function. *Best Pract. Res. Clin. Endocrinol. Metabolism* 17, 305–322. doi:10.1016/s1521-690x(03)00042-3

Reaven, G. M., Brand, R. J., Chen, Y. D., Mathur, A. K., and Goldfine, I. (1993). Insulin Resistance and Insulin Secretion aAre Determinants of Oral Glucose Tolerance i Normal Individuals. *Diabetes* 42, 1324–1332. doi:10.2337/diabetes.42.9.1324

Rigler, R., Pramanik, A., Jonasson, P., Kratz, G., Jansson, O. T., Nygren, P.-Å., et al. (1999). Specific Binding of Proinsulin C-Peptide to Human Cell Membranes. *Proc. Natl. Acad. Sci. U.S.A.* 96, 13318–13323. doi:10.1073/pnas.96.23.13318

Schiavon, M., Herzig, D., Hepprich, M., Donath, M. Y., Bally, L., and Dalla Man, C. (2021). Model-Based Assessment of C-Peptide Secretion and Kinetics in Post Gastric Bypass Individuals Experiencing Postprandial Hyperinsulinemic Hypoglycemia. *Front. Endocrinol.* 83, 611253. doi:10.3389/fendo.2021.611253

Steiner, D. F., Cunningham, D., Spigelman, L., and Aten, B. (1967). Insulin Biosynthesis: Evidence for a Precursor. *Science* 157, 697–700. doi:10.1126/science.157.3789.697

Tolić, I. M., Mosekilde, E., and Sturis, J. (2000). Modeling the Insulin-Glucose Feedback System: The Significance of Pulsatile Insulin Secretion. *J. Theor. Biol.* 207, 361–375. doi:10.1006/jtbi.2000.2180

Tommerdahl, K. L., Brinton, J. T., Vigers, T., Cree-Green, M., Zeitler, P. S., Nadeau, K. J., et al. (2021). Delayed Glucose Peak and Elevated 1-Hour Glucose on the Oral Glucose Tolerance Test Identify Youth With Cystic Fibrosis With Lower Oral Disposition Index. *J. Cyst. Fibros.* 20, 339–345. doi:10.1016/j.jcf.2020.08.020

Topp, B., Promislow, K., Devries, G., Miura, R. M., and Finegood, D. T. (2000). A Model of B -Cell Mass, Insulin, and Glucose Kinetics: Pathways to Diabetes. *J. Theor. Biol.* 206, 605–619. doi:10.1006/jtbi.2000.2150

Venugopal, S. K., Mowery, M. L., and Jialal, I. (2021). *C Peptide*. StatPearls.

Watanabe, R. M., and Bergman, R. N. (2000). Accurate Measurement of Endogenous Insulin Secretion Does Not Require Separate Assessment of C-Peptide Kinetics. *Diabetes* 49, 373–382. doi:10.2337/diabetes.49.3.373

Watanabe, R. M., Steil, G. M., and Bergman, R. N. (1998). Critical Evaluation of the Combined Model Approach for Estimation of Prehepatic Insulin Secretion. *Am. J. Physiology-Endocrinology Metabolism* 274, E172–E183. doi:10.1152/ajpendo.1998.274.1.e172

Wilcox, G. (2005). Insulin and Insulin Resistance. *Clin. Biochem. Rev.* 26, 19

Conflict of Interest: The authors declare that the research was conducted in the absence of any commercial or financial relationships that could be construed as a potential conflict of interest.

Publisher's Note: All claims expressed in this article are solely those of the authors and do not necessarily represent those of their affiliated organizations, or those of the publisher, the editors and the reviewers. Any product that may be evaluated in this article, or claim that may be made by its manufacturer, is not guaranteed or endorsed by the publisher.

frontiers | Frontiers in Physiology

TYPE Original Research
PUBLISHED 05 August 2022
DOI 10.3389/fphys.2022.895118

OPEN ACCESS

EDITED BY
John D. Imig,
Medical College of Wisconsin,
United States

REVIEWED BY
Dominik H. Pesta,
German Aerospace Center (DLR),
Germany
Nepton Soltani,
Isfahan University of Medical
Sciences, Iran

*CORRESPONDENCE
Cecilia Diniz Behn,
cdinizbe@mines.edu

SPECIALTY SECTION
This article was submitted to Metabolic Physiology,
a section of the journal
Frontiers in Physiology

RECEIVED 13 March 2022
ACCEPTED 08 July 2022
PUBLISHED 05 August 2022

CITATION
Hampton GS, Bartlette K, Nadeau KJ, Cree-Green M and Diniz Behn C (2022), Mathematical modeling reveals differential dynamics of insulin action models on glycerol and glucose in adolescent girls with obesity.
Front. Physiol. 13:895118.
doi: 10.3389/fphys.2022.895118

Mathematical modeling reveals differential dynamics of insulin action models on glycerol and glucose in adolescent girls with obesity

Griffin S. Hampton[1], Kai Bartlette[1], Kristen J. Nadeau[2,3], Melanie Cree-Green[2,3] and Cecilia Diniz Behn[1,2]*

[1]Department of Applied Mathematics and Statistics, Colorado School of Mines, Golden, CO, United States, [2]Division of Pediatric Endocrinology, University of Colorado Anschutz Medical Campus, Aurora, CO, United States, [3]Ludeman Center for Women's Health Research, University of Colorado Anschutz Medical Campus, Aurora, CO, United States

Under healthy conditions, the pancreas responds to a glucose challenge by releasing insulin. Insulin suppresses lipolysis in adipose tissue, thereby decreasing plasma glycerol concentration, and it regulates plasma glucose concentration through action in muscle and liver. Insulin resistance (IR) occurs when more insulin is required to achieve the same effects, and IR may be tissue-specific. IR emerges during puberty as a result of high concentrations of growth hormone and is worsened by youth-onset obesity. Adipose, liver, and muscle tissue exhibit distinct dose-dependent responses to insulin in multi-phase hyperinsulinemic-euglycemic (HE) clamps, but the HE clamp protocol does not address potential differences in the dynamics of tissue-specific insulin responses. Changes to the dynamics of insulin responses would alter glycemic control in response to a glucose challenge. To investigate the dynamics of insulin acting on adipose tissue, we developed a novel differential-equations based model that describes the coupled dynamics of glycerol concentrations and insulin action during an oral glucose tolerance test in female adolescents with obesity and IR. We compared these dynamics to the dynamics of insulin acting on muscle and liver as assessed with the oral minimal model applied to glucose and insulin data collected under the same protocol. We found that the action of insulin on glycerol peaks approximately 67 min earlier ($p < 0.001$) and follows the dynamics of plasma insulin more closely compared to insulin action on glucose as assessed by the parameters representing the time constants for insulin action on glucose and glycerol ($p < 0.001$). These findings suggest that the dynamics of insulin action show tissue-specific differences in our IR adolescent population, with adipose tissue responding to insulin more quickly compared to muscle and liver. Improved understanding of the tissue-specific dynamics of insulin action may provide novel insights into the progression of metabolic disease in patient populations with diverse metabolic phenotypes.

KEYWORDS

glycerol, glucose, insulin, insulin resisitance, lipolysis, mathematical model

Introduction

The obesity epidemic now affects a significant portion of the world, causing insulin resistance and metabolic dysregulation in multiple organs of the body. The worldwide prevalence of overweight and obesity has approximately doubled from 1980 to 2015, affecting adults and children of all ages, and is forecasted to reach levels over 50% by 2030 (Kelly et al., 2008; Chooi et al., 2019). The metabolic syndrome as defined in the National Health and Nutrition Examination Survey (NHANES) is related to insulin resistance (IR) and shows an increased risk for developing type 2 diabetes and cardiovascular disease. The metabolic syndrome was calculated to affect 34.7% of the U.S. population in 2016, with a significant increase in the incidence in young adults from 2011 to 2016 (Aguilar et al., 2015; Hirode and Wong, 2020). Related to this obesity and metabolic dysfunction, approximately 34.2 million adults in the United States have type 2 diabetes (T2D) (Centers for Disease Control and Prevention, 2020), and among youth the incidence rate of T2D is also increasing and expected to quadruple from 2010 to 2050 (Imperatore et al., 2012; Mayer-Davis et al., 2017; American Diabetes, 2020). Of grave concern, T2D appears to be much more aggressive in youth than in adults, including poor response to interventions effective in adults, and early onset of diabetes complications (RISE Consortium and Investigators, 2019; Group et al., 2021; Utzschneider et al., 2021). Even when dysglycemia is already present, adolescents secrete much higher concentrations of insulin than adults, likely driven by their marked IR (RISE Consortium, 2018; Utzschneider et al., 2020). This high morbidity and the unique physiologic features of insulin sensitivity and secretion in youth drive the necessity to specifically investigate the systems involved in metabolic disease development in youth. By better understanding the unique pathology of metabolic disease in youth, better treatments can be developed and personalized for individuals.

Metabolic dysregulation often arises from an imbalance in energy consumption and expenditure. During fasting, energy is primarily provided from energy stored in adipose and hepatic tissue. In a healthy individual, when energy is acquired through ingesting food, the mechanisms that provide endogenous energy sources are suppressed, so that the ingested fuel can be used and stored. Insulin facilitates the transition from an endogenous to exogenous energy source, and it manages glycerol, free fatty acid (FFA), and glucose systems across different metabolic states. In addition to suppressing the release of glucose from the liver and stimulating glucose uptake in hepatic and peripheral tissues (Petersen and Shulman, 2018), insulin is the most potent antilipolytic hormone: it suppresses lipolysis, and reduces the use of FFA as an energy source. IR is defined as a decreased biological response to insulin, which leads to increased insulin secretion, eventually causing pancreatic β-cell failure and T2D (Ronald Kahn, 1978; Arner, 2002; Cree-Green et al., 2019a). IR is tissue specific, and it may manifest in individual tissues at different points in disease progression. It is hypothesized that the development of IR in adipose tissue, resulting in excess circulating FFA and glycerol, may induce IR in other tissues (Arner and Rydén, 2015). Elevated FFA concentrations may contribute to dysglycemia in multiple ways, including impairing β-cell insulin secretion and vascular function, and directly inducing hepatic and skeletal muscle IR (Arner, 2001; Arner, 2002; Arner and Rydén, 2015; Sondergaard et al., 2017), thereby emphasizing the importance of characterizing adipose IR.

The gold standard in assessing insulin action on adipose tissue is a low dose hyperinsulinemic euglycemic (HE) clamp with stable isotope tracers. The HE clamp determines the steady state concentration of insulin, that is, necessary to suppress FFA and/or glycerol release into circulation. Using different insulin infusion rates as part of a multi-step clamp with glucose and glycerol tracers, the insulin sensitivity of adipose, liver, and peripheral tissue can be determined (Conte et al., 2012). While effective at quantifying some aspects of adipose health, the HE clamp is resource intensive and narrow in application as it relies on steady state values produced from glucose and insulin infusions rather than the coordinated physiologic response that occurs with oral nutrient ingestion (Sondergaard et al., 2017). Moreover, the HE clamp does not provide insight into the dynamics of insulin action on adipose, liver, or muscle tissue. An insulin-modified frequently sampled intravenous glucose tolerance test (IM-FSIVGTT) is a dynamic test where glucose is administered intravenously followed by an insulin bolus, showing metabolic dynamics under non-physiologic circumstances. An oral glucose tolerance test (OGTT) is a more physiologically complete dynamic test where participants ingest glucose orally through a sugary drink, allowing for the contribution of multiple gut hormones that may also play a role in the coordinated response to nutrition. Therefore, to focus on the dynamic response of adipose, liver, and muscle tissue to insulin under a more physiologic state, we quantify the dynamics of insulin action on glycerol and glucose during an oral glucose tolerance test (OGTT).

Both glycerol and FFA are released during lipolysis, but glycerol is a better marker of lipolysis due to differences in recycling between glycerol and FFA. FFA can either be released from adipose cells into the bloodstream or be recycled within adipose cells in a process by which the FFA are reincorporated into triacylglycerides and absorbed by neighboring cells prior to entry to the bloodstream (Coppack et al., 1999; Landau, 1999; Reshef et al., 2003; Wolfe and Chinkes, 2005; Magkos et al., 2012; Cree-Green et al., 2016; Cree-Green et al., 2019a; Cree-Green et al., 2019b). The process of intracellular and intratissue recycling complicates the dynamics of FFA and must be considered when evaluating adipose metabolism with FFA. In contrast, because adipose tissue lacks the expression of glycerol kinase (Steinberg et al., 1961), glycerol is not recycled in adipose tissue as it cannot be

reincorporated into triacylglycerides. Instead, circulating glycerol produced by lipolysis is taken up primarily by the liver *via* hepatic glycerol kinase expression, allowing glycerol to be phosphorylated and reincorporated into triacylglycerides (Coppack et al., 1999; Jensen, 1999; Landau, 1999). The absence of local glycerol recycling in adipose makes glycerol an appealing metabolite to track adipose metabolism. Whereas lipolysis from adipose tissues is the primary source for intravascular glycerol, a small proportion of glycerol is also produced *via* glycogenolysis and gluconeogenesis (Rotondo et al., 2019). These synthetic processes are regulated by glycerol-3-phosphate phosphatase and phosphoglycolate phosphatase which control the amount of glycerol made by glycogenolysis in the fasting state, and then gluconeogenesis in the fed state (Possik et al., 2022). It is estimated that up to 10%–15% of intravascular glycerol during prolonged fasting may be attributed to these processes, but the proportion attributed in the fed state is not as clear. The fasting contribution from glycogenolysis is higher with long fasting durations. In our study, participants had a monitored fast of 12 h, so the contribution from glycogenolysis is expected to be low. The contribution from gluconeogenesis is related to serum glucose concentrations. As none of our participants had diabetes, the contribution from this pathway is also expected to be low. Therefore, we consider changes in glycerol concentration to primarily reflect insulin-mediated changes in lipolysis.

Mathematical models of glucose metabolism have contributed a fundamental understanding of interactions in glucose and insulin dynamics (Ajmera et al., 2013; Cobelli et al., 2014). These models describe how insulin induces glucose uptake by peripheral tissue and reduces glucose production from endogenous sources under different experimental conditions, and the Oral Minimal Model (OMM) describes glucose dynamics during an OGTT (Bergman et al., 1979; Bergman, 1989; Dalla Man et al., 2002; Ha et al., 2016; Bartlette et al., 2021). Although insulin concentrations may be modeled directly (Bergman RNB et al., 1981; Picchini et al., 2005; Ramos-Roman et al., 2012; Ha et al., 2016), an intermediate variable of insulin action is often introduced to account for the delay between changes in insulin concentrations and observed effects on glucose concentrations (Bergman, 1989; Dalla Man et al., 2002), and this delay may increase as insulin sensitivity decreases. The concepts of glucose metabolic modeling have also been extended to other tissues and metabolic systems including adipose tissue (Roy and Parker, 2006; Periwal et al., 2008; Ramos-Roman et al., 2012; Thomaseth et al., 2014; Li et al., 2016; Young and Periwal, 2016). In previous work we modeled glycerol dynamics with an implicit insulin effect on the glycerol rate of appearance that was estimated using glycerol stable isotope tracer data (Diniz Behn et al., 2020). Periwal and colleagues proposed a model of interacting FFA and insulin dynamics to measure adipose metabolism during an IM-FSIVGTT (Periwal et al., 2008). Their model used a Hill function to represent insulin action-dependent lipolysis and described both glucose and FFA dynamics using a single insulin action term, suggesting that the dynamics of insulin action on glucose and FFA were similar in this study. These models have been successfully employed to assess adipose metabolism in translational studies utilizing IVGTTs (Adler-Wailes et al., 2013; Levine et al., 2020).

To characterize the dynamics of orally-stimulated adipose metabolism, we develop a differential-equations based mathematical model that describes the interaction between glycerol and insulin concentrations during an OGTT. We use the modeling infrastructure of existing FFA models as a basis for our glycerol-insulin model, and we explicitly represent the effects of insulin on lipolysis. We apply the glycerol-insulin model and the OMM to OGTT data from a population of obese and overweight adolescent girls with and without polycystic ovary syndrome (PCOS). This population is characterized by a significant degree of IR and metabolic dysregulation (Bartlette et al., 2021; Ware et al., 2022). To quantify tissue-specific insulin action, we compare simulation results and model parameters associated with the glycerol model and the OMM. The differences in the dynamics of insulin action on glycerol and glucose systems were the primary focus of this study.

Methods

Participants

The development of the glycerol model and analysis of insulin action dynamics was conducted on data collected in the APPLE (Androgens and Post-Prandial LivEr metabolism: liver and fat regulation in overweight adolescent girls; NCT02157954) study. This study was performed to explore metabolic abnormalities associated with PCOS and develop new adolescent specific models to understand IR. It was approved by the Colorado Multiple Institutional Review Board. All participants provided informed consent if they were 18–21 years old or parental consent and participant assent if they were 12–17 years old.

The participants were recruited for this cross-sectional study from pediatric clinics at Children's Hospital Colorado. The inclusion criteria were age 12–21 years, female sex, postpubertal Tanner Stage 5 status, at least 18 months post-menarche, and overweight/obese status (BMI $\geq$ 90th percentile for age and sex). The participants had a sedentary lifestyle (<3 h routine exercise per week, validated with both a 3-day activity recall and 7-day accelerometer use). The exclusion criteria were a confirmed diagnosis of diabetes (HbA1c $\geq$ 6.5%), pregnancy, anemia, liver diseases other than non-alcoholic fatty liver disease (NAFLD), an alanine transferase (ALT) level greater than 125 IU/L, and use of medications known to affect insulin

TABLE 1 Population description. These values are reported as population numbers or means ± the standard deviation.

Variable	Values
Physical characteristics	
Number (n)	66
Age (years)	15.6 ± 2
Race (n) White/Black	59/7
Ethnicity (n) Hispanic/non-Hispanic	35/31
Disease State (n) Obese Control/PCOS/PCOS + drug	18/33/15
BMI (kg/m^2)	35.5 ± 5.7
Weight (kg)	95.8 ± 16.9
Fat Free Mass (kg)	49.6 ± 7.3
Fat Mass (kg)	42.9 ± 10.8
Height (cm)	164.1 ± 7.1
Waist Circumference (cm)	106.5 ± 11.9
Metabolic Characteristics	
6h Insulin Sensitivity (dL/kg/min per $\mu U/mL$)	2.9 ± 2.4 × 10^{-4}
Fasting glucose (mg/dl)	90 ± 9
2-h glucose (mg/dl)	142 ± 25
Fasting glycerol (μmol/L)	118 ± 26
Fasting FFA (μmol/L)	625 ± 139
Fasting Insulin (μU/mL)	26 ± 15
Peak Insulin (μU/mL)	361 ± 207
Peak Insulin Time (min)	84 ± 47

sensitivity or glucose metabolism (including systemic steroids and antipsychotics) in the last 6 months. Metformin and oral contraceptives were excluded in all participants except in metformin (n = 6) and contraceptive (n = 10) sub-cohorts. Participants with PCOS were defined according to the NIH criteria: 1) an irregular menstrual cycle and 2) clinical and/or biochemical evidence of hyperandrogenism (Zawadzki JD, 1992). Total body fat and fat free mass percentages was assessed by standard DEXA methods (Hologic, Waltham, MA).

From the ninety-two studied participants, the population analyzed in this paper was a subset of sixty-six participants (18 with normal menses and forty-eight with PCOS, described in Table 1). Of the ninety-two study participants the following were excluded: Sixteen with missing OGTT time points precluding modeling and 10 participants randomized to receive exanatide during the OGTT, because exenatide is known to alter insulin dynamics.

Protocol

Each participant had two study-visits: 1) an initial consent/screening for eligibility; 2) an overnight monitored fast during the follicular phase of the menstrual cycle followed by a six-hour OGTT. Before the metabolic study visit, participants refrained from physical activity for 3 days. The afternoon and evening prior to the OGTT, each participant consumed an isocaloric diet (65% carbohydrate, 15% protein, 20% fat). After the evening meal, each participant refrained from activity and followed a monitored inpatient 12-h fast, followed by a frequently sampled OGTT. Baseline fasting metabolite concentrations were determined prior to the OGTT. At 8 a.m., participants ingested 75 g glucose and 25 g of fructose. Fructose was included to distinguish abnormal hepatic fat metabolism. The drink was consumed in a three-minute window at time 0 and blood samples were taken at the following time points: −20, −10, 0, 10, 20, 30, 45, 60, 75, 90, 105, 120, 135, 150, 165, 180, 210, 240, 300, and 360 min. Blood glucose was measured at the bedside with the StatStrip® Hospital Glucose Monitoring System (Novo Biomedical, Waltham, MA, United States). Serum insulin was measured with radioimmunoassay (Millipore, Billerica, MA, United States). Serum glycerol concentrations were obtained from an ELISA assay (R-Biopharm, Washington, MO, United States).

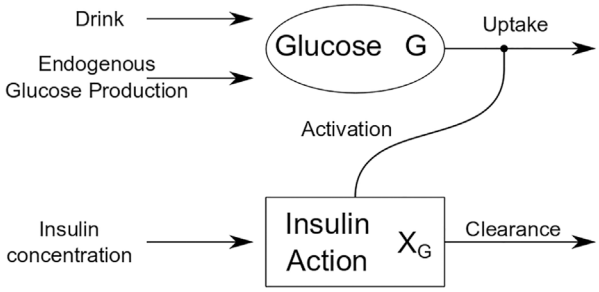

FIGURE 1
Schematic of oral minimal model (OMM).

Oral minimal model for glucose dynamics

OGTT glucose dynamics for each participant were described using the Oral Minimal Model (OMM) (Dalla Man et al., 2002), a one-compartment mathematical model that describes the effect of insulin on glucose and provides an estimate of whole-body insulin sensitivity (S_I), as reported previously (Bartlette et al., 2021). Figure 1 is a schematic that shows how insulin action affects the uptake term of the glucose dynamics.

The oral minimal model equations are

$$\dot{G} = -[S_G + X_G]G + S_G G_b + \frac{Ra_{meal}}{V} \tag{1}$$

$$\dot{X}_G = \begin{cases} -p_2^G X_G & , I(t) < I_b \\ -p_2^G X_G + p_3 (I(t) - I_b) & , I(t) \geq I_b \end{cases} \tag{2}$$

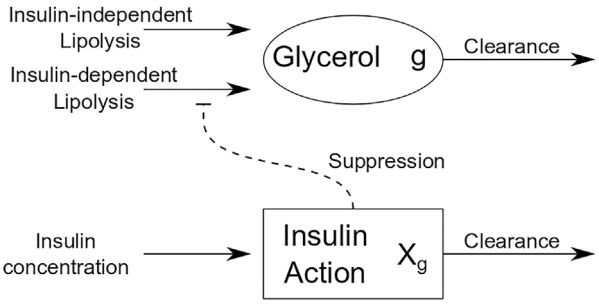

FIGURE 2
Schematic of glycerol model.

where $G(t)$ is glucose concentration in mg/dL; $X_G(t)$ is insulin action on glucose; $I(t)$ is the insulin concentration; G_b and I_b are basal glucose and insulin concentrations, respectively; S_G is the glucose effectiveness; p_2^G is a time constant of insulin action; p_3 is a constants of insulin action clearance and appearance; and $Ra_{meal}(\alpha, t)$ is a piecewise-linear function describing the rate of appearance of exogenous glucose in the bloodstream. The initial values for the OMM are $G(0) = G_b$ and $X_G(0) = 0$. Six-hour OGTT data from this population were fit to the OMM implemented in SAAM II (SAAM II software v 2.2, The Epsilon group, Charlottesville, VA, United States) as we previously detailed in Bartlette et al. (2021). The parameters we determined in this prior study were used to model the glucose dynamics for all participants in the present study. The insulin action profiles generated from the best-fit parameters were the focus of comparison between insulin-mediated glucose and glycerol dynamics.

Glycerol dynamics model

Informed by models of FFA dynamics, we developed a differential equations-based model for glycerol dynamics that utilizes the concept of insulin action as an intermediate variable between measured insulin and its action on adipose tissue. Figure 2 is a schematic of insulin action on glycerol dynamics that illustrates insulin action on glycerol production. By contrast with insulin action's role to activate glucose uptake in OMM, insulin action in the glycerol model suppresses glycerol production. The equations for the glycerol model are as follows:

$$\dot{g} = -S_g g + l_0 + \frac{l_2}{1 + \left(\frac{X_g}{X_2}\right)^A} \tag{3}$$

$$\dot{X}_g = \begin{cases} -p_2^g X_g & , I(t) < I_b \\ -p_2^g X_g + p_2^g (I(t) - I_b) & , I(t) \geq I_b \end{cases} \tag{4}$$

where $g(t)$ is the concentration of glycerol in μ mol/L; $X_g(t)$ is insulin action on glycerol; p_2^g is a time constant of insulin action; $I(t)$ is the insulin concentration; I_b is the basal insulin concentration; S_g is the effectiveness of glycerol uptake; l_0 is the insulin independent lipolysis rate; l_2 is the insulin dependent (suppressible) lipolysis rate; X_2 scales insulin action; and A affects how aggressively changes in insulin action result in changes of lipolysis suppression. Lipolysis is modeled as the sum of an insulin independent lipolysis rate, l_0, and a Hill function representing insulin action-dependent lipolysis and describing the transition from maximum lipolysis rate, $l_0 + l_2$, to the minimum lipolysis rate, l_0, as insulin action increases. The Hill function is the functional form that was determined to best fit the dynamics of FFA suppression (Periwal et al., 2008).

Glycerol model fitting process

Before the glycerol model was fit to glycerol data for each participant, the data were truncated to reflect the time period from the drink ingestion (t = 0) to the time at which the participant's glucose concentration reached a nadir concentration following the glucose excursion induced by the drink. The choice to fit data from t = 0 to the glucose concentration nadir avoided physiological complications due to the high prevalence of reactive hypoglycemia in this population, and it provided a standard check point by which to compare participants. More details are included in the Discussion.

The basal concentration of insulin was determined by averaging the concentrations at timepoints −20, −10, and 0 min. The model was then fit to the truncated data in MATLAB (Mathworks, Natick, MA) using the interior point algorithm FMINCON and the built-in ode solver ODE23S with an absolute tolerance of 1e-10. The FMINCON algorithm minimized an objective function analogous to the objective function described in Periwal et al. (2008); Li et al. (2016). Briefly, this objective function uses single spectrum analysis with only one eigenvalue retained to generate a representative smoothing of the data. Variance of the data is calculated by squaring the standard deviation of the squared difference between the experimental data and the representative smooth curve generated from the single spectrum analysis. The error term is the sum of the square differences between the experimental data and the numeric solution produced by ODE23S divided by the calculated variance. As in previous work, we fixed the parameter A to 2 because the model was not sensitive to this parameter and fixing it improved model identifiability (Li et al., 2016).

Lipolysis parameters were seeded in a physiological range between 0 and approximately 200% of the analogous parameter values reported by Periwal and colleagues (Periwal et al., 2008). The S_g and p_2^g parameters were seeded between 0 and 1. If the initial parameters did not produce a valid model state (i.e., model states were not real or positive), all parameters would be

randomly reseeded until the initial model state was valid. For the optimization, all parameters were constrained to be nonnegative and parameters representing proportions, S_g and p_2^g were restricted to range between 0 and 1. The glycerol and insulin concentration data for each participant were fit with FMINCON 75 times. The solution with the lowest objective function value of the 75 runs was selected as the best fit parameter set.

Analysis of insulin action dynamics

All analysis was done in MATLAB (Mathworks, Natick, MA). To quantify the differences in insulin action dynamics associated with glucose and glycerol, we defined three metrics on the insulin action profiles. The first metric determines the difference in time between the insulin action peak for each metabolite and the peak insulin concentration. The magnitudes of each delay were computed for both glucose and glycerol for all participants and compared with a Wilcoxon signed rank test. The Wilcoxon test was chosen to compare the two distributions because the data are paired and not normally distributed. Since the dynamics of glucose and glycerol come from the same participant, using the same insulin concentrations as a forcing function, the samples are not independent.

The second metric determines the difference in time between the insulin action peak for glucose and the insulin action peak for glycerol. This measure describes the relative timing of insulin action for each metabolite. The difference in timing for glucose and glycerol action was evaluated using a one-sample Student's t-test to establish if the difference was equal to zero. The third metric determines the difference in the normalized insulin actions at the time point associated with the glucose nadir (i.e., the lowest glucose value after the glucose peak). This measure quantifies the relative strength of insulin on the glucose system compared to the glycerol system at the time of the glucose nadir. To compute this measure, the insulin action curves for each metabolite were normalized by the peak insulin action values, respectively, and then the insulin action values at the time point associated with the glucose nadir were determined. The normalized glycerol insulin action nadir value was subtracted from the normalized glucose insulin action nadir value to obtain the relative difference in insulin actions at the nadir. The relative difference in the normalized insulin actions at the nadir was evaluated with a one-sample Student's t-test to test if the difference was equal to zero.

In addition to these metrics comparing the insulin action profiles, and we also compared the estimated parameters p_2^G and p_2^g that govern the insulin action dynamics for glucose and glycerol, respectively. Qualitatively, larger insulin action time constants reflect smaller delays from the insulin concentration profile while smaller insulin action time constants reflect larger delays from the insulin concentration profile. Since the insulin action time constants have an exponential effect on insulin action, we compared the magnitude of time constant values for each metabolic system using $log_{10}(p_2^G)$ and $log_{10}(p_2^g)$. The $log_{10}(p_2^g)$ and $log_{10}(p_2^G)$ parameter distributions were not approximately normal. We compared $log_{10}(p_2^G)$ and $log_{10}(p_2^g)$ with a Wilcoxon signed rank test.

Results

Mathematical modeling of glucose and glycerol dynamics

For each participant we fit OMM and the glycerol model to OGTT data. Following ingestion of the drink, glucose and insulin concentrations increased and glycerol concentrations decreased for all participants. Although the functional form for insulin action was the same for both models, we found that obtaining good fits to the glucose and glycerol data required separate representations of the dynamics of insulin action on each metabolite. Figure 3 shows the OMM and glycerol model fits to glucose and glycerol dynamics, respectively, for two representative individuals from our cohort. These participants were selected to show different dynamic features associated with varying degrees of glycemic dysregulation in this population. The first participant's insulin profile has a single insulin peak (SIP). The second participant's insulin profile has a secondary peak prior to the main peak resulting in a double insulin peak (DIP). The SIP participant reaches peak insulin concentration at 75 min while the DIP participant's insulin peaks at 90 min. The magnitude of the insulin response for the DIP participant is large compared to that of the SIP participant, more than doubling peak insulin from the approximately 300 μ U/mL in the SIP participant to approximately 700 μ U/mL in the DIP participant. In addition, the DIP participant exhibits an insufficient initial insulin response, an extended period of hyperglycemia, and an excursion below the basal glucose level to a nadir glucose level of 58 mg/dl of glucose, all indicators of poor control of central metabolism. The DIP participant is one a subset of individuals in our cohort who exhibits a hypoglycemic response. Both participants show an increase in glycerol concentrations above basal levels after the glucose nadir.

Dynamics of glucose insulin action are delayed relative to dynamics of glycerol insulin action

Each simulated glucose and glycerol profile has a corresponding insulin action profile. Insulin action profiles for the representative participants are shown in Figure 4. Both glucose and glycerol insulin action time traces rely on the same insulin concentration time series as a forcing function,

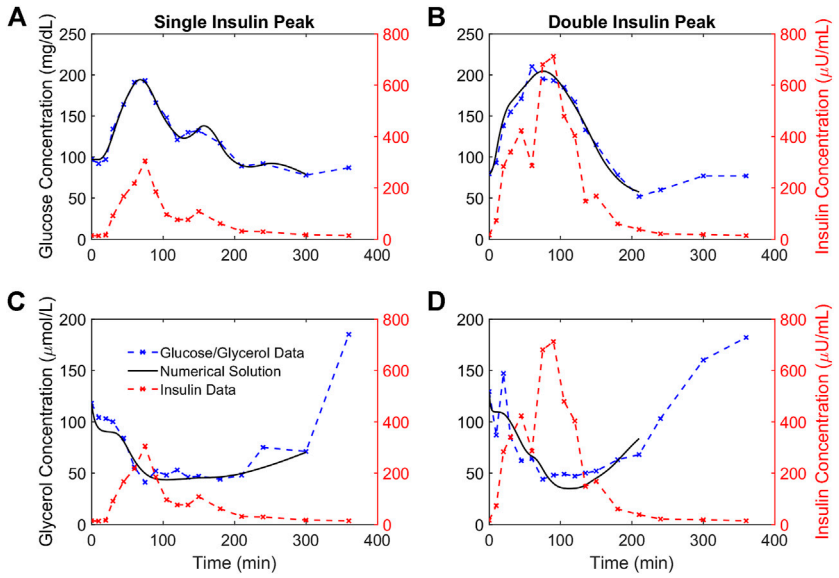

FIGURE 3
Numerical solutions and OGTT data for glucose and glycerol in two representative participants. **(A,B)**. The numerical solutions for glucose (black) are shown relative to the data (blue) and insulin (red) concentrations for two representative participants demonstrating a single insulin peak **(A)** and a double insulin peak **(B)**, respectively. **(C,D)**. The numerical solutions for glycerol (black) are shown relative to the data (blue) and insulin (red) concentrations for the same representative participants and show the suppression of glycerol concentrations in response to insulin concentrations. The lowest glucose concentration following the glucose excursion is taken to be the end point for the glucose and glycerol numerical solutions for each individual.

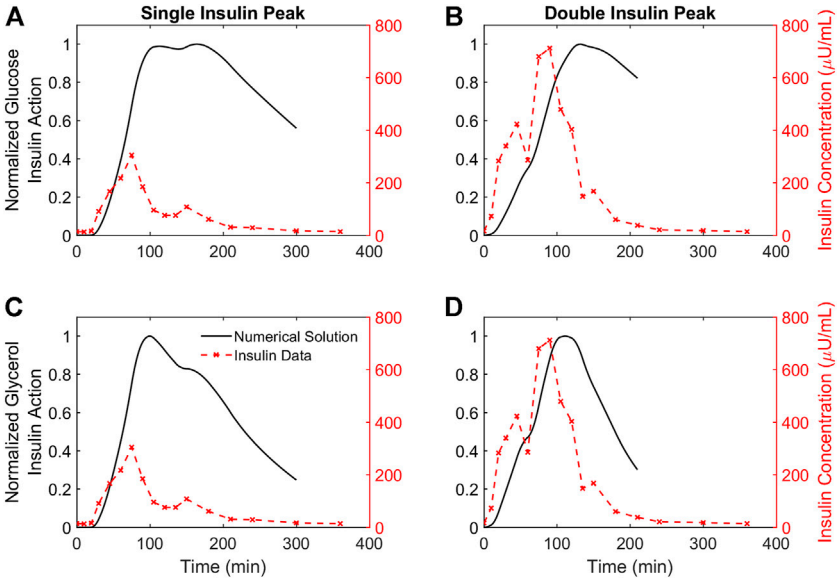

FIGURE 4
Time courses of insulin action on glucose and glycerol for two representative participants. **(A,B)**. The time course of insulin action on glucose plotted against insulin concentrations for two representative participants demonstrating a single insulin peak **(A)** and a double insulin peak **(B)**, respectively. **(C,D)**. The time course of insulin action on glycerol plotted against insulin concentrations for the same two representative participants. All insulin action concentrations are normalized by their maximum value. Insulin concentrations not normalized, and the DIP participant has higher insulin secretion compared to the SIP participant.

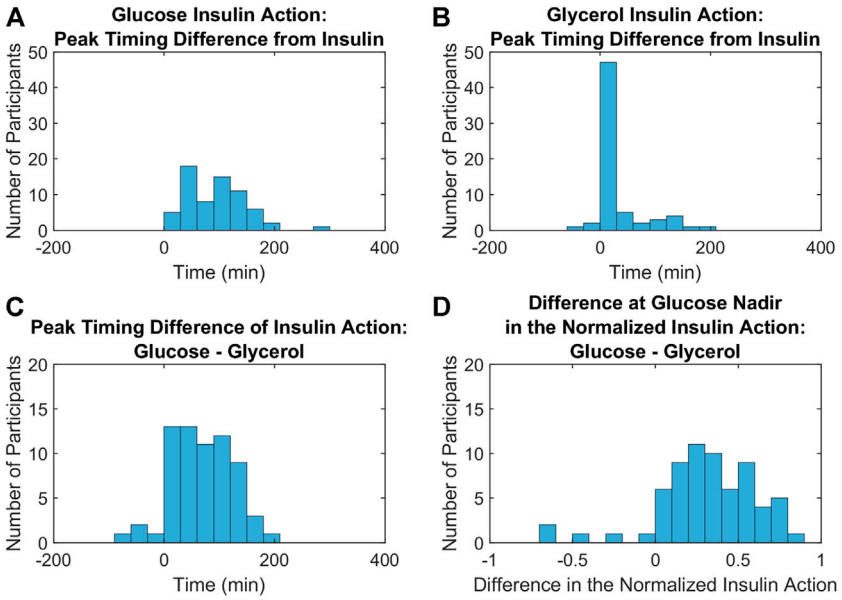

FIGURE 5
Metrics comparing the dynamics of insulin action on glucose and glycerol across all participants. **(A,B)**. Histograms of the differences between glucose **(A)** and glycerol **(B)** insulin action peak timing from insulin peak timing show that insulin peaks are closer to glycerol insulin action peaks compared to glucose insulin action peaks (Wilcoxon signed rank test, $p < 0.001$). **(C)**. A histogram of the differences between glucose and glycerol insulin action peak timing show that this difference is significantly greater than 0 (Student's t-test, $p < 0.001$, 95% confidence interval: 67.38 ± 13.52), indicating that peak glucose insulin action occurs at a later time compared to peak glycerol insulin action. **(D)**. A histogram of the differences between normalized insulin actions for glucose and glycerol at the glucose nadir shows that the normalized insulin action for glucose is greater than the normalized insulin action for glycerol at this time point (Student's t-test, $p < 0.001$, 95% confidence interval: 0.3120 ± 0.0736) and indicates that insulin action on glucose has stronger relative action at the glucose nadir.

but distinct dynamics for glucose and glycerol in response to insulin give rise to qualitatively different insulin action time traces. For both individuals, the glucose insulin action time trace shows a greater delay relative to the insulin time trace while the dynamics of the glycerol insulin action time trace follow insulin dynamics more closely. This observation that glucose insulin action has a greater delay relative to changing insulin concentration than the glycerol insulin action is consistent throughout the population and can be quantified using several metrics.

The results from three metrics comparing distinct features of the insulin action profiles for glucose and glycerol in all participants are depicted in the histograms in Figure 5. The differences between glucose insulin action and insulin peak timing are larger and more variable compared to the differences between glycerol insulin action and insulin peak timing (Wilcoxon signed rank test, $p < 0.001$) reflecting the relatively later timing of the glucose insulin action peak (Figures 5A,B). This relatively later timing of glucose insulin action is also seen in the difference in the timing of insulin action peaks for glucose and glycerol, where the glycerol insulin action peak time is subtracted from the glucose insulin action peak time (Figure 5C). The glycerol insulin action peak time was determined to be earlier compared to the glucose insulin action peak time with a difference between peak times significantly different from 0 (Student's t-test, $p < 0.001$, 95% confidence interval: 67.38 ± 13.52). The normalized glucose insulin action is greater than the normalized glycerol insulin action at the glucose concentration nadir (Figure 5D). The difference in normalized insulin action was positive and significantly different from 0 (Student's t-test, $p < 0.001$, 95% confidence interval: 0.3120 ± 0.0736). This difference indicates that glycerol insulin action terminates earlier compared to glucose insulin action relative to the timing of the glucose excursion. All of these metrics suggest that the timing of insulin action differs between tissues: glycerol insulin action on adipose tissue initiates and terminates earlier relative to glucose insulin action on hepatic tissue and muscle.

Differences in the insulin action time constant

For glucose and glycerol insulin action models, the insulin action time constant parameters, p_2^G and p_2^g, respectively, govern the dynamics of insulin action. As the insulin action time constant parameters approach one, the insulin action curve approaches the plasma insulin curve. When the distributions

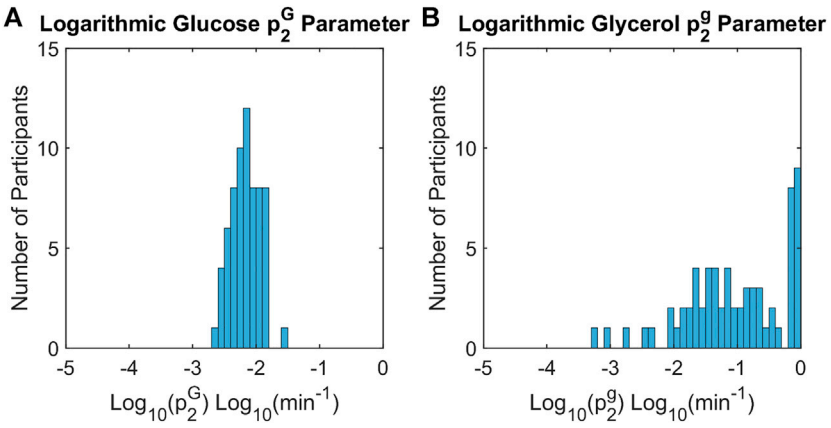

FIGURE 6
Histograms of insulin action time constants for glucose and glycerol across all participants. The time constants for insulin action on glucose, p_2^G, **(A)** are consistently smaller than the time constants for insulin action on glycerol, p_2^g, **(B)** (Wilcoxon signed rank test, $p < 0.001$). This indicates that the time course of insulin action on glucose is more delayed than the time course of insulin action on glycerol relative to insulin concentration data.

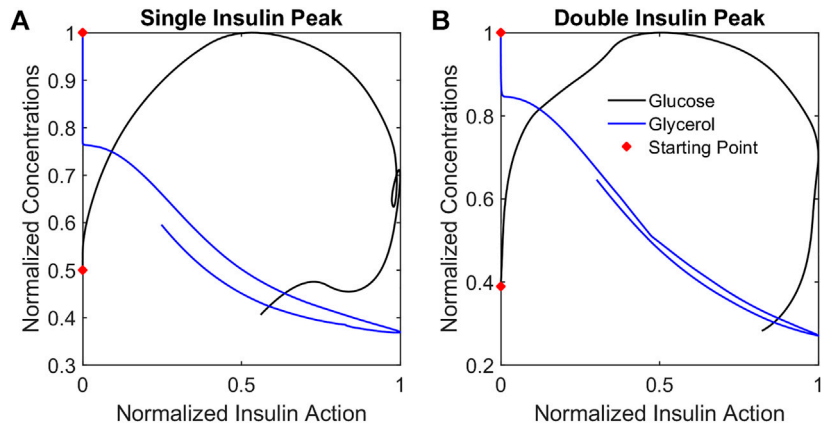

FIGURE 7
Metabolite phase plane trajectories summarize qualitative differences in glucose and glycerol dynamics relative to insulin action. Plotting normalized metabolite concentrations against normalized insulin action concentrations for the representative participants SIP **(A)** and DIP **(B)** reveals that glycerol concentrations change in a diagonal out-and-back pattern while the glucose concentrations change in a cyclic clockwise pattern reflecting the different dynamics of the responses.

of p_2^G and p_2^g were compared across all participants, the p_2^g values for the glycerol model were much greater and were distributed across the range 0–1. To evaluate the effect of p_2^G and p_2^g on each model, the parameters were base 10 log transformed and compared. The distribution of the log transformed p_2^G and p_2^g values in all participants are shown in Figure 6. The estimates of the log-transformed parameters were significantly different (Wilcoxon signed rank test, $p < 0.001$) and show a distinct difference in magnitude with p_2^g approximately two orders larger in magnitude than p_2^G. The difference in estimated glycerol p_2^g and glucose p_2^G parameters indicates that insulin has a more immediate effect on glycerol insulin action than on glucose insulin action.

Summary of differences in insulin action dynamics

To illustrate how insulin action changes relative to each metabolite, trajectories were considered in the metabolite-insulin action phase plane. Phase planes for each representative participant are shown in Figure 7. In each

phase plane, the insulin action and metabolite were normalized by their maximum value. The phase planes show that changes in glycerol tracked more closely with changes in glycerol insulin action compared to changes in glucose and glucose insulin action. Specifically, the trajectory for the glycerol model showed an out and back diagonal path with glycerol and glycerol insulin action changing together. By contrast, the trajectory for the glucose model showed a cyclic path reflecting a time lag in changes in glucose insulin action relative to changes in glucose concentration.

Discussion

Summary of results

This study introduced a model of interacting glycerol and insulin dynamics in response to an OGTT and compared the dynamics of insulin acting on glucose and glycerol in a population of adolescent girls with obesity and with or without PCOS. To our knowledge, this glycerol model is the first mathematical model to describe interactions between glycerol and insulin dynamics. It successfully simulated glycerol concentration data over time from the ingestion of the drink to the post-excursion glucose nadir, and it demonstrated a suppression in glycerol concentrations in response to insulin action. Comparison of results from the glycerol model to results from OMM simulations of glucose and insulin dynamics showed that the dynamics of insulin action on glucose were delayed when compared to the dynamics of insulin action on glycerol.

Differential dynamics for glucose and glycerol in adolescent girls

We quantified the dynamics of insulin action on glucose and glycerol based on model parameters and characteristics of the modeled insulin action using several metrics. All of these metrics showed that the dynamics of insulin action on glucose were delayed relative to the dynamics of insulin action on glycerol during the OGTT, and distinct representations of insulin action on glucose and glycerol were necessary to describe the metabolite data from our adolescent cohort.

Although we represent adipose metabolism through glycerol instead of FFA, the difference in dynamics we observe for insulin acting on glucose compared to insulin acting on glycerol likely reflects the extreme IR with compensatory hyperinsulinemia in our adolescent cohort. Our cohort has a significant degree of IR, accompanied by impaired glucose tolerance, with an average two-hour glucose measurement $\geq$ 140 mg/dl. Low insulin sensitivity suggests a slower insulin response, possibly increasing the delay in insulin action on the glucose system compared to the action of insulin on the glycerol system. The delayed timing of the insulin peaks in our cohort reflects extreme IR consistent with similar populations of adolescents with dysmetabolism (Cree-Green et al., 2018a; RISE Consortium, 2018). In normoglycemic non-obese youth, peak insulin concentrations occur at 30 min post drink, while the insulin peak is at 120 min in adolescents with prediabetes and diabetes (RISE Consortium, 2018; Tommerdahl et al., 2021). Our cohort has an insulin peak at 84 ± 47 min. However, the higher insulin concentrations required as a result of IR may also play a role in the observed delay of insulin action on the glucose system. The average peak insulin concentration for a healthy adolescent insulin profile is approximately 55 μ U/mL (Tommerdahl et al., 2021). The individuals in our cohort have an average peak insulin concentration of 361 μ U/mL. Whereas the insulin concentration needed to suppress lipolysis in this population, 40–50 μ U/mL, is reached quickly after consuming the drink, there is a much longer delay associated with reaching the peak insulin concentration which drives maximal glucose uptake (Cree-Green et al., 2016).

Adolescents have different metabolic characteristics compared to adults due to pubertally-mediated changes in insulin sensitivity, which present in addition to effects of obesity (RISE Consortium, 2018). Growth hormone alters both lipolysis and glucose metabolism, reducing insulin sensitivity in muscle and peripheral tissue, with concentrations peaking during the rapid growth phase of puberty (Moller and Jorgensen, 2009; Kim and Park, 2017). Growth hormone may preferentially influence IR in glucose metabolism compared to adipose metabolism producing a distinct metabolic phenotype in adolescents compared to phenotypes where IR is induced by other metabolic pathways. A tissue-specific difference in IR in adolescents could produce differential metabolic dynamics and is consistent with our findings that data in this cohort requires separate models for insulin action on glucose and glycerol during an OGTT.

By contrast, Periwal and colleagues described glucose and FFA dynamics in an IM-FSIVGTT and a mixed meal tolerance test (MMTT) in African American and Caucasian premenopausal women using a single model with one form of insulin action (Periwal et al., 2008; Li et al., 2016). In addition to the dissimilarities between study populations, distinct dynamics of glucose, insulin, glycerol and FFA among experimental protocols may contribute to the differences in our findings. In an IM-FSIVGTT, plasma glucose concentrations peak at the beginning of the protocol, and the initial early peak in insulin reflects the injection of exogenous insulin and may interact with the endogenous glucose-insulin dynamics and diminish endogenous insulin release. In an OGTT, ingested glucose is slowly absorbed and typically peaks at least 20 min after the administration of the drink (Cree-Green et al., 2018b; RISE Consortium, 2018); endogenous insulin is released in response to increased plasma glucose concentrations and acts on glycerol and glucose in a concentration-dependent manner. In an MMTT, the absorbance of glucose is slower compared to an OGTT due to the presence of fat and protein (Li et al., 2016).

Thus, although, the glucose and FFA model captured the dynamics of two very disparate methods of increasing glucose and insulin in an adult population, the temporality of changes in glucose, insulin, and FFA were similar within each protocol (all fast in an IM-FSIVGTT and all slow in a MMTT). By contrast, an OGTT may highlight distinct dynamics between adipose and glucose metabolism by producing physiologic interactions between glucose and endogenous insulin dynamics in the context of glucose absorbance, that is, slower compared to an IM-FSIVGTT and faster compared to an MMTT. Thus, differences in study populations and protocols likely contributed to the differences in temporality and rate of changes between glucose, insulin, and glycerol and necessitated distinct representations of insulin action on glucose and glycerol in our study compared to previous work with FFAs (Periwal et al., 2008; Li et al., 2016).

Possible physiologic basis for difference in dynamics

Insulin regulation of the metabolic pathways for glucose and glycerol occurs through distinct mechanisms. The elevation of glucose concentration triggers the release of insulin. The insulin then acts so that glucose concentrations decrease back to basal levels. When glucose concentrations return to normal, insulin secretion also decreases. Thus, the interaction between glucose and insulin is bidirectional. Conversely, the interaction between glycerol and insulin is unidirectional. Insulin induces the suppression of lipolysis by regulating the activity of hormone sensitive lipase (Stralfors and Honnor, 1989; Arner, 2001). When insulin concentrations decrease, activation of hormone sensitive lipase stops, and glycerol concentrations increase. However, glycerol concentration has no effect on insulin concentration.

Limitations

This model makes several simplifying assumptions about glycerol biochemistry. First, although we expect lipolysis to be the primary source of glycerol in our protocol, glycolysis may play a role (Rotondo et al., 2019). Second, the structure of this glycerol model assumes that the maximum lipolysis rate occurs in the initial fasted state, and, therefore, it cannot describe rebounds in glycerol concentrations above basal levels. In many participants in our cohort (both SIP and DIP), glycerol concentrations post-suppression rose above basal levels, suggesting the involvement of other metabolic pathways. This post-suppression rebound was particularly pronounced in the approximately 10% of participants demonstrating reactive hypoglycemia (RHG) (Ware et al., 2022). Hypoglycemia is characterized as a condition where blood sugar falls below 60 mg/dl, resulting in warning symptoms and the secretion of counterregulatory hormones working to rapidly increase blood sugar levels (Desouza et al., 2010; Casertano et al., 2021; Ware et al., 2022). Along with glucagon, catecholamines are released during a RHG response, stimulating lipolysis (Fanelli et al., 2020). The current glycerol model does not account for these additional metabolic pathways, so we truncated the data at the glucose nadir to avoid trying to represent two distinct physiological conditions (the initial glucose excursion and the recovery of lipolysis above basal rates) with a single set of parameters. Future work should consider extensions of the glycerol model that account for the counterregulatory response.

There are several additional limitations to this study. This model was developed in a highly IR population of adolescent girls with a high incidence of non-alcoholic fatty liver disease (NAFLD), a condition associated with adipose dysmetabolism. Application of the model to data from healthy populations as well as other IR or dysglycemic populations is important to verify the generalizability of this glycerol-insulin model to the range of dynamics associated with adipose metabolism. For example, in a healthy individual, glycerol may be suppressed earlier in response to a smaller plasma insulin peak.

Summary and implications

In summary, we have proposed a novel differential equations-based model of interactions between glycerol and insulin dynamics that provides a better understanding of glycerol dynamics relative to other metabolic processes like glucose metabolism. In addition, this model demonstrates that during an OGTT, insulin action on glucose is more delayed compared to insulin action on glycerol in our cohort of IR adolescent girls. Although tissue-specific actions of insulin are known to be concentration dependent, to our knowledge this is the first study to establish a difference in the dynamics of distinct insulin actions. Future work examining the mechanisms implicated in this difference and the significance of altered relative glycerol and glucose dynamics to metabolic disease development and progression is needed to alleviate the growing burden of metabolic dysregulation.

Data availability statement

The datasets presented in this article are not readily available because an appropriate institutional data sharing agreement is required. Requests to access the datasets should be directed to Melanie Cree-Green, Melanie.Green@childrenscolorado.org.

Ethics statement

The studies involving human participants were reviewed and approved by the Colorado Multiple Institutional Review Board. Written informed consent to participate in this study was provided by the participants' legal guardian/next of kin.

Author contributions

GSH, MCG, and CDB contributed to conception and design of the study. KJN and MCG collected the data. GSH, KB, and CDB implemented the mathematical models. GSH and CDB performed the statistical analysis. GSH wrote the first draft of the manuscript. MCG and CDB wrote sections of the manuscript. All authors contributed to manuscript revision, read, and approved the submitted version.

Funding

This research was supported by National Institutes of Health (NIH) grants BIRCWH K12HD057022, NIDDK K23DK107871; Doris Duke Foundation 2015212; Children's Hospital Colorado/Colorado School of Mines Collaborative Pilot Award; Mines Undergraduate Research Fellowship; Boettcher Foundation; Boettcher-Webb Warring grant; National Science Foundation Grant DMS 1853511; Nutrition and Obesity Research Core Pilot Grant P30 DK048520; and University of Colorado NIH CTSI protocol micro-grant. This research was also supported by NIH/NCATS Colorado CTSA Grant Number UL1 TR001082.

Acknowledgments

The authors would like to thank Laura Pyle for helpful discussions of the statistical approach. The authors would like to thank Yesenia Garcia-Reyes, Gregory Coe, and Haseeb Rahat for assistance in the APPLE study. The authors would like to thank the participants, their families and the CTRC nurses and staff.

Conflict of interest

The authors declare that the research was conducted in the absence of any commercial or financial relationships that could be construed as a potential conflict of interest.

Publisher's note

All claims expressed in this article are solely those of the authors and do not necessarily represent those of their affiliated organizations, or those of the publisher, the editors and the reviewers. Any product that may be evaluated in this article, or claim that may be made by its manufacturer, is not guaranteed or endorsed by the publisher.

References

Adler-Wailes, D. C., Periwal, V., Ali, A. H., Brady, S. M., McDuffie, J. R., Uwaifo, G. I., et al. (2013). Sex-associated differences in free fatty acid flux of obese adolescents. *J. Clin. Endocrinol. Metab.* 98 (4), 1676–1684. doi:10.1210/jc.2012-3817

Aguilar, M., Bhuket, T., Torres, S., Liu, B., and Wong, R. J. (2015). Prevalence of the metabolic syndrome in the United States, 2003-2012. *JAMA* 313 (19), 1973–1974. doi:10.1001/jama.2015.4260

Ajmera, I., Swat, M., Laibe, C., Le Novere, N., and Chelliah, V. (2013). The impact of mathematical modeling on the understanding of diabetes and related complications. *CPT. Pharmacometrics Syst. Pharmacol.* 2, e54. doi:10.1038/psp.2013.30

American Diabetes, A. (2020). 13. Children and adolescents: Standards of medical care in diabetes-2020. *Diabetes Care* 43 (1), S163–S182. doi:10.2337/dc20-S013

Arner, P. (2001). Free fatty acids - do they play a central role in type 2 diabetes? *Diabetes Obes. Metab.* 3, 11–19. doi:10.1046/j.1463-1326.2001.00031.x

Arner, P. (2002). Insulin resistance in type 2 diabetes: role of fatty acids. *Diabetes. Metab. Res. Rev.* 18 (2), S5–S9. doi:10.1002/dmrr.254

Arner, P., and Rydén, M. (2015). Fatty acids, obesity and insulin resistance. *Obes. Facts* 8 (2), 147–155. doi:10.1159/000381224

Bartlette, K., Carreau, A. M., Xie, D., Garcia-Reyes, Y., Rahat, H., Pyle, L., et al. (2021). Oral minimal model-based estimates of insulin sensitivity in obese youth depend on oral glucose tolerance test protocol duration. *Metabol. Open* 9, 100078. doi:10.1016/j.metop.2021.100078

Bergman, R. N., Ider, Y. Z., Bowden, C. R., and Cobelli, C. (1979). Quantitative estimation of insulin sensitivity. *Am. J. Physiol.* 236 (6), E667–E677. doi:10.1152/ajpendo.1979.236.6.E667

Bergman, R. N. (1989). Lilly lecture 1989. Toward physiological understanding of glucose tolerance. Minimal-model approach. *Diabetes* 38 (12), 1512–1527. doi:10.2337/diab.38.12.1512

Bergman RNB, C. R., and Cobelli, C. (1981). "The Minimal Model approach to quantification of factors controlling glucose disposal in man," in *Carbohydrate metabolism*. Editor R. N. CCB (John Wiley & Sons), 13, 269–296.

Casertano, A., Rossi, A., Fecarotta, S., Rosanio, F. M., Moracas, C., Di Candia, F., et al. (2021). An overview of hypoglycemia in children including a comprehensive practical diagnostic flowchart for clinical use. *Front. Endocrinol.* 12, 684011. doi:10.3389/fendo.2021.684011

Chooi, Y. C., Ding, C., and Magkos, F. (2019). The epidemiology of obesity. *Metabolism.* 92, 6–10. doi:10.1016/j.metabol.2018.09.005

Cobelli, C., Dalla Man, C., Toffolo, G., Basu, R., Vella, A., Rizza, R., et al. (2014). The oral minimal model method. *Diabetes* 63 (4), 1203–1213. doi:10.2337/db13-1198

RISE Consortium and Investigators, R. C. (2019). Effects of treatment of impaired glucose tolerance or recently diagnosed type 2 diabetes with metformin alone or in combination with insulin glargine on beta-cell function: Comparison of responses in youth and adults. *Diabetes* 68 (8), 1670–1680. doi:10.2337/db19-0299

RISE Consortium (2018). Metabolic contrasts between youth and adults with impaired glucose tolerance or recently diagnosed type 2 diabetes: I. Observations using the hyperglycemic clamp. *Diabetes Care* 41 (8), 1696–1706. doi:10.2337/dc18-0244

Conte, C., Fabbrini, E., Kars, M., Mittendorfer, B., Patterson, B. W., Klein, S., et al. (2012). Multiorgan insulin sensitivity in lean and obese subjects. *Diabetes Care* 35 (6), 1316–1321. doi:10.2337/dc11-1951

Centers for Disease Control and Prevention (2020). *National diabetes statistics report*. Atlanta, GA: Centers for Disease Control and Prevention, US Department of Health and Human Services.

Coppack, S. W., Persson, M., Judd, R. L., and Miles, J. M. (1999). Glycerol and nonesterified fatty acid metabolism in human muscle and adipose tissue *in vivo*. *Am. J. Physiol.* 276 (2), E233–E240. doi:10.1152/ajpendo.1999.276.2.E233

Cree-Green, M., Bergman, B. C., Cengiz, E., Fox, L. A., Hannon, T. S., Miller, K., et al. (2019). Metformin improves peripheral insulin sensitivity in youth with type 1 diabetes. *J. Clin. Endocrinol. Metab.* 104 (8), 3265–3278. doi:10.1210/jc.2019-00129

Cree-Green, M., Bergman, B. C., Coe, G. V., Newnes, L., Baumgartner, A. D., Bacon, S., et al. (2016). Hepatic steatosis is common in adolescents with obesity and

PCOS and relates to De novo lipogenesis but not insulin resistance. *Obes. (Silver Spring)* 24 (11), 2399–2406. doi:10.1002/oby.21651

Cree-Green, M., Cai, N., Thurston, J. E., Coe, G. V., Newnes, L., Garcia-Reyes, Y., et al. (2018). Using simple clinical measures to predict insulin resistance or hyperglycemia in girls with polycystic ovarian syndrome. *Pediatr. Diabetes* 19 (8), 1370–1378. doi:10.1111/pedi.12778

Cree-Green, M., Wiromrat, P., Stuppy, J. J., Thurston, J., Bergman, B. C., Baumgartner, A. D., et al. (2019). Youth with type 2 diabetes have hepatic, peripheral, and adipose insulin resistance. *Am. J. Physiol. Endocrinol. Metab.* 316 (2), E186–E195. doi:10.1152/ajpendo.00258.2018

Cree-Green, M., Xie, D., Rahat, H., Garcia-Reyes, Y., Bergman, B. C., Scherzinger, A., et al. (2018). Oral glucose tolerance test glucose peak time is most predictive of prediabetes and hepatic steatosis in obese girls. *J. Endocr. Soc.* 2 (6), 547–562. doi:10.1210/js.2018-00041

Dalla Man, C., Caumo, A., and Cobelli, C. (2002). The oral glucose minimal model: Estimation of insulin sensitivity from a meal test. *IEEE Trans. Biomed. Eng.* 49 (5), 419–429. doi:10.1109/10.995680

Desouza, C. V., Bolli, G. B., and Fonseca, V. (2010). Hypoglycemia, diabetes, and cardiovascular events. *Diabetes Care* 33 (6), 1389–1394. doi:10.2337/dc09-2082

Diniz Behn, C., Jin, E. S., Bubar, K., Malloy, C., Parks, E. J., Cree-Green, M., et al. (2020). Advances in stable isotope tracer methodology part 1: hepatic metabolism *via* isotopomer analysis and postprandial lipolysis modeling. *J. Investig. Med.* 68 (1), 3–10. doi:10.1136/jim-2019-001109

Fanelli, C. G., Lucidi, P., Bolli, G. B., and Porcellati, F. (2020). *Hypoglycemia*. Springer International Publishing, 615–652.

Group, T. S., Bjornstad, P., Drews, K. L., Caprio, S., Gubitosi-Klug, R., Nathan, D. M., et al. (2021). Long-term complications in youth-onset type 2 diabetes. *N. Engl. J. Med. Overseas. Ed.* 385 (5), 416–426. doi:10.1056/nejmoa2100165

Ha, J., Satin, L. S., and Sherman, A. S. (2016). A mathematical model of the pathogenesis, prevention, and reversal of type 2 diabetes. *Endocrinology* 157 (2), 624–635. doi:10.1210/en.2015-1564

Hirode, G., and Wong, R. J. (2020). Trends in the prevalence of metabolic syndrome in the United States, 2011-2016. *JAMA* 323 (24), 2526–2528. doi:10.1001/jama.2020.4501

Imperatore, G., Boyle, J. P., Thompson, T. J., Case, D., Dabelea, D., Hamman, R. F., et al. (2012). Projections of type 1 and type 2 diabetes burden in the U.S. population aged <20 years through 2050: dynamic modeling of incidence, mortality, and population growth. *Diabetes Care* 35 (12), 2515–2520. doi:10.2337/dc12-0669

Jensen, M. D. (1999). Regional glycerol and free fatty acid metabolism before and after meal ingestion. *Am. J. Physiol.* 276 (5), E863–E869. doi:10.1152/ajpendo.1999.276.5.E863

Kelly, T., Yang, W., Chen, C. S., Reynolds, K., and He, J. (2008). Global burden of obesity in 2005 and projections to 2030. *Int. J. Obes.* 32 (9), 1431–1437. doi:10.1038/ijo.2008.102

Kim, S. H., and Park, M. J. (2017). Effects of growth hormone on glucose metabolism and insulin resistance in human. *Ann. Pediatr. Endocrinol. Metab.* 22 (3), 145–152. doi:10.6065/apem.2017.22.3.145

Landau, B. R. (1999). Glycerol production and utilization measured using stable isotopes. *Proc. Nutr. Soc.* 58 (4), 973–978. doi:10.1017/s0029665199001287

Levine, J. A., Han, J. M., Wolska, A., Wilson, S. R., Patel, T. P., Remaley, A. T., et al. (2020). Associations of GlycA and high-sensitivity C-reactive protein with measures of lipolysis in adults with obesity. *J. Clin. Lipidol.* 14 (5), 667–674. doi:10.1016/j.jacl.2020.07.012

Li, Y., Chow, C. C., Courville, A. B., Sumner, A. E., and Periwal, V. (2016). Modeling glucose and free fatty acid kinetics in glucose and meal tolerance test. *Theor. Biol. Med. Model.* 13, 8. doi:10.1186/s12976-016-0036-3

Magkos, F., Fabbrini, E., Conte, C., Patterson, B. W., and Klein, S. (2012). Relationship between adipose tissue lipolytic activity and skeletal muscle insulin resistance in nondiabetic women. *J. Clin. Endocrinol. Metab.* 97 (7), E1219–E1223. doi:10.1210/jc.2012-1035

Mayer-Davis, E. J., Lawrence, J. M., Dabelea, D., Divers, J., Isom, S., Dolan, L., et al. (2017). Incidence trends of type 1 and type 2 diabetes among youths, 2002-2012. *N. Engl. J. Med.* 376 (15), 1419–1429. doi:10.1056/NEJMoa1610187

Moller, N., and Jorgensen, J. O. (2009). Effects of growth hormone on glucose, lipid, and protein metabolism in human subjects. *Endocr. Rev.* 30 (2), 152–177. doi:10.1210/er.2008-0027

Periwal, V., Chow, C. C., Bergman, R. N., Ricks, M., Vega, G. L., Sumner, A. E., et al. (2008). Evaluation of quantitative models of the effect of insulin on lipolysis and glucose disposal. *Am. J. Physiol. Regul. Integr. Comp. Physiol.* 295 (4), R1089–R1096. doi:10.1152/ajpregu.90426.2008

Petersen, M. C., and Shulman, G. I. (2018). Mechanisms of insulin action and insulin resistance. *Physiol. Rev.* 98 (4), 2133–2223. doi:10.1152/physrev.00063.2017

Picchini, U., De Gaetano, A., Panunzi, S., Ditlevsen, S., and Mingrone, G. (2005). A mathematical model of the euglycemic hyperinsulinemic clamp. *Theor. Biol. Med. Model.* 2 (1), 44. doi:10.1186/1742-4682-2-44

Possik, E., Schmitt, C., Al-Mass, A., Bai, Y., Cote, L., Morin, J., et al. (2022). Phosphoglycolate phosphatase homologs act as glycerol-3-phosphate phosphatase to control stress and healthspan in *C. elegans*. *Nat. Commun.* 13 (1), 177. doi:10.1038/s41467-021-27803-6

Ramos-Roman, M. A., Lapidot, S. A., Phair, R. D., and Parks, E. J. (2012). Insulin activation of plasma nonesterified fatty acid uptake in metabolic syndrome. *Arterioscler. Thromb. Vasc. Biol.* 32 (8), 1799–1808. doi:10.1161/ATVBAHA.112.250019

Reshef, L., Olswang, Y., Cassuto, H., Blum, B., Croniger, C. M., Kalhan, S. C., et al. (2003). Glyceroneogenesis and the triglyceride/fatty acid cycle. *J. Biol. Chem.* 278 (33), 30413–30416. doi:10.1074/jbc.R300017200

Ronald Kahn, C. (1978). Insulin resistance, insulin insensitivity, and insulin unresponsiveness: A necessary distinction. *Metabolism.* 27 (12), 1893–1902. doi:10.1016/s0026-0495(78)80007-9

Rotondo, F., Ho-Palma, A. C., Romero, M. D. M., Remesar, X., Fernandez-Lopez, J. A., Alemany, M., et al. (2019). Higher lactate production from glucose in cultured adipose nucleated stromal cells than for rat adipocytes. *Adipocyte* 8 (1), 61–76. doi:10.1080/21623945.2019.1569448

Roy, A., and Parker, R. S. (2006). Dynamic modeling of free fatty acid, glucose, and insulin: An extended "minimal model. *Diabetes Technol. Ther.* 8 (6), 617–626. doi:10.1089/dia.2006.8.617

Sondergaard, E., Espinosa De Ycaza, A. E., Morgan-Bathke, M., and Jensen, M. D. (2017). How to measure adipose tissue insulin sensitivity. *J. Clin. Endocrinol. Metab.* 102 (4), 1193–1199. doi:10.1210/jc.2017-00047

Steinberg, D., Vaughan, M., Margolis, S., Price, H., and Pittman, R. (1961). Studies of triglyceride biosynthesis in homogenates of adipose tissue. *J. Biol. Chem.* 236 (6), 1631–1637. doi:10.1016/s0021-9258(19)63276-x

Stralfors, P., and Honnor, R. C. (1989). Insulin-induced dephosphorylation of hormone-sensitive lipase. Correlation with lipolysis and cAMP-dependent protein kinase activity. *Eur. J. Biochem.* 182 (2), 379–385. doi:10.1111/j.1432-1033.1989.tb14842.x

Thomaseth, K., Brehm, A., Pavan, A., Pacini, G., and Roden, M. (2014). Modeling glucose and free fatty acid kinetics during insulin-modified intravenous glucose tolerance test in healthy humans: role of counterregulatory response. *Am. J. Physiol. Regul. Integr. Comp. Physiol.* 307 (3), R321–R331. doi:10.1152/ajpregu.00314.2013

Tommerdahl, K. L., Brinton, J. T., Vigers, T., Cree-Green, M., Zeitler, P. S., Nadeau, K. J., et al. (2021). Delayed glucose peak and elevated 1-hour glucose on the oral glucose tolerance test identify youth with cystic fibrosis with lower oral disposition index. *J. Cyst. Fibros.* 20 (2), 339–345. doi:10.1016/j.jcf.2020.08.020

Utzschneider, K. M., Tripputi, M. T., Kozedub, A., Barengolts, E., Caprio, S., Cree-Green, M., et al. (2021). Differential loss of beta-cell function in youth vs. adults following treatment withdrawal in the Restoring Insulin Secretion (RISE) study. *Diabetes Res. Clin. Pract.* 178, 108948. doi:10.1016/j.diabres.2021.108948

Utzschneider, K. M., Tripputi, M. T., Kozedub, A., Mather, K. J., Nadeau, K. J., Edelstein, S. L., et al. (2020). β-cells in youth with impaired glucose tolerance or early type 2 diabetes secrete more insulin and are more responsive than in adults. *Pediatr. Diabetes* 21 (8), 1421–1429. doi:10.1111/pedi.13113

Ware, M., Carreau, A., Garcia-Reyes, Y., Rahat, H., Diniz Behn, C., and Cree-Green, M. (2022). Reactive hypoglycemia following a sugar challenge is accompanied by higher insulin in adolescent girls with obesity. *J. Investig. Med.* 70, 112-337.

Wolfe, R. R., and Chinkes, D. L. (2005). *Isotope tracers in metabolic research: Principles and practice of kinetic analysis*. 2nd ed. (Hoboken, N.J.: Wiley-Liss), 474. vii.

Young, L. H., and Periwal, V. (2016). Metabolic scaling predicts posthepatectomy liver regeneration after accounting for hepatocyte hypertrophy. *Liver Transpl.* 22 (4), 476–484. doi:10.1002/lt.24392

Zawadzki JD, A. (1992). "Diagnostic criteria for polycystic ovary syndrome: towards a rational approach," in *Polycystic ovary syndrome* (Boston: Blackwell Scientific Publications), 39–50.

frontiers | Frontiers in Physiology

TYPE Original Research
PUBLISHED 01 September 2022
DOI 10.3389/fphys.2022.936101

OPEN ACCESS

EDITED BY
Stephanie Therese Chung,
National Institutes of Health (NIH),
United States

REVIEWED BY
Juan Guillermo Diaz Ochoa,
PERMEDIQ GmbH, Germany
Jeppe Sturis,
Novo Nordisk, Denmark

*CORRESPONDENCE
William Ott,
ott@math.uh.edu
Bhargav R. Karamched,
bkaramched@fsu.edu

SPECIALTY SECTION
This article was submitted to Metabolic Physiology, a section of the journal Frontiers in Physiology

RECEIVED 10 May 2022
ACCEPTED 05 August 2022
PUBLISHED 01 September 2022

CITATION
Karamched BR, Hripcsak G, Leibel RL, Albers D and Ott W (2022), Delay-induced uncertainty in the glucose-insulin system: Pathogenicity for obesity and type-2 diabetes mellitus. *Front. Physiol.* 13:936101. doi: 10.3389/fphys.2022.936101

Delay-induced uncertainty in the glucose-insulin system: Pathogenicity for obesity and type-2 diabetes mellitus

Bhargav R. Karamched[1,2,3]*, George Hripcsak[4], Rudolph L. Leibel[5,6], David Albers[4,7] and William Ott[8]*

[1]Department of Mathematics, Florida State University, Tallahassee, FL, United States, [2]Institute of Molecular Biophysics, Florida State University, Tallahassee, FL, United States, [3]Program in Neuroscience, Florida State University, Tallahassee, FL, United States, [4]Department of Biomedical Informatics, Columbia University, New York, NY, United States, [5]Division of Molecular Genetics, Department of Pediatrics, Vagelos College of Physicians and Surgeons, Columbia University Irving Medical Center, NY, NY, United States, [6]Naomi Berrie Diabetes Center, Columbia University Irving Medical Center, NY, NY, United States, [7]Section of Informatics and Data Science, Department of Pediatrics, Department of Biomedical Engineering, and Department of Biostatistics and Informatics, University of Colorado Anschutz Medical Campus, Aurora, CO, United States, [8]Department of Mathematics, University of Houston, Houston, TX, United States

We have recently shown that physiological delay can induce a novel form of sustained temporal chaos we call delay-induced uncertainty (DIU) (Karamched et al. (Chaos, 2021, 31, 023142)). This paper assesses the impact of DIU on the ability of the glucose-insulin system to maintain homeostasis when responding to the ingestion of meals. We address two questions. First, what is the nature of the DIU phenotype? That is, what physiological macrostates (as encoded by physiological parameters) allow for DIU onset? Second, how does DIU impact health? We find that the DIU phenotype is abundant in the space of intrinsic parameters for the Ultradian glucose-insulin model—a model that has been successfully used to predict glucose-insulin dynamics in humans. Configurations of intrinsic parameters that correspond to high characteristic glucose levels facilitate DIU onset. We argue that DIU is pathogenic for obesity and type-2 diabetes mellitus by linking the statistical profile of DIU to the glucostatic theory of hunger.

KEYWORDS

delay-induced uncertainty, glucostatic hypothesis, lyapunov exponent, obesity, shear, theory of rank-one maps, type-2 diabetes mellitus, ultradian model

1 Introduction

Clinical and laboratory practice throughout biomedicine and biochemistry proceeds from the assumption that the dynamics of measured quantities are predictable. For instance, a clinician administers medication to a patient based on the supposition that the medical intervention will not induce an unexpectedly erratic response. The presence of sustained temporal chaos would fundamentally undermine the assumption of predictability. Such chaos has been observed in certain classical physiological models

(Abarbanel et al. (1993); Li and Yorke (2004); Mackey and Glass (1977); Glass et al. (1988); Glass and Malta (1990)).

We recently proposed a novel route through which physiological delay can induce sustained temporal chaos for concrete dynamical systems of interest in biomedicine (Karamched et al. (2021)). We termed the resulting chaos *delay-induced uncertainty* (DIU). We argued that DIU is relevant for glycemic management in the intensive care unit by exhibiting it for the Ultradian model, an archetypal model of glucose-insulin dynamics (Sturis et al. (1991); Drozdov and Khanina (1995)). Tools from the general theory of nonuniformly hyperbolic dynamical systems and the theory of rank-one maps yielded a precise characterization of the dynamical and statistical profiles of DIU. Clinicians may find DIU difficult to interpret because these profiles can be subtle.

DIU is potentially relevant for any physiological system wherein delayed regulatory feedback controls try to maintain healthy homeostasis. Examples include pulmonary and respiratory dynamics (Mackey and Glass (1977); Sottile et al. (2018)), cardiac dynamics (Christini and Glass (2002)), female endocrine dynamics (Graham et al. (2020); Urteaga et al. (2019)), and neurological dynamics (Stroh et al. (2020); Claassen et al. (2013); Hodgkin and Huxley (1952)). Indeed, the use of mathematical physiology within medicine has broad potential (Albers et al. (2018a); Zenker et al. (2007)).

This paper is a first attempt to assess the impact of DIU on the ability of the glucose-insulin system to maintain homeostasis when responding to the ingestion of meals. We work with the Ultradian model as we did before (Karamched et al. (2021)), but in a different regime. Our previous work focused on glycemic management in the intensive care unit (ICU) and therefore considered the regime wherein the intrinsic (unforced) system admits a glycemic oscillation (limit cycle). Here, we work in the regime wherein the intrinsic system admits a stable stationary state. In this regime, meals (glucose kicks) move trajectories away from the stationary point. After each kick, the glucose-insulin control system tries to efficiently return to the fixed point. We are therefore interested in how DIU impacts *return to equilibrium*.

In the context of return to equilibrium, the recipe for DIU has three ingredients. First, delay renders the unforced system excitable by weakening the stability of the stationary point. Second, shear is present near this stationary point. One can think of shear as velocity gradients. Third, external forcing (glucose kicking) interacts with shear during the relaxation phase between kicks. This interaction stretches and folds the phase space, creating hyperbolicity in the dynamics and producing sustained temporal chaos.

Here, we show that the physiological architecture of the glucose-insulin system possesses all three ingredients in the DIU recipe. We offer substantial evidence for the following two conjectures.

1) The DIU phenotype is abundant in the space of intrinsic parameters. In other words, a variety of physiological macrostates (as encoded by intrinsic parameters) lead to DIU emergence.
2) DIU is pathogenic for obesity and type-2 diabetes mellitus (T2DM).

This paper is a call to action—a first step toward verifying these conjectures.

Given the importance of elucidating obesity pathogenesis (Schwartz et al. (2017)), the DIU pathogenicity conjecture is the primary contribution of this work. The two-part argument supporting it links the statistical distribution of glucose that DIU induces to the glucostatic theory (Chaput and Tremblay (2009); Mayer (1955)). First, when DIU is present, glucose level dips below its mean more frequently. Second, glucostatic theory asserts that such dips induce hunger. See Figure 1 for an illustration of this two-part argument. This conjectured form of obesity pathogenesis acts on long timescales (months and years). As we will show, DIU becomes more probable as intrinsic parameters move into regions of parameter space that correspond to elevated characteristic glucose levels. Development of early-stage obesity and T2DM would therefore act as a feedback mechanism by promoting DIU, leading to disease progression.

We work with the Ultradian model for two primary reasons, validity and flexibility. The model includes two major negative feedback loops describing effects of insulin on glucose use and glucose production. Both loops include glucose-based stimulation of insulin secretion. External forcing can include both meal ingestion and glucose infusion. The Ultradian model can be tuned so that the unforced system admits a limit cycle, as in (Karamched et al. (2021)), or a stationary state. Importantly, it has been used to accurately predict glucose dynamics in humans (Albers et al. (2017)).

2 The Ultradian model

In this section we describe the Ultradian glucose-insulin model (Sturis et al. (1991); Drozdov and Khanina (1995); Keener and Sneyd (1998)), the external forcing drive that we use for simulations, and intrinsic system parameters that we hypothesize can facilitate DIU onset.

The Ultradian model is a compartment model with three state variables: plasma glucose (G), plasma insulin (I_p), and interstitial insulin (I_i). See Figure 2 for the model schematic. These three state variables are coupled to a three-stage linear delay filter, producing a six-dimensional phase space. The model includes two major negative feedback loops describing effects of insulin on glucose use and glucose production. Both loops include glucose-based stimulation of insulin secretion. The Ultradian model includes physiologic delay, but the system is *finite-dimensional* because the delay assumes the form of a three-stage linear filter.

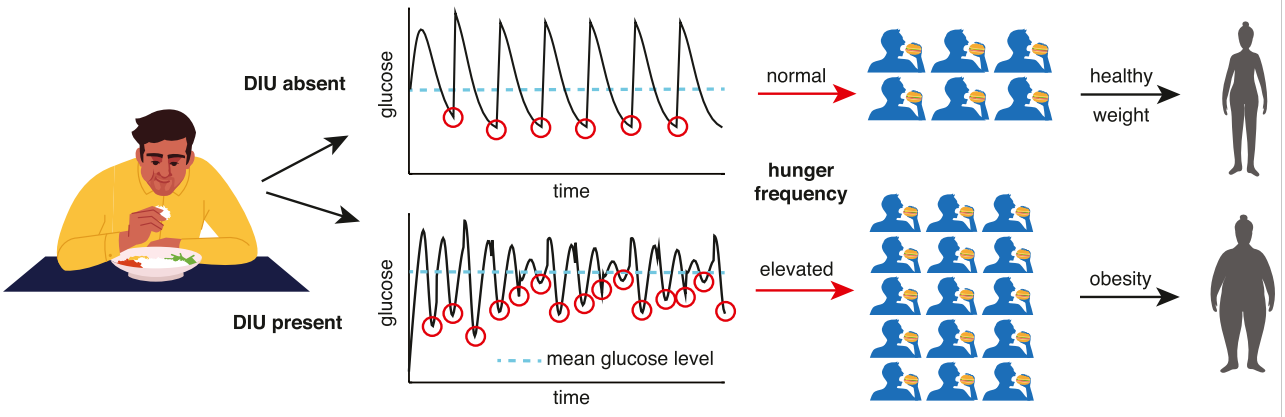

FIGURE 1
How DIU may be pathogenic for obesity and T2DM. When DIU is present, glucose level dips below its mean more frequently (bottom row). The glucostatic hypothesis asserts that such dips induce hunger. DIU would therefore impute elevated hunger frequency, leading to obesity on long timescales.

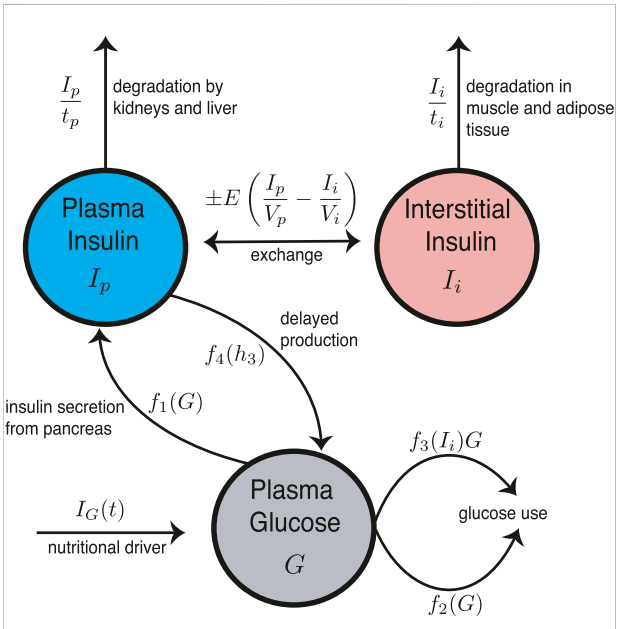

FIGURE 2
Schematic for the Ultradian model of glucose-insulin dynamics. Note the important delayed regulatory feedback between I_p and G.

The full model is given by

$$\frac{dI_p}{dt} = f_1(G) - E\left(\frac{I_p}{V_p} - \frac{I_i}{V_i}\right) - \frac{I_p}{t_p} \tag{1a}$$

$$\frac{dI_i}{dt} = E\left(\frac{I_p}{V_p} - \frac{I_i}{V_i}\right) - \frac{I_i}{t_i} \tag{1b}$$

$$\frac{dG}{dt} = f_4(h_3) + I_G(t) - f_2(G) - f_3(I_i)G \tag{1c}$$

$$\frac{dh_1}{dt} = \frac{1}{t_d}\left(I_p - h_1\right) \tag{1d}$$

$$\frac{dh_2}{dt} = \frac{1}{t_d}\left(h_1 - h_2\right) \tag{1e}$$

$$\frac{dh_3}{dt} = \frac{1}{t_d}\left(h_2 - h_3\right), \tag{1f}$$

where $f_1(G)$ represents the rate of insulin production, $f_2(G)$ represents insulin-independent glucose use, $f_3(I_i)G$ represents insulin-dependent glucose use, and $f_4(h_3)$ represents delayed insulin-dependent glucose use. The functional forms of f_1, f_2, f_3, and f_4 are given by

$$f_1(G) = \frac{R_m}{1 + \exp\left(\frac{-G}{V_g C_1} + a_1\right)} \tag{2a}$$

$$f_2(G) = U_b\left(1 - \exp\left(\frac{-G}{C_2 V_g}\right)\right) \tag{2b}$$

$$f_3(I_i) = \frac{1}{C_3 V_g}\left(U_0 + \frac{U_m - U_0}{1 + (\kappa I_i)^{-\beta}}\right) \tag{2c}$$

$$f_4(h_3) = \frac{R_g}{1 + \exp\left(\alpha\left(\frac{h_3}{C_5 V_p} - 1\right)\right)}, \tag{2d}$$

with

$$\kappa = \frac{1}{C_4}\left(\frac{1}{V_i} - \frac{1}{E t_i}\right). \tag{3}$$

Table 1 summarizes the meaning of each model parameter and provides the set of nominal parameter values.

2.1 Pulsatile glucose forcing drives

The term $I_G(t)$ in Eq.1c represents the external nutritional drive. We call system (1) without this term the *intrinsic system* or

TABLE 1 Full list of intrinsic parameters for the Ultradian glucose-insulin model (Albers et al. (2017)). Note that IIGU and IDGU denote insulin-independent glucose utilization and insulin-dependent glucose utilization, respectively.

Ultradian model parameters

Name	Nominal value	Meaning
V_p	3 L	plasma volume
V_i	11 L	interstitial volume
V_g	10 L	glucose space
E	0.2 L min^{-1}	exchange rate for insulin between remote and plasma compartments
t_p	6 min	time constant for plasma insulin degradation (via kidney and liver filtering)
t_i	100 min	time constant for remote insulin degradation (via muscle and adipose tissue)
t_d	10.5 min	delay between plasma insulin and glucose production
R_m	209 mU min^{-1}	linear constant affecting insulin secretion
a_1	6.6	exponential constant affecting insulin secretion
C_1	300 mg L^{-1}	exponential constant affecting insulin secretion
C_2	144 mg L^{-1}	exponential constant affecting IIGU
C_3	100 mg L^{-1}	linear constant affecting IDGU
C_4	80 mU L^{-1}	factor affecting IDGU
C_5	26 mU L^{-1}	exponential constant affecting IDGU
U_b	72 mg min^{-1}	linear constant affecting IIGU
U_0	4 mg min^{-1}	linear constant affecting IDGU
U_m	94 mg min^{-1}	linear constant affecting IDGU
R_g	180 mg min^{-1}	linear constant affecting IDGU
α	7.5	exponential constant affecting IDGU
β	1.772	exponent affecting IDGU

unforced system. In this paper, we consider an idealized nutritional drive $I_G(t)$ that consists of pulsatile kicks. This drive models meals that are eaten and digested instantaneously. That is, we assume that the nutritional content of each meal immediately affects the glucose state variable in the Ultradian system. The idealized nutritional drive is given by

$$I_G(t) = \sum_{n=1}^{\infty} A_n \delta(t - T_n), \tag{4}$$

where $\delta(t)$ is the Dirac delta distribution (unit impulse), T_n is the time of meal n, and A_n is the amount of carbohydrate in meal n. Importantly, this pulsatile drive does not overwhelm the intrinsic dynamics. On the contrary, it can interact subtly with intrinsic shear to produce DIU, as we will see.

The form of $I_G(t)$ in Eq. 4 induces the following dynamics. Between two consecutive kicks ($T_{n-1} < t < T_n$), Ultradian dynamics evolve according to system (1) with $I_G(t) = 0$. At time T_n of meal n, the glucose state variable, G, undergoes the instantaneous change $G \mapsto G + A_n$. That is, at time T_n we pause the flow generated by the intrinsic system and apply the diffeomorphism

$$\left(I_p, I_i, G, h_1, h_2, h_3\right) \mapsto \left(I_p, I_i, G + A_n, h_1, h_2, h_3\right) \tag{5}$$

to the phase space. We call this diffeomorphism followed by flow of the intrinsic system cycle the *kick-relaxation cycle*.

In reality, meals produce glucose perturbations that are temporally localized but not instantaneous. Nevertheless, we have strong evidence that the emergence of DIU (or the absence of such emergence) is sensitive to neither the exact timing of the pulses nor to their shape. In previous work (Karamched et al. (2021)), we examined the emergence of DIU for the Ultradian model when the delay parameter t_d is tuned so that the intrinsic system admits a limit cycle (sustained oscillatory dynamics). There, we showed that DIU can emerge when each inter-meal time is drawn from an exponential distribution (Poissonian inter-meal timing) and when the drive 4) is replaced with square pulses of duration 30 min that arrive at 8 a.m., noon, and 6 PM. Here, we elect to work with drive 4) and consider only periodic pulsing ($T_n = nT$, where $T \in \mathbb{R}_{>0}$ is the inter-kick time) with constant kick amplitude ($A_n = A$ for all $n \in \mathbb{Z}_{\geqslant 0}$) in order to focus on how intrinsic parameters impact DIU emergence. Our previous work indicates that our new results for periodic pulsatile forcing will continue to hold for more complex forcing drives.

2.2 Key intrinsic parameters for DIU emergence

We hypothesize that intrinsic (unrelated to the forcing drive) parameters directly linked to G, the glucose state variable, play a key role in DIU onset. This hypothesis is partially inspired by recent work that established a positive correlation between mean glucose levels and glucose variance (Albers et al. (2018b)). Our numerical experiments examine the impact of the following parameters on DIU emergence.

- R_g - the uninhibited hepatic glucose production rate
- U_b - the maximal insulin-independent glucose usage rate
- U_0 - the basal insulin-dependent glucose usage rate
- α - the inhibition of hepatic glucose production
- a_1 - the basal glucose-based insulin inhibition
- C_1 - the sensitivity of insulin production to glucose

Importantly, each of these intrinsic parameters has a concrete physiological interpretation.

3 Methods

The maximal Lyapunov exponent as a diagnostic tool. We use the maximal Lyapunov exponent, $\Lambda_{\max}$, as a DIU diagnostic: $\Lambda_{\max} > 0$ indicates DIU whereas $\Lambda_{\max} < 0$ indicates its absence. Computing $\Lambda_{\max}$ requires solving system (1). We do this in the following way. During the relaxation intervals (T_{n-1}, T_n) between kicks, we integrate the unforced differential equations using the MATLAB `ode23s` solver. At kick times T_n, we pause the differential equation solver and apply the diffeomorphism of phase space induced by the kick (see Eq. 5).

We compute the maximal Lyapunov exponent in the following way. We track two solutions to system (1), initially separated by $d_0 = 10^{-8}$. One of these solutions can be thought of as a base solution and the other as a perturbation. After the first kick-relaxation cycle, we compute the separation d_1 between the solutions and store the quantity $\log(d_1/d_0)$ in a vector. We then renormalize by rescaling the secondary orbit so that the distance between the solutions resets to d_0. We proceed in this manner for 10^5 kick-relaxation cycles. This produces a vector containing 10^5 values of $\log(d_1/d_0)$. Averaging over the vector produces $\Lambda_{\max}$. The maximal Lyapunov exponent consequently quantifies the amount of expansion per kick-relaxation cycle.

4 Results

We have designed our numerical experiments to support two primary conjectures. These conjectures are the animating force behind this paper.

1) The DIU phenotype is abundant in the space of intrinsic parameters. In other words, a variety of physiological macrostates (as encoded by intrinsic parameters) lead to DIU emergence.
2) DIU is pathogenic for obesity and T2DM.

4.1 Numerical experiments: Design, rationale, and expectations

Tuning of intrinsic parameters. To support the conjecture that the DIU phenotype is abundant in the space of intrinsic parameters, we begin by setting the intrinsic parameters in the unforced Ultradian model to the nominal values listed in Table 1. Crucially, the delay timescale t_d acts as a bifurcation parameter for the intrinsic system. There exists a value $t_d^\star$ at which the intrinsic system undergoes a supercritical Hopf bifurcation. The intrinsic system admits a stable stationary point $(I_{p,\mathrm{eq}}, I_{i,\mathrm{eq}}, G_{\mathrm{eq}}, h_{1,\mathrm{eq}}, h_{2,\mathrm{eq}}, h_{3,\mathrm{eq}})$ for $t_d < t_d^\star$ (homeostasis) that gives birth to a stable limit cycle (glycemic oscillation) for $t_d > t_d^\star$. For our numerical experiments, we set t_d to the nominal value 10.5 min, a value strictly less than $t_d^\star$, thereby placing the intrinsic system in the stable stationary point regime. This is the appropriate regime for our current study because we are interested in how the dynamical variables relax to homeostatic levels between glucose kicks.

Using the nominal values of the intrinsic parameters as a starting point, we look for DIU along six one-dimensional slices of parameter space. We select a parameter from the list given in Section 2.2 and then vary this parameter while holding all other intrinsic parameters fixed.

Testing for DIU onset. Having set the intrinsic parameters, we test for DIU onset by tuning the external pulsatile forcing drive (4). For the sake of simplicity, we select a kick amplitude A and set $A_n = A$ for all $n \in \mathbb{Z}_{\geqslant 0}$. We work with periodic kicks, so we set $T_n = nT$, where T is the time between consecutive kicks. The forcing drive 4) for the experiments is therefore given by

$$I_G(t) = A \sum_{n=1}^{\infty} \delta(t - nT). \tag{6}$$

To test for DIU onset, we compute the maximal Lyapunov exponent $\Lambda_{\max}$ as a function of T.

Expectations. DIU may or may not emerge as T increases, depending on the dynamics of the intrinsic flow near the stationary point. If contraction to the stationary state is strong and shear near the stationary state is weak, DIU will not emerge. The maximal Lyapunov exponent $\Lambda_{\max}$ will indicate this by remaining negative as T increases. In fact, $\Lambda_{\max}$ will *decrease* as T increases because the phase space has more time to contract between kicks as T increases.

On the other hand, if contraction to the stationary state is weak and shear near the stationary state is strong, then DIU can

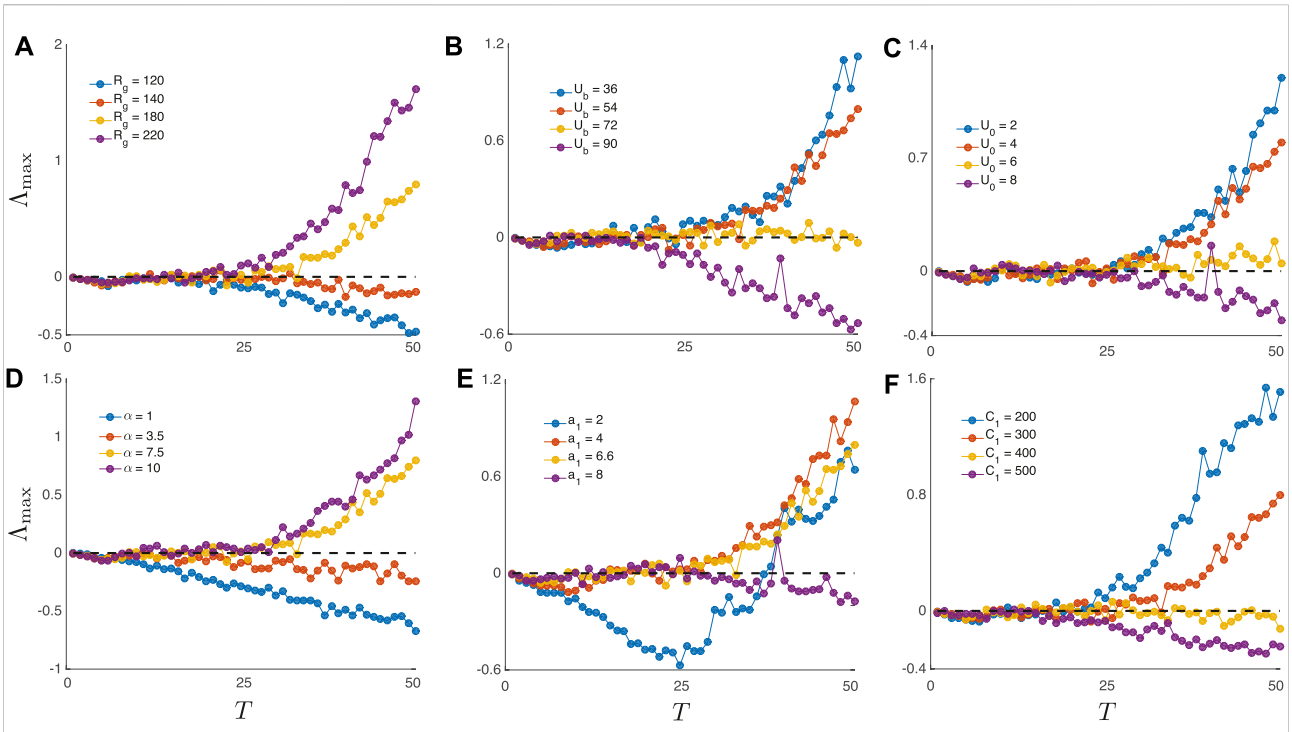

FIGURE 3
The DIU phenotype is abundant in the space of intrinsic parameters. Plots show the maximal Lyapunov exponent Λ_{max} as a function of inter-kick time T for the time-T map induced by the Ultradian system (1) with T-periodic pulsatile forcing (6). DIU is present when $\Lambda_{max} > 0$ and absent when $\Lambda_{max} < 0$. As T increases, DIU emerges when intrinsic parameters are tuned so as to increase characteristic glucose levels. Intrinsic parameters are set to the nominal values in Table 1 except for the single intrinsic parameter that is tuned in each panel: **(A)** R_g; **(B)** U_b; **(C)** U_0; **(D)** α; **(E)** a_1; **(F)** C_1. Kick amplitude: A = 10 mg/dl.

emerge as T increases. This can happen because when T is large, shear has a long time to act between kicks. Shear causes the phase space to stretch and fold, thereby producing DIU. In our experiments, a transition from $\Lambda_{max} < 0$ to $\Lambda_{max} > 0$ as T increases indicates that DIU has emerged.

4.2 The DIU phenotype is abundant in the space of intrinsic parameters

Figure 3 illustrates how Λ_{max} varies with T as we individually tune each of the six parameters identified in Section 2.2. Each panel corresponds to tuning a single parameter while holding all other intrinsic parameters fixed at the nominal values. Importantly, DIU emerges in every one of the six panels when we tune the selected parameter so as to increase characteristic glucose levels in the intrinsic dynamics.

Figure 4 confirms the expected link between strength of contraction to the stationary point, shear near the stationary point, and DIU emergence. For Figure 4, we replace the periodic pulsatile forcing used to generate Figure 3 with a forcing signal that consists of three kicks (meals). After the final kick, the glucose variable converges to the equilibrium level G_{eq} as $t \to \infty$.

The panels in Figure 4 indicate that our experiments have captured two behaviors. Either we see rapid convergence to G_{eq} (as in Figure 4D (top)), or we see slow convergence to G_{eq} by way of a damped oscillation (as in Figure 4D (bottom)). Notice that in each panel of Figure 4, we tune the same parameter that we tune in the corresponding panel of Figure 3, while holding all other intrinsic parameters fixed at the nominal values.

Comparing Figures 3, 4 shows that without exception, *the geometry of the glucose trajectory predicts whether or not DIU will emerge*. If we observe rapid convergence to G_{eq}, as in Figure 4D (top) for instance, then DIU does not emerge. If, however, we observe slow convergence to G_{eq} by way of a damped oscillation, as in Figure 4D (bottom) for instance, then DIU emerges.

Figure 5 illustrates the DIU dynamical profile and acts as a companion to Figure 4. Each glucose trajectory in Figure 5 results from forcing with periodic pulsatile kicks 6) and corresponds to a companion glucose trajectory in Figure 4 (produced by applying only three kicks). When contraction toward the equilibrium glucose level G_{eq} is strong (Figures 4A–F (top)), driving with periodic pulsatile kicks produces rhythmic behavior (Figures 5A–F (top)). When periodic pulsatile kicks produce DIU, glucose trajectories exhibit sustained temporal chaos (Figures 5A–F (bottom)).

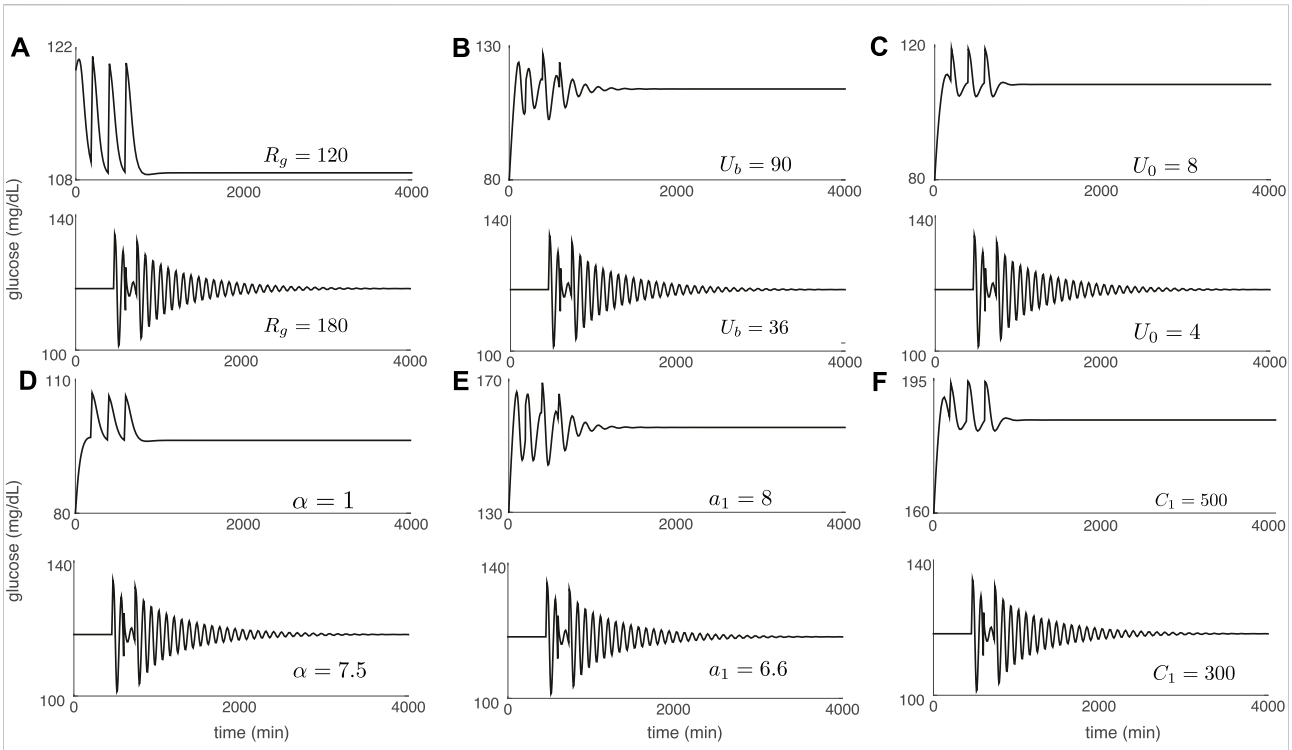

FIGURE 4
Glucose trajectories generated by the Ultradian system (1) with forcing that consists of three glucose kicks spaced 100 min apart. After the final kick, the glucose level converges to the equilibrium value G_{eq}. Convergence is either rapid (top of each panel) or via a slow damped oscillation (bottom of each panel). Intrinsic parameters are set to the nominal values in Table 1 except for the single intrinsic parameter that is tuned in each panel: **(A)** R_g; **(B)** U_b; **(C)** U_0; **(D)** α; **(E)** a_1; **(F)** C_1. Kick amplitude: A = 10 mg/dl.

4.3 DIU is pathogenic for obesity and T2DM

We have established that the DIU phenotype is abundant in the space of intrinsic parameters for the Ultradian model. But why does this matter? Delayed regulatory feedback pathways are common in mathematical physiology. Since DIU emerges in a natural way for the Ultradian model, it may appear in a variety of physiological models. When present, DIU can profoundly impact medical practice because medicine proceeds from the assumption that the outcome of an intervention can be predicted when the state of the patient at the time of intervention is known. Sustained temporal chaos undercuts this assumption. See (Karamched et al. (2021)) for an assessment of the impact of DIU on glycemic management in the intensive care unit.

Here, we conjecture that DIU is pathogenic for obesity and T2DM. This conjecture is based on how the statistical signature of DIU links to the glucostatic theory. The glucostatic theory asserts that drops in blood glucose levels induce hunger and therefore energy intake (Chaput and Tremblay (2009); Mayer (1955)). If such drops are frequent in time and sizable in magnitude, excess energy intake could result.

Figure 6 shows that DIU induces frequent, sizable drops in blood glucose levels! We start with all intrinsic parameters set at the nominal values and we then tune R_g, the uninhibited hepatic glucose production rate. Figure 6 shows glucose distributions for the time-T map induced by Ultradian dynamics 1) with T-periodic pulsatile forcing (6). That is, each histogram gives the distribution of

$$\{G(nT): n \in \mathbb{Z}_{\geqslant 0}\} \tag{7}$$

for a different value of R_g. We set T = 100 min. When R_g = 120 mg/min (Figure 6A), a value for which DIU is absent, the glucose distribution is essentially a Dirac measure concentrated at the mean. (Blue indicates the mean of the glucose distribution and orange indicates the distribution itself.) However, when R_g = 180 mg/min (Figure 6B), a value for which DIU is present, the glucose distribution is approximately Gaussian. This is as it should be—the mathematical theory behind DIU predicts Gaussian statistics when DIU is present. Notice that the variance of the approximately Gaussian distribution is large. This means that the glucose level frequently drops well below its mean. In light of glucostatic theory, this observation directly supports the conjecture that DIU is pathogenic for obesity and T2DM.

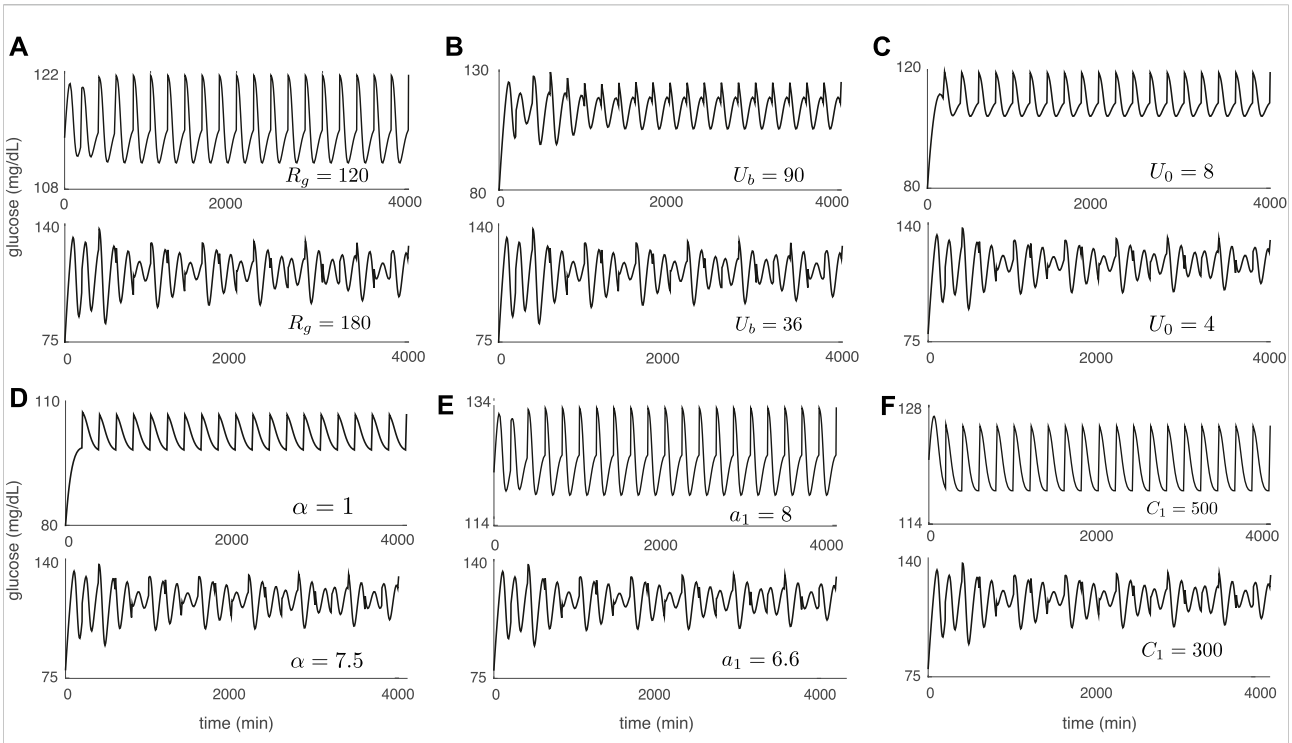

FIGURE 5
Sustained temporal chaos associated with DIU. Plots show glucose trajectories produced by the Ultradian system (1) with T-periodic pulsatile forcing (6). Each trajectory in Figure 5 corresponds to a companion trajectory in Figure 4. When DIU is absent, T-periodic pulsatile forcing results in a rhythmic glucose signal (top of each panel). When DIU is present, we observe sustained temporal chaos (bottom of each panel). Intrinsic parameters are set to the nominal values in Table 1 except for the single intrinsic parameter that is tuned in each panel: **(A)** R_g; **(B)** U_b; **(C)** U_0; **(D)** α; **(E)** a_1; **(F)** C_1. Forcing parameters: A = 10 mg/dl, T = 100 min.

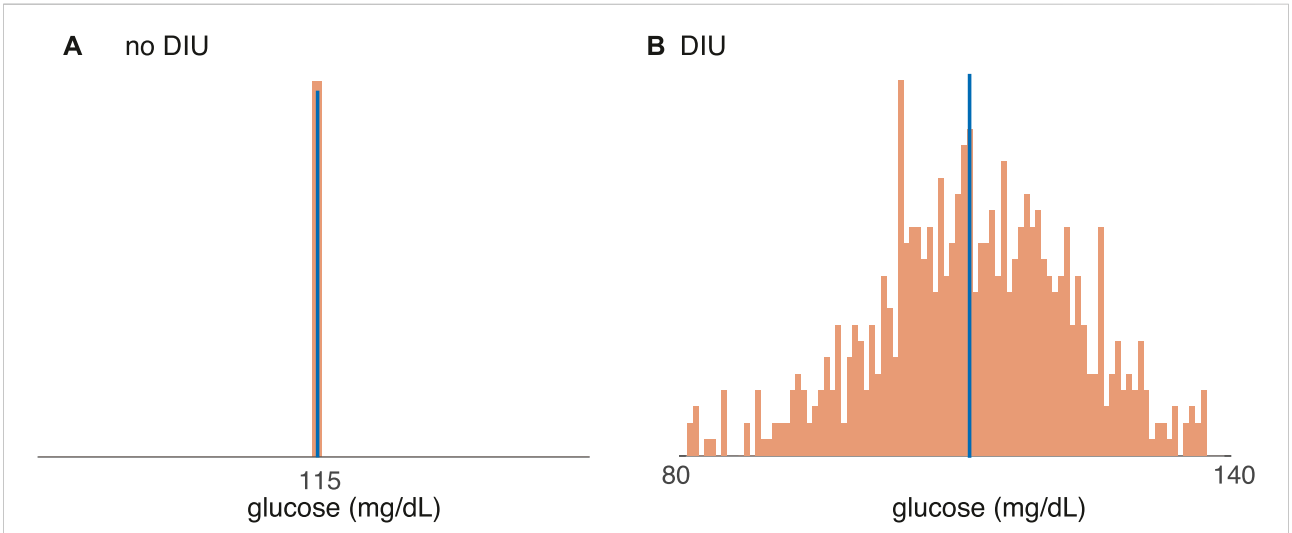

FIGURE 6
Support for the conjecture that DIU is pathogenic for obesity and T2DM. Distributions of the glucose variable (7) for the time-T map induced by the Ultradian system (1) with T-periodic pulsatile forcing (6). Blue bar indicates mean. **(A)** When R_g = 120 mg/min, DIU is absent and the glucose distribution concentrates at the mean. **(B)** When R_g = 180 mg/min, DIU is present. Consistent with the mathematical structure of the DIU profile, the glucose distribution is approximately Gaussian. All of the other intrinsic parameters are set to the nominal values in Table 1. Forcing parameters: A = 10 mg/dl, T = 100 min.

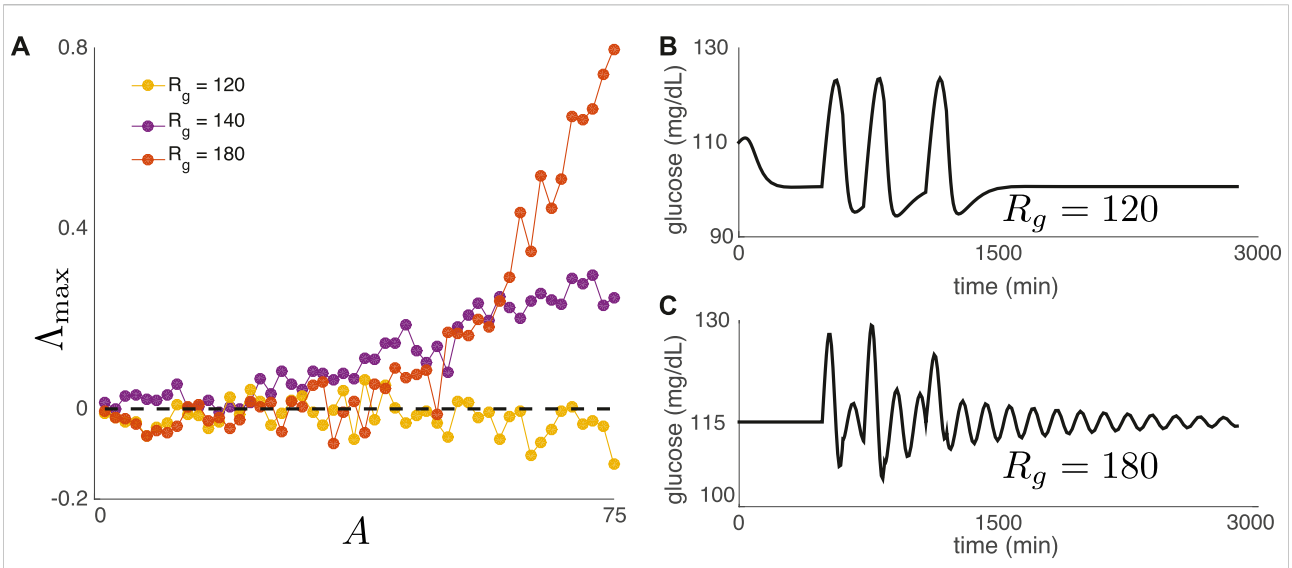

FIGURE 7
DIU phenotype for a realistic nutritional driver. **(A)** We have replaced (6) with the exponential-type drive in (8). Meals are consumed daily at 8 a.m., noon, and 6 p.m. Plot shows Λ_{max} as a function of meal amplitude A for three values of R_g **(B,C)** We replace (8) with a single day of meals (three meals). Rapid return to equilibrium correlates with the absence of DIU, while slow, oscillatory return to equilibrium correlates with the presence of DIU. Here, A = 50 mg/(dL · min) and υ = 1/120 min^{-1}.

4.4 DIU emerges for generic pulsatile meal drives

Our results do not depend on the precise form of the pulsatile forcing that appears in (6). The forcing need not be periodic, and it need not consist of δ-pulses. DIU should emerge for a generic pulsatile forcing drive as long as the forcing interacts with intrinsic shear[1].

To support this claim, we have varied the intrinsic parameter R_g to test for DIU emergence after replacing 6) with

$$I_G(t) = A\sum_{n=1}^{\infty}\Theta(t-m_n)e^{-\upsilon(t-m_n)}, \tag{8}$$

where $A > 0$ denotes meal amplitude, $\Theta(t)$ is the Heaviside function, $\upsilon > 0$ is a constant, and m_n denotes the time of meal n. For this set of experiments, meals are consumed daily at 8 a.m., noon, and 6 p.m. Figure 7A shows Λ_{max} as a function of meal amplitude A for three values of R_g. For two of the three values of R_g, the top Lyapunov exponent becomes positive as A increases, indicating DIU onset. For Figure 7bc, we replace (8) with a single day of meals (three meals) in order to show that the nature of return to equilibrium correlates with DIU onset. Rapid return to equilibrium correlates with the absence of DIU (Figure 7B), while slow, oscillatory return to equilibrium correlates with the presence of DIU (Figure 7C).

1 Here we compute Λ_{max} by averaging over time intervals of length 12 h.

5 Discussion

We have found that DIU is abundant in the space of parameters for the Ultradian glucose-insulin model. Such DIU could result in obesity and T2DM if induced low-glucose excursions produce excess hunger frequently enough, but much work remains to verify the conjecture that DIU is pathogenic for obesity and T2DM. Crucially, DIU and the theory behind it must be anchored to data. Methods for DIU detection directly from data should be developed for the clinical and self-care settings. The impact of DIU on the techniques by which models are fit to data should be assessed.

We have assumed in this paper that the intrinsic parameters in the Ultradian model do not vary over time. On long timescales, however, DIU may affect physiological state. At the modeling level, this would correspond to DIU causing intrinsic model parameters to drift (perhaps slowly) over time. Such drift might enhance the pathogenicity of DIU through a feedback mechanism: When DIU is present, intrinsic parameters may slowly drift into a region of parameter space that is even more favorable for DIU. A mathematical investigation of this phenomenon would involve developing a theory of DIU for nonstationary dynamical systems.

We have shown here that the DIU phenotype is abundant in the space of intrinsic parameters for the Ultradian model. An important next step will be to precisely characterize the DIU phenotype in terms of physiological architecture. Such a characterization may reveal the most essential physiological mechanisms that lead to DIU onset. Mathematically speaking,

we must quantify shear near stationary states of flows. Shear near limit cycles has received considerable attention (Ott and Stenlund (2010); Wang and Young (2003)). Shear near stationary states, though, has only been quantified in dimension two (Ott (2008)).

The rigorous mathematical theory behind DIU is known as the theory of rank-one maps. This theory has been developed for finite-dimensional dynamical systems (Wang and Young (2001, 2008; 2013)). The Utradian model is finite-dimensional as a dynamical system because the delay in the Ultradian model takes the form of a three-stage linear filter. The theory of rank-one maps therefore characterizes the sustained temporal chaos that we see in the Ultradian model. However, models that include explicit delays—systems of nonlinear delay differential equations—permeate mathematical physiology. Models that include explicit delays are infinite-dimensional when viewed as dynamical systems. Important infinite-dimensional analogs of the Ultradian model have been studied (Li et al. (2006); Li and Kuang (2007)). The theory of rank-one maps must be extended to infinite-dimensional dynamical systems in order to analyze delay differential equations in the DIU context. See (Lu et al. (2013)) for an approach that combines the existing theory of rank-one maps with invariant manifold techniques.

When assessing the impact of DIU on a given physiological system, one should ask the following questions. Are we interested in precisely predicting the temporal evolution of individual orbits, or do we care more about the statistics of the system? What are the relevant timescales? For the glucose-insulin system, we have now studied two contrasting settings. In the ICU context, we showed that DIU can disrupt single-orbit prediction on short timescales (Karamched et al. (2021)). In the present paper, we have argued that over long timescales, DIU-induced glucose statistics may be pathogenic for obesity and T2DM.

Data availability statement

The original contributions presented in the study are included in the article/supplementary materials, further inquiries can be directed to the corresponding author/s. The code used to generate all figures is available here: https://github.com/Bargo727/DIU.

Author contributions

BK performed the simulations. BK and WO wrote the first draft of the manuscript. All authors contributed to subsequent revisions.

Funding

This work has been supported by the National Science Foundation under grant DMS 1816315 (WO) and by the National Institutes of Health under grants LM006910 (GH), R01DK052431 (RL), P30DK26687 (RL), and LM012734 (DA).

Acknowledgments

BK would like to thank his wife, Hajra Habib, for her unending support.

Conflict of interest

The authors declare that the research was conducted in the absence of any commercial or financial relationships that could be construed as a potential conflict of interest.

Publisher's note

References

Abarbanel, H. D., Brown, R., Sidorowich, J. J., and Tsimring, L. S. (1993). The analysis of observed chaotic data in physical systems. *Rev. Mod. Phys.* 65, 1331–1392. doi:10.1103/RevModPhys.65.1331

Albers, D. J., Elhadad, N., Claassen, J., Perotte, R., Goldstein, A., and Hripcsak, G. (2018b). Estimating summary statistics for electronic health record laboratory data for use in high-throughput phenotyping algorithms. *J. Biomed. Inf.* 78, 87–101. doi:10.1016/j.jbi.2018.01.004

Albers, D. J., Levine, M., Gluckman, B., Ginsberg, H., Hripcsak, G., and Mamykina, L. (2017). Personalized glucose forecasting for type 2 diabetes using data assimilation. *PLoS Comput. Biol.* 13, e1005232. doi:10.1371/journal.pcbi.1005232

Albers, D. J., Levine, M. E., Stuart, A., Mamykina, L., Gluckman, B., and Hripcsak, G. (2018a). Mechanistic machine learning: How data assimilation leverages physiologic knowledge using bayesian inference to forecast the future, infer the present, and phenotype. *J. Am. Med. Inf. Assoc.* 25, 1392–1401. doi:10.1093/jamia/ocy106

Chaput, J., and Tremblay, A. (2009). The glucostatic theory of appetite control and the risk of obesity and diabetes. *Int. J. Obes.* 33, 46–53. doi:10.1038/ijo.2008.221

Christini, D. J., and Glass, L. (2002). Introduction: Mapping and control of complex cardiac arrhythmias. *Chaos* 12, 732–739. doi:10.1063/1.1504061

Claassen, J., Perotte, A., Albers, D., Kleinberg, S., Schmidt, J. M., Tu, B., et al. (2013). Nonconvulsive seizures after subarachnoid hemorrhage: Multimodal detection and outcomes. *Ann. Neurol.* 74, 53–64. doi:10.1002/ana.23859

Drozdov, A., and Khanina, H. (1995). A model for ultradian oscillations of insulin and glucose. *Math. Comput. Model.* 22, 23–38. doi:10.1016/0895-7177(95)00108-E

Glass, L., Beuter, A., and Larocque, D. (1988). Time delays, oscillations, and chaos in physiological control systems. *Math. Biosci.* 90, 111–125. doi:10.1016/0025-5564(88)90060-0

Glass, L., and Malta, C. P. (1990). Chaos in multi-looped negative feedback systems. *J. Theor. Biol.* 145, 217–223. doi:10.1016/s0022-5193(05)80127-4

Graham, E., Elhadad, N., and Albers, D. (2020). Reduced model for female endocrine dynamics: Validation and functional variations. *arXiv Prepr. arXiv: 2006.05034*.

Hodgkin, A. L., and Huxley, A. F. (1952). A quantitative description of membrane current and its application to conduction and excitation in nerve. *J. Physiol.* 117, 500–544. doi:10.1113/jphysiol.1952.sp004764

Karamched, B., Hripcsak, G., Albers, D., and Ott, W. (2021). Delay-induced uncertainty for a paradigmatic glucose–insulin model. *Chaos* 31, 023142. doi:10.1063/5.0027682

Keener, J., and Sneyd, J. (1998). *Mathematical physiology, interdisciplinary applied mathematics, vol. 8*. New York: Springer-Verlag, xx+766.

Li, J., and Kuang, Y. (2007). Analysis of a model of the glucose-insulin regulatory system with two delays. *SIAM J. Appl. Math.* 67, 757–776. doi:10.1137/050634001

Li, J., Kuang, Y., and Mason, C. (2006). Modeling the glucose-insulin regulatory system and ultradian insulin secretory oscillations with two explicit time delays. *J. Theor. Biol.* 242, 722–735. doi:10.1016/j.jtbi.2006.04.002

Li, T. Y., and Yorke, J. A. (2004). "Period three implies chaos," in *The theory of chaotic attractors* (Berlin, Germany: Springer), 77–84.

Lu, K., Wang, Q., and Young, L. S. (2013). Strange attractors for periodically forced parabolic equations. *Mem. Am. Math. Soc.* 224, 1. doi:10.1090/S0065-9266-2012-00669-1

Mackey, M. C., and Glass, L. (1977). Oscillation and chaos in physiological control systems. *Science* 197, 287–289. doi:10.1126/science.267326

Mayer, J. (1955). Regulation of energy intake and the body weight: The glucostatic theory and the lipostatic hypothesis. *Ann. N. Y. Acad. Sci.* 63, 15–43. doi:10.1111/j.1749-6632.1955.tb36543.x

Ott, W., and Stenlund, M. (2010). From limit cycles to strange attractors. *Commun. Math. Phys.* 296, 215–249. doi:10.1007/s00220-010-0994-y

Ott, W. (2008). Strange attractors in periodically-kicked degenerate Hopf bifurcations. *Commun. Math. Phys.* 281, 775–791. doi:10.1007/s00220-008-0499-0

Schwartz, M. W., Seeley, R. J., Zeltser, L. M., Drewnowski, A., Ravussin, E., Redman, L. M., et al. (2017). Obesity pathogenesis: An Endocrine Society scientific statement. *Endocr. Rev.* 38, 267–296. doi:10.1210/er.2017-00111

Sottile, P. D., Albers, D., Higgins, C., Mckeehan, J., and Moss, M. M. (2018). The association between ventilator dyssynchrony, delivered tidal volume, and sedation using a novel automated ventilator dyssynchrony detection algorithm. *Crit. Care Med.* 46, e151–e157. doi:10.1097/CCM.0000000000002849

Stroh, J., Bennett, T., Kheyfets, V., and Albers, D. (2020). Estimating intracranial pressure via low-dimensional models: Toward a practical tool for clinical decision support at multi-hour timescales. *bioRxiv*.

Sturis, J., Polonsky, K., Mosekilde, E., and Van Cauter, E. (1991). Computer model for mechanisms underlying ultradian oscillations of insulin and glucose. *Am. J. Physiol.* 260, E801–E809. doi:10.1152/ajpendo.1991.260.5.E801

Urteaga, I., Bertin, T., Hardy, T. M., Albers, D. J., and Elhadad, N. (2019). Multi-task Gaussian processes and dilated convolutional networks for reconstruction of reproductive hormonal dynamics. *arXiv Prepr. arXiv:1908.10226*.

Wang, Q., and Young, L. S. (2013). Dynamical profile of a class of rank-one attractors. *Ergod. Th. Dynam. Sys.* 33, 1221–1264. doi:10.1017/S014338571200020X

Wang, Q., and Young, L. S. (2003). Strange attractors in periodically-kicked limit cycles and Hopf bifurcations. *Commun. Math. Phys.* 240, 509–529. doi:10.1007/s00220-003-0902-9

Wang, Q., and Young, L. S. (2001). Strange attractors with one direction of instability. *Commun. Math. Phys.* 218, 1–97. doi:10.1007/s002200100379

Wang, Q., and Young, L. S. (2008). Toward a theory of rank one attractors. *Ann. Math.* (2), 167349–167480. doi:10.4007/annals.2008.167.349

Zenker, S., Rubin, J., and Clermont, G. (2007). From inverse problems in mathematical physiology to quantitative differential diagnoses. *PLoS Comput. Biol.* 3, e204. doi:10.1371/journal.pcbi.0030204

frontiers | Frontiers in Physiology

TYPE Original Research
PUBLISHED 06 September 2022
DOI 10.3389/fphys.2022.911616

OPEN ACCESS

EDITED BY
Cecilia Diniz Behn,
Colorado School of Mines, United States

REVIEWED BY
Laura Burattini,
Marche Polytechnic University, Italy
Everardo Magalhaes Carneiro,
State University of Campinas, Brazil

*CORRESPONDENCE
Vijaya Subramanian,
vsubram6@jhu.edu
Jonatan I. Bagger,
jonatan.ising.bagger@regionh.dk

SPECIALTY SECTION
This article was submitted to Metabolic Physiology,
a section of the journal
Frontiers in Physiology

RECEIVED 02 April 2022
ACCEPTED 19 July 2022
PUBLISHED 06 September 2022

CITATION
Subramanian V, Bagger JI, Holst JJ, Knop FK and Vilsbøll T (2022), A glucose-insulin-glucagon coupled model of the isoglycemic intravenous glucose infusion experiment.
Front. Physiol. 13:911616.
doi: 10.3389/fphys.2022.911616

A glucose-insulin-glucagon coupled model of the isoglycemic intravenous glucose infusion experiment

Vijaya Subramanian[1]*, Jonatan I. Bagger[2,3,4]*, Jens J. Holst[3,5], Filip K. Knop[2,3,4,6] and Tina Vilsbøll[2,4,6]

[1]Institute for Computational Medicine, Johns Hopkins University, Baltimore, MD, United States, [2]Center for Clinical Metabolic Research, Herlev and Gentofte Hospital, University of Copenhagen, Hellerup, Denmark, [3]Novo Nordisk Foundation Center for Basic Metabolic Research, Faculty of Health and Medical Sciences, University of Copenhagen, Copenhagen, Denmark, [4]Clinical Research, Steno Diabetes Center Copenhagen, Herlev, Denmark, [5]Department of Biomedical Sciences, Faculty of Health and Medical Sciences, University of Copenhagen, Copenhagen, Denmark, [6]Department of Clinical Medicine, Faculty of Health and Medical Sciences, University of Copenhagen, Copenhagen, Denmark

Type 2 diabetes (T2D) is a pathophysiology that is characterized by insulin resistance, beta- and alpha-cell dysfunction. Mathematical models of various glucose challenge experiments have been developed to quantify the contribution of insulin and beta-cell dysfunction to the pathophysiology of T2D. There is a need for effective extended models that also capture the impact of alpha-cell dysregulation on T2D. In this paper a delay differential equation-based model is developed to describe the coupled glucose-insulin-glucagon dynamics in the isoglycemic intravenous glucose infusion (IIGI) experiment. As the glucose profile in IIGI is tailored to match that of a corresponding oral glucose tolerance test (OGTT), it provides a perfect method for studying hormone responses that are in the normal physiological domain and without the confounding effect of incretins and other gut mediated factors. The model was fit to IIGI data from individuals with and without T2D. Parameters related to glucagon action, suppression, and secretion as well as measures of insulin sensitivity, and glucose stimulated response were determined simultaneously. Significant impairment in glucose dependent glucagon suppression was observed in patients with T2D (duration of T2D: 8 (6–36) months) relative to weight matched control subjects (CS) without diabetes (k_1 $(mM)^{-1}$: 0.16 ± 0.015 (T2D, n = 7); 0.26 ± 0.047 (CS, n = 7)). Insulin action was significantly lower in patients with T2D (a_1 $(10\ pM\ min)^{-1}$: 0.000084 ± 0.0000075 (T2D); 0.00052 ± 0.00015 (CS)) and the Hill coefficient in the equation for glucose dependent insulin response was found to be significantly different in T2D patients relative to CS (h: 1.4 ± 0.15; 1.9 ± 0.14). Trends in parameters with respect to fasting plasma glucose, HbA1c and 2-h glucose values are also presented. Significantly, a negative linear relationship is observed between the glucagon suppression parameter, k_1, and the three markers for diabetes and is thus indicative of the role of glucagon in exacerbating the pathophysiology of diabetes (Spearman Rank Correlation: (n = 12; (–0.79, 0.002), (–0.73,.007), (–0.86,.0003)) respectively).

KEYWORDS

glucagon action, glucagon suppression, glucagon secretion, insulin sensitivity, insulin secretion, hysteresis, type 2 diabetes

1 Introduction

Glucose homeostasis is maintained primarily by the action of the two pancreatic hormones, insulin and glucagon, in conjunction with a host of other modulators. (Röder et al., 2016). Beta- and alpha-cell dysfunction both contribute to the pathophysiology of type 2 diabetes (T2D). (Burcelin et al., 2008; Ashcroft and Rorsman, 2012; Cryer, 2012; Cerf, 2013; Godoy-Matos, 2014; Moon and Won, 2015; Eizirik et al., 2020). Reduced insulin secretion from the pancreatic beta-cells and reduced insulin sensitivity in various tissues in the body lead to high postprandial glucose excursions. (DeFronzo and Tripathy, 2009; Montanya, 2014; Titchenell et al., 2016; Santoleri and Titchenell, 2019). In addition, higher basal levels of glucagon and impaired suppression of glucagon secretion is implicated in elevated fasting and post-prandial glucose levels in individuals with T2D. (Unger and Orci, 1975; Gerich, 1988; Dunning and Gerich, 2007; Lee et al., 2011). Theoretical models of glucose, insulin and glucagon dynamics can be used to quantify the extent of dysregulation in hormonal control of glucose homeostasis in T2D by fitting the models to data from various glucose challenge experiments. (Bergman et al., 1979; Bergman et al., 1981; Mari et al., 2002a; Dalla Man et al., 2002; Ferrannini et al., 2005; Dalla Man et al., 2006; Panunzi et al., 2007; Palumbo et al., 2013; Kelly et al., 2019; Bergman, 2021; Morettini et al., 2021).

The oral glucose tolerance test (OGTT) and the intravenous glucose tolerance test (IVGTT) have been used to quantify different aspects of plasma glucose regulation. (Panunzi et al., 2007; Cobelli et al., 2014; Bergman, 2021). The advantage of the OGTT is that it represents a physiological response to oral ingestion of nutrients. The challenge from a mathematical modeling point of view is that stimulation of the gut results not only in glucose dependent insulin secretion but also numerous confounding factors, e.g., the incretin effect. (Nauck et al., 1986; Knop et al., 2007; Nauck and Meier, 2016). Gut mediated effects do not come into play when glucose is administered intravenously. In a typical IVGTT, both first phase and second phase insulin secretion are observed in response to glucose challenge. (Bergman et al., 1981; Caumo and Luzi, 2004). Another method for studying glucose-insulin-glucagon dynamics is the isoglycemic intravenous glucose infusion (IIGI), which matches the glucose excursion observed during an OGTT but does not stimulate incretin secretion. (Bagger et al., 2011; Bagger et al., 2014; Nauck and Meier, 2016). Historically, IIGI has been used to obtain a quantitative measure of the incretin effect based on the differential insulin response observed in the OGTT and the corresponding IIGI experiment. In an IIGI, the typical first phase insulin response followed by the slower second phase of the bolus IVGTT is not observed. Instead, a single phase that tracks glucose concentration is observed. The shape of the insulin response is closer to that observed during oral ingestion because the delivery of glucose to the beta cells mimics normal physiological graded delivery from oral glucose administration. (Caumo and Luzi, 2004). Thus, the data from such experiments can be used to estimate parameters of glucose dependent insulin response in addition to insulin sensitivity by fitting a suitable minimal model of glucose regulation without confounding factors from the gut.

While the role of insulin mediated regulation of glucose homeostasis is well established and the contribution to the pathophysiology of T2D has been extensively quantified (Mari et al., 2002b; Panunzi et al., 2007; Cobelli et al., 2009; Cobelli et al., 2014; Bergman, 2021), the role of glucagon and alpha-cell dysregulation is less well studied from a computational perspective. Models have been developed to study glucagon secretion from the alpha cells or pancreatic islets addressing glucose dependent intrinsic and paracrine regulation. (Diderichsen and Göpel, 2006; Fridlyand and Philipson, 2012; Watts and Sherman, 2014; Briant et al., 2016; Watts et al., 2016; Briant et al., 2018; Zmazek et al., 2021). At the whole-body systems level, glucagon dynamics has been included in complex models that describe regulation of glucose homeostasis by the interplay between different organ systems. (Cobelli et al., 1982; Sulston et al., 2006; Kim et al., 2007; De Gaetano and Hardy, 2019). These models included many coupled differential equations and large number of parameters which make them less amenable to validation based on data from glucose challenge experiments for example. On the other hand, minimal models such as those developed for assessing insulin sensitivity and beta cell function are particularly useful in highlighting the contribution of specific impairments to the pathophysiology of diabetes and are more easily validated with data. (Bergman et al., 1979; Mari et al., 2002a; Dalla Man et al., 2002; Ferrannini et al., 2005; Panunzi et al., 2007; Bergman, 2021). The drawback with the glucose-insulin models is that they do not include the dynamics of the counter-regulator glucagon in establishing glucose homeostasis. A more complete minimal model which includes glucagon dynamics coupled to insulin and glucose dynamics would be self-consistent and yield information on glucagon action, secretion and suppression in addition to insulin related parameters. A few minimal models have included glucagon dynamics during IVGTT and OGTT respectively. (Kelly et al., 2019; Morettini et al., 2021). Glucagon dynamics has been described differently in each of the previous models (complex and minimal) particularly with respect to the regulation of glucagon secretion and suppression. In the paper by Morettini et al. (2021), a glucagon-c-peptide

coupled model which did not include glucose dynamics was developed to describe suppression of glucagon secretion during OGTT. As the model did not include glucose dynamics, parameters related to glucagon action and secretion, insulin sensitivity, and secretion could not be determined simultaneously. In the IVGTT minimal model, (Kelly et al., 2019), the dynamics of glucose, insulin and glucagon were all included. In the description of glucagon dynamics, glucagon suppression is assumed to be linearly dependent on plasma insulin concentration and glucagon secretion occurs only when glucose levels drop below baseline. Experimental evidence from human islet level studies indicates that glucagon suppression at low glucose is controlled primarily through intrinsic regulation by glucose. (Tian et al., 2011; Walker et al., 2011; Yu et al., 2019). At high glucose, the intrinsic regulation is modulated by glucose dependent paracrine effects mediated by somatostatin. (Briant et al., 2016; Briant et al., 2018). In the paper by Elliot et al., (Elliott et al., 2015), insulin and somatostatin have been shown to act synergistically in regulating glucagon concentrations at high glucose in human islets. In the hypoglycemic range Bolli et al. (1984) have shown that glucagon secretion is regulated exclusively by glucose. Though the nature of paracrine regulation and the factors that mediate it are uncertain there is consensus on the observation that it occurs in a glucose dependent manner. In the OGTT model, (Morettini et al., 2021), glucagon suppression is attributed exclusively to insulin, ignoring intrinsic regulation by glucose. In the IVGTT minimal model, (Kelly et al., 2019), glucagon suppression is again attributed to insulin at glucose levels above baseline. In the comprehensive models, insulin dependent hyperbolic tangent functions, (Cobelli et al., 1982), quadratic functions, (Kim et al., 2007), and inverse functions (Sulston et al., 2006) have been used to describe glucagon suppression but it is unclear why the particular forms were chosen.

In this paper, a parsimonious model based on delay differential equations, that extends previous insulin-glucose models (Panunzi et al., 2007) was developed to include glucagon dynamics. The coupled model allows for the determination of parameters related to both insulin and glucagon regulation of glucose homeostasis in one step. Glucagon and insulin response to glucose are modeled on dose response data from human islet level studies of alpha and beta cell secretion in contrast to previous models. (Walker et al., 2011). The glucagon dynamics is described by a phenomenological model based on the data from IIGI experiments. Glucagon secretion and suppression are shown to be regulated by glucose as in reference (Walker et al., 2011; De Gaetano and Hardy, 2019) but the magnitude of the suppression is varied during the course of the dynamics. This allows for the description of the prolonged suppression of glucagon secretion and resulting delayed recovery to baseline as observed in the data which is likely due to paracrine effects. The model thus incorporates intrinsic and possible paracrine regulation in a glucose dependent manner and is described in detail in the methods section.

The model developed is fit simultaneously to glucose, insulin and glucagon data from IIGI experiments on individuals with T2D and without diabetes (CS) previously published in the papers by Bagger et al. among others. (Bagger et al., 2011; Mari et al., 2013; Bagger et al., 2014; Alskär et al., 2016; Guiastrennec et al., 2016; Røge et al., 2017; Tura et al., 2017). There are significant advantages of fitting IIGI over OGTT data namely: 1) there are fewer parameters in the model as exogenous glucose arrival is a known quantity unlike in an OGTT; 2) hormone secretory and suppression parameters determined are free of gut mediated effects; 3) parameters that could not be estimated from fitting OGTT data, because of gut stimulation can be determined from IIGI, such as the Hill coefficient in the glucose dependent insulin response; 4) the data from the IIGI experiments also reveal unusual behavior in the insulin response in T2D patients such as significant time delays in insulin secretion, quantification of which would give another tool to distinguish between T2D and control subjects (CS); and 5) there have also been questions regarding insulin response contributing to post prandial glucose lowering below baseline, a phenomenon observed particularly when exogenous glucose loads are high. (Saha, 2006; Parekh et al., 2014). A related pathophysiology is reactive hypoglycemia where glucose levels drop well below baseline and patients present with the Whipple's triad. (Ahmadpour and Kabadi, 1997; Brun et al., 2000; Suzuki et al., 2016). If there is a lag in insulin return to baseline, i.e., if high levels of insulin secretion persist after plasma glucose levels start dropping, then it would explain postprandial glucose lowering. Modeling the glucose dependent insulin response using a hysteresis model should reveal if a lag in insulin recovery to baseline levels exists and causes postprandial hypoglycemia.

In this paper, the role of alpha- and beta-cell dysfunction in T2D is quantified and highlighted. The question of whether hysteresis in insulin secretion plays a role in postprandial hypoglycemia is also addressed. In addition, correlations between the parameters determined and the hallmarks of T2D, fasting plasma glucose (FPG), hemoglobin A1c (HbA1c) and 2-h plasma glucose (2 h PG) values are presented and highlighted.

2 Modeling and data analysis

2.1 Glucose-insulin-glucagon model

In this paper, a parsimonious model that includes glucagon dynamics was developed to describe the coupled glucose-insulin-glucagon system and is presented in Eqs 1–3. The model is an extension of the delay differential equation model of Panunzi

et al. (Panunzi et al., 2007; De Gaetano et al., 2008). Equation 1 describes glucose dynamics. The rate of change of glucose is given by a source term depending on glucagon and the exogenous glucose infused during the IIGI experiment and clearance terms depending on glucose and insulin. The first term in Eq. 1 represents glucose dependent glucose clearance as in the Bergman model (Bergman et al., 1979) and is first order in glucose with rate constant S_G. The second term represents insulin dependent glucose clearance and is first order in insulin and glucose. The rate constant a_1 gives a measure of insulin sensitivity; it is analogous to the parameter S_I in the Bergman minimal model and K_{xgI} in the paper by Panunzi et al. Hepatic glucose production is assumed to be driven primarily by glucagon and is given by the third term in Eq. 1. It is first order in glucagon concentration and the rate constant a_2 gives a measure of glucagon action in the liver. Hepatic glucose production would likely also depend on other substrates such as glycogen in glycogenolysis, but they are assumed to be in excess and the pseudo first order (Keeler et al., 2018) dependence on glucagon used should be sufficient. In the model of De Gaetano et al., (De Gaetano and Hardy, 2019), glucagon is included in the fast dynamics, but they use saturation kinetics to describe glucagon-dependent hepatic glucose production while a first order dependence is used in the paper by Kelly et al. (2019) As the extent of insulin dependent suppression of hepatic glucose production is uncertain, it was not included in this model (Gastaldelli et al., 2001; Adkins et al., 2003; Kaplan et al., 2008). The rate of glucose arrival in the plasma, $R_{IIGI,}$ is determined from the glucose infusion rate, $G_{infusion}$, during the IIGI as shown in Eq. 6. In the underlying experiments, the glucose infusion was manually adjusted in the IIGI protocol to match the OGTT profile. The average amount of glucose infused every 15 min was used to approximate the actual glucose infusion rate which involved adjustments every 5 min.

In Eq. 2 describing insulin dynamics, n_1 is the insulin degradation constant, γ_1 is a measure of insulin secretion and $\psi(G[t])$ is the dose-response relationship for glucose-dependent insulin secretion. Two models were used to describe insulin dynamics. The dose-response function, $\psi(G[t])$, is represented by a Hill function, Eq. 4a, in Model 1. While the Hill function has been used by other researchers, (Panunzi et al., 2007), the parameter K in Eq. 4 in this paper is fixed at the value obtained by fitting dose-response data from *in vitro* human pancreatic islet level studies (Walker et al., 2011) and is set at 17 mM.

As some researchers (Mari et al., 2002a; Keenan et al., 2012; Parekh et al., 2014) have raised the possibility of hysteresis-like behavior in insulin secretion in response to exogenous glucose influx, in Model 2, Eq. 4b was used to fit the IIGI data. In the hysteresis model, insulin secretory response to glucose depends on whether glucose levels are increasing or decreasing. The Hill coefficient h_1 controls the response when glucose levels are increasing and h_2 describes the secretory response when

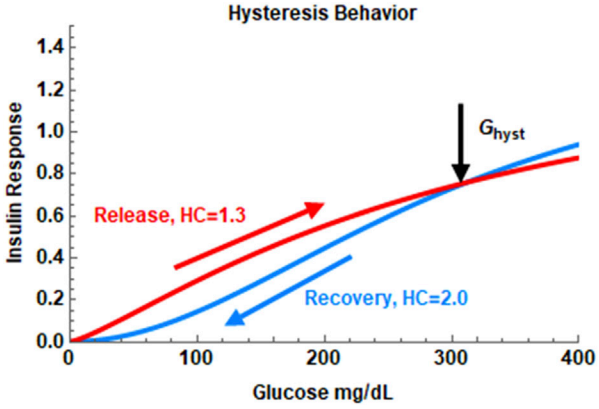

FIGURE 1
The hysteresis behavior of the insulin dose-response in Model 2. In this example, the Hill coefficient, h, is set at 1.3 during the insulin release phase and set at 2.0 during the recovery phase. The hysteresis turning point is set at the maximum of the glucose profile in the IIGI experiment.

glucose levels are decreasing. C_1 is an adjustment constant determined to make the two curves meet at the hysteresis point, (G_{hyst}, t_{hyst}). A sample plot showing hysteretic dose-response is shown in Figure 1. Here h_1 is set to be lower than h_2. Two Hill equations are used here as studies at the islet level indicate that the physiological dose-response shows this behavior. Logistic functions have been used in the paper by Keenan et al. to model hysteresis in c-peptide secretion. (Keenan et al., 2012). Changes in insulin secretory patterns with time have also been modeled using different potentiation factors as in the work by Mari et al. which is in turn derived from deconvolution of c-peptide kinetics. (Mari et al., 2002a).

Glucagon dynamics is described by Eq. 3 and is the sum of two terms, a clearance term, and a glucose dependent response term. Glucagon degradation or clearance is assumed to be first order in glucagon with degradation constant, $n_{2,}$ which was obtained from the literature. (Alford et al., 1976). The second term describes the response to glucose. Islet level (Walker et al., 2011) and other studies (De Gaetano and Hardy, 2019) indicate that glucagon levels decrease exponentially as a function of glucose elevation. Preliminary investigations while modeling OGTT experiments showed that the glucagon dynamics shows hysteresis like behavior in response to glucose challenge. The suppression of glucagon in response to glucose challenge follows a different glucose dependence than the recovery after the plasma glucose level reaches a maximum. Thus, the glucagon dose-response is given by two different exponential terms (Eq. 5), one when glucose level is rising and a different one when glucose level is falling. The change in behavior is assumed to occur at the maximum of the glucose curve occurring at glucose concentration G_{hyst}, and time t_{hyst}. G_{hyst} is determined by finding the maximum of the plasma glucose profile, ie., the

IIGI data, numerically and t_{hyst} is the time at which the maximum occurs (Wolfram Research, Inc, 2019). The reason for this slow recovery of glucagon levels post glucose influx is uncertain but likely due to paracrine modulation of glucagon secretion while the early suppression is likely due to intrinsic regulation by glucose. As both paracrine regulators, insulin and somatostatin, are secreted in a glucose dependent manner, here the paracrine modulation is also assumed to occur in a glucose dependent manner without explicit dependence on insulin or somatostatin concentration. The two exponential glucose dependent response terms were able to capture glucagon dynamics reasonably well during the 240 min duration of the IIGI experiment as shown in the results section. This persistent suppression of glucagon was also observed by Gerich (Mitrakou et al., 1990; Gerich, 1993) and in a larger study by Faerch et al. (Færch et al., 2016) The suppression and recovery constants are k_1 and k_2 respectively. The rate constant γ_2 is a measure of glucagon secretion. The parameters τ, τ_1 and τ_2 represent possible time delays in glucose distribution, insulin secretion and glucagon suppression respectively.

$$\frac{dG[t]}{dt} = -(S_G + a_1 I[t])G[t] + a_2 A[t] + R_{IIGI}[t-\tau] \Big/ V \quad (1)$$

$$\frac{dI[t]}{dt} = -n_1 I(t) + \gamma_1 \psi(G[t-\tau_1]) \quad (2)$$

$$\frac{dA[t]}{dt} = -n_2 A(t) + \gamma_2 \phi(G[t-\tau_2]) \quad (3)$$

$$\psi_{Hill} = \frac{1.5 G[t]^h}{K^h + G[t]^h} \quad (a)$$

$$\psi_{Hysteresis} = \begin{cases} \dfrac{1.5 G[t]^{h_1}}{K^{h_1} + G[t]^{h_1}}, t < t_{hyst} \\ \dfrac{C_1 G[t]^{h_2}}{K^{h_2} + G[t]^{h_2}}, t \geq t_{hyst} \end{cases} \quad (b) \quad (4)$$

$$\phi(G[t-\tau_2]) = \begin{cases} e^{-k_1 G[t-t_2]}, t < t_{hyst} \\ e^{-k_2 G[t-t_2]} + yshift, t \geq t_{hyst} \end{cases} \quad (5)$$

$$yshift = e^{-k_1 G_{hyst}}$$

$$R_{IIGI} mg\,(kg\ min)^{-1} = G_{Infusion}(g) \Big/ 15(min) \times \frac{1000}{(subject\ weight\ (kg))} \quad (6)$$

2.2 Parameter estimation and statistics

Models 1 and 2 were simultaneously fit to glucose, insulin and glucagon data from IIGI tests on eight patients with diabetes (T2D) and eight weight matched control subjects (CS) without diabetes. (Bagger et al., 2011; Bagger et al., 2014). The glucose infusion in IIGI was manually adjusted to obtain a glucose profile that matches the OGTT glucose profile. The data available from the glucose infusion was the total amount of glucose infused in 15-min blocks for a total of 240 min. A uniform glucose infusion rate was thus used for every 15-min block of the infusion experiment as described in Eq. 6. This approximates the actual infusion rate which was adjusted every 5 min. As this approximation was applied across all patients, trends in estimated parameters within groups and between groups should likely be unaffected.

The parameters that were determined from the fit are glucagon action a_2, secretion γ_2 and suppression k_1, insulin action a_1, secretion γ_1 and the Hill coefficients h, or h_1 and h_2 depending on the model used. As the exogenous glucose arrival, R_{IIGI} is continuous but not smooth, the time delay terms could not be estimated using the Levenberg-Marquardt algorithm in all subjects. The times delays, τ, τ_1, τ_2, were therefore adjusted manually. The glucagon recovery parameter k_2 was also adjusted manually. These parameters were adjusted to obtain a reasonable visual fit before running the Levenberg-Marquardt algorithm to estimate the other parameters. The time delays as well as k_2 were easy to set manually as good visual fits were obtained over a relatively narrow range of parameter values. No constraints were set on the values. The parameters n_1, n_2 and S_G were obtained from the literature and set at 0.14 min^{-1}, (Duckworth et al., 1998), 0.08 min^{-1}, (Alford et al., 1976; De Gaetano and Hardy, 2019; Grøndahl et al., 2021), and 0.014 min^{-1} (Dalla Man et al., 2002) respectively. V was fixed at 1.35 dL/kg. (Man et al., 2005).

The fitting was done using the nonlinear regression package NonLinearModelFit in Wolfram Mathematica, Version 12.0. (Wolfram Research, Inc, 2019). The Levenberg-Marquardt algorithm was used for the least-squares minimization. This package also provides all the statistics related to the fits.

A weighted least-squares regression was used for some of the subjects to improve the fits. The weights were determined using the coefficient of variation (CV) for glucose, insulin, and glucagon concentrations. The CVs used were 2%, 3% and 5.5% for glucose, insulin, and glucagon respectively. The caveat with using a constant CV in least squares fitting is that the fit is skewed heavily towards lower data values.

Significance of differences in parameters between groups (T2D vs. CS) was tested using the non-parametric Mann-Whitney *U* test. (MannWhitneyTest. Wolfram Research, 2010). The *p* values <0.05 indicated significant differences between groups based on the null hypothesis that the median difference is zero. Correlations between parameters were determined using the nonparametric Spearman Rank Test. Comparison of Model 1 and Model 2 was done based on the Akaike Information Criterion corrected for small sample size (AICc). (Akaike, 1974; Portet, 2020).

Identifiability of parameters determined was checked using publicly available software, STRIKE-GOLDD Version 3.0. (Villaverde et al., 2016; Villaverde et al., 2019). All parameters in the model that were estimated using the least-squares fitting were assessed to be locally structurally identifiable.

Model validation (Hasdemir et al., 2015) was carried out by simulating data from IIGI experiments that matched OGTT glucose profiles with varying glucose loads (Bagger et al., 2014) on the same set of patients with T2D and CS as in this study. The results are presented in the supplementary section.

3 Experimental methods

The experimental methods are discussed in detail in the paper by Bagger et al. (Bagger et al., 2011; Bagger et al., 2014) A brief overview of the individuals and methods used is presented here.

3.1 Subjects

Eight patients (3 male) with T2D [mean age, 57 (range 40–75) years.; body mass index (BMI), 29 (25–34) kg/m^2; duration of diabetes, 8 (6–36) months] and eight gender-, age-, and BMI-matched healthy control individuals [age, 57 (38–74) years.; BMI, 29 (26–33) kg/m^2] were studied. All patients with T2D were diagnosed based on the criteria of the World Health Organization. (Expert Committee on the Diagnosis, 2003).

3.2 Experimental design

Participants were subject to OGTT followed by IIGI on a subsequent day. The subjects were studied in the morning in a recumbent position after an overnight fast (10 h) fast. On OGTT days, the participants ingested 75 g glucose dissolved in 300 g water. Blood samples were drawn 15, 10, 0 before and 5, 10, 15, 20, 25, 30, 35, 40, 45, 50, 60, 70, 90, 120, 150, 180, 240 min after ingestion of glucose. IIGI was performed using a sterile 20% wt/vol glucose infusion. The infusion rate was adjusted aiming at duplication of the plasma glucose profiles determined on the corresponding OGTT day. Blood was sampled as on the OGTT days. Analytical methods used to determine glucose, insulin and glucagon concentrations are described in Bagger et al. (Bagger et al., 2014).

4 Results

In the first and second subsections, the fits obtained using Model 1 for CS are discussed first, followed by the fits for patients with T2D, and trends within groups presented. In the third subsection, the parameters obtained for CS and patients with T2D are compared. In the fourth subsection correlations with hemoglobin A1c (HbA1c), fasting plasma glucose (FPG) and 2-h plasma glucose (2 h PG) will be presented and implications for categorizing patients with T2D in terms of impaired glucagon suppression in addition to insulin sensitivity will be discussed. In the fourth subsection the question of possible hysteresis behavior in glucose dependent insulin secretion will be explored by comparing Models 1 and 2 of insulin secretion. The implications with respect to postprandial glucose lowering will be discussed.

4.1 Control subjects

The glucose infusion data was first converted to a plasma glucose arrival profile using Eq. 6. The glucose arrival rate profile in four CS subjects is plotted in Figure 2, panel A. This figure highlights the significant variation in glucose arrival profiles between the different subjects that could have an impact on extent of glucose excursions post glucose infusion. In addition, the shape of the plasma glucose profile in IIGI is also dictated by the shape of the exogenous glucose input, which in turn depends on the glucose excursions during the prior OGTTs.

The coupled Eqs 1–3 with insulin response given by Eq. 4a) were then fit to the data. A reasonable fit with low standard errors was not obtained for CS 6. The IIGI experiments involve manual adjustment of glucose infusion rates to obtain glucose profiles that match the OGTT profiles which sometimes result in overshoot in plasma glucose values that may trigger first phase insulin secretion which is likely what happened in CS 6 and could not be fit with this model. This subject was excluded from further study. The fits obtained for the remaining seven CS subjects are presented in Figure 3 and the estimated and manually adjusted parameters in Table 1. The fits were uniformly good for CS subjects with high coefficient of determination (adjusted R^2) values >0 .97. The standard errors in all the estimated parameters were low and the p-values for all the parameters <0.05 except for a_1 of patient 2. The average values, standard errors of the mean and ranges of the parameters are presented in Table 3.

The CS subjects showed a wide range of insulin sensitivities, a_1, 0.000055–0.0012. Subjects two and four showed lower insulin sensitivity relative to other CS subjects. The range in insulin sensitivities can be attributed to the fact that the CS subjects were weight matched to the T2D group (average BMI = 29). The glucose dependent insulin secretion parameter γ_1 showed modest variation with one outlier, CS subject 4. The Hill coefficient, h, was divided into two groups, one centered around h = 2.0 and another around h = 1.35. Subjects with higher values of h have a steeper insulin dose-response to glucose. In general, there were no time delays in the CS subjects with respect to insulin secretion or action except for a 12-min delay in insulin secretion in CS 2 who also had the lowest insulin sensitivity.

The glucagon suppression parameter k_1 in CS subjects was clustered around 0.26, close to the value of 0.25 determined from human islet level studies. Only one subject, CS 2, had anomalously low glucagon suppression. The average glucagon recovery parameter k_2 was 0.50 and shows that glucagon recovery is much slower than suppression in CS subjects. The glucagon action parameter, a_2, which is a measure of glucagon effectiveness in glucose release appeared to be significantly attenuated in CS 2 and 4 relative to the others; the average value was determined to be 0.25. The glucagon secretion parameter γ_2 in normal subjects did not show a huge spread except for CS 4 who had a much

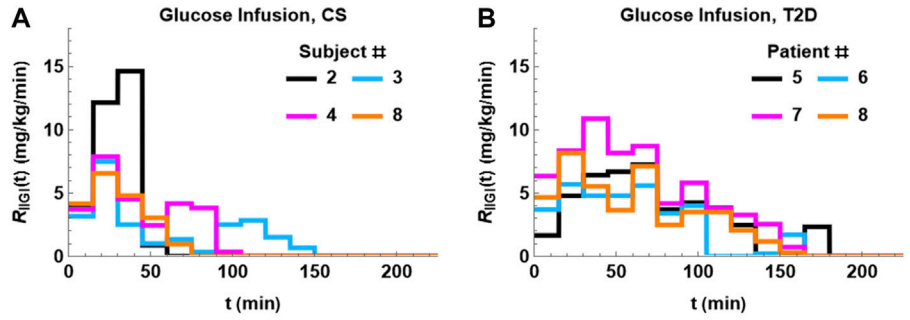

FIGURE 2
Glucose arrival profiles, R_{IIGI}, determined using Eq. 6. There is significant difference between the profiles both within groups and between groups. The profiles tend be more bimodal in CS subjects **(A)**. The glucose arrival profile for T2D **(B)** is unimodal and more prolonged relative to CS.

higher value relative to others. No time delays, τ_2, were observed in glucagon suppression.

There was also a short time delay, τ, in R_{IIGI} in CS subjects two and three of 3 and 5 min respectively. This behavior was observed in most patients with T2D.

4.2 Patients with T2D

The coupled Eqs. 1– 3 with the plasma glucose arrival profile determined using Eq. 6 were fit to the data. The fits for the patients with T2D are shown in Figure 4 and the estimated parameters in Table 2. The adjusted R^2 values for the fit were high for all patients (>0.98). The SE values were low and p values were <0.05 for all parameters except for the insulin sensitivity parameter a_1 in three patients. The fits for those three patients were particularly sensitive to initial guess values for the nonlinear least-squares regression. Possible reasons for the difficulty in fitting these patients might be: 1) The baseline glucagon data for subjects one and two did not match the values on OGTT day indicating greater uncertainty in glucagon data points. 2) T2D subject three had multiple data values near the detection limit of glucagon. The average values, standard errors of the mean and ranges of the parameters are presented in Table 3. Of the eight patients studied patient four could not be fit, likely due to the overshoot in infused glucose as described previously and was excluded from further study.

Patients with T2D showed a large delay in insulin secretion, τ_1, with a mean value of 26 min. The insulin sensitivities, a_1, in patients with T2D were narrowly distributed around the mean value of 0.000084. The insulin secretion parameter, γ_1, had an average of value of 5.5 and a narrow spread of 1.1. The Hill coefficient clustered around two values, four patients around h = 1.75 and three patients around h = 1.0.

The glucagon suppression parameter in patients with T2D was below 0.2 for all subjects except subject 8. Values of glucagon action, a_2, were mixed with four subjects showing significantly higher values than the other three. The glucagon secretion parameters, γ_2, were evenly distributed about the mean except for subject 8. A time delay, τ_2, of 5 minutes was observed in one patient.

The glucose arrival rate R_{IIGI} profile in four patients with T2D is plotted in Figure 2, panel B. The infusion profiles are unimodal and prolonged, extending to 180 min in some subjects. The infusion profiles in T2D show less variability than the CS subjects. Remarkably, a time delay, τ, had to be introduced in R_{IIGI} and had an average of 7 min with 12 min being the longest delay.

4.3 Comparison of patients with T2D and CS subjects

Mean values and ranges of the parameters for patients with T2D and CS subjects are presented in Table 3. The Mann-Whitney U test was used to compare the median differences between T2D and CS parameters. The results of the comparison test are presented in Table 4. There are significant differences (p-value<0.05) between five of the T2D and CS parameters, namely: the insulin sensitivity parameter, a_1, the glucagon suppression parameter k_1, the Hill coefficient, h, in the insulin dose-response curve and the time delays in insulin secretion and exogenous glucose arrival.

Insulin sensitivity, a_1, is much lower in patients with T2D than CS subjects except for two outliers CS 2 and four who had insulin sensitivities on par with patients with T2D. Homa-IR (84) is a method of estimating insulin resistance from fasting glucose and insulin levels. The insulin sensitivity parameters determined using Model 1 showed a positive correlation with 1/HomaIR (n = 14 (CS and T2D patients), Spearman Rank Test correlation =

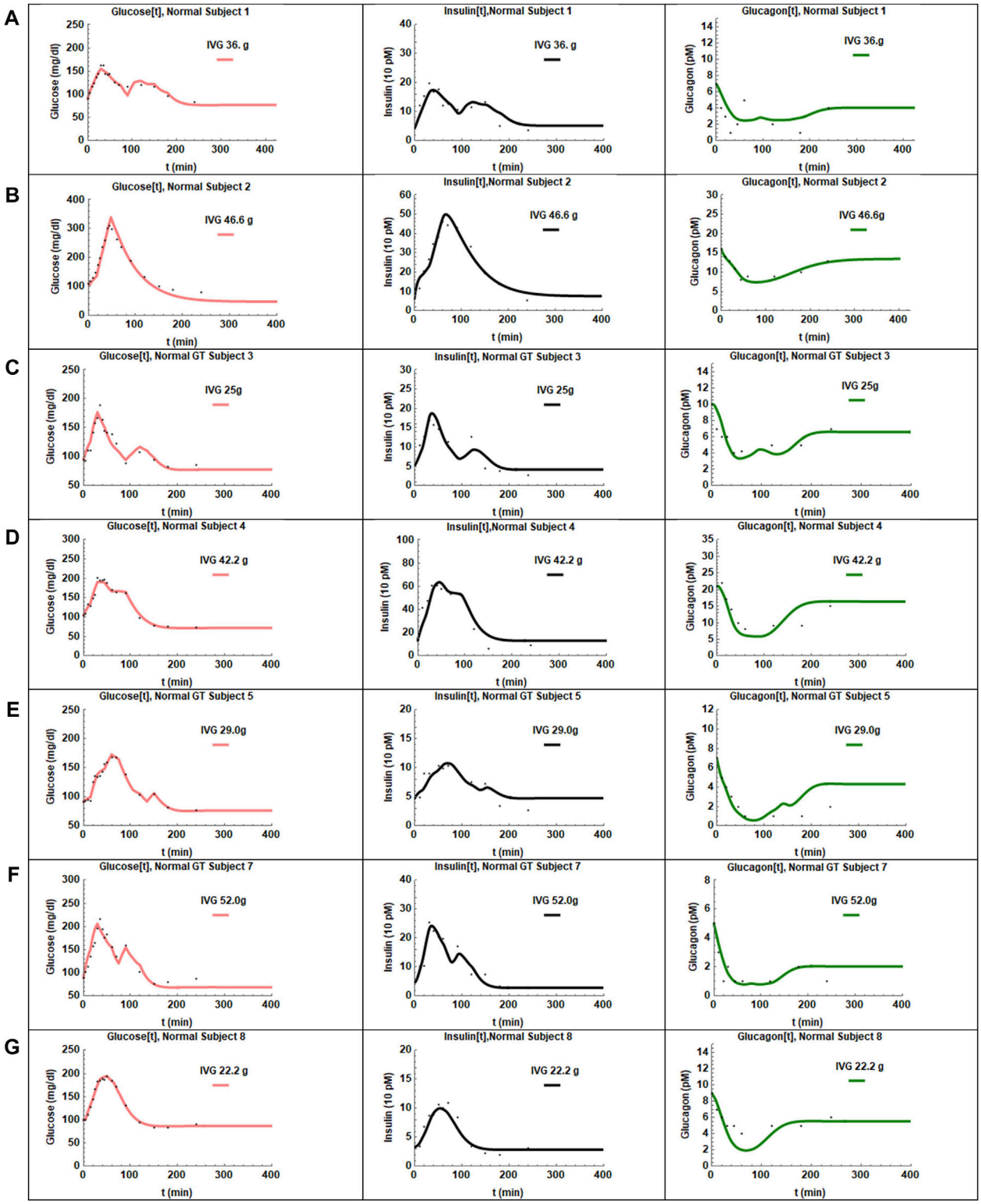

FIGURE 3
The fits obtained for the seven CS subjects are presented in panels **(A–G)**. The adjusted R^2 values were >0.97 for all the fits. The glucose profiles were fit the best by the model. In some cases, the insulin recovery was not captured perfectly **(D,E)**. Glucagon shows very slow recovery and is captured reasonably well by the hysteresis model except for one subject **(E)**.

TABLE 1 Parameters obtained from fitting the coupled Model 1 to the seven CS subjects.

CS#	Parameter								
	a_1	a_2	γ_1	γ_2	k_1	k_2	h	τ	τ_I
1	0.00061	0.33	8.7	1.7	0.25	0.55	2.0	-	-
2	0.000055	0.052	9.3	1.3	0.046	0.35	1.4	3.0	12
3	0.00071	0.20	8.7	3.6	0.27	0.55	2.2	5.3	-
4	0.00012	0.068	21	8.1	0.26	0.45	1.9	-	-
5	0.00032	0.28	3.2	3.4	0.48	0.55	1.3	-	-
7	0.0012	0.59	8.9	0.92	0.24	0.50	2.3	-	-
8	0.00063	0.25	3.2	2.9	0.28	0.55	1.9	-	-

0.70, p value =.0056). The Hill coefficient, h, which is a measure of the rapidity of the insulin response to glucose elevation, is higher in CS subjects than T2D subjects. Insulin secretion is delayed on average by 26 min in patients with T2D. In addition, there was delay of ~10 min in R_{IIGI} circulation in patients with T2D.

The glucagon suppression constant k_1 is significantly lower in patients with T2D relative to CS. Glucagon action in the liver is not significantly different between CS and T2D though there is significant variation within groups. The glucagon secretion parameter is not significantly different between T2D and CS groups in this study.

The glucose infusion profiles are also different between the two groups. The infusion profiles of the CS subjects are bimodal (two peaks), shorter, and show more variability relative to patients with T2D. The infusion profile in patients with T2D is unimodal and more prolonged lasting up to 180 min in some cases.

4.3.1 Trends in parameters

Fasting plasma glucose (FPG), HbA1c and 2 h OGTT plasma glucose levels are all used to diagnose diabetes. (Diabetes Association, 2022). The parameters obtained from the fits were plotted against FPG, HbA1c and 2 h PG (which is approximately matched to 2 h OGTT glucose) to see which parameters correlated with these determinants of diabetes. The contribution of parameters related to glucagon dynamics to impaired FPG, HbA1c and 2 h PG levels is established. As this model differs significantly from previously established models, parameters related to insulin sensitivity and dose-response are classified based on correlations with FPG, HbA1c and 2 h PG. As the sample size is small, the cut-off valus separating T2D and CS are tentatively assigned by visual inspection of Figure 5 and not through statistical tools such as receiver operating characteristic (ROC) curves.

In panel A, the glucagon suppression parameter, k_1, is plotted against HbA1c, FPG and 2 h PG. A linear trend was observed in all three cases with glucose dependent glucagon suppression constant decreasing with increasing A1c, FG and 2 h PG. Two outliers are observed, CS subject 5 with very high suppression and CS subject 2 with very low suppression. The patients with T2D and CS subjects separate into two distinct non-overlapping quadrants, particularly when plotted against 2 h PG. The k_1 value of 0.2 serves as the demarcation between CS and T2D groups. The Spearman Rank Correlation Coefficient and the p-value between k_1 and HbA1c, FPG, and 2 h PG with and without the two outliers are: (n = 14; (−0.46,0.1), (−0.67,.009), (−0.75, 0.002)), and (n = 12; (−0.79, 0.002), (−0.73,.007), (−0.86,.0003)) respectively.

In panel B, the insulin sensitivity parameter, a_1, is plotted against HbA1c, FPG and 2 h PG. All patients with T2D show uniformly low values of insulin sensitivity and again fall into a separate quadrant. Two CS subjects overlap with patients with T2D with respect to a_1. The demarcation for a_1 values between T2D and CS is set at 0.0002 which would place CS 2 and 4 in the diabetes group.

In panel C the glucagon action parameter, a_2, is plotted against HbA1c, FPG and 2 h PG. The action parameter is a measure of glucagon dependent glucose release from the liver. The glucagon action parameter is not significantly different between the two groups. There are no clear trends with respect to a_2 though within the T2D group, 2 h PG values increase linearly with increasing a_2.

In panel D the Hill coefficient which describes the steepness of the glucose dependent insulin response is plotted against HbA1c, FPG and 2 h PG. The Hill coefficient decreases with increasing HbA1c and FPG levels. A value of h = 2 appears to be closer to normal secretory response and h = 1 appears to be the low end of the response.

In Panel E, the total glucose infused in the IIGI experiment is plotted against HbA1c, FPG and 2 h PG. The premise of the IIGI experiment is that if the insulin response to glucose challenge is entirely glucose dependent, with no incretin effect, then the amount of glucose infused will be identical to that of the OGTT glucose challenge experiment. In this case it would be 75 g glucose as in the matching OGTT. The lower the amount of glucose required, the greater the incretin effect. (Nauck et al., 1986). A strong linear relationship is seen with 2 h PG levels particularly within the T2D group. The T2D patient three who showed no incretin effect, had the highest 2 h PG level. The Spearman Rank Correlation Coefficient and the p-value between $Glucose_{Infused}$ and HbA1c, FPG, and 2 h PG are (0.74,.0025), (0.72,.0035), and (0.88,.000039) respectively.

In Panel F insulin secretion parameter γ_1 is presented. There is no difference between the insulin secretion parameter between the T2D and CS groups and no trends with respect to HbA1c, FPG or 2 h PG. This implies that incretin effects are primarily responsible for differences in insulin secretion between the two groups under OGTT conditions.

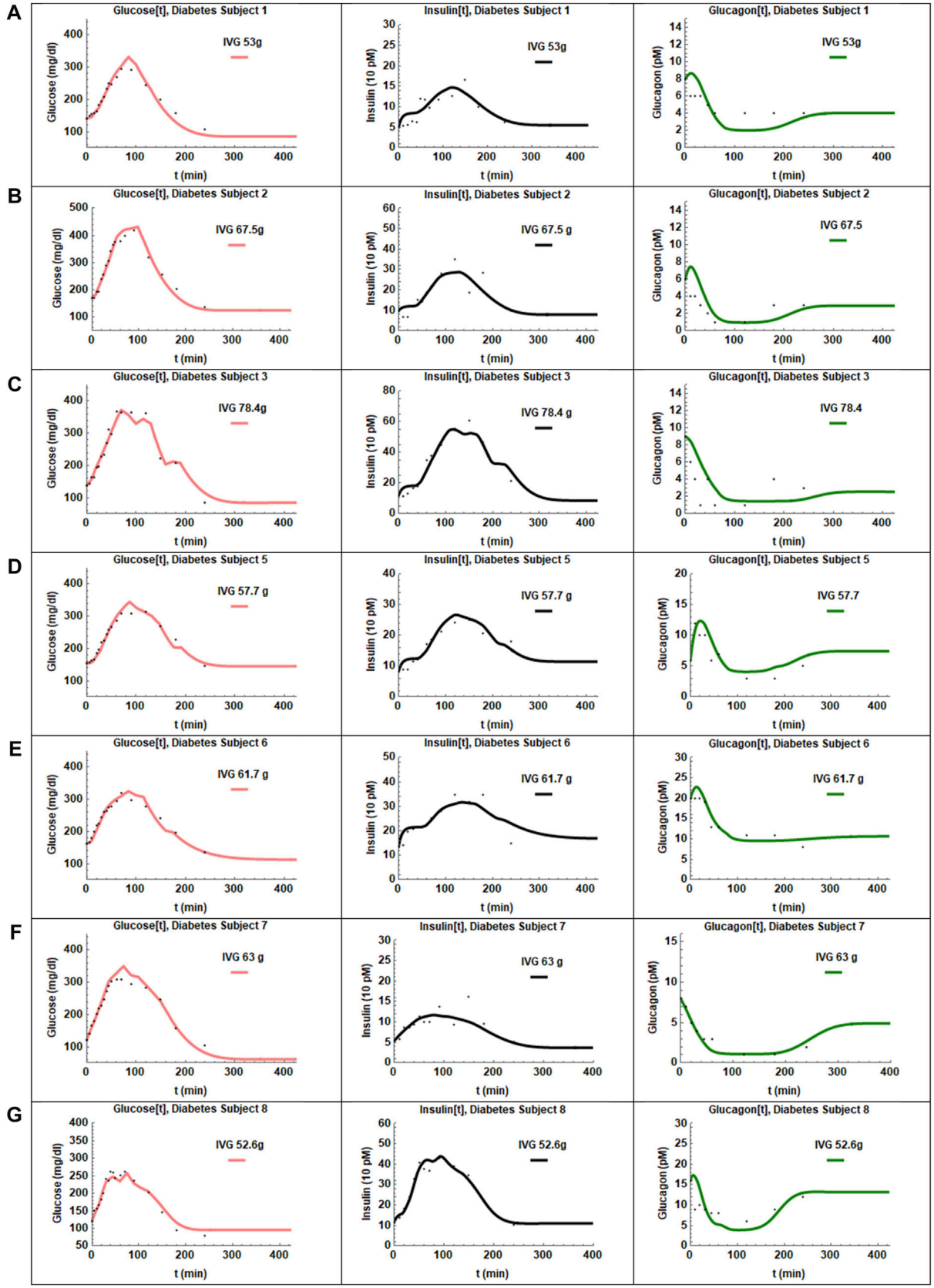

FIGURE 4
The fits obtained for the seven patients with T2D are presented in panels **(A–G)**. The adjusted R^2 values were >0.98 for all subjects. The glucose and insulin profiles were fit best by the model. Glucagon recovery is slow as seen in panels **(A–G)** and again described reasonably well by the hysteresis model.

TABLE 2 Parameters obtained from fitting the coupled Model 1 to patients with T2D.

T2D#	Parameter								
	a_1	a_2	γ_1	γ_2	k_1	k_2	h	τ	τ_1
1	0.00010	0.30	2.7	2.8	0.17	0.60	1.1	10	30
2	0.000085	0.50	4.2	3.6	0.17	0.45	1.7	8	30
3	0.000094	0.49	8.9	1.9	0.13	0.65	1.8	10	35
5	0.000072	0.29	4.6	4.0	0.14	0.33	1.6	12	30
6	0.000050	0.16	5.8	5.2	0.10	0.65	1.0	10	45
7	0.00011	0.18	2.0	1.4	0.16	0.45	1.0	-	-
8	0.000080	0.11	10	8.6	0.23	0.45	1.9	-	15

In Panel G, the glucagon secretion parameter γ_2 is plotted as a function of HbA1C, FPG and 2 h PG. There is trend towards increasing HbA1c and fasting glucose with increasing glucagon secretion within the T2D group. No pattern was seen with respect to 2 h glucose.

4.4 Hysteresis in insulin secretion

To assess the role of hysteresis in glucose dependent insulin secretion, Model 1 without hysteresis, Eq. 4a was compared with Model 2, where insulin secretion is described by Eq. 4b. In Model 1, the insulin secretion is described by a single Hill function with coefficient h. In the hysteresis model, insulin secretion is described by two Hill functions with coefficients h_1 and h_2. The Hill coefficients h_1 and h_2 are varied between the rising and recovery phases of insulin secretion, but the parameter K is assumed to be constant and same in both models.

The results in Section 4, describe the fits obtained with Model 1 for CS and T2D subjects. The parameters obtained using the hysteresis Model 2 are presented in Tables 5, 6. The fits are presented in Supplementary Figures S3, 4. Visually the fits for the different subjects are not very different for Model 1 and Model 2. In Model 2, the Hill coefficients h_2 is greater than h_1 for all CS subjects. Thus, insulin levels fall more steeply when glucose is declining. In the patients with T2D $h_1 \sim h_2$ indicating there is no hysteresis and the results are essentially equivalent to the Model 1. The values of h in Model 1 were comparable to h_2 in Model 2 in CS subjects. In patients with T2D, h was comparable to h_1 and h_2, in other words, a single Hill equation is sufficient to describe insulin dose-response.

In Model 1, h was significantly higher in CS subjects compared to patients with T2D. In Model 2, h_2 is significantly higher in CS subjects relative to patients with T2D. So, both models show a change in behaviour in patients with T2D.

Model comparison is made based on the Akaike Information Criterion with small sample correction (AICc). (Akaike, 1974). This criterion gives an estimate of whether the model with more parameters reduces the error sufficiently to justify the increase in complexity. The Akaike criterion can only be used to compare models using the same data set, so the AICc values are presented in Tables 7, 8 for individual CS and T2D subjects respectively. The lower the AICc value, the better the fit. The differences in AICc values are given in column 4. The AICc differences were variable with some subjects fit better by Model 1 and others by Model 2. The criterion cannot therefore be used to pick one model over the other.

5 Discussion

T2D is a disease that is manifested when insulin resistance and beta- and alpha-cell dysfunction occur. (Topp et al., 2000; Topp et al., 2007; Burcelin et al., 2008; Ashcroft and Rorsman, 2012; Ha et al., 2016). As these three determinants of diabetes

TABLE 3 Average values, standard errors, and ranges of the parameters in patients with T2D and CS subjects.

ACT	Mean		SEM		Range	
	T2D	CS	T2D	CS	T2D	CS
a_1 ($\times 10^{-5}$)						
(10 pM min)$^{-1}$	8.4	52	0.75	15	5.-11	5.5–120
a_2 mg/dL (pM min)$^{-1}$	0.29	0.25	0.059	0.069	0.11–0.5	0.052–0.59
γ_1 10 pM min^{-1}	5.5	9.0	1.1	2.2	2.0–10	3.2–21
γ_2 pM min^{-1}	3.9	3.1	0.92	0.92	1.4–8.6	0.92–8.12
k_1 (mM)$^{-1}$	0.16	0.26	0.015	0.047	0.1–0.23	0.046–0.48
k_2 (mM)$^{-1}$	0.51	0.50	0.046	0.029	0.33–0.60	0.35–0.55
h	1.4	1.9	0.15	0.14	1.0–1.9	1.3–2.3
τ_1 (min)$^{-1}$	26	1.7	5.5	1.7	0.-45	0.-12
τ (min)$^{-1}$	7.1	1.2	1.9	0.80	0.-12	3.0–5.3

TABLE 4 Results of the Mann-Whitney *U* test. The insulin sensitivity parameter, a_1, the glucagon suppression parameter k_1, the Hill coefficient h, the insulin secretion time delay τ_1 and the infused glucose R_{IIGI} time delay τ, are found to be significantly different between the T2D and CS groups.

Parameter	Mann-whitney *U* test (T2D vs. CS) *p*-value
a_1	0.015
a_2	0.70
γ_1	0.28
γ_2	0.37
k_1	0.021
k_2	0.95
h	0.039
τ	0.006
τ_1	0.039

TABLE 5 Parameters determined from fitting the hysteresis Model 2 to data from CS subjects. The parameters obtained are similar to that for Hill Model 1. The values of h_1 are lower than h_2 in all subjects implying a steeper glucose dependent dose-response during the insulin recovery phase.

CS#	a_1	a_2	γ_1	γ_2	k_1	k_2	h_1	h_2	τ_1/τ
1	0.00053	0.34	6.0	2.9	0.35	0.55	1.4	1.8	–/–
2	0.000058	0.092	9.0	2.0	0.077	0.35	1.3	1.8	14/3.5
3	0.00062	0.18	5.7	4.7	0.31	0.55	1.4	2.3	6./5
4	0.00011	0.070	16	8.8	0.28	0.55	1.1	2.2	–/–
5	0.00034	0.28	2.7	3.3	0.46	0.45	0.94	1.4	–/–
7	0.0011	0.58	8.6	0.96	0.24	0.55	2.2	2.4	–/–
8	0.00063	0.22	2.7	2.9	0.25	0.45	1.3	1.7	–/–

TABLE 6 Parameters determined from fitting the hysteresis Model 2 to data from patients with T2D. The parameters a_1-k_2 are comparable to that for Hill Model 1. The value of h_1 is approximately equal to h_2 in all subjects implying there is no hysteresis in diabetic subjects. Only subject eight showed a significant drop in h_2 compared to h_1.

T2D#	a_1	a_2	γ_1	γ_2	k_1	k_2	h_1	h_2	τ_1/τ
1	0.000092	0.33	2.6	2.5	0.17	0.4	1.2	1.3	30/10
2	0.000075	0.57	4.5	3.6	0.18	0.35	1.4	2.0	30/8
3	0.000081	0.45	9.2	2.1	0.13	0.65	2.3	2.0	30/10
5	0.000072	0.26	4.5	4.5	0.14	0.41	1.5	1.4	30/12
6	0.0001	0.19	5.4	4.2	0.097	0.65	0.9	0.95	45/10
7	0.00011	0.18	2.0	1.1	0.15	0.45	1.1	0.90	–/–
8	0.00011	0.12	10	5.1	0.18	0.3	2.2	1.2	15/-

are intrinsically coupled, it is important to quantify parameters related to them in a self-consistent manner without splitting the coupled dynamics into separate subsystems. The parsimonious coupled system of delay differential equations used in this paper allow for estimation of all parameters in a single step. The coupled glucose-insulin-glucagon model was used to fit data from IIGI experiments to quantify glucagon action, suppression, and secretion as well as insulin resistance and secretion, without the confounding influence of incretins and other gut mediated factors. The results presented in Section 4 show that the model captures the coupled dynamics correctly and yields parameters related to both alpha and beta cell dysfunction and insulin resistance in one step. As this is a new extended model based on delay differential equations, some comparisons will be made with parameters related to insulin resistance and secretion from the single delay differential model of De Gaetano et al., where the coupled insulin-glucose dynamics was studied. (Panunzi et al., 2007; De Gaetano and Hardy, 2019).

Alpha cell dysfunction is known to contribute to both fasting and postprandial hyperglycemia in T2D. (Dunning and Gerich, 2007; Burcelin et al., 2008; Lund et al., 2014). Increased glucagon secretion, lowered glucagon suppression and differences in glucagon action could contribute to elevated fasting glucose levels and continued glucose production in the post prandial state. In this study, the glucagon suppression parameter, k_1, was found to be significantly lower in patients with T2D relative to CS. The parameter also showed clear linear relationship with respect to HbA1c, FPG and 2 h PG values. There was strong negative correlation with all three indicators of diabetes. HbA1c levels have been shown to correlate better with post-prandial glucose levels and less with fasting glucose levels. (Landgraf, 2004; Hershon et al., 2019). Two hr PG values are reflective of postprandial glucose excursions. This shows that glucagon suppression is impaired in T2D and has an impact on both fasting and postprandial glucose levels and likely exacerbates hyperglycemia in patients with T2D.

The glucagon secretion parameter γ_2 was not significantly different between CS and patients with T2D in this study. In the paper by Unger et al. (1970) similarly, statistically significant differences were not observed in fasting glucagon levels between CS and T2D subjects but when hyperglycemia was induced by glucose infusion in the CS so as to simulate the fasting hyperglycemia of T2D patients, mean glucagon fell significantly below the T2D mean, indicating the level of glucagonemia is high for the prevailing glycemia in T2D. This is also in line with former observations measuring hepatic glucose output using radiolabeled isotopes showing a clear positive correlation between baseline glucose and hepatic glucose output. (Baron et al., 1987). Even with great basal variation in basal glucagon the hepatic glucose output was suppressible

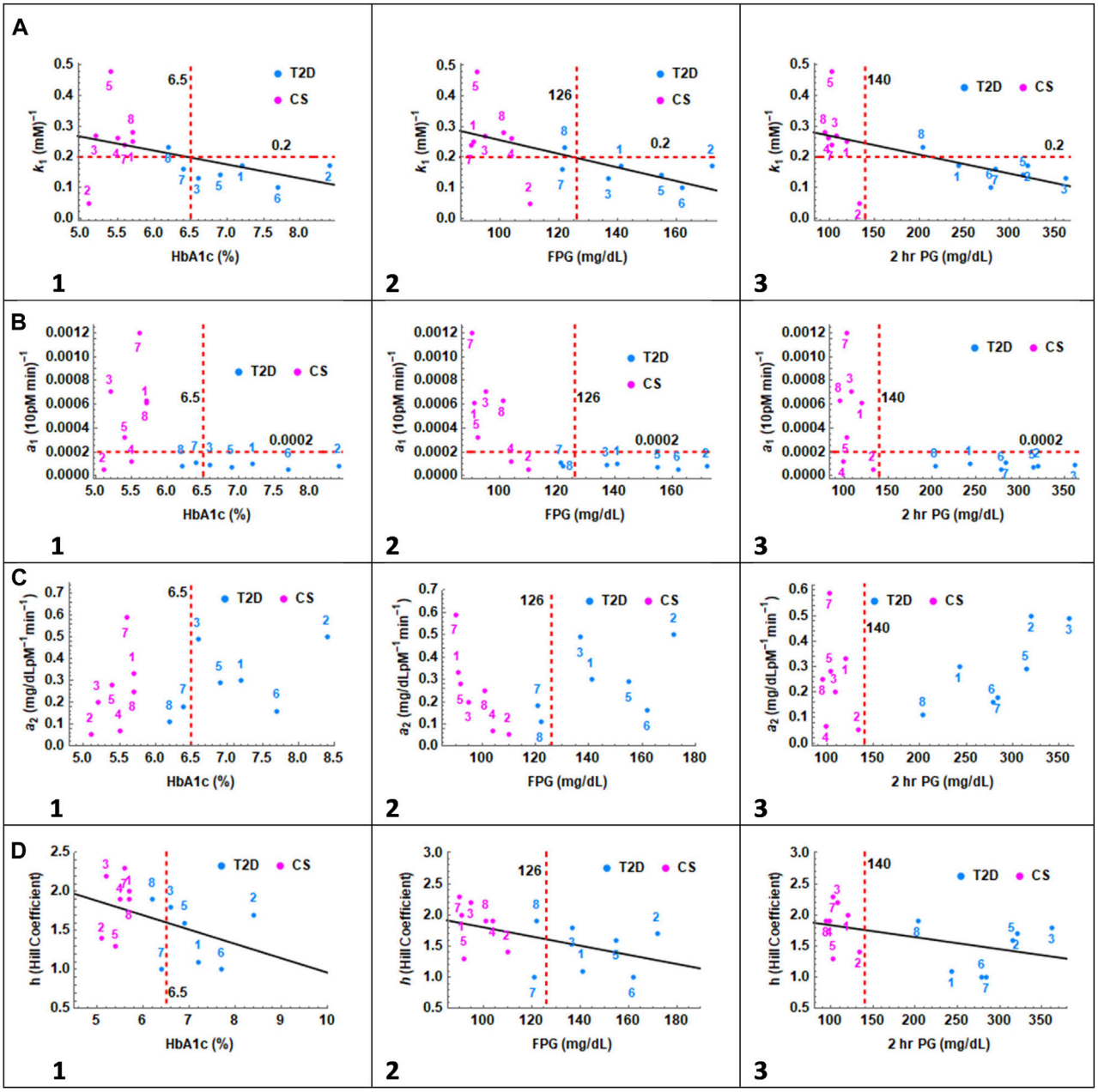

FIGURE 5
In the series of panels **(A)** through **(G)**, the parameters related to glucagon suppression k_1, insulin action a_1, glucagon action a_2, Hill coefficient h, infused glucose, insulin secretion γ_1 and glucagon secretion γ_2 are plotted as a function of HbA1c, FPG and 2 h PG values. In panel **(A)** 1, 2, and 3, CS and T2D subjects partition into distinct quadrants except for one CS subject. A linear relationship is observed between glucagon suppression and HbA1c, FPG, and 2 h PG. The cutoff value separating patients with T2D, and CS subjects is set at 0.2. In Panel **(B)**, the correlation with insulin sensitivity parameter a_1 is presented. CS subjects and patients with T2D again partition into two distinct quadrants except for CS 2 and 4. The cutoff value separating patients with T2D, and CS subjects is 0.0002. In panel **(C)** no clear distinction between patients with T2D and CS subjects is observed with respect to glucagon action parameter a_2. In Panel **(D)**, the Hill coefficient, h, is trending higher in CS subjects toward h = two and in patients with T2D towards h = 1. In Panel **(E)**, infused glucose, an indicator of the incretin effect, shows a linear trend with respect to HbA1C, FPG and 2 h PG, particularly in patients with T2D. In panel **(F)**, no difference in insulin secretion parameter, γ_1, between CS and T2D is observed. In panel **(G)**, patients with T2D show a weak linear trend towards higher HbA1c and FPG values with increasing glucagon secretion parameter.

by suppressing glucagon alone in pancreatic clamp (using somatostatin and basal insulin infusion). (Baron et al., 1987).

The glucagon action parameter, a_2, which is a measure of how effective it is in hepatic glucose production, is not significantly different between the CS and T2D subjects and is thus not the

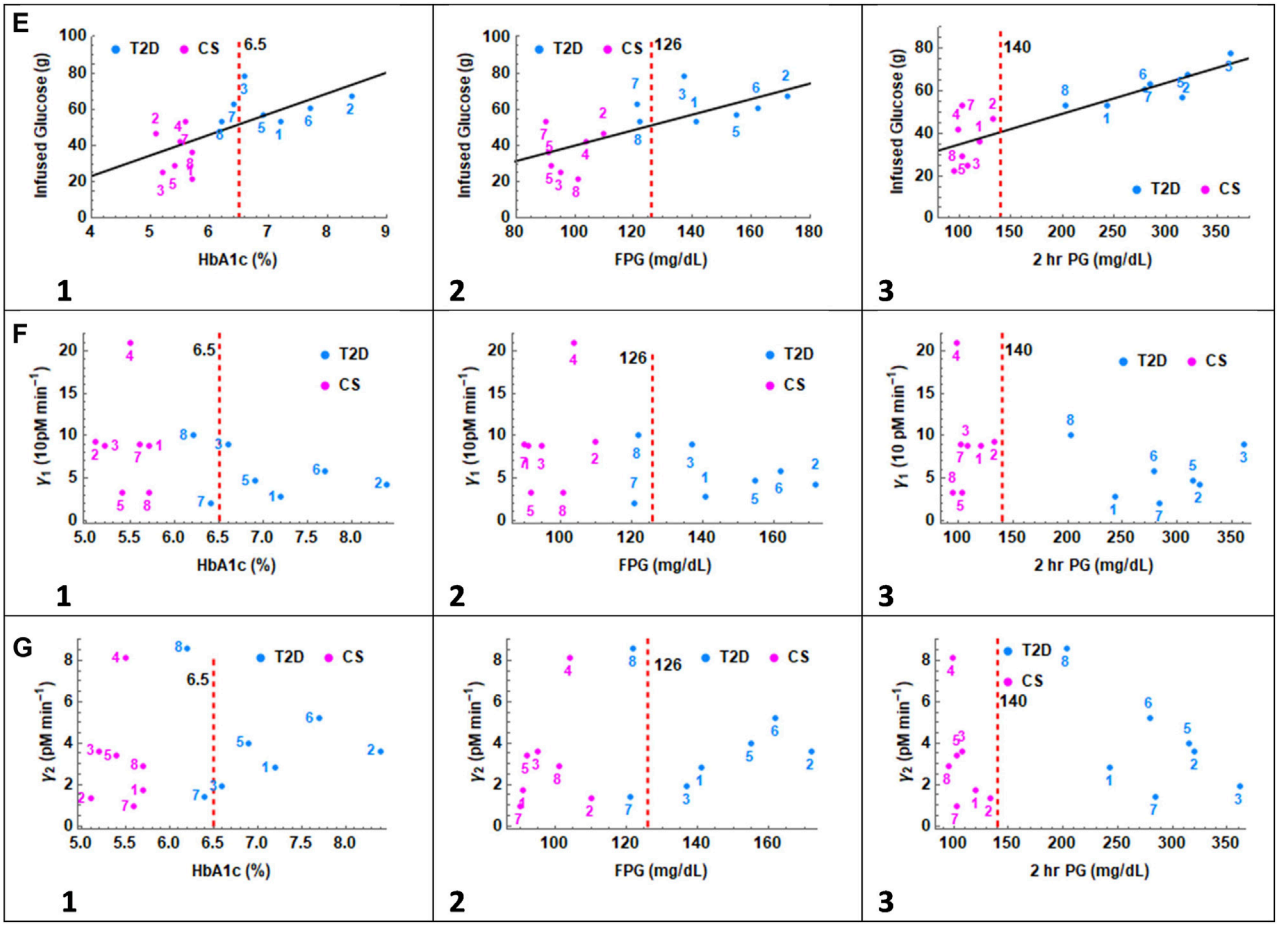

FIGURE 5
coninued

likely cause of elevated fasting and post prandial plasma glucose levels.

Modeling IIGI gives information regarding glucose stimulated insulin secretion. In model 1, there are three parameters describing insulin secretion: 1) a measure of the magnitude of insulin secretion, γ_1. 2) the steepness of the response based on the Hill coefficient, h, in the dose-response expression, ψ and 3) the time delay in insulin response, τ_1. A point to note is that differences in hepatic insulin extraction (HPE) may exist between subjects and the

TABLE 7 Values of the Akaike Information Criterion corrected for small sample size (AICc) is presented for patients with T2D. Smaller AICc values indicate a better fit. The AICc values are not uniformly less for one model over the other in all patients.

Pat#(T2D)	Akaike information criterion (AICc)		AICc difference (model 1-Model2)
	Model 1 (Hill)	Model 2 (hysteresis)	
1	309	303	+6
2	318	317	+1
3	321	323	−2
5	296	301	−5
6	290	292	−2
7	232	233	−1
8	301	297	+4

TABLE 8 Values of the Akaike Information Criterion corrected for small sample size (AICc) is presented for CS subjects. Smaller AICc values indicate a better fit. The AICc values are not uniformly less for one model over the other.

Pat#(CS)	Akaike information criterion (AICc)		AICc difference
Model 1-model 2	Model 1 (Hill)	Model 2 (hysteresis)	
1	256	257	−1
2	299	305	−6
3	236	227	+9
5	279	268	+11
6	229	231	−2
7	253	256	−3
8	217	216	+1

insulin secretion parameters determined are reflective of post HPE plasma insulin levels. The differences in HPE could also account for the some of the variation in plasma insulin levels between subjects but is not considered here. (Bojsen-Møller et al., 2018; Santoleri and Titchenell, 2019; Piccinini and Bergman, 2020).

The parameter γ_1 which is a measure of glucose dependent insulin secretion was not significantly different between T2D and CS subjects. There may be multiple reasons for this observation. The patients with T2D in this study were newly diagnosed and thus in the early stages of disease progression. This result is also consistent with the estimation of the incretin effects from the IIGI experiments in this study which showed that the incretin dependent insulin response is the dominant factor in differentiating between the levels of insulin secretion in CS and T2D subjects. The incretin dependent insulin secretion was found to be significantly impaired in patients with T2D. (Bagger et al., 2011).

Though the insulin secretion parameter was not significantly different, the steepness of the insulin response as reflected by the Hill coefficient, h, is significantly different between the two groups. A value of h = 2 appears to be closer to normal secretory response, observed in CS subjects with higher insulin sensitivity and h = 1 appears to be the low end of the response observed in T2D subjects who have much lower insulin sensitivity. A point of note is that the CS subjects in this study were weight matched to the patients with T2D and the T2D patients were newly diagnosed. It is possible that a clearer demarcation between CS and T2D groups with respect to the Hill coefficient might become evident when studying a wider spectrum of T2D and CS subjects. In the paper by De Gaetano et al., the average estimated value for the Hill coefficient in normal individuals was 2.4.

Significant differences in time delay in glucose stimulated insulin secretion, τ_1, was observed between CS and T2D subjects. There was a significant time delay in only one CS subject who also had low insulin sensitivity whereas most T2D had large time delays in insulin secretion. The reason for the delay in insulin secretion is unclear but might be partly related to the delay in exogenous glucose (R_{IIVG})

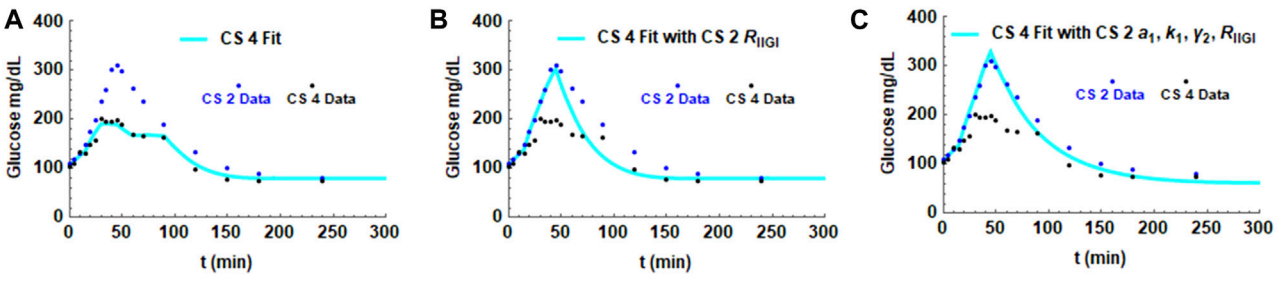

FIGURE 6
Simulations showing the effect of the exogenous glucose arrival R_{IIGI} on the glucose profile. Parameters in the fit for CS 4 were substituted with the values obtained from the CS 2 fit. Panel **(A)** shows the fit with all CS 4 parameters. Panel **(B)** shows the effect of substituting CS 2 glucose infusion, R_{IIGI}, in the simulation. Panel **(C)** shows the impact of substituting CS 2 insulin sensitivity parameter a_1, glucagon secretion parameter k_1 and glucagon secretion parameter γ_2 in addition to R_{IIGI} on the CS 4 fit.

arrival observed in the patients with T2D. In the paper by De Gaetano where they fit data from IVGTT on normal subjects, a delay in the insulin secretion term had to be introduced to produce the characteristic second phase insulin secretion profile. This result is very different from that observed in this IIGI study where no significant delays were observed in glucose stimulated insulin secretion in the CS subjects.

The insulin sensitivity parameter showed significant differences between T2D and CS subjects following established trends. The magnitude of the average insulin sensitivity of 0.0005 $(10\ pM\ min)^{-1}$ in CS subjects is near the lower end of the glucose sensitivity parameter estimates in normal subjects in the paper by De Gaetano et al. In addition, two CS subjects had insulin sensitivities that were on par with T2D patients. This is likely because the CS group was weight matched to the patients with T2D in this study. In fact, some CS subjects showed very high levels of insulin secretion indicative of the compensatory phase in response to falling insulin sensitivities. A cut-off value of 0.0002 $(10\ pM\ min)^{-1}$ separating T2D and CS was tentatively assigned though a much larger study would be required to correctly identify the cut-off based on ROC curves for example. The insulin sensitivity measures determined in this study correlated well with HOMA-IR values. Though HOMA-IR is considered to be a measure of hepatic insulin resistance it has been found to correlate well with insulin sensitivity measures from the hyperinsulinemic-euglycemic clamp, for example. (Matthews et al., 1985).

As seen in Figure 2, the exogenous glucose that is infused has distinct profiles for the different subjects that is particularly apparent in CS patients. To delineate the influence of infused glucose on post infusion glucose profiles, the effect of substituting R_{IIGI} of one patient with that of another was studied. In order to make a meaningful inference, two CS subjects, 2 and 4, who had similar parameters including similar amounts of total glucose infused (Table 1; Figure 3 Panel B and D), but showed very different post infusion glucose profiles were chosen for the simulations. In Figure 6A, the fit obtained for CS 4 (light blue solid line) as well as the glucose data for CS 2 and CS 4 are shown. In the second simulation (Figure 6B), all parameters of the CS 4 fit were retained but the exogenous glucose infusion R_{IIGI} of CS 2 was substituted. This causes the CS 4 glucose profile to spike very much like that seen in CS 2. In Panel C, 4 parameters of CS 2 were substituted retaining only insulin secretion and glucagon action parameters. It is shown that patient four transitions to patient two completely. The effect of the exogenous glucose profile is dramatic in this case. This result indicates that rate of glucose arrival could have a big impact on glucose dynamics. As IIGI is isoglycemic with the corresponding OGTT this suggests that rate of glucose arrival from the gut could play a role in glucose dynamics post oral ingestion as well and account in part for the differences in glucose excursions between subjects. The role of gastric emptying in glucose homeostasis has been studied by several researchers where this effect has been observed, eg., Holst et al. and references therein. (Brener et al., 1983; Horowitz et al., 1993; Holst et al., 2016). This possibility has been suggested in the paper by Fiorentino et al. where the role of sodium-glucose co-transporters is investigated. (Fiorentino et al., 2017). This result may also have direct relevance to the findings in the paper by Utzschneider et al. where they made an association between plasma glucose profile shape and beta cell function in newly diagnosed T2D patients. (Utzschneider et al., 2021).

A consequence of ingesting large glucose loads is often a lowering of glucose to values below baseline levels or postprandial hypoglycemia. (Saha, 2006; Parekh et al., 2014). This phenomenon is seen in most of the subjects in this study, particularly the CS subjects. One explanation could be that delayed recovery of glucagon to baseline levels causes the glucose levels in turn to fall below baseline. In the paper by Wang, G., (Wang, 2014)., hysteresis in insulin action is hypothesized to cause postprandial hypoglycemia. As modeling in this study with constant insulin action, a_1, was able to reproduce the plasma glucose profiles correctly, including the postprandial dip, hysteresis behaviour in insulin secretion was considered a possibility instead. If insulin secretion falls off more slowly after glucose levels start falling, it could contribute to post-prandial lowering of glucose below baseline. The fits of the hysteresis model 2, showing $h_1<h_2$ in CS subjects, on the contrary, predict insulin levels returning to baseline levels more sharply than the rise. The hysteresis model of glucose dependent insulin secretion thus does not appear to explain post-prandial hypoglycemia. Secondly, the hysteresis model 2, with one extra parameter, did not provide a significantly improved description of the dynamics relative to the Hill model 1 as indicated by the AICc criterion.

Modeling IIGI is shown to reveal different levels of impairment in alpha- and beta-cell function and insulin action in T2D. The contribution of various parameters to glucose homeostasis, particularly those related to glucagon dynamics have been estimated. Quantification of the significant impairment in glucagon suppression in patients with T2D should help in classifying patients based on alpha-cell dysregulation. Changes in insulin dose-response parameters in T2D without the confounding influence of incretins and other gut mediated factors as well as first phase insulin release have been determined. The importance of considering exogenous glucose arrival on exacerbating postprandial glucose excursions is highlighted using model simulations. In

addition to T2D, the model developed was also used to explore the role of hysteresis in insulin secretion in explaining phenomena such as post prandial glucose lowering and a related pathophysiology reactive hypoglycemia. Results from this study show that hysteresis in insulin secretion is not the likely cause of postprandial glucose lowering. While the model developed is shown to be very effective in determining parameters related to the coupled dynamics from IIGI data, shortcomings of fitting IIGI data are that some of the parameters had to be adjusted manually. Future work would include fitting the model to larger sets of data which would allow for classification of patients based on cut-off values of parameters related to both alpha- and beta-cell impairment determined from ROC curves.

Data availability statement

The original contributions presented in the study are included in the article/Supplementary Material, further inquiries can be directed to the corresponding authors.

Ethics statement

The studies involving human participants were reviewed and approved by the Scientific-Ethical Committee of the Capital Region of Denmark (registration no. H-A-2007-0048), the Danish Data Protection Agency (registration j. nr. 2007- 41-1058) and at www.ClinicalTrials.gov (ID NCT00529048). The study was conducted according to the principles of the Helsinki Declaration II. The patients/participants provided their written informed consent to participate in this study.

Author contributions

VS: Development of computational model, Fitting model to data, Analysis of results, and Manuscript preparation. JB: Conduction of experimental procedures and collection of samples, Delivery of raw data, Interpretation of results, and Manuscript preparation. JH: Biochemical analysis of glucagon, Interpretation of results, and Manuscript review. FK: Conductor of experimental protocol, Interpretation of results, and Manuscript review. TV: Principal Investigator and Conductor of experimental protocol, Interpretation of results, and Manuscript review.

Funding

(VS) This work was facilitated by financial and institutional support from the Whiting School of Engineering, JH University. The research and open access publication charges were partially funded by the NIH K25 grant number DK131328. (JB) Original work was funded by an unrestricted research grant (no. 34851) from the Investigator Initiated Studies Program of Merck&Co.

Acknowledgments

(VS) Many useful discussions with Professor Patrik Rorsman are gratefully acknowledged. A special thank you to Dr Arthur Sherman for many useful discussions and editing the manuscript. Thanks also to Dr Shankar Subramaniam for useful discussions regarding glucose homeostasis. Thanks to Vinayak Harihar for editing the manuscript and many useful suggestions. Thanks to the reviewers for helpful critiques and suggestions.

Conflict of interest

The authors declare that the research was conducted in the absence of any commercial or financial relationships that could be construed as a potential conflict of interest.

Publisher's note

Supplementary material

The Supplementary Material for this article can be found online at: https://www.frontiersin.org/articles/10.3389/fphys.2022.911616/full#supplementary-material

References

Adkins, A., Basu, R., Persson, M., Dicke, B., Shah, P., Vella, A., et al. (2003). Higher insulin concentrations are required to suppress gluconeogenesis than glycogenolysis in nondiabetic humans. *Diabetes* 52 (9), 2213–2220. doi:10.2337/diabetes.52.9.2213

Ahmadpour, S., and Kabadi, U. M. (1997). Pancreatic α-cell function in idiopathic reactive hypoglycemia. *Metabolism.* 46 (6), 639–643. doi:10.1016/s0026-0495(97)90006-8

Akaike, H. (1974). A new look at the statistical model identification. *IEEE Trans. Autom. Contr.* 19 (6), 716–723. doi:10.1109/tac.1974.1100705

Alford, F. P., Bloom, S. R., and Nabarro, J. D. N. (1976). Glucagon metabolism in man. Studies on the metabolic clearance rate and the plasma acute disappearance time of glucagon in normal and diabetic subjects. *J. Clin. Endocrinol. Metab* 42(5): 830–838. doi:10.1210/jcem-42-5-830

Alskär, O., Bagger, J. I., Røge, R. M., Knop, F. K., Karlsson, M. O., Vilsbøll, T., et al. (2016). Semimechanistic model describing gastric emptying and glucose absorption in healthy subjects and patients with type 2 diabetes. *J. Clin. Pharmacol.* 56 (3), 340–348. doi:10.1002/jcph.602

Diabetes Association, American (2022). *Classification and Diagnosis of Diabetes : Standards of Medical Care in Diabetes — 2022*, 17–38.

Ashcroft, F. M., and Rorsman, P. (2012). Diabetes mellitus and the β -cell : The last ten years. *Cell.* 148 (6), 1160–1171. doi:10.1016/j.cell.2012.02.010

Bagger, J. I., Knop, F. K., Lund, A., Holst, J. J., and Vilsbøll, T. (2014). Glucagon responses to increasing oral loads of glucose and corresponding isoglycaemic intravenous glucose infusions in patients with type 2 diabetes and healthy individuals. *Diabetologia* 57 (8), 1720–1725. doi:10.1007/s00125-014-3264-2

Bagger, J. I., Knop, F. K., Lund, A., Vestergaard, H., Holst, J. J., and Vilsbøll, T. (2011). Impaired regulation of the incretin effect in patients with type 2 diabetes. *J. Clin. Endocrinol. Metab.* 96 (3), 737–745. doi:10.1210/jc.2010-2435

Baron, A. D., Schaeffer, L., Shragg, P., and Kolterman, O. G. (1987). Role of hyperglucagonemia in maintenance of increased rates of hepatic glucose output in type II diabetics. *Diabetes* 36 (3), 274–283. doi:10.2337/diab.36.3.274

Bergman, R. N., Ider, Y. Z., Bowden, C. R., and Cobelli, C. (1979). Quantitative estimation of insulin sensitivity. *Am. J. Physiol.* 5 (6), E667–E677. doi:10.1152/ajpendo.1979.236.6.E667

Bergman, R. N. (2021). Origins and history of the minimal model of glucose regulation. *Front. Endocrinol.* 11, 583016. doi:10.3389/fendo.2020.583016

Bergman, R. N., Phillips, L. S., and Cobelli, C. (1981). Physiologic evaluation of factors controlling glucose tolerance in man. Measurement of insulin sensitivity and β-cell glucose sensitivity from the response to intravenous glucose. *J. Clin. Investig.* 68 (6), 1456–1467. doi:10.1172/jci110398

Bojsen-Møller, K. N., Lundsgaard, A. M., Madsbad, S., Kiens, B., and Holst, J. J. (2018). Hepatic insulin clearance in regulation of systemic insulin concentrations-role of carbohydrate and energy availability. *Diabetes* 67 (11), 2129–2136. doi:10.2337/db18-0539

Bolli, G., de Feo, P., Perriello, G., De Cosmo, S., Compagnucci, P., Santeusanio, F., et al. (1984). Mechanisms of glucagon secretion during insulin-induced hypoglycemia in man Role of the beta cell and arterial hyperinsulinemia. *J. Clin. Investig.* 73 (4), 917–922. doi:10.1172/JCI111315

Brener, W., Hendrix, T. R. M. P., and McHugh, P. R. (1983). Regulation of the gastric emptying of glucose. *Gastroenterology* 85 (1), 76–82. doi:10.1016/s0016-5085(83)80232-7

Briant, L., Salehi, A., Vergari, E., Zhang, Q., and Rorsman, P. (2016). Glucagon secretion from pancreatic α-cells. *Ups. J. Med. Sci.* 121 (2), 113–119. doi:10.3109/03009734.2016.1156789

Briant, L. J. B., Reinbothe, T. M., Spiliotis, I., Miranda, C., Rodriguez, B., and Rorsman, P. (2018). δ-cells and β-cells are electrically coupled and regulate α-cell activity via somatostatin. *J. Physiol.* 596 (2), 197–215. doi:10.1113/JP274581

Brun, J. F., Fedou, C., and Mercier, J. (2000). Postprandial reactive hypoglycemia. *Diabetes Metab.* 26 (5), 337–351.

Burcelin, R., Knauf, C., and Cani, P. D. (2008). Pancreatic alpha-cell dysfunction in diabetes. *Diabetes Metab.* 34, S49–S55. doi:10.1016/S1262-3636(08)73395-0

Caumo, A., and Luzi, L. (2004). First-phase insulin secretion: Does it exist in real life? Considerations on shape and function. *Am. J. Physiol. Endocrinol. Metab.* 287 (3 50-3), 371–385. doi:10.1152/ajpendo.00139.2003

Cerf, M. E. (2013). Beta cell dysfunction and insulin resistance. *Front. Endocrinol. (Lausanne).* 4 (MAR), 1–12. doi:10.3389/fendo.2013.00037

Cobelli, C., Federspil, G., Pacini, G., Salvan, A., and Scandellari, C. (1982). An integrated mathematical model of the dynamics of blood glucose and its hormonal control. *Math. Biosci.* 58 (1), 27–60. doi:10.1016/0025-5564(82)90050-5

Cobelli, C., Man, C. D., Sparacino, G., Magni, L., Nicolao, G. De, and Kovatchev, B. P. (2009). Diabetes: Models, signals, and control. *IEEE Rev. Biomed. Eng.* 2, 54–96. doi:10.1109/RBME.2009.2036073

Cobelli, C., Man, C. D., Toffolo, G., Basu, R., Vella, A., and Rizza, R. (2014). The oral minimal model method. *Diabetes* 63 (4), 1203–1213. doi:10.2337/db13-1198

Cryer, P. E. (2012). Minireview: Glucagon in the pathogenesis of hypoglycemia and hyperglycemia in diabetes. *Endocrinology* 153 (3), 1039–1048. doi:10.1210/en.2011-1499

Dalla Man, C., Camilleri, M., and Cobelli, C. (2006). A system model of oral glucose absorption: Validation on gold standard data. *IEEE Trans. Biomed. Eng.* 53 (12), 2472–2478. doi:10.1109/TBME.2006.883792

Dalla Man, C., Caumo, A., and Cobelli, C. (2002). The oral glucose minimal model: Estimation of insulin sensitivity from a meal test. *IEEE Trans. Biomed. Eng.* 49 (5), 419–429. doi:10.1109/10.995680

De Gaetano, A., and Hardy, T. A. (2019). A novel fast-slow model of diabetes progression: Insights into mechanisms of response to the interventions in the Diabetes Prevention Program. *PLoS One* 14 (10), e0222833–39. doi:10.1371/journal.pone.0222833

De Gaetano, A., Hardy, T., Beck, B., Abu-raddad, E., Palumbo, P., Bue-valleskey, J., et al. (2008). Mathematical models of diabetes progression. *Am. J. Physiol.* 295 (6). doi:10.1152/ajpendo.90444.2008

DeFronzo, R. A., and Tripathy, D. (2009). Skeletal muscle insulin resistance is the primary defect in type 2 diabetes. *Diabetes Care* 32 (2), S157–S163. doi:10.2337/dc09-S302

Diderichsen, P. M., and Göpel, S. O. (2006). Modelling the electrical activity of pancreatic α-cells based on experimental data from intact mouse islets. *J. Biol. Phys.* 32 (3–4), 209–229. doi:10.1007/s10867-006-9013-0

Duckworth, W. C., Bennett, R. G., and Hamel, F. G. (1998). Insulin degradation: Progress and potential. *Endocr. Rev.* 19 (5), 608–624. doi:10.1210/edrv.19.5.0349

Dunning, B. E., and Gerich, J. E. (2007). The role of α-cell dysregulation in fasting and postprandial hyperglycemia in type 2 diabetes and therapeutic implications. *Endocr. Rev.* 28 (3), 253–283. doi:10.1210/er.2006-0026

Eizirik, D. L., Pasquali, L., and Cnop, M. (2020). Pancreatic β-cells in type 1 and type 2 diabetes mellitus: Different pathways to failure. *Nat. Rev. Endocrinol.* 16 (7), 349–362. doi:10.1038/s41574-020-0355-7

Elliott, A. D., Ustione, A., and Piston, D. W. (2015). Somatostatin and insulin mediate glucose-inhibited glucagon secretion in the pancreatic alpha-cell by lowering cAMP. *Am. J. Physiol. Endocrinol. Metab.* 308, E130–E143. doi:10.1152/ajpendo.00344.2014

Expert committee on the Diagnosis and classification of diabetes mellitus. *Diabetes Care.* 2003;26(1):S5–S20.

Færch, K., Vistisen, D., Pacini, G., Torekov, S. S., Johansen, N. B., Witte, D. R., et al. (2016). Insulin resistance is accompanied by increased fasting glucagon and delayed glucagon suppression in individuals with normal and impaired glucose regulation. *Diabetes* 65 (11), 3473–3481. doi:10.2337/db16-0240

Ferrannini, E., Gastaldelli, A., Miyazaki, Y., Matsuda, M., Mari, A., and DeFronzo, R. A. (2005). beta-Cell function in subjects spanning the range from normal glucose tolerance to overt diabetes: a new analysis. *J. Clin. Endocrinol. Metab.* 90 (1), 493–500. doi:10.1210/jc.2004-1133

Fiorentino, T. V., Suraci, E., Arcidiacono, G. P., Cimellaro, A., Mignogna, C., Presta, I., et al. (2017). Duodenal sodium/glucose cotransporter 1 expression under fasting conditions is associated with postload hyperglycemia. *J. Clin. Endocrinol. Metab.* 102 (11), 3979–3989. doi:10.1210/jc.2017-00348

Fridlyand, L. E., and Philipson, L. H. (2012). A computational systems analysis of factors regulating α cell glucagon secretion. *Islets* 4 (4), 262–283. doi:10.4161/isl.22193

Gastaldelli, A., Toschi, E., Pettiti, M., Frascerra, S., Quin, A., Sironi, A. M., et al. (2001). Effect of physiological hyperinsulinemia on gluconeogenesis in nondiabetic subjects and in type 2 diabetic patients. *Diabetes* 50 (8), 1807–1812. doi:10.2337/diabetes.50.8.1807

Gerich, J. E. (1993). Control of glycaemia. *Baillieres Clin. Endocrinol. Metab.* 7, 551–586. doi:10.1016/s0950-351x(05)80207-1

Gerich, J. E. (1988). Lilly lecture 1988. Glucose counterregulation and its impact on diabetes mellitus. *Diabetes* 37 (12), 1608–1617. doi:10.2337/diab.37.12.1608

Godoy-Matos, A. F. (2014). The role of glucagon on type 2 diabetes at a glance. *Diabetol. Metab. Syndr.* 6, 91. doi:10.1186/1758-5996-6-91

Grøndahl, M. F. G., Lund, A. B., Bagger, J. I., Petersen, T. S., Wewer Albrechtsen, N. J., Holst, J. J., et al. Glucagon clearance is preserved in type 2 diabetes. , . 2021; 71(1):73–82. doi:10.2337/db21-0024

Guiastrennec, B., Sonne, D. P., Hansen, M., Bagger, J. I., Lund, A., Rehfeld, J. F., et al. (2016). Mechanism-based modeling of gastric emptying rate and gallbladder emptying in response to caloric intake. *CPT. Pharmacometrics Syst. Pharmacol.* 5 (12), 692–700. doi:10.1002/psp4.12152

Ha, J., Satin, L. S., and Sherman, A. S. (2016). A mathematical model of the pathogenesis, prevention, and reversal of type 2 diabetes. *Endocrinology* 157 (2), 624–635. doi:10.1210/en.2015-1564

Hasdemir, D., Hoefsloot, H. C. J., and Smilde, A. K. (2015). Validation and selection of ODE based systems biology models: How to arrive at more reliable decisions. *BMC Syst. Biol.* 9 (1), 32–19. doi:10.1186/s12918-015-0180-0

Hershon, K. S., Hirsch, B. R., and Odugbesan, O. (2019). Importance of postprandial glucose in relation to A1C and cardiovascular disease. *Clin. Diabetes* 37 (3), 250–259. doi:10.2337/cd18-0040

Holst, J. J., Gribble, F., Horowitz, M., and Rayner, C. K. (2016). Roles of the gut in glucose homeostasis. *Diabetes Care* 39 (6), 884–892. doi:10.2337/dc16-0351

Horowitz, M., Edelbroek, M. A. L., Wishart, J. M., and Straathof, J. W. (1993). Relationship between oral glucose tolerance and gastric emptying in normal healthy subjects. *Diabetologia* 36 (9), 857–862. doi:10.1007/BF00400362

Kaplan, W., Sunehag, A. L., Dao, H., and Haymond, M. W. (2008). Short-term effects of recombinant human growth hormone and feeding on gluconeogenesis in humans. *Metabolism.* 57 (6), 725–732. doi:10.1016/j.metabol.2008.01.009

Keeler, J., de Paula, J., and Atkins, P. (2018). *Atkins' physical chemistry*. 11th ed., 1. Oxford University Press.

Keenan, D. M., Basu, R., Liu, Y., Basu, A., Bock, G., and Veldhuis, J. D. (2012). Logistic model of glucose-regulated C-peptide secretion: Hysteresis pathway disruption in impaired fasting glycemia. *Am. J. Physiol. Endocrinol. Metab.* 303 (3), E397–E409. doi:10.1152/ajpendo.00494.2011

Kelly, R. A., Fitches, M. J., Webb, S. D., Pop, S. R., Chidlow, S. J., Sotsky, M. J., et al. (2019). Modelling the effects of glucagon during glucose tolerance testing. *Theor. Biol. Med. Model.* 16 (1), 21–17. doi:10.1186/s12976-019-0115-3

Kim, J., Saidel, G. M., and Cabrera, M. E. (2007). Multi-scale computational model of fuel homeostasis during exercise: Effect of hormonal control. *Ann. Biomed. Eng.* 35 (1), 69–90. doi:10.1007/s10439-006-9201-x

Knop, F. K., Vilsbøll, T., Højberg, P. V., Larsen, S., Madsbad, S., Vølund, A., et al. (2007). Reduced incretin effect in type 2 diabetes. *Diabetes* 56, 1951–1959. doi:10.2337/db07-0100

Landgraf, R. (2004). The relationship of postprandial glucose to HbA1c. *Diabetes. Metab. Res. Rev.* 20 (2), S9–S12. doi:10.1002/dmrr.517

Lee, Y., Wang, M. Y., Du, X. Q., Charron, M. J., and Unger, R. H. (2011). Glucagon receptor knockout prevents insulin-deficient type 1 diabetes in mice. *Diabetes* 60 (2), 391–397. doi:10.2337/db10-0426

Lund, A., Bagger, J. I., Christensen, M., Knop, F. K., and Vilsbøll, T. (2014). Glucagon and type 2 diabetes: The return of the alpha cell. *Curr. Diab. Rep.* 14 (12), 555–557. doi:10.1007/s11892-014-0555-4

Man, C. D., Yarasheski, K. E., Caumo, A., Robertson, H., Toffolo, G., Polonsky, K. S., et al. (2005). Insulin sensitivity by oral glucose minimal models: Validation against clamp. *Am. J. Physiol. Endocrinol. Metab.* 289 (6), 954–959. doi:10.1152/ajpendo.00076.2005

MannWhitneyTest. Wolfram Research (2010). *Wolfram lang funct*.

Mari, A., Bagger, J. I., Ferrannini, E., Holst, J. J., Knop, F. K., and Vilsbøll, T. (2013). Mechanisms of the incretin effect in subjects with normal glucose tolerance and patients with type 2 diabetes. *PLoS One* 8 (9), e73154. doi:10.1371/journal.pone.0073154

Mari, A., Schmitz, O., Gastaldelli, A., Oestergaard, T., Nyholm, B., and Ferrannini, E. (2002). Meal and oral glucose tests for assessment of β-cell function: Modeling analysis in normal subjects. *Am. J. Physiol. Endocrinol. Metab.* 283 (6 46-6), 1159–1166. doi:10.1152/ajpendo.00093.2002

Mari, A., Tura, A., Gastaldelli, A., and Ferrannini, E. (2002). Assessing insulin secretion by modeling in multiple-meal tests: Role of potentiation. *Diabetes* 51 (L), S221–S226. doi:10.2337/diabetes.51.2007.s221

Matthews, D. R., Hosker, J. P., Rudenski, A. S., Naylor, B. A., Treacher, D. F., and Turner, R. C. (1985). Homeostasis model assessment: Insulin resistance and β-cell function from fasting plasma glucose and insulin concentrations in man. *Diabetologia* 28 (7), 412–419. doi:10.1007/BF00280883

Mitrakou, A., Kelley, D., Veneman, T., Jenssen, T., Pangburn, T., Reilly, J., et al. (1990). Contribution of abnormal muscle and liver glucose metabolism to postprandial hyperglycemia in NIDDM. *Diabetes* 39 (11), 1381–1390. doi:10.2337/diab.39.11.1381

Montanya, E. (2014). *Insulin resistance compensation: not just a matter of β-cells?*, 63. Diabetes, 832–834.

Moon, J. S., and Won, K. C. (2015). Pancreatic α-cell dysfunction in type 2 diabetes: Old kids on the block 39(1):1. 9. doi:10.4093/dmj.2015.39.1.1

Morettini, M., Burattini, L., Göbl, C., Pacini, G., Ahrén, B., and Tura, A. (2021). Mathematical model of glucagon kinetics for the assessment of insulin-mediated glucagon inhibition during an oral glucose tolerance test. *Front. Endocrinol.* 12, 611147. doi:10.3389/fendo.2021.611147

Nauck, M., Stöckmann, F., Ebert, R., and Creutzfeldt, W. (1986). Reduced incretin effect in Type 2 (non-insulin-dependent) diabetes. *Diabetologia* 29 (1), 46–52. doi:10.1007/BF02427280

Nauck, M. A., and Meier, J. J. (2016). The incretin effect in healthy individuals and those with type 2 diabetes: Physiology, pathophysiology, and response to therapeutic interventions. *Lancet. Diabetes Endocrinol.* 4 (6), 525–536. doi:10.1016/S2213-8587(15)00482-9

Palumbo, P., Ditlevsen, S., Bertuzzi, A., and Gaetano, A. De (2013). Mathematical modeling of the glucose – insulin system : A review. *Math. Biosci.* 244 (2), 69–81. doi:10.1016/j.mbs.2013.05.006

Panunzi, S., Palumbo, P., and De Gaetano, A. (2007). A discrete single delay model for the intra-venous glucose tolerance test. *Theor. Biol. Med. Model.* 4, 35–16. doi:10.1186/1742-4682-4-35

Parekh, S., Bodicoat, D. H., Brady, E., Webb, D., Mani, H., MoStafa, S., et al. (2014). Clinical characteristics of people experiencing biochemical hypoglycaemia during an oral glucose tolerance test : Cross-sectional analyses from a UK multi-ethnic population. *Diabetes Res. Clin. Pract.* 104 (3), 427–434. doi:10.1016/j.diabres.2014.02.013

Piccinini, F., and Bergman, R. N. (2020). The measurement of insulin clearance. *Diabetes Care* 43 (9), 2296–2302. doi:10.2337/dc20-0750

Portet, S. (2020). A primer on model selection using the Akaike Information Criterion. *Infect. Dis. Model.* 5, 111–128. doi:10.1016/j.idm.2019.12.010

Röder, P. V., Wu, B., Liu, Y., and Han, W. (2016). Pancreatic regulation of glucose homeostasis. *Exp. Mol. Med.* 48 (3), e219.

Røge, R. M., Bagger, J. I., Alskär, O., Kristensen, N. R., Klim, S., Holst, J. J., et al. (2017). Mathematical modelling of glucose-dependent insulinotropic polypeptide and glucagon-like peptide-1 following ingestion of glucose. *Basic Clin. Pharmacol. Toxicol.* 121 (4), 290–297. doi:10.1111/bcpt.12792

Saha, B. (2006). Post prandial plasma glucose level less than the fasting level in otherwise healthy individuals during routine screening. *Indian J. Clin. biochem.* 21 (2), 67–71. doi:10.1007/BF02912915

Santoleri, D., and Titchenell, P. M. (2019). Resolving the paradox of hepatic insulin resistance. *Cell. Mol. Gastroenterol. Hepatol.* 7 (2), 447–456. doi:10.1016/j.jcmgh.2018.10.016

Sulston, K. W., Ireland, W. P., and Praught, J. C. (2006). Hormonal effects on glucose regulation. *Atlantic* 1 (1), 31–46.

Suzuki, K., Katsura, D., Sagara, M., Aoki, C., Nishida, M., and Aso, Y. (2016). Postprandial reactive hypoglycemia treated with a low-dose alpha-glucosidase inhibitor : Voglibose may suppress oxidative stress and prevent endothelial dysfunction. *Int. Med.* 55 (8), 949–953. doi:10.2169/internalmedicine.55.5737

Tian, G., Sandler, S., Gylfe, E., and Tengholm, A (2011). Glucose- and hormone-induced cAMP oscillations in α- and β-cells within intact pancreatic islets. *Diabetes* 60 (5), 1535–1543. doi:10.2337/db10-1087

Titchenell, P. M., Quinn, W. J., Lu, M., Chu, Q., Lu, W., Li, C., et al. (2016). Direct hepatocyte insulin signaling is required for lipogenesis but is dispensable for the suppression of glucose production. *Cell. Metab.* 23 (6), 1154–1166. doi:10.1016/j.cmet.2016.04.022

Topp, B., Promislow, K., Devries, G., Miura, R. M., and Finegood, D. T. (2000). A model of β-cell mass, insulin, and glucose kinetics: Pathways to diabetes. *J. Theor. Biol.* 206 (4), 605–619. doi:10.1006/jtbi.2000.2150

Topp, B. G., Atkinson, L. L., and Finegood, D. T. (2007). Dynamics of insulin sensitivity , Beta-cell function , and Beta-cell mass during the development of diabetes in fa/fa rats. *Am. J. Physiol. Endocrinol. Metab.* 293, E1730–E1735. doi:10.1152/ajpendo.00572.2007

Tura, A., Bagger, J. I., Ferrannini, E., Holst, J. J., Knop, F. K., Vilsbøll, T., et al. (2017). Impaired beta cell sensitivity to incretins in type 2 diabetes is insufficiently compensated by higher incretin response. *Nutr. Metab. Cardiovasc. Dis.* 27 (12), 1123–1129. doi:10.1016/j.numecd.2017.10.006

Unger, R. H., Aguilar-Parada, E., Müller, W. A., and Eisentraut, A. M. (1970). Studies of pancreatic alpha cell function in normal and diabetic subjects. *J. Clin. Investig.* 49 (4), 837–848. doi:10.1172/JCI106297

Unger, R. H., and Orci, L. (1975). The essential role of glucagon in the pathogenesis of diabetes mellitus. *Lancet* 84, 14–16. doi:10.1016/s0140-6736(75)92375-2

Utzschneider, K. M., Younes, N., Rasouli, N., Barzilay, J. I., Banerji, M. A., Cohen, R. M., et al. (2021). Shape of the OGTT glucose response curve: Relationship with β-cell function and differences by sex, race, and BMI in adults with early type 2 diabetes treated with metformin. *BMJ Open Diabetes Res. Care* 9 (1), e002264. doi:10.1136/bmjdrc-2021-002264

Villaverde, A. F., Barreiro, A., and Papachristodoulou, A. (2016). Structural identifiability of dynamic systems biology models. *PLoS Comput. Biol.* 12 (10), e1005153–22. doi:10.1371/journal.pcbi.1005153

Villaverde, A. F., Evans, N. D., Chappell, M. J., and Banga, J. R. (2019). Input-dependent structural identifiability of nonlinear systems. *IEEE Control Syst. Lett.* 3 (2), 272–277. doi:10.1109/lcsys.2018.2868608

Walker, J. N., Ramracheya, R., Zhang, Q., Johnson, P. R. V., Braun, M., and Rorsman, P. (2011). Regulation of glucagon secretion by glucose: Paracrine. *Diabetes Obes. Metab.* 13, 95–105. doi:10.1111/j.1463-1326.2011.01450.x

Wang, G. (2014). Raison d'être of insulin resistance: The adjustable threshold hypothesis. *J. R. Soc. Interface* 11 (101), 20140892. doi:10.1098/rsif.2014.0892

Watts, M., Ha, J., Kimchi, O., and Sherman, A. (2016). Paracrine regulation of glucagon secretion: The β/α/δ model. *Am. J. Physiol. Endocrinol. Metab.* 310 (8), E597-E611–E611. doi:10.1152/ajpendo.00415.2015

Watts, M., and Sherman, A. (2014). Modeling the pancreatic α-cell: Dual mechanisms of glucose suppression of glucagon secretion. *Biophys. J.* 106 (3), 741–751. doi:10.1016/j.bpj.2013.11.4504

Wolfram Research, Inc. (2019). *Mathematica, Version 12.0*. Champaign, IL.

Yu, Q., Shuai, H., Ahooghalandari, P., Gylfe, E., and Tengholm, A. (2019). *Glucose controls glucagon secretion by directly modulating cAMP in alpha cells*, 1212–24.

Zmazek, J., Grubelnik, V., Markovič, R., and Marhl, M. (2021). Role of cAMP in double switch of glucagon secretion. *Cells* 10 (4), 896. doi:10.3390/cells10040896

frontiers | Frontiers in Physiology

TYPE Original Research
PUBLISHED 28 November 2022
DOI 10.3389/fphys.2022.923704

OPEN ACCESS

EDITED BY
Cecilia Diniz Behn,
Colorado School of Mines, United States

REVIEWED BY
Justin R. Ryder,
University of Minnesota Twin Cities, United States
Rongjing Ding,
Peking University, China
Sushant Singh,
Amity University, Raipur, India

*CORRESPONDENCE
George Hripcsak,
hripcsak@columbia.edu

SPECIALTY SECTION
This article was submitted to Metabolic Physiology, a section of the journal Frontiers in Physiology

RECEIVED 19 April 2022
ACCEPTED 11 October 2022
PUBLISHED 28 November 2022

CITATION
Richter LR, Albert BI, Zhang L, Ostropolets A, Zitsman JL, Fennoy I, Albers DJ and Hripcsak G (2022), Data assimilation on mechanistic models of glucose metabolism predicts glycemic states in adolescents following bariatric surgery.
Front. Physiol. 13:923704.
doi: 10.3389/fphys.2022.923704

Data assimilation on mechanistic models of glucose metabolism predicts glycemic states in adolescents following bariatric surgery

Lauren R. Richter[1], Benjamin I. Albert[1], Linying Zhang[1], Anna Ostropolets[1], Jeffrey L. Zitsman[2], Ilene Fennoy[3], David J. Albers[1,4,5] and George Hripcsak[1]*

[1]Department of Biomedical Informatics, Columbia University Irving Medical Center, New York, NY, United States, [2]Division of Pediatric Surgery, Department of Surgery, Columbia University Irving Medical Center, New York, NY, United States, [3]Division of Pediatric Endocrinology, Metabolism, and Diabetes, Department of Pediatrics, Columbia University Irving Medical Center, New York, NY, United States, [4]Department of Bioengineering, University of Colorado Anschutz Medical Campus, Aurora, CO, United States, [5]Department of Biomedical Informatics, University of Colorado Anschutz Medical Campus, Aurora, CO, United States

Type 2 diabetes mellitus is a complex and under-treated disorder closely intertwined with obesity. Adolescents with severe obesity and type 2 diabetes have a more aggressive disease compared to adults, with a rapid decline in pancreatic β cell function and increased incidence of comorbidities. Given the relative paucity of pharmacotherapies, bariatric surgery has become increasingly used as a therapeutic option. However, subsets of this population have sub-optimal outcomes with either inadequate weight loss or little improvement in disease. Predicting which patients will benefit from surgery is a difficult task and detailed physiological characteristics of patients who do not respond to treatment are generally unknown. Identifying physiological predictors of surgical response therefore has the potential to reveal both novel phenotypes of disease as well as therapeutic targets. We leverage data assimilation paired with mechanistic models of glucose metabolism to estimate pre-operative physiological states of bariatric surgery patients, thereby identifying latent phenotypes of impaired glucose metabolism. Specifically, maximal insulin secretion capacity, σ, and insulin sensitivity, S_I, differentiate aberrations in glucose metabolism underlying an individual's disease. Using multivariable logistic regression, we combine clinical data with data assimilation to predict post-operative glycemic outcomes at 12 months. Models using data assimilation sans insulin had comparable performance to models using oral glucose tolerance test glucose and insulin. Our best performing models used data assimilation and had an area under the receiver operating characteristic curve of 0.77 (95% confidence interval 0.7665, 0.7734) and mean average precision of 0.6258 (0.6206, 0.6311). We show that data assimilation extracts knowledge from mechanistic models of glucose metabolism to infer future glycemic states from limited clinical data. This method can provide a pathway to predict long-term, post-surgical glycemic states by estimating the

contributions of insulin resistance and limitations of insulin secretion to pre-operative glucose metabolism.

KEYWORDS

type 2 diabetes, data assimilation, mechanistic models of glucose metabolism, pediatrics, bariatric surgery, machine learning, obesity

1 Introduction

As obesity rates rise in the United States, so too does the prevalence of type 2 diabetes mellitus (T2DM) in children and adolescents (Skelton et al., 2009; Hales et al., 2017h). While a number of pharmacotherapies exist to treat T2DM, there are few options approved for use in younger patients, who typically have more aggressive disease (TODAY Study Group, 2021; American Diabetes Association Professional Practice Committee, 2022). As such, bariatric surgery is increasingly used as a treatment for severe obesity and prevention or reversal of T2DM, despite risk of operative complications (Hsia et al., 2012; Aung et al., 2016; Beamish and Reinehr, 2017; Inge et al., 2018a; Armstrong et al., 2019; Bolling et al., 2019; Karasko, 2019; Khattab and Sperling, 2019; American Diabetes Association Professional Practice Committee Draznin et al., 2022). Many patients benefit with significant, sustained weight loss, improvement in quality of life, and improvement of obesity-related comorbidities (Inge et al., 2016; Rubino et al., 2016; Beamish and Reinehr, 2017; Pedroso et al., 2018; Inge et al., 2019). However, an ill-defined subset of this population have sub-optimal outcomes (Montero et al., 2011; Livhits et al., 2012; Toh et al., 2017; Inge et al., 2018a; Inge et al., 2018b). Predicting which patients are most likely to benefit from surgery and how they will benefit is a current challenge aimed to minimize unnecessary risk during a critical period of growth and development.

The prevalence of impaired glucose metabolism (IGM)—here referring to a heterogenous population with impaired glucose tolerance (IGT), impaired fasting glucose (IFG), prediabetes (preDM), or T2DM— is increasing in pediatric populations, and may be underestimated (Sinha et al., 2002; Lee et al., 2006; Nowicka et al., 2011; Buse et al., 2013; Dabelea et al., 2014). IGM is progressive and often goes undiagnosed until later in disease history. It is associated with insulin resistance (IR), the need for more insulin to achieve physiologic effects, i.e., peripheral glucose uptake and suppression of hepatic glucose production (HGP). In the obese state, IR is almost guaranteed as it is directly related to visceral adiposity (Kahn and Flier, 2000), but the extent to which the pancreas can compensate exists on a spectrum. Insulin sensitivity (S_I) is a measure of the effectiveness of insulin in promoting glucose uptake. It is reciprocally related to insulin resistance. In this context, T2DM is an example extreme IGM, with significant IR coupled with β cell dysfunction and resultant hyperglycemia (Prentki and Nolan, 2006; American Diabetes Association Professional Practice Committee, 2022). The extent to which function can be rescued after progression to T2DM is modifiable to some degree (Lim et al., 2011; Pajvani and Accili, 2015; Taylor et al., 2019; Richter et al., 2020; Holst and Madsbad, 2021; Bartolomé et al., 2022). Duration of disease negatively impacts the probability of resolution, and lifestyle interventions resulting in weight loss during the early prediabetic phase are more likely to prevent progression (Knowler et al., 2002).

Reversal of preDM and prevention of T2DM are therefore considered to be one of the major benefits of bariatric surgery in this age group for which there are limited other options (Aung et al., 2016; Armstrong et al., 2019; Bolling et al., 2019; Khattab and Sperling, 2019; American Diabetes Association Professional Practice Committee Draznin et al., 2022). Indeed, when compared to pharmacologic or lifestyle interventions, bariatric surgery is overall the most successful intervention with respect to glycemic improvements and sustained weight loss (Schauer et al., 2012; Courcoulas et al., 2014; Mingrone et al., 2015). The specific surgery has clear impact on outcomes. The three most prevalent bariatric surgeries in the U.S. are adjustable gastric banding (AGB), Roux-en-Y gastric bypass (RYGB), and vertical sleeve gastrectomy (VSG). In AGB, an inflatable band is placed around the upper part of the stomach creating a small pouch. In RYGB, the jejunum is directly connected to a remnant small pouch of stomach, thereby bypassing the majority of the stomach and the duodenum. In VSG, the majority of the stomach is removed along the greater curvature, creating a narrow tube or sleeve. While AGB is thought to act through purely restrictive mechanisms, VSG and RYGB restrict food intake and increase malabsorption, alter secretion of gut hormones related to satiety and insulin secretion, e.g., glucagon-like peptide-1 (GLP-1) and ghrelin, and change bile acid composition through the change in macronutrients present in areas of the small intestine (Seeley et al., 2015; Mulla et al., 2018; Akalestou et al., 2022). These differing effects can have profound impact on insulin resistance in particular, and the success of VSG and RYGB in comparison to AGB has led to their increased usage (Mulla et al., 2018). Depending on how remission is defined, meta-analyses have shown that 20–80% of adults will have some degree of improvement in T2DM at medium-to-long term follow up (Yip et al., 2013; Elbahrawy et al., 2018; Tsilingiris et al., 2019; Purnell et al., 2021),

although there is suggestion of continued impaired β cell function and overestimation of success (Ramos-Levi et al., 2013a; Laferrère and Pattou, 2018). Smaller prospective studies focusing on adolescents suggest T2DM remission may occur in up to 80–90% of patients and improvement of preDM may occur in 70–80% of patients following Roux-en-Y gastric bypass (RYGB), the most drastic surgery that is recommended for adolescents with respect to metabolic intervention and risk of complications (Inge et al., 2014; Inge et al., 2017; Olbers et al., 2017; Stefater and Inge, 2017). However, small sample sizes and relatively homogenous populations (> 70% non-Hispanic white) limit generalizability of results. Predicting which patients are likely to have remission or partial remission of IGM as a result of surgery and thus not develop T2DM remains a challenging task (Ramos-Levi et al., 2013b; Wang et al., 2015; Tsilingiris et al., 2019).

Given the complexity of medical decision making in adolescent bariatric surgery, accurately assessing benefits vs. risks for an individual is critical for patients and their care teams. Glucose dysregulation and obesity can compound existing surgical risks and increase the chance of complications. Although adolescents have lower complication rates compared to their adult counterparts, they may still experience wound infections, anastomotic strictures, leaks, wound dehiscence, abdominal hernias, dehydration, and venous thromboembolism (Lamoshi et al., 2020). In patients with diabetes, poor wound healing and risk of infection are serious considerations and can directly impact the success of the surgery and need for revision (Keidar, 2011). In the long term, patients also have significant malabsorption post-bariatric surgery, resulting in multiple vitamin and mineral deficiencies requiring lifelong supplementation (Bal et al., 2012; Lamoshi et al., 2020). The consequences of this decreased nutrition can be great in adolescents who are still undergoing their growth spurts and accruing bone during their pubertal years (Lamoshi et al., 2020; Weiner et al., 2020; Ou et al., 2022). Although advancements have been made to minimize risk of post-operative complications, improve wound healing, and optimize post-operative nutrition, bariatric surgery remains an aggressive measure taken to improve a patient's health (Crossan and Sheer, 2022; Dewberry et al., 2022). Therefore, providing accurate information about a patient's current diabetic state the probability of improvement with surgery can allow for more informed decision making.

Previous studies using statistical or traditional machine learning techniques to predict T2DM outcomes have generally focused on relatively homogenous adult populations who underwent RYGB, with or without genetic information included in analysis. Because available data are sparse, these approaches are subject to error and are not often validated in pediatric populations (Aminian et al., 2017; Cao et al., 2020; Kam et al., 2020). Varying definitions of what successful glycemic outcomes mean also complicate prediction (Buse et al., 2009; Holst and Madsbad, 2021). Outside of surgery type, other potential predictors include anthropometrics (weight, height, body mass index [BMI]), pre-operative disease severity, use of anti-diabetic medications, and presence of comorbidities (DeMaria et al., 2007; Livhits et al., 2012; Dixon et al., 2013; Robert et al., 2013; Panunzi et al., 2015; Wang et al., 2015; Shen et al., 2019). Associations are also seen with baseline biomarkers such as fasting glucose, insulin, C-peptide, triglycerides (TG), C-reactive protein (CRP), and hemoglobin A1c (HbA1c) levels (Ortega et al., 2012; Courcoulas et al., 2013; Inge et al., 2014; Pedersen et al., 2016; Yan et al., 2017). These features, particularly pre-operative disease severity (as measured by duration of disease, labs, and medications) are more homogenous in adolescents, who frequently have preDM rather than T2DM, and are therefore on fewer medications, if any. Additionally, adolescents tend to have lower HbA1c values at baseline prior to undergoing bariatric surgery compared to their adult counterparts. As such, features that are useful predictors in adult surgical response are not necessarily translatable to adolescents.

To provide more personalized predictions, Pedersen, et al. incorporated genetic and clinical information in an artificial neural network to accurately predict short-term discontinuation of diabetes medications at 30 days (Pedersen et al., 2016). The majority of candidate genetic markers were associated with insulin secretion, glucose clearance, or insulin sensitization. While genetics certainly play a role in T2DM, pre-operative genetic analyses are not currently practical for every patient (Hatoum et al., 2011; Okser et al., 2013; Rouskas et al., 2014).

These prior studies provide evidence that an individual's underlying physiology has long-term implications for treatment outcomes, but existing methods to approximate these physiological pathways may not be practical for use in adolescents (Lee, 2007; Brown and Yanovski, 2014). Glucose tolerance and insulin resistance are frequently estimated using point or dynamic lab proxies due to the expensive and invasive nature of the gold standard for measurement, the hyperinsulinemic-euglycemic clamp (Muniyappa et al., 2018). Oral glucose tolerance tests (OGTTs) are one such approximation used to screen for and diagnose dysglycemia (Olson et al., 2010; Muniyappa et al., 2018; American Diabetes Association Professional Practice Committee, 2022). After fasting (usually overnight), patients are given a fixed dose of liquid glucose (typically 75 g) after which glucose levels are measured at timed intervals. OGTTs can vary in the types of labs drawn, the frequency of sampling, and the duration of the procedure (Muniyappa et al., 2018). In common clinical practice, glucose is measured over two or three hours. Measurements of insulin and C-peptide are not the standard of care; their assays are

relatively costly and lack of standardization makes their interpretation less straightforward (Manley et al., 2007; Little et al., 2008; Miller et al., 2009; Tohidi et al., 2017). As such, these labs are typically only collected in research settings.

Fasting insulin and glucose measurements can be used to calculate indices such as the homeostatic model assessment of insulin resistance (HOMA-IR), which can approximate parameters such as peripheral and hepatic insulin sensitivity $hepa_{S_I}$ as would be assessed in clamp studies or frequently sampled intravenous GTTs (FSIVGTT), a silver standard (Matthews et al., 1985; Bergman et al., 1987; Yeckel et al., 2004). Interpretation of these indices can vary by patient characteristics (e.g., age, sex, ethnicity, body habitus) (Wallace et al., 2004; Gunczler and Lanes, 2006; Nathan et al., 2007; Shaibi et al., 2011; Gutch et al., 2015; Arslanian et al., 2019; Tagi et al., 2019; Kim et al., 2020). In particular, HOMA-IR may not be sensitive to improvements in insulin sensitivity in adolescents (Shaibi et al., 2011; Bryant et al., 2014).

Several mechanistic models of glucose and insulin metabolism have been empirically developed and validated against clamp or FSIVGTT studies to mathematically describe glucose metabolism. Models such as the meal model (Dalla Man et al., 2007), oral minimal model (Cobelli et al., 2014), and ultradian model (Sturis et al., 1991) incorporate insulin secretion rates and glucose elimination to estimate states over varying timescales. Topp et al. developed a mechanistic model that incorporates more granular β cell dynamics, which was extended by Ha et al. to model the development of type 2 diabetes over time and quantify the extent to which different insults in the system contribute to disease (Topp et al., 2000; Ha et al., 2016; Ha and Sherman, 2020). Represented as a system of ordinary differential equations (ODEs), these models have the potential to allow for patient-level characterization of glucose metabolism.

Extracting clinical knowledge from these models is not straightforward, as both the models themselves and their results are often viewed as too abstract for application in clinical practice. However, within these mechanistic models are clinically meaningful physiologic parameters when applied to the appropriate problems, e.g. assessing insulin sensitivity's relationship with lipoprotein metabolism (Chung et al., 2022). Furthermore, while clamp studies represent a patient's physiologic state and glucose excursions at a specific point in time, mechanistic models have the potential to elucidate more long-term physiologic states that are difficult to capture clinically.

Knowledge within mechanistic models of glucose metabolism can be exploited via data assimilation, a family of methods frequently used in meteorology and aerospace science (Evensen, 2009; Law et al., 2015). Data assimilation leverages the underlying information about the system contained in these mechanistic models to update current and past states using filtering and smoothing, updates that in turn provide the ability to forecast future states by running the estimated model forward in time. Various filters exist that allow for parameterization and propagation of state uncertainty for non-linear systems such as glucose homeostasis (Kalman, 1960; Wan et al., 2001; Julier and Uhlmann, 2004). In previous work, we used the ultradian and meal models with an unscented Kalman filter (UKF), a sequential method that propagates uncertainty in non-linear systems, as well as deterministic and stochastic optimization methods using techniques such as Markov chain Monte Carlo (MCMC) to estimate both states and parameters, generating a real-time, personalized forecast from free-living data (Albers et al., 2017; Levine et al., 2017). In the free-living data context where data are sparse, we developed a constrained (Albers et al., 2019) version of the ensemble Kalman filter (EnKF) method (Evensen, 2009) that made state and parameter estimates more robust. We also successfully applied these methods to real-time glucose forecasting in the setting of T2DM with OGTT data (Mulgrave et al., 2020). Whereas in the free-living case the focus was accurate glucose state determination, the OGTT case focused more on parameter estimates as a marker for underlying disease.

Here, we take this prior work to further demonstrate the validity of using physiologic parameters inferred from mechanistic models of glucose metabolism to predict impaired glucose metabolism (IGM) in adolescents at 12-months post-bariatric surgery as compared to other clinical information. We use data assimilation to estimate parameters from an extension of the model initially proposed by Topp et al. incorporating β cell mass (Ha and Sherman, 2020), partially represented in Figure 1. We then train logistic regression models leveraging these parameter estimates derived from data assimilation on a cohort of adolescents who underwent vertical sleeve gastrectomy (VSG) or laparascopic adjustable gastric banding (AGB) at our institution between 2006 and 2020.

2 Materials and methods

2.1 Extraction of clinical data

Data were collected retrospectively from Columbia University Irving Medical Center (CUIMC) from adolescent patients aged 10–21 who had bariatric surgery between 2006 and 2020. Records were first selected based on the presence of bariatric surgery procedure codes with a diagnosis of obesity on the same day (n = 396), a 120-minute OGTT measuring glucose and insulin (at 0, 30, 60, and 120 min) within one year prior to surgery (n = 202), a pre-operative HbA1c within 120 days of the OGTT (n = 202), and at least one post-operative outcome documented within 6–18 months post-surgery (n = 176). These patients were seen through the Center for Adolescent Bariatric Surgery (CABS) at CUIMC. Patients with diganosis codes associated with type 1, cystic fibrosis-related, or

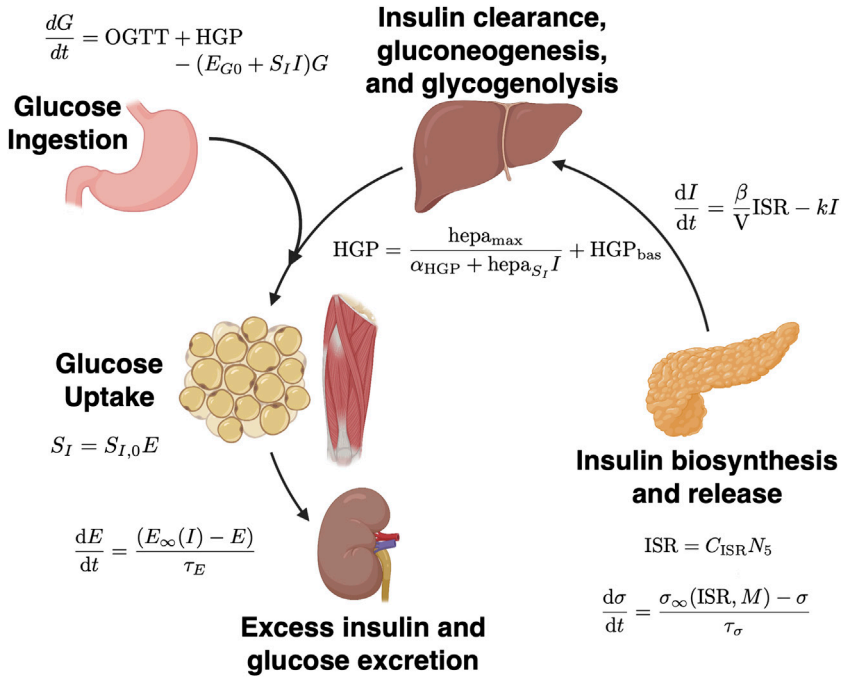

FIGURE 1
Schematic of mechanistic models of glucose metabolism. Underlying physiologic processes are represented by a series of ordinary differential equations (ODEs). Solutions lie on discrete spaces based on patient physiology at the time of measurements. In data assimilation, after reverse parameter estimation at discrete time points (i.e., insulin secretion capacity, σ, and insulin sensitivity, S_I), the system state is updated and the ODEs are solved again. Figure adapted from Tokarz et al. (Tokarz et al., 2018) and created with BioRender.com. Relevant equations are outlined in Methods and in Ha and Sherman 2020 (Ha and Sherman, 2020).

gestational diabetes mellitus were excluded. Features as outlined above were extracted for patients who met criteria.

2.2 Data pre-processing and manual feature selection

In addition to features necessary to include patients (OGTT glucose and insulin measurements and HbA1c), additional laboratory variables were selected *a priori*. These labs were pre-operative thyroid stimulating hormone (TSH), thyroxine (T4), free T4 (FT4), triiodothyronine (T3), aspartate transaminase (AST), alanine transaminase (ALT), total cholesterol (TC), high-density lipoprotein (HDL), low-density lipoprotein (LDL), triglycerides (TG), and C-peptide. Age was used as a continuous variable. Categorical features included surgery type, demographic data (self-reported race, ethnicity, and sex), and pre-operative presence of specific comorbidities associated with insulin resistance and T2DM: liver disease (including non-alcoholic steatohepatitis [NASH] and non-alcoholic fatty liver disease [NAFLD]), polycystic ovary syndrome (PCOS), dyslipidemia, hypertension (HTN), obstructive sleep apnea (OSA), thyroid disease, metabolic syndrome (MetS), T2DM (by diagnosis code), and abnormal glucose metabolism (by diagnosis code). To be coded as having the comorbidity of interest without manual chart review, at least 25% of all encounters within the appropriate time window had to contain a related diagnosis code (5 years pre-operative; 6–18 months post-operative) (Perotte and Hripcsak, 2013). Features missing in more than 25% of the sample were removed from analysis. The closest labs obtained prior to surgery and the pre-operative OGTT were included as features if there were multiple lab results within the appropriate time window. HOMA-IR was calculated using mass units (Matthews et al., 1985) as follows in Eq. 1:

$$\text{IR}_{\text{HOMA}} = \frac{G_0 \times I_0}{405} \quad (1)$$

where G_0 is fasting glucose in mg/dL and I_0 is fasting insulin in μIU/mL.

For continuous variables, outliers were defined as those values outside 1.5× the interquartile range (IQR). However, after manual chart review, none of the outliers were removed as none were found to be spurious measurements.

TABLE 1 Outcome definitions for classification as having impaired glucose metabolism (IGM) or normal glucose metabolism (NGM) at 12 months post-bariatric surgery.

	Normal glucose metabolism (NGM)	Impaired glucose metabolism (IGM)	
		Prediabetes	Type 2 diabetes mellitus
HbA1c (%)	< 5.7	5.7–6.4	≥ 6.5
G_0 (mg/dL)	< 100	100–125	≥ 126
G_{120} (mg/dL)	< 140	140–199	≥ 200
Anti-diabetic medications	None	Metformin or GLP-1a	All other drug classes
Diagnosis codes in encounters within 6–18 months post-op	None or < 25%	Abnormal Glucose in ≥ 25% of encounters	T2DM in ≥ 25% of encounters

G, glucose; GLP-1a, Glucagon-Like Peptide-1 agonist; OGTT, oral glucose tolerance test; OSA, obstructive sleep apnea; T2DM, type 2 diabetes mellitus.

Due to non-normal distributions of the majority of continuous variables, numeric features were scaled and standardized using power transformation with the Box-Cox method (Box and Cox, 1964) prior to hyperparameter tuning. Missing values (n = 7, all thyroid function tests) were imputed using iterative imputation using five nearest features with sampling from the prior distribution (Buck, 1960; Buuren and Groothuis-Oudshoorn, 2011; Pedregosa et al., 2011).

In total, we used 21 continuous clinical variables, 23 categorical variables (three multinomial, 11 binary), and six continuous parameter estimates from data assimilation (mean and standard deviations of maximal insulin secretion capacity [σ], insulin sensitivity [S_I], and their product [σ^*S_I] for an individual's estimated distributions). Models including HOMA-IR as a feature did not include data assimilation estimates. After data pre-processing, a total of 49 features were included in the most comprehensive model.

2.3 Outcome labelling

Patient post-operative outcome classification was coded as a binary variable indicating the presence or absence of impaired glucose metabolism (IGM) at 12 months. To be classified as having IGM, patients could have any one of the following criteria occur in the 6–18-month post-operative window: ≥ 2 elevated HbA1c values, post-operative OGTT G_0 ≥ 100 mg/dL, post-operative OGTT G_{120} ≥ 140 mg/dL, anti-diabetic drug use (including metformin), or presence of diagnosis codes for T2DM or abnormal glucose metabolism in ≥ 25% of encounters in the post-op window (American Diabetes Association Professional Practice Committee, 2022). If multiple specimens for the same lab were collected within the 6-18-month window, the latest labs were used. Outcome definitions are shown in Table 1.

2.4 Predictive model training and evaluation

Regularized logistic regression models were trained to predict impaired glucose metabolism (IGM) as a binary outcome on varied subsets of the features as input. The data were first split into 70–30 train-test sets. Hyperparameters were tuned on the train set with stratified nested k-fold cross-validation. Tuned hyperparameters included regularization method ($L2$ vs. $L1$), regularization constant ($\lambda = \alpha^*n$), learning rate [$f(\alpha)$], and max iterations. The loss function was binary cross-entropy loss with balanced class weight. The optimizer was stochastic gradient descent with an adaptive learning rate. To ensure model robustness to random data splitting, we performed 30 independent train-test splits and the results were averaged. The hyperparameters associated with the minimum loss in training were selected for model evaluation.

Because our dataset was imbalanced with respect to outcomes, we chose class weights in the logistic regression models that were inversely proportional to the class frequency. To evaluate the performance of the prediction models, we computed area under the Receiver Operating Characteristic curve (AUROC), precision, recall, and average precision (AP) on out-of-bag estimates from 1,000 bootstrapped samples (n = 176). Average precision refers to the weighted mean of precision with respect to recall at all probability thresholds for classification and focuses on how well the models predict the positive class (in our case, post-operative IGM). It is analogous to the area under the precision-recall curve (AUPRC) and better suited for imbalanced datasets compared to accuracy. Baseline performance of a naïve classifier would have an AUPRC equal to the proportion of the positive class in the data (here, 0.318).

2.5 Mechanistic glucose metabolism modeling

Relevant equations used in our study are briefly outlined below, with a full description of the model available in the supplemental materials of Ha and Sherman 2020 (Ha and Sherman, 2020; Sherman, 2022).

Eq. 2 describes change in glucose over time as a function of the glucose flux during the OGTT (OGTT), hepatic glucose production (HGP), insulin sensitivity (S_I), the insulin-independent effectiveness of glucose (E_{G0}), current glucose (G), and insulin (I). It is given as:

$$\frac{dG}{dt} = \text{OGTT} + \text{HGP} - (E_{G0} + S_I I)G \tag{2}$$

where HGP is a decreasing function of I and hepatic insulin sensitivity (hepa_{S_I}) and E_{G0} represents insulin-independent glucose uptake by peripheral tissues, here fixed at 0.0118 min^{-1}.

Eqs. 3, 4 describe change in insulin over time as a function of β cell mass (β), volume of distribution (V), insulin secretion rate (ISR), and insulin (I). ISR is a function of calcium ion concentration in the β cell cytosol (C_{ISR}) and the number of primed insulin vesicles at the β cell membrane (N_5). They are given as:

$$\frac{dI}{dt} = \frac{\beta}{V}\text{ISR} - kI \tag{3}$$

$$\text{ISR} = C_{\text{ISR}} N_5 \tag{4}$$

where k is a rate constant of insulin clearance. The precise form of C_{ISR} as a function of glucose (G) and ATP-dependent potassium ion channel (K^+-ATP) density (γ) can be determined by expanding the equations derived from a slight modification of the steady state of the previously published exocytosis model (Chen et al., 2008).

Eq. 5 shows the change in γ, the density of the β cell membrane ATP-dependent potassium ion channel (K^+-ATP), as an increasing function of glucose (G) on a scale of hours to days. This describes the shift in glucose-dependent insulin secretion in the setting of chronic hyperglycemia, where increases in channel density lead to decreases in insulin secretion. Because of the short time scale of the OGTT, γ was fixed at −0.076 as in prior work (Sherman, 2022) and this equation was not explicitly solved in our methods. It is provided here for clarity on how chronic hyperglycemia affects β cell structure and is given as:

$$\frac{d\gamma}{dt} = \frac{\gamma_\infty(G) - \gamma}{\tau_\gamma} \tag{5}$$

where $\gamma_\infty(G)$ is an increasing sigmoidal function of glucose and τ_γ is a time constant.

From the insulin exocytosis model, Eqs. 6, 7 describe the change in the number of vesicles in the β cell granule-membrane complex during docking and priming (N_6 and N_5, respectively) as functions of K^+-ATP channel density (γ), glucose (G), maximal insulin secretion capacity (σ), and the baseline insulin vesicle priming rate, r_2^0 (Chen et al., 2008). These equations are given as:

$$\frac{dN_5}{dt} = C_{5,5}N_5 + C_{5,6}N_6 \tag{6}$$

$$\frac{dN_6}{dt} = C_{6,0} + C_{6,5}N_5 + C_{6,6}N_6 \tag{7}$$

where $C_{i,j}$ represents the cytosol calcium ion concentration at a given state in exocytosis: $C_{5,5}$ is a function of G and γ; $C_{5,6}$ and $C_{6,6}$ are functions of G, γ, and r_2^0; $C_{6,0}$ is a function of G, γ, and σ, and; $C_{6,5}$ is a constant.

Eq. 8 describes the change in the maximal insulin secretion capacity, σ, to compensate for chronic hyperglycemia on a scale of hours to days. It is a unitless scale factor. During the OGTT, σ is assumed to be at steady state. σ is a function of insulin secretion rate (ISR) and β cell metabolism (M), where σ increases with increases in ISR and decreases as M increases.

$$\frac{d\sigma}{dt} = \frac{\sigma_\infty(\text{ISR}, M) - \sigma}{\tau_\sigma} \tag{8}$$

Parameters and non-estimated initial states were set according to their values in previous research (Ha and Sherman, 2020; Sherman, 2022). In experiments where measured insulin values were not included in the estimation optimization, I_0 was set as 5.63 μIU/mL. The parameters estimated without using a patient's insulin values are denoted with an, $\overline{\sigma S_I}$ and $\overline{\sigma^* S_I}$.

2.6 Estimating parameters using data assimilation

In our methods, we estimated two parameters via data assimilation, insulin sensitivity, S_I, and maximal insulin secretion capacity, σ. Ordinary differential equations were solved using a Rosenbrock-W method (Rosenbrock23) (Rackauckas and Nie, 2017) within the bounds of [0.005, 3] for S_I and [0.01, 10] for σ. The posterior distributions of the parameters and the product $\sigma^* S_I$ were estimated based on a 500,000 iteration Random Walk Metropolis-Hastings MCMC (Hastings, 1970) chain (excluding a burn-in of 50,000 iterations), assuming a normal distribution error model and uniform priors. A decrease in autocorrelation approaching 0 was appreciated with increasing lags (k) near k = 500 to support chain convergence, and the number of iterations and burn-in were selected to be orders of magnitude larger than k (Roy, 2019). Acceptance rate varied with each patient between 0.2–0.5. Multiple independent chains for a subset of 10 patients provided confidence in the reproducibility of the estimates. The means and standard deviations of the parameters were calculated from the remaining 450,000 iterations (Ge et al., 2018) in an individual's chain, and these summary statistics were included in logistic regression models.

TABLE 2 Pre-operative demographic comparisons by binary post-operative outcome at 12 months. For continuous variables, medians with their 95% CI are shown. Categorical variables are shown as a percentage and count. Significant *p*-values for Mann-Whitney-U tests after Bonferroni correction are in bold ($p < 0.001$).

Variable Name	− IGM *n* = 120	+ IGM *n* = 56	*p*-value
Pre-operative IGM status[#]	**45 (54)**	**83.9 (47)**	**< 0.0001**
Operation Age (years)	16.9 (16.6, 17.1)	16.8 (16.5, 17.5)	0.3034
Pre-operative BMI (kg/m^2)	45.93 (44.66, 47.92)	48.25 (46.20, 51.24)	0.0712
Male (%)	27.5 (33)	33.9 (19)	0.4880
Race			
Asian	0 (0)	3.6 (2)	0.1000
Black	17.5 (21)	28.6 (16)	0.1390
Native American	0 (0)	1.8 (1)	0.3180
Other	2.5 (3)	7.1 (4)	0.2110
Pacific Islander	0.8 (1)	0 (0)	1.0000
White	58.3 (70)	46.4 (26)	0.1890
Unknown	20.8 (25)	16.1 (9)	0.5890
Ethnicity			
Hispanic	42.5 (51)	51.8 (29)	0.3220
Non-Hispanic	53.3 (64)	51.8 (29)	0.9760
Declined	1.7 (2)	1.8 (1)	1.0000
Unknown	9.2 (11)	1.8 (1)	0.1060
Surgery Type			
Roux-en-Y (RYGB)	0.8 (1)	0 (0)	1.0000
Gastric Band (AGB)	42.5 (51)	60.7 (34)	0.0370
Sleeve Gastrectomy (VSG)	55.8 (67)	39.3 (22)	0.0600
Other[x]	0.8 (1)	0 (0)	1.0000
ICD Codes			
Abnormal Glucose[°]	13.3 (16)	33.9 (19)	0.0030
T2DM	8.3 (10)	23.2 (13)	0.0130
Dyslipidemia	29.2 (35)	35.7 (20)	0.4850
GERD	13.3 (16)	14.3 (8)	1.0000
Hypertension	21.7 (26)	41.1 (23)	0.0130
Liver Disease[+]	17.5 (21)	21.4 (12)	0.6780
Metabolic Syndrome	29.2 (35)	32.1 (18)	0.8220
OSA	35 (42)	42.9 (24)	0.4030
PCOS (F, *n* = 87, 37)	19.5 (17)	48.6 (18)	0.0021
Thyroid Disease	4.2 (5)	8.9 (5)	0.2930

[#]Patients with pre-operative IGM had any one of the IGM definitions pre-operatively. This variable was not used in training any of the models.
[x]Other surgeries refers to non-specific procedure codes for restrictive bariatric surgery.
[+]Liver disease includes non-alcoholic fatty liver disease, non-alcoholic steatohepatitis, and unspecified chronic liver disease.
[°]Abnormal glucose diagnosis codes exclude any kind of diabetes mellitus.
Abbreviations: BMI, body mass index; CI, confidence interval; GERD, gastroesophageal reflux disease; IGM, impaired glucose metabolism; OSA, obstructive sleep apnea; PCOS, polycystic ovary syndrome; T2DM, type 2 diabetes mellitus.

2.7 Descriptive statistics

The majority of continuous features were not normally distributed, so non-parametric methods were used to calculate descriptive statistics on non-transformed data. These data are reported as medians with 95% confidence intervals around the median. The Mann-Whitney-U tests were used to compare continuous variables under these circumstances. χ^2 or Fisher's

TABLE 3 Pre-operative laboratory value comparisons by binary post-operative outcome at 12 months. Medians with their 95% CI are shown. Significant *p*-values for Mann-Whitney-U tests after Bonferroni correction are in bold ($p < 0.002$).

Variable Name	− NGM $n = 120$	+ IGM $n = 56$	*p*-value
Baseline HbA1c (%)	**5.4 (5.3, 5.5)**	**5.8 (5.7, 6.0)**	**< 0.0001**
Baseline HOMA-IR	**3.13 (2.76, 3.52)**	**4.53 (3.75, 5.57)**	**1.987×10^{-3}**
OGTT Measurements			
G_0 (mg/dL)	86.5 (84, 88)	87.5 (86, 93)	0.1081
G_{30} (mg/dL)	**128 (123, 134)**	**140.5 (134, 146)**	**1.312×10^{-3}**
G_{60} (mg/dL)	**115.5 (113, 121)**	**133.5 (127, 154)**	**2.2×10^{-4}**
G_{120} (mg/dL)	**98 (93, 104)**	**113.5 (109, 122)**	**1.5×10^{-4}**
I_0 (μIU/mL)	14.5 (13.0, 17.0)	20.0 (17.0, 24.0)	4.033×10^{-3}
I_{30} (μIU/mL)	65.0 (52.0, 81.0)	70.5 (52.0, 87.0)	0.8265
I_{60} (μIU/mL)	63.0 (50.0, 72.0)	62.5 (49.0, 90.0)	0.9456
I_{120} (μIU/mL)	**36.5 (27.0, 50.0)**	**58.5 (47.0, 94.0)**	**1.17×10^{-4}**
Other Labs			
Total Cholesterol (mg/dL)	164 (159, 171)	164 (155, 170)	0.6057
HDL Cholesterol (mg/dL)	42 (41, 44)	43 (41, 47)	0.3700
HDL Cholesterol (mg/dL) (M, $n = 33, 19$)	39 (35, 44)	39 (34, 44)	0.9317
HDL Cholesterol (mg/dL) (F, $n = 87, 37$)	43 (42, 47)	46 (43, 51)	0.2019
LDL Cholesterol (mg/dL)	94 (92, 104)	101 (94, 105)	0.7447
Triglycerides (mg/dL)	103 (93, 113)	87.5 (78, 114)	0.4017
ALT (IU/L)	18.5 (16, 21)	20 (17, 25)	0.3676
AST (IU/L)	19 (18, 19)	18 (18, 21)	0.8286
TSH (μIU/L)	2.3 (2.0, 2.7)	2.8 (2.3, 3.7)	0.4416
Free T4 (ng/dL)	1.14 (1.1, 1.17)	1.16 (1.13, 1.22)	0.2113
Total T4 (μg/dL)	8.2 (8.0, 8.8)	8.7 (8.3, 9.3)	0.3143

Abbreviations: ALT, alanine aminotransferase; AST, aspartate aminotransferase; CI, confidence interval; G, glucose; HbA1c, hemoglobin A1c; HDL, high-density lipoprotein; HOMA-IR, homeostatic model assessment of insulin resistance; I, insulin; IGM, impaired glucose metabolism; LDL, low-density lipoprotein; NGM, normal glucose metabolism; OGTT, oral glucose tolerance test; TSH, thyroid stimulating hormone; T4, thyroxine.

exact tests were used to compare categorical variables depending on the frequencies of the categories. Two-tailed Student's *t*-tests were used to compare means and 95% confidence intervals of bootstrapped coefficient estimates and scoring metrics.

3 Results

3.1 Description of data

Out of 396 adolescents who underwent bariatric surgery, 248 had pre-operative OGTTs. Of 202 patients without any missing values in their pre-operative OGTT glucose and insulin measurements, 176 had follow-up within the appropriate time window and were further analyzed. All potential classification methods for impaired glucose metabolism (IGM) demonstrated class imbalance, with ~35% ($n = 56$) of patients with meeting post-operative criteria for IGM as outlined above. Pre-operative characteristics by group are shown in Tables 2, 3. Using the same criteria to classify IGM post-operatively, 101 of the 176 (57.4%) met criteria for IGM pre-operatively. At baseline, patients who had higher probabilities of having IGM post-operatively were more insulin resistant as

TABLE 4 Data assimilation-derived mechanistic model parameter estimate comparisons by binary post-operative outcome at 12 months. The parameters S_I, σ, and σ^*S_I refer to the means of the posterior distributions for each patient. Overlined parameters were estimated without insulin values. For comparisons, medians and 95% confidence intervals of the median are shown. All comparisons had significant *p*-values for Mann-Whitney-U test after Bonferroni correction ($p < 0.008$).

Parameter Name	− IGM $n = 120$	+ IGM $n = 56$	*p*-value
$\overline{S_I}$	0.403 (0.249, 0.571)	0.086 (0.054, 0.207)	1.70×10^{-5}
S_I	0.356 (0.284, 0.420)	0.155 (0.129, 0.178)	< 0.0001
$\overline{\sigma^*S_I}$	0.947 (0.651, 1.539)	0.207 (0.157, 0.379)	< 0.0001
σ^*S_I	0.908 (0.763, 1.510)	0.255 (0.146, 0.547)	< 0.0001
$\bar{\sigma}$	4.715 (4.414, 4.976)	4.083 (3.582, 4.399)	0.0011
σ	3.424 (2.627, 4.630)	1.596 (1.195, 3.169)	0.0003

Abbreviations: IGM, impaired glucose metabolism; σ, maximal insulin secretion capacity; S_I, insulin sensitivity.

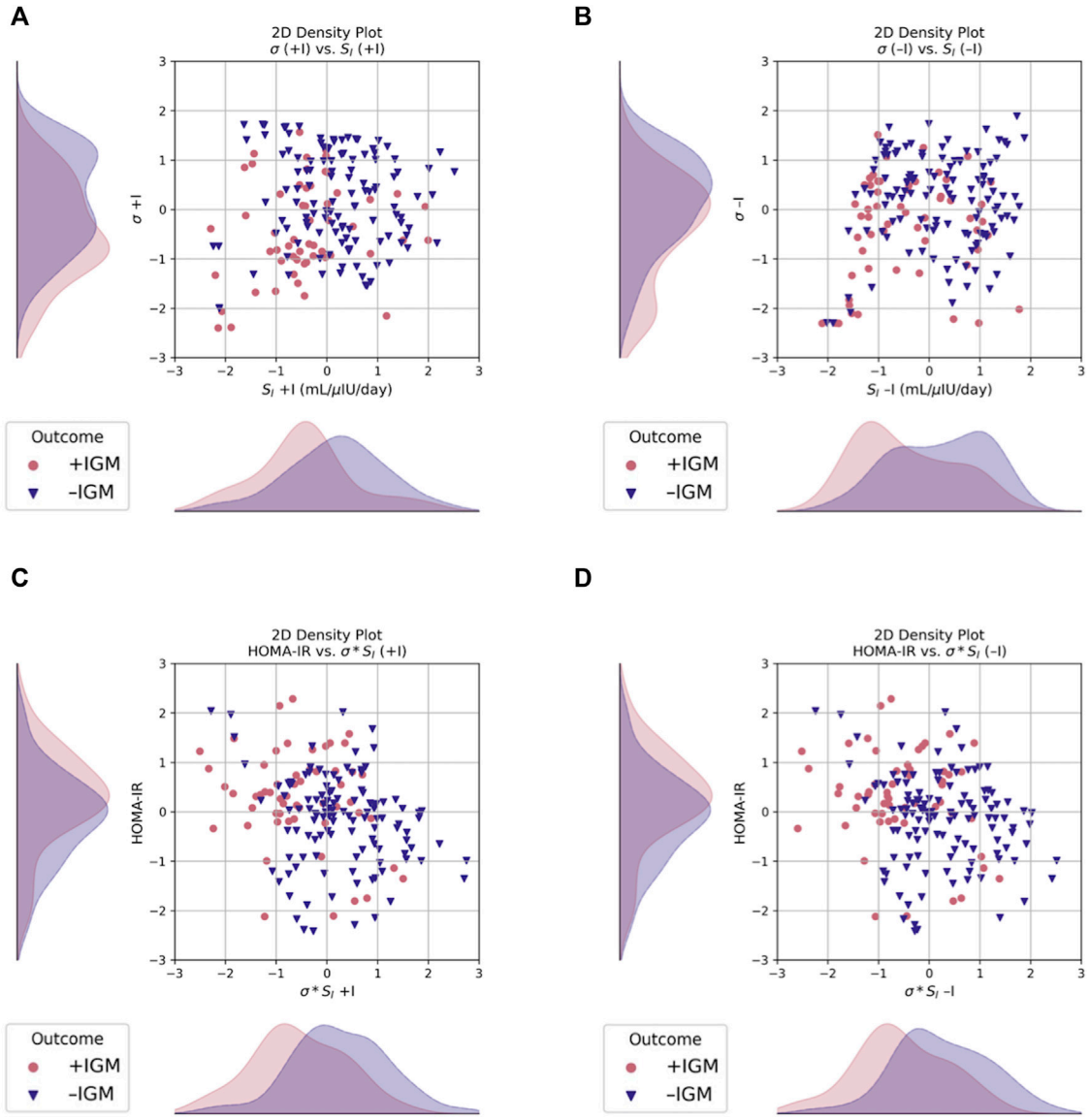

FIGURE 2
Scatter and 2D kernel density estimation plots, stratified by post-operative outcome at 12 months. Data are shown after Box-Cox transformation for visualization. **(A)** Incorporating measured insulin measurements in the data assimilation estimations increases separation of the estimated probability distributions of σ between groups, as compared to **(B)** without insulin, where S_I is more separated but σ has more overlap. **(C)** σ*S_I had better separation compared to HOMA-IR when estimated both with and **(D)** without insulin. Blue triangles, normal glucose metabolism (–IGM); red circles, impaired glucose metabolism (+IGM).

measured by HOMA-IR, had higher G_{30}, G_{60}, and G_{120} values, and had higher I_{120} values.

A total of 202 patients met inclusion criteria, but 26 of them did not have follow-up within 6–18 months of surgery. One patient was lost to follow-up due to death within three months of surgery. The proportions of patients lost to follow-up were statistically different between those with pre-operative IGM (Fisher's exact test $p = 0.035$): nine met two or more pre-operative IGM criteria (three with elevated G_0, one with elevated G_{120}, six with multiple elevated HbA1c values, one on anti-diabetic medication).

3.2 Data assimilation results

Parameter estimates from data assimilation are summarized in Table 4 and the probability distribution of

TABLE 5 AUROC comparisons between models trained on subsets of features with and without data assimilation. Models are presented in alphabetical order with the better performing model on the left (Model A). Clinical Vars refers to all clinical features in Tables 2, 3 except pre-operative IGM status and HOMA-IR. Clinical Vars^{-Ins} refers to the same set of features in Clinical Vars after removing insulin measurements. Overlined parameters were estimated without insulin values. Significant *p*-values for two-tailed Student's *t*-test after Bonferroni correction are shown in bold ($p < 0.004$).

	Model A	A AUROC Mean (95% CI)	Model B	B AUROC Mean (95% CI)	*p*-value
1	**Clinical Vars**	**0.7655 (0.7622, 0.7689)**	**Clinical Vars^{-Ins} + $\overline{\sigma^*S_I}$**	**0.7511 (0.7475, 0.7547)**	**< 0.0001**
2	Clinical Vars + HOMA-IR	0.7659 (0.7625, 0.7692)	Clinical Vars	0.7655 (0.7622, 0.7689)	0.8942
3	Clinical Vars^{-Ins} + $\overline{\sigma^*S_I}$	0.7511 (0.7475, 0.7547)	Clinical Vars^{-Ins}	0.7491 (0.7455, 0.7527)	0.4351
4	Clinical Vars + σ + S_I + σ^*S_I	0.7678 (0.7644, 0.7713)	Clinical Vars	0.7655 (0.7622, 0.7689)	0.3573
5	Clinical Vars + σ + S_I + σ^*S_I	0.7678 (0.7644, 0.7713)	Clinical Vars + HOMA-IR	0.7659 (0.7625, 0.7692)	0.4282
6	Clinical Vars + σ^*S_I	0.7700 (0.7665, 0.7734)	Clinical Vars	0.7655 (0.7622, 0.7689)	0.0728
7	Clinical Vars + σ^*S_I	0.7700 (0.7665, 0.7734)	Clinical Vars + HOMA-IR	0.7659 (0.7625, 0.7692)	0.0952
8	**Glucose + Insulin + HbA1c + σ^*S_I**	**0.7627 (0.7594, 0.7659)**	**Glucose + Insulin + HbA1c + σ + S_I + σ^*S_I**	**0.7451 (0.7416, 0.7486)**	**< 0.0001**
9	**Glucose + Insulin + σ + S_I + σ^*S_I**	**0.7463 (0.743, 0.7496)**	**Glucose + Insulin**	**0.7337 (0.7303, 0.7371)**	**< 0.0001**
10	$\overline{\sigma^*S_I}$	0.7380 (0.7346, 0.7415)	Glucose + Insulin	0.7337 (0.7303, 0.7371)	0.0790
11	$\overline{\sigma^*S_I}$	0.7380 (0.7346, 0.7415)	Glucose + Insulin + HOMA-IR	0.7317 (0.7283, 0.7350)	0.0089

Abbreviations: CI, confidence interval; HbA1c, hemoglobin A1c; HOMA-IR, homeostatic model assessment of insulin resistance; σ, maximal insulin secretion capacity; S_I, insulin sensitivity.

TABLE 6 Average precision comparisons between models trained on subsets of features with and without data assimilation. Models are presented in the same order as in Table 5. Clinical Vars refers to all clinical features in Tables 2, 3 except pre-operative IGM status and HOMA-IR. Clinical Vars^{-Ins} refers to the same set of features in Clinical Vars after removing insulin measurements. Overlined parameters were estimated without insulin values. Significant *p*-values for two-tailed Student's *t*-test after Bonferroni correction are shown in bold ($p < 0.004$).

	Model A	A AP Mean (95% CI)	Model B	B AP Mean (95% CI)	p-value
1	Clinical Vars	0.6200 (0.6148, 0.6252)	Clinical Vars^{-Ins} + $\overline{\sigma^*S_I}$	0.613 (0.6074, 0.6185)	0.0700
2	Clinical Vars + HOMA-IR	0.6209 (0.6155, 0.6262)	Clinical Vars	0.6200 (0.6148, 0.6252)	0.8200
3	Clinical Vars^{-Ins} + $\overline{\sigma^*S_I}$	0.613 (0.6074, 0.6185)	Clinical Vars^{-Ins}	0.6075 (0.6021, 0.6129)	0.1665
4	Clinical Vars + σ + S_I + σ^*S_I	0.6253 (0.6197, 0.6308)	Clinical Vars	0.6200 (0.6148, 0.6252)	0.8835
5	Clinical Vars + σ + S_I + σ^*S_I	0.6253 (0.6197, 0.6308)	Clinical Vars + HOMA-IR	0.6209 (0.6155, 0.6262)	0.2656
6	Clinical Vars + σ^*S_I	0.6258 (0.6206, 0.6311)	Clinical Vars	0.6200 (0.6148, 0.6252)	0.1244
7	Clinical Vars + σ^*S_I	0.6258 (0.6206, 0.6311)	Clinical Vars + HOMA-IR	0.6209 (0.6155, 0.6262)	0.1966
8	**Glucose + Insulin + HbA1c + σ^*S_I**	**0.6156 (0.6105, 0.6207)**	**Glucose + Insulin + HbA1c + σ + S_I + σ^*S_I**	**0.5936 (0.5882, 0.599)**	**< 0.0001**
9	**Glucose + Insulin + σ + S_I + σ^*S_I**	**0.5841 (0.5791, 0.5892)**	**Glucose + Insulin**	**0.5695 (0.5644, 0.5745)**	**0.0001**
10	**$\overline{\sigma^*S_I}$**	**0.5990 (0.5939, 0.6041)**	**Glucose + Insulin**	**0.5695 (0.5644, 0.5745)**	**< 0.0001**
11	**$\overline{\sigma^*S_I}$**	**0.5990 (0.5939, 0.6041)**	**Glucose + Insulin + HOMA-IR**	**0.5662 (0.5611, 0.5713)**	**< 0.0001**

Abbreviations: AP, average precision; CI, confidence interval; HbA1c, hemoglobin A1c; HOMA-IR, homeostatic model assessment of insulin resistance; σ, maximal insulin secretion capacity; S_I, insulin sensitivity.

their means across the cohort as estimated by kernel density estimation are shown in Figure 2. The post-operative + IGM group had statistically significantly lower baseline insulin sensitivity (S_I) and maximal insulin secretion capacity (σ) values compared to the post-operative − IGM group, irrespective of inclusion of insulin in the data assimilation.

The marginal posterior densities of the parameters were estimated for each individual patient using MCMC. The marginal posterior density of S_I was sharply peaked away from its bounds on manual inspection for a random subset of patients, giving us confidence in its mean estimator. The density for σ^*S_I was also sharply peaked away from its bounds (not shown).

3.3 Prediction model results

For the most complex model, data assimilation estimates were negatively correlated with the probability of having post-operative impaired glucose metabolism (IGM) at 12 months. Across models that contained them, HbA1c and I_{120} were positively correlated with the probability of having post-operative IGM at 12 months. However, the model coefficients were overall not significantly different from zero for all models (not shown). When ranked by magnitude, the largest coefficients, when included, were coefficients for HbA1c, I_{120}, and G_{60}.

Selected AUROC and average precision score comparisons are shown in Tables 5, 6, respectively.

The best performing model used all available clinical variables (n features = 43) and σ^*S_I with an AUROC of 0.77 (95% CI 0.7665, 0.7734) and average precision of 0.6258 (95% CI 0.6206, 0.6311). Our most comprehensive models using all clinical data had similar performances regardless of whether data assimilation estimates or HOMA-IR were included (Tables 5, 6, rows 1–7).

4 Discussion

4.1 Data assimilation estimates can add clinical information that improves prediction

Our best-performing model used the aforementioned clinical variables combined with the product of maximal insulin secretion capacity and insulin sensitivity, σ^*S_I, with an AUROC of 0.77 (95% CI 0.7665, 0.7734) and average precision of 0.6258 (95% CI 0.6206, 0.6311). This model was nominally better than one using clinical variables alone with an AUROC of 0.7655 (95% CI 0.7622, 0.7689) and average precision of 0.6200 (95% CI 0.6148, 0.6252), but the differences were not significant at p = 0.0728 and 0.1244, respectively (Tables 5, 6, row 6).

4.2 Data assimilation estimates can infer missing information encoded in insulin measurements

The comparability of our most comprehensive models suggests that the information added by data assimilation is captured in an extensive, but not exhaustive, clinical dataset. Embedded in the electronic health record (EHR) data was a powerful experiment where the effects of bariatric surgery could be thoroughly investigated. Models incorporating insulin, in general, outperformed models that did not include it. However, when insulin measurements are missing, data assimilation can add physiologic information that approaches the predictive ability of the full clinical dataset. For example, when using all other clinical features *except* insulin, the model using the product $\overline{\sigma^*S_I}$ had nominally improved performance to the model not including any data assimilation estimates, although the p-value was not significant (AUROC 0.7511 [0.7475, 0.7547] vs. 0.7491 [0.7455, 0.7527], respectively, p = 0.4351; AP 0.6130 [0.6074, 0.6185] vs. 0.6075 [0.6021, 0.6129], p = 0.1665) (Tables 5, 6, row 3). While the performance of this same model using $\overline{\sigma^*S_I}$ performed worse than the model using the full clinical dataset including insulin (AUROC 0.7511 [0.7475, 0.7547] vs. 0.7655 [0.7622, 0.7689], p < 0.0001; AP 0.6130 [0.6074, 0.6185] vs. 0.6200 [0.6148, 0.6252], p = 0.0700) (Tables 5, 6, row 1), its AUROC was non-inferior at 98.5% with p = 0.2326.

Our models further suggest that σ^*S_I, even when estimated sans insulin, can represent the information within an OGTT using glucose and insulin. When compared, our model trained on only $\overline{\sigma^*S_I}$ had similar or better performance as compared to models trained on the glucose and insulin measurements from an OGTT (AUROC 0.7380 [0.7346, 0.7415] vs. 0.7337 [0.7303, 0.7371], p = 0.079; AP 0.5990 [0.5939, 0.6041] vs. 0.5695 [0.5644, 0.5745], p < 0.0001) (Tables 5, 6, row 10). The predictive performance of $\overline{\sigma^*S_I}$ is demonstrated again in comparison with the model incorporating HOMA-IR, which requires a fasting insulin measurement (AUROC 0.7380 [0.7346, 0.7415] vs. 0.7317 [0.7283, 0.7350], p = 0.0089; 0.5990 [0.5939, 0.6041] vs. 0.5662 [0.5611, 0.5713], p < 0.0001) (Tables 5, 6, row 11).

4.3 The mechanistic models were validated using clinical data

The mechanistic models were able to be well estimated, achieving a stable solution with a unique minimum, using our clinical dataset. Furthermore, the mechanistic model output did not contradict nor add unvalidated information, in that the parameters estimated corresponded to variables associated with glucose and insulin metabolism, and not to other clinical variables (e.g., demographics, thyroid function).

4.4 Uncertainty of data assimilation estimates results in reduced performance in logistic regression

When included in the model, HbA1c and insulin measures (particularly I_{120}) were frequently ranked as the most important predictors by magnitude. The improved prediction ability using A1c or insulin was not replicated by substituting them with data assimilation estimates not using insulin (not shown). While not a complete substitute

for the information contained in HbA1c or insulin, when maximal insulin secretion capacity (σ), insulin sensitivity (S_I), or σ^*S_I are estimated using insulin measurements, they still improve performance when added to models containing OGTT insulin (AUROC 0.7463 [0.743, 0.7496] vs. 0.7337 [0.7303, 0.7371], $p < 0.0001$; AP 0.5841 [0.5791, 0.5892] vs. 0.5695 [0.5644, 0.5745], $p = 0.0001$) (Tables 5, 6, row 9).

Although in most models the feature coefficients were not statistically different from zero (not shown), the standard deviation of maximal insulin secretion capacity (σ) is given more importance than the actual estimated parameters themselves and HbA1c in the models using all three data assimilation estimates. Furthermore, in the presence of insulin, regularization consistently shrinks the coefficient for insulin sensitivity (S_I), whereas the coefficient for maximal insulin secretion capacity (σ) increases. The variance in σ's estimation and its overlapping distributions between groups compared to that of S_I, even when estimated using insulin measurements, likely contributes to the loss of predictive power (Figure 2). Using σ^*S_I in lieu of σ and S_I separately improves model performance (AUROC 0.7627 [0.7594, 0.7659] vs. 0.7451 [0.7416, 0.7486], $p < 0.0001$; AP 0.6156 [0.6105, 0.6207] vs. 0.5936 [0.5882, 0.599], $p < 0.0001$) (Tables 5, 6, row 8).

4.5 Disease subtypes can be described by parameter estimates

Differences in pre-operative insulin sensitivity (S_I) and maximal insulin secretion capacity (σ) estimates were seen between outcome groups when estimated both with and without measured insulin ($p < 0.05$, Figure 2 and Table 4). Regardless of a patient's pre-operative glycemic status, S_I better distinguished those patients who would have post-operative impaired glucose metabolism (IGM) compared to either σ or σ^*S_I (Figure 2).

Those with post-operative IGM tended to have lower baseline S_I and σ values compared to those without it, demonstrating that both may contribute to a patient's disease, although not necessarily equally. Additionally, those with post-operative IGM had higher pre-operative HbA1c, G_{30}, G_{60}, and G_{120} and I_{120} values ($p < 0.05$, Table 3). This may reflect defects in second phase insulin secretion, which is associated with decreases in insulin secretion capacity (Ha and Sherman, 2020). Notably, σ^*S_I and S_I values were not correlated with baseline BMI values, demonstrating a seeming disconnect between whole-body adiposity and insulin sensitivity (not shown). Other physiologic parameters that were not estimated using data assimilation in this study, such as insulin secretion rate (ISR) and hepatic insulin sensitivity ($hepa_{S_I}$), may reveal other disease phenotypes and patient characterizations that could be explored in future work.

4.6 Fixed mechanistic model parameters may differ between adolescents and adults

Not all parameters in the mechanistic models can be estimated simultaneously. All models have potential limitations in generalizability beyond the populations studied during initial development. Use of fixed parameters with values derived from clinical studies in adults may not optimally estimate parameters during pubertal states, where hormonal crosstalk greatly influences energy homeostasis. For example, adolescence is marked by a drastic decrease in insulin sensitivity independent of adiposity; euglycemia is achieved by a compensatory and proportional increase in insulin secretion (Hannon et al., 2006). Insulin secretion rates will therefore be elevated in this age group compared to their adult counterparts, and estimated parameter bounds may differ considerably.

Other parameters which may be relatively constant in adulthood might be more dynamic in adolescents. Obesity and age impact β cell mass and proliferation, which were set as fixed components of these mechanistic models (Saisho et al., 2013; Michaliszyn et al., 2014). The fasting value of γ, representing the K^+-ATP channel density on the β cells, was set to its example value of −0.076 (Sherman, 2022). However, γ plays an important role in regulating β cell physiology and glucose-mediated insulin secretion. Not properly tuning the fasting value of γ may adversely affect the estimates of the parameters regulating β cell physiology such as maximal insulin secretion capacity (σ) and insulin priming rate (r_2^0). These effects likely reduced the prediction capabilities of our estimates.

Finally, the assumption that estimates based on the 120-min-OGTT approximate parameters as they would be estimated by a hyperinsulinemic euglycemic clamp may be violated in adolescents. Recently, validation of the oral minimal model in adolescents showed that the 120-min-OGTT underestimates insulin sensitivity compared to longer OGTTs, which is not the case for adults (Bartlette et al., 2021). Complicating this suboptimal approximation is the erratic behavior of OGTT measurements, even in euglycemic patients. Glucose and insulin assays can be imprecise, particularly in periods where glucose and insulin are changing rapidly (i.e., after a meal), and removing spurious OGTT measurements can improve performance (Abohtyra et al., 2022).

4.7 Binary classification of outcomes obscures a heterogenous population

Because of the relatively rare frequency of overt diabetes pre-operatively and varying sensitivity of common measurements in adolescents, the post-operative glucose metabolism outcome was coded as a binary variable: normal glucose metabolism (NGM) or

impaired glucose metabolism (IGM). However, there are likely multiple sub-phenotypes present in these groups, which would negatively impact prediction models.

Though the diagnostic threshold for T2DM is HbA1c ≥ 6.5%, we used HbA1c ≥ 5.7%, the threshold for preDM, to indicate any IGM to improve sensitivity for detecting T2DM in adolescents (Nowicka et al., 2011). The exact interpretation of HbA1c must be considered along with an individual's hemoglobin concentration and structure (Radin, 2014). In particular, studies have shown that traditional HbA1c thresholds for T2DM (≥ 6.5%) are imperfect for diagnosis in adults and may significantly underestimate the prevalence of T2DM in adolescents (Nowicka et al., 2011; American Diabetes Association Professional Practice Committee Draznin et al., 2022). Furthermore, given the frequency of anemia in bariatric surgery patients, HbA1c may misrepresent average blood glucose levels and thus, normal values are insufficient to exclude IGM phenotypes. As such, HbA1c was used as a feature in a logistic regression rather than as the outcome in a linear regression.

All patients were included for analysis regardless of pre-operative IGM status. Notably, neither hyperinsulinism nor insulin resistance were used to code IGM. As insulin resistance is tightly coupled with visceral adiposity, the likelihood that all patients had insulin resistance as the only manifestation of their IGM phenotype is high; this is supported by the lower S_I values and elevated HOMA-IR calculations of patients at baseline (Kahn and Flier, 2000; Stern et al., 2005). Nonetheless, the decision to focus on glucose rather than insulin perturbations in outcome labeling likely impaired the ability of our models to identify those with IGM-like phenotypes post-operatively, particularly as the outcome is not granular enough to distinguish this heterogenous population.

4.8 Limitations

4.8.1 Small sample size

Our methods were hindered by a small, imbalanced, and homogenous sample from a single institution. In addition to increasing sample size by using incomplete OGTT data, future work could address class imbalance by under sampling the majority class or removing redundant information. Our sample size relative to features was exacerbated by patient attrition, likely not at random.

4.8.2 Bias in clinical measures

Our cohort is more diverse with respect to ethnicity and race compared to previously reported studies, which may impact the ability of a model to predict outcomes when using estimators such as HbA1c. Race differences in outcomes have been seen in other studies and have been attributed to poor calibration of models or measurements across heterogenous populations (Wallace et al., 2004; Olson et al., 2010; Tharakan et al., 2017). However, race differences between Black and white adolescents have also been noted in hyperinsulinemic-euglycemic clamp studies, so the true difference in T2DM development is still unclear (Michaliszyn et al., 2017).

4.8.3 Complexity and validation of electronic health records

Our study did not occur in the context of a clinical trial and is subject to the constraints of EHR data. The most effective use of EHR data applies knowledge of how data are inputted into the system while also understanding the underlying medical decision making process. Improper automatic encoding of features or outcomes could have negatively impacted our models' predictive abilities. In the case of our analyses, features such comorbidities and drug information are less reliable than laboratory values, and awareness of missing data is not guaranteed—that is, the EHR datasets are not complete (Weiskopf et al., 2013). For example, formal diagnoses of obesity-related liver diseases (i.e., NAFLD and NASH) use a liver biopsy to confirm pathology, which can be done while a patient is undergoing bariatric surgery. However, the diagnosis codes for *suspected* liver disease may not be reflected in the EHR, and if they are inputted, they are done so irregularly. This was the case in our patient sample, where many of the comorbidities were mentioned within the patient assessment and/or radiology impressions of notes, but not listed as a visit-associated diagnosis code frequently enough to be marked as present by our criteria. Relatedly, medication data are sparse and often inaccurate, with unreliable start and stop dates. Diet information, which is undoubtedly important in this context, is not typically represented at all in structured datasets. Information about mental health and psychiatric comorbidities is intentionally difficult to access for secondary use, and social stigmas surrounding mental health reduce confidence that, absent documentation, no comorbidities are present. Similarly, social determinants of health such as food insecurity, exposure to discrimination, and exposure to adverse childhood events are not captured in this dataset. Compounding these limitations are existing health disparities in access bariatric surgery, leading to selection bias (Tsui et al., 2021).

Manual chart review is the gold standard for extracting clinical information, but this is time intensive and subject to human error. It also cannot account for truly missing information. As this relates to our methods, to avoid misclassifying patients with post-operative IGM, we erred on the side of underestimating the proportion of patients with specific comorbidities by requiring at least 25% of encounters to contain the relevant diagnosis codes and structured documentation of medications. This may have classified patients as not having IGM post-operatively when in fact they did have some impaired metabolism.

4.8.4 Limitations related to the use of mechanistic models

The use of mechanistic models and oridnary differential equations inherently limits the number of parameters that can be estimated concurrently. Combined with the limitations related to our retrospective, observational analysis, we are limited in our ability to verify the estimated values with respect to a patient's true physiology. There are several physiologic estimates from data assimilation that could be of use clinically, such as pre-hepatic insulin secretion rate (ISR) or hepatic insulin sensitivity ($hepa_{S_I}$). Both ISR and $hepa_{S_I}$ are difficult to capture clinically, and estimation using OGTTs is complex (Cauter et al., 1992; Kjems et al., 2000). However, our choices to estimate maximal insulin secretion capacity (σ) and insulin sensitivity (S_I) limited our ability to estimate other such important parameters. Generally in our results, more information improved predictions and model accuracy varied in a smooth and logical way. While this does not prove that the ISR estimates incorporated into σ are their true values, it demonstrates that these imperfect features have potential utility in improving patient-level predictions related to surgical outcomes.

Related to the limitations of mechanistic models, our predictive models did not incorporate estimates of hepatic insulin sensitivity ($hepa_{S_I}$) because $hepa_{S_I}$ was necessarily fixed in our equations to better estimate σ and S_I. However, mismatch between peripheral and hepatic insulin sensitivity may better describe subgroups of adolescents with IGM compared to peripheral insulin resistance alone, particularly in the setting of physiologic pubertal insulin resistance (Hannon et al., 2006). Future work should incorporate this critical component of glucose-insulin metabolism into descriptions of patient phenotypes.

Also absent in these models are the effects of circulating incretins, i.e., glucagon-like peptide-1 (GLP-1) and glucose-dependent insulinotropic polypeptide or gastric inhibitory polypeptide (GIP). These gut-secreted, insulinotropic hormones are implicated as one potential therapeutic mechanism of action in metabolic surgeries through their actions on insulin secretion and hepatic insulin clearance (Fetner et al., 2005; Hutch and Sandoval, 2017). Supporting this is the general success of novel classes of anti-diabetic drugs leveraging GLP-1 receptor agonists to manage T2DM and obesity in adults and adolescents (Kelly et al., 2020). However, GLP-1 and GIP are not directly represented in the mechanistic models we used, nor is it currently feasible to directly measure their levels in an outpatient clinical setting. Changes in incretins are indirectly reflected in changes in maximal insulin secretion capacity, σ, where increases in GLP-1 lead to increases in σ through the exocytosis model (Ha and Sherman, 2020). If these mechanistic models are employed to predict future physiologic states on a longer time scale, it is critical to include models which incorporate incretin effects to better model post-surgical physiology.

4.9 Future directions

Our model could not capture all features to confidently predict post-surgical glycemic states as a dichotomous outcome despite an extensive collection of laboratory data. We do not believe that these estimates should be broadly disseminated to preclude or exclude patients from receiving indicated care. Rather, with future validation, parameters like σ and S_I could inform expectations with respect to potential outcomes. Patients intending to have their prediabetic or diabetic states completely reversed should be informed of the possibility that they may not completely resolve with surgery alone. Quantifying that uncertainty may be accomplished using models like the ones described here. By providing more informed consent, we hope that more patients will be able to have meaningful discussions with their care teams to improve long-term surgical outcomes.

Future studies can incorporate using more longitudinal data to see the trends in insulin secretion capacity (σ) and insulin sensitivity (S_I) in the pre-, peri-, and post-operative periods. Applying more granular outcome definitions on a continuous scale may better capture patients who might improve in the severity of their disease, but not sufficiently to resolve impaired glucose metabolism. Alternatively, unsupervised machine learning methods could be applied on a larger cohort of patients to identify different pre-operative phenotypes.

Investigation into additional features that may improve predictive performance can also inform future work. Focusing on the direct effects of surgery itself may provide more insight into patient outcomes, especially when certain surgeries (e.g., sleeve gastrectomy or RYGB) have larger metabolic impacts as compared to relatively metabolically modest restrictive procedures like gastric banding. Using models that directly incorporate the effects of GLP-1 and its secretion in response to glucose ingestion, such as that developed by De Gaetano et al., (De Gaetano et al., 2013) should be included in future work, as should assessment of the change in GLP-1 secretion patterns post-operatively. Prospective studies with larger sample sizes or measurement of more stable insulin byproducts such as C-peptide during OGTTs could improve model performance both by adding a more specific feature and through improvement of data assimilation estimates. Manual chart review can provide information about pre- and post-operative anthropometrics to better quantify adiposity. Alternatively, methods to estimate fat-free body mass using more readily available clinical data could be explored. Inclusion of other candidate biomarkers associated with glucose and insulin metabolism such as incretins, growth factors, inflammatory markers, and carrier proteins could be added. Variables related to behaviors (including diet), mental health, and social determinants of health should also be included in future studies attempting prediction in this same population.

This research is a starting point for further investigation into the use of mechanistic models and data assimilation

applied to clinical problems. In addition to application of similar techniques to clinical problems outside of prediction, research focusing on solving strategies with sparse or irregularly sampled clinical data could provide robust and reliable methods for future studies.

5 Conclusion

We demonstrate that data assimilation captures predictive information about glucose metabolism that is not readily apparent from OGTT measurements alone. Further, we validated that our chosen mechanistic model does not add any additional information than it is meant to represent. The clinical variables combined with the product of maximal insulin secretion capacity and insulin sensitivity, σ^*S_1, produced the best-performing model with AUROC = 0.77 and average precision = 0.6258. This model was nominally better than one using clinical variables alone with AUROC = 0.7655, but the difference was not significant at $p = 0.07$. In some cases, using the individual components of insulin secretion capacity (σ) and insulin sensitivity (S_I) along with their product reduced prediction model performance.

Looking at whether insulin measurement can be replaced by data assimilation, we found that the model using clinical variables with insulin (AUROC = 0.7655) performed better than the models using clinical variables without insulin but combined with $\overline{\sigma^*S_I}$ (AUROC = 0.7511, $p < 0.001$). We also found, however, that the difference was small and non-inferior at 98.5%, implying that similar performance can be achieved even without insulin measurements.

If we limit our model inputs to OGTT glucose and insulin values, we found adding data assimilation estimates of insulin secretion capacity and insulin sensitivity (σ, S_I, and σ^*S) significantly increased performance ($p < 0.001$). Models using $\overline{\sigma^*S_I}$ alone, estimated without insulin, performed marginally better than models using OGTT glucose and insulin with respect to AUROC (0.7380 vs. 0.7337, $p = 0.08$) and had significant improvements in average precision (0.5990 vs. 0.5695, $p < 0.001$).

While data assimilation alone does not significantly improve prediction ability compared to a maximal dataset, the separation of parameter distributions may provide insight into how underlying physiologic processes contribute to a patient's disease. In this adolescent cohort, low insulin sensitivity *and* low maximal insulin secretion capacity distinguish those patients who are less likely to see glycemic benefits from bariatric surgery. While knowing the extent to which defects in glucose-insulin metabolism contribute to disease is not sufficient to confidently predict surgical outcomes, future research can leverage mechanistic models to infer a patient's physiology even when certain data are absent.

Data availability statement

The original contributions presented in the study are included in the article/supplementary materials, further inquiries can be directed to the corresponding author.

Author contributions

LR, IF, BA, DA, and GH contributed to the conception and design of the study. LR and AO extracted structured and unstructured clinical data from the EHR. IF and JZ provided clinical care for patients in the Center for Adolescent Bariatric Surgery. LR performed manual chart review where necessary. LR cleaned and pre-processed data. BA and DA coded the mechanistic models, and BA performed MCMC fitting. LR and LZ developed the logistic regression models. LR wrote the first draft of the manuscript. BA, LZ, DA, and GH wrote sections of the manuscript. All others contributed to manuscript revision, read, and approved the submitted version.

Funding

This work was supported by NIH Grant Nos. R01 LM006910 (GH, LZ, AO), R01 LM012734 (GH and DA), and T15 LM007079 (LR and BA).

Acknowledgments

We acknowledge the excellent support, guidance, and advice from Arthur S. Sherman and Joon Ha to ensure sound use and encoding of their models in this clinical application.

Conflict of interest

The authors declare that the research was conducted in the absence of any commercial or financial relationships that could be construed as a potential conflict of interest.

The handling Editor CDB declared a past co-authorship with authors DA and GH.

Publisher's note

References

Abohtyra, R. M., Chan, C. L., Albers, D. J., and Gluckman, B. J. (2022). Inferring insulin secretion rate from sparse patient glucose and insulin measures. *Endocrinol. Incl. Diabetes Mellitus Metabolic Dis.* doi:10.1101/2022.03.10.22272234

Akalestou, E., Miras, A. D., Rutter, G. A., and le Roux, C. W. (2022). Mechanisms of weight loss after obesity surgery. *Endocr. Rev.* 43, 19–34. doi:10.1210/endrev/bnab022

Albers, D. J., Blancquart, P-A., Levine, M. E., Seylabi, E. E., and Stuart, A. (2019). Ensemble kalman methods with constraints. *Inverse Probl.* 35, 095007. doi:10.1088/1361-6420/ab1c09

Albers, D. J., Levine, M., Gluckman, B., Ginsberg, H., Hripcsak, G., and Mamykina, L. (2017). Personalized glucose forecasting for type 2 diabetes using data assimilation. *PLoS Comput. Biol.* 13, e1005232. doi:10.1371/journal.pcbi.1005232

American Diabetes Association Professional Practice CommitteeDraznin, B., Aroda, V. R., Bakris, G., Benson, G., and Brown, F. M. (2022). 14. Children and adolescents: *Standards of medical Care in diabetes—2022. Diabetes Care* 45, S208–S231. doi:10.2337/dc22-S014

American Diabetes Association Professional Practice Committee (2022). 2. Classification and diagnosis of diabetes: *Standards of medical Care in diabetes—2022. Diabetes Care* 45, S17–S38. doi:10.2337/dc22-S002

Aminian, A., Brethauer, S. A., Andalib, A., Nowacki, A. S., Jimenez, A., Corcelles, R., et al. (2017). Individualized metabolic surgery score: Procedure selection based on diabetes severity. *Ann. Surg.* 266, 650–657. doi:10.1097/SLA.0000000000002407

Armstrong, S. C., Bolling, C. F., Michalsky, M. P., and Reichard, K. W. (2019). Pediatric metabolic and bariatric surgery: Evidence, barriers, and best practices. *Pediatrics* 144, e20193223. doi:10.1542/peds.2019-3223

Arslanian, S., El ghormli, L., Young Kim, J., Bacha, F., Chan, C., Ismail, H. M., et al. (2019). The shape of the glucose response curve during an oral glucose tolerance test: Forerunner of heightened glycemic failure rates and accelerated decline in β-cell function in TODAY. *Diabetes Care* 42, 164–172. doi:10.2337/dc18-1122

Aung, L., Lee, W-J., Chen, S. C., Ser, K. H., Wu, C. C., Chong, K., et al. (2016). Bariatric surgery for patients with early-onset vs late-onset type 2 diabetes. *JAMA Surg.* 151, 798–805. doi:10.1001/jamasurg.2016.1130

Bal, B. S., Finelli, F. C., Shope, T. R., and Koch, T. R. (2012). Nutritional deficiencies after bariatric surgery. *Nat. Rev. Endocrinol.* 8, 544–556. doi:10.1038/nrendo.2012.48

Bartlette, K., Carreau, A-M., Xie, D., Garcia-Reyes, Y., Rahat, H., Pyle, L., et al. (2021). Oral minimal model-based estimates of insulin sensitivity in obese youth depend on oral glucose tolerance test protocol duration. *Metabol. Open* 9, 100078. doi:10.1016/j.metop.2021.100078

Bartolomé, A., Suda, N., Yu, J., Zhu, C., Son, J., Ding, H., et al. (2022). Notch-mediated Ephrin signaling disrupts islet architecture and β cell function. *JCI Insight* 7, e157694. doi:10.1172/jci.insight.157694

Beamish, A. J., and Reinehr, T. (2017). Should bariatric surgery be performed in adolescents? *Eur. J. Endocrinol.* 176, D1-D15. D1–D15. doi:10.1530/EJE-16-0906

Bergman, R. N., Prager, R., Volund, A., and Olefsky, J. M. (1987). Equivalence of the insulin sensitivity index in man derived by the minimal model method and the euglycemic glucose clamp. *J. Clin. Investig.* 79, 790–800. doi:10.1172/JCI112886

Bolling, C. F., Armstrong, S. C., Reichard, K. W., and Michalsky, M. P. (2019). Metabolic and bariatric surgery for pediatric patients with severe obesity. *Pediatrics* 144, e20193224. doi:10.1542/peds.2019-3224

Box, G. E. P., and Cox, D. R. (1964). An analysis of transformations. *J. R. Stat. Soc. Ser. B* 26, 211–243. doi:10.1111/j.2517-6161.1964.tb00553.x

Brown, R. J., and Yanovski, J. A. (2014). Estimation of insulin sensitivity in children: Methods, measures and controversies. *Pediatr. Diabetes* 15, 151–161. doi:10.1111/pedi.12146

Bryant, M., Ashton, L., Brown, J., Jebb, S., Wright, J., Roberts, K., et al. (2014). Systematic review to identify and appraise outcome measures used to evaluate childhood obesity treatment interventions (CoOR): Evidence of purpose, application, validity, reliability and sensitivity. *Health Technol. Assess.* 18, 1–380. doi:10.3310/hta18510

Buck, S. F. (1960). A method of estimation of missing values in multivariate data suitable for use with an electronic computer. *J. R. Stat. Soc. Ser. B* 22, 302–306. doi:10.1111/j.2517-6161.1960.tb00375.x

Buse, J. B., Caprio, S., Cefalu, W. T., Ceriello, A., Del Prato, S., Inzucchi, S. E., et al. (2009). How do we define cure of diabetes? *Diabetes Care* 32, 2133–2135. doi:10.2337/dc09-9036

Buse, J. B., Kaufman, F. R., Linder, B., Hirst, K., El Ghormli, L., Willi, S., et al. (2013). Diabetes screening with hemoglobin A1c versus fasting plasma glucose in a multiethnic middle-school cohort. *Diabetes Care* 36, 429–435. doi:10.2337/dc12-0295

Buuren, S. van, and Groothuis-Oudshoorn, K. (2011). Mice : Multivariate imputation by chained equations in *R. J. Stat. Softw.* 45. doi:10.18637/jss.v045.i03

Cao, Y., Näslund, I., Näslund, E., Ottosson, J., Montgomery, S., and Stenberg, E. (2020). Using convolutional neural network to predict remission of diabetes after gastric bypass surgery: A machine learning study from the scandinavian obesity surgery register. *Endocrinol. Incl. Diabetes Mellitus Metabolic Dis.* doi:10.1101/2020.11.03.20224956

Cauter, E. V., Mestrez, F., Sturis, J., and Polonsky, K. S. (1992). Estimation of insulin secretion rates from C-peptide levels: Comparison of individual and standard kinetic parameters for C-peptide clearance. *Diabetes* 41, 368–377. doi:10.2337/diab.41.3.368

Chen, Y., Wang, S., and Sherman, A. (2008). Identifying the targets of the amplifying pathway for insulin secretion in pancreatic β-cells by kinetic modeling of granule exocytosis. *Biophys. J.* 95, 2226–2241. doi:10.1529/biophysj.107.124990

Chung, S. T., Katz, L. E. L., Stettler-Davis, N., Shults, J., Sherman, A., Ha, J., et al. (2022). The relationship between lipoproteins and insulin sensitivity in youth with obesity and abnormal glucose tolerance. *J. Clin. Endocrinol. Metabolism* 107, 1541–1551. doi:10.1210/clinem/dgac113

Cobelli, C., Dalla Man, C., Toffolo, G., Basu, R., Vella, A., and Rizza, R. (2014). The oral minimal model method. *Diabetes* 63, 1203–1213. doi:10.2337/db13-1198

Courcoulas, A. P., Christian, N. J., Belle, S. H., Berk, P. D., Flum, D. R., Garcia, L., et al. (2013). Weight change and health outcomes at 3 Years after bariatric surgery among individuals with severe obesity. *JAMA* 310, 2416–2425. doi:10.1001/jama.2013.280928

Courcoulas, A. P., Goodpaster, B. H., Eagleton, J. K., Belle, S. H., Kalarchian, M. A., Lang, W., et al. (2014). Surgical vs medical treatments for type 2 diabetes mellitus: A randomized clinical trial. *JAMA Surg.* 149, 707–715. doi:10.1001/jamasurg.2014.467

Crossan, K., and Sheer, A. J. (2022). "Surgical options in the treatment of severe obesity," in StatPearls. *StatPearls publishing: Treasure island, FL.* Available at: https://www.ncbi.nlm.nih.gov/books/NBK576372/(accessed Sep 13 2022).

Dabelea, D., Mayer-Davis, E. J., Saydah, S., Imperatore, G., Linder, B., Divers, J., et al. (2014). Prevalence of type 1 and type 2 diabetes among children and adolescents from 2001 to 2009. *JAMA* 311, 1778–1786. doi:10.1001/jama.2014.3201

Dalla Man, C., Rizza, R. A., and Cobelli, C. (2007). Meal simulation model of the glucose-insulin system. *IEEE Trans. Biomed. Eng.* 54, 1740–1749. doi:10.1109/TBME.2007.893506

De Gaetano, A., Panunzi, S., Matone, A., Samson, A., Vrbikova, J., Bendlova, B., et al. (2013). Routine OGTT: A robust model including incretin effect for precise identification of insulin sensitivity and secretion in a single individual. *PLoS ONE* 8, e70875. doi:10.1371/journal.pone.0070875

DeMaria, E. J., Portenier, D., and Wolfe, L. (2007). Obesity surgery mortality risk score: Proposal for a clinically useful score to predict mortality risk in patients undergoing gastric bypass. *Surg. Obes. Relat. Dis.* 3, 134–140. doi:10.1016/j.soard.2007.01.005

Dewberry, L. C., Niemiec, S. M., Hilton, S. A., Louiselle, A. E., Singh, S., Sakthivel, T. S., et al. (2022). Cerium oxide nanoparticle conjugation to microRNA-146a mechanism of correction for impaired diabetic wound healing. *Nanomedicine.* 40, 102483. doi:10.1016/j.nano.2021.102483

Dixon, J. B., Chuang, L-M., Chong, K., Chen, S. C., Lambert, G. W., Straznicky, N. E., et al. (2013). Predicting the glycemic response to gastric bypass surgery in patients with type 2 diabetes. *Diabetes Care* 36, 20–26. doi:10.2337/dc12-0779

Elbahrawy, A., Bougie, A., Loiselle, S-E., Demyttenaere, S., Court, O., and Andalib, A. (2018). Medium to long-term outcomes of bariatric surgery in older adults with super obesity. *Surg. Obes. Relat. Dis.* 14, 470–476. doi:10.1016/j.soard.2017.11.008

Evensen, G. (2009). *Data assimilation: The ensemble kalman filter*. Berlin, Heidelberg: Springer Berlin Heidelberg Springer e-books.

Fetner, R., McGinty, J., Russell, C., Pi-Sunyer, F. X., and Laferrère, B. (2005). Incretins, diabetes, and bariatric surgery: A review. *Surg. Obes. Relat. Dis.* 1, 589–597. doi:10.1016/j.soard.2005.09.001

Ge, H., Xu, K., and Ghahramani, Z. (2018). Turing: A language for flexible probabilistic inference. In *Int. Conf. Artif. Intell. Statistics*, 9-11. Spain: AISTATS, 1682–1690.

Gunczler, P., and Lanes, R. (2006). Relationship between different fasting-based insulin sensitivity indices in obese children and adolescents. *J. Pediatr. Endocrinol. Metab.* 19, 259–265. doi:10.1515/JPEM.2006.19.3.259

Gutch, M., Kumar, S., Razi, S. M., Gupta, K. K., and Gupta, A. (2015). Assessment of insulin sensitivity/resistance. *Indian J. Endocrinol. Metab.* 19, 160–164. doi:10.4103/2230-8210.146874

Ha, J., Satin, L. S., and Sherman, A. S. (2016). A mathematical model of the pathogenesis, prevention, and reversal of type 2 diabetes. *Endocrinology* 157, 624–635. doi:10.1210/en.2015-1564

Ha, J., and Sherman, A. (2020). Type 2 diabetes: One disease, many pathways. *Am. J. Physiol. Endocrinol. Metab.* 319, E410-E426–E426. doi:10.1152/ajpendo.00512.2019

Hales, C. M., Carroll, M. D., Fryar, C. D., and Ogden, C. L. (2017h). *Prevalence of obesity among adults and youth: United States, 2015–2016*. Hyattsville, MD: National Center for Health Statistics.//www.cdc.gov/nchs/data/databriefs/db288.pdf.

Hannon, T. S., Janosky, J., and Arslanian, S. A. (2006). Longitudinal study of physiologic insulin resistance and metabolic changes of puberty. *Pediatr. Res.* 60, 759–763. doi:10.1203/01.pdr.0000246097.73031.27

Hastings, W. K. (1970). Monte Carlo sampling methods using Markov chains and their applications. *Biometrika* 57, 97–109. doi:10.1093/biomet/57.1.97

Hatoum, I. J., Greenawalt, D. M., Cotsapas, C., Reitman, M. L., Daly, M. J., and Kaplan, L. M. (2011). Heritability of the weight loss response to gastric bypass surgery. *J. Clin. Endocrinol. Metab.* 96, E1630–E1633. doi:10.1210/jc.2011-1130

Holst, J. J., and Madsbad, S. (2021). What is diabetes remission? *Diabetes Ther.* 12, 641–646. doi:10.1007/s13300-021-01032-y

Hsia, D. S., Fallon, S. C., and Brandt, M. L. (2012). Adolescent bariatric surgery. *Arch. Pediatr. Adolesc. Med.* 166, 757–766. doi:10.1001/archpediatrics.2012.1011

Hutch, C. R., and Sandoval, D. (2017). The role of GLP-1 in the metabolic success of bariatric surgery. *Endocrinology* 158, 4139–4151. doi:10.1210/en.2017-00564

Inge, T. H., Coley, R. Y., Bazzano, L. A., Xanthakos, S. A., McTigue, K., Arterburn, D., et al. (2018). Comparative effectiveness of bariatric procedures among adolescents: The PCORnet bariatric study. *Surg. Obes. Relat. Dis.* 14, 1374–1386. doi:10.1016/j.soard.2018.04.002

Inge, T. H., Courcoulas, A. P., Jenkins, T. M., Michalsky, M. P., Brandt, M. L., Xanthakos, S. A., et al. (2019). Five-year outcomes of gastric bypass in adolescents as compared with adults. *N. Engl. J. Med.* 380, 2136–2145. doi:10.1056/NEJMoa1813909

Inge, T. H., Courcoulas, A. P., Jenkins, T. M., Michalsky, M. P., Helmrath, M. A., Brandt, M. L., et al. (2016). Weight loss and health status 3 Years after bariatric surgery in adolescents. *N. Engl. J. Med.* 374, 113–123. doi:10.1056/NEJMoa1506699

Inge, T. H., Jenkins, T. M., Xanthakos, S. A., Dixon, J. B., Daniels, S. R., Zeller, M. H., et al. (2017). Long-term outcomes of bariatric surgery in adolescents with severe obesity (FABS-5+): A prospective follow-up analysis. *Lancet. Diabetes Endocrinol.* 5, 165–173. doi:10.1016/S2213-8587(16)30315-1

Inge, T. H., Laffel, L. M., Jenkins, T. M., Marcus, M. D., Leibel, N. I., Brandt, M. L., et al. (2018). Comparison of surgical and medical therapy for type 2 diabetes in severely obese adolescents. *JAMA Pediatr.* 172, 452–460. doi:10.1001/jamapediatrics.2017.5763

Inge, T. H., Zeller, M. H., Jenkins, T. M., Helmrath, M., Brandt, M. L., Michalsky, M. P., et al. (2014). Perioperative outcomes of adolescents undergoing bariatric surgery: The teen–longitudinal assessment of bariatric surgery (Teen-LABS) study. *JAMA Pediatr.* 168, 47–53. doi:10.1001/jamapediatrics.2013.4296

Julier, S. J., and Uhlmann, J. K. (2004). Unscented filtering and nonlinear estimation. *Proc. IEEE* 92, 401–422. doi:10.1109/jproc.2003.823141

Kahn, B. B., and Flier, J. S. (2000). Obesity and insulin resistance. *J. Clin. Investig.* 106, 473–481. doi:10.1172/JCI10842

Kalman, R. E. (1960). A new approach to linear filtering and prediction problems. *J. Basic Eng.* 82, 35–45. doi:10.1115/1.3662552

Kam, H., Tu, Y., Pan, J., Han, J., Zhang, P., Bao, Y., et al. (2020). Comparison of four risk prediction models for diabetes remission after roux-en-Y gastric bypass surgery in obese Chinese patients with type 2 diabetes mellitus. *Obes. Surg.* 30, 2147–2157. doi:10.1007/s11695-019-04371-9

Karasko, D. (2019). Weight loss in adolescents after bariatric surgery: A systematic review. *J. Pediatr. Health Care* 33, 26–34. doi:10.1016/j.pedhc.2018.05.010

Keidar, A. (2011). Bariatric surgery for type 2 diabetes reversal: The risks. *Diabetes Care* 34, S361–S266. doi:10.2337/dc11-s254

Kelly, A. S., Auerbach, P., Barrientos-Perez, M., Gies, I., Hale, P. M., Marcus, C., et al. (2020). A randomized, controlled trial of liraglutide for adolescents with obesity. *N. Engl. J. Med.* 382, 2117–2128. doi:10.1056/NEJMoa1916038

Khattab, A., and Sperling, M. A. (2019). Obesity in adolescents and youth: The case for and against bariatric surgery. *J. Pediatr.* 207, 18–22. doi:10.1016/j.jpeds.2018.11.058

Kim, J. Y., Tfayli, H., Bacha, F., Lee, S., Michaliszyn, S. F., Yousuf, S., et al. (2020). β-cell function, incretin response, and insulin sensitivity of glucose and fat metabolism in obese youth: Relationship to OGTT-time-to-glucose-peak. *Pediatr. Diabetes* 21, 18–27. doi:10.1111/pedi.12940

Kjems, L. L., Christiansen, E., Vølund, A., Bergman, R. N., Madsbad, S., and Volund, A. (2000). Validation of methods for measurement of insulin secretion in humans *in vivo*. *Diabetes* 49, 580–588. doi:10.2337/diabetes.49.4.580

Knowler, W. C., Barrett-Connor, E., Fowler, S. E., Hamman, R. F., Lachin, J. M., Walker, E. A., et al. (2002). Reduction in the incidence of type 2 diabetes with lifestyle intervention or metformin. *N. Engl. J. Med.* 346, 393–403. doi:10.1056/NEJMoa012512

Laferrère, B., and Pattou, F. (2018). Weight-independent mechanisms of glucose control after roux-en-Y gastric bypass. *Front. Endocrinol.* 9, 530. doi:10.3389/fendo.2018.00530

Lamoshi, A., Chernoguz, A., Harmon, C. M., and Helmrath, M. (2020). Complications of bariatric surgery in adolescents. *Semin. Pediatr. Surg.* 29, 150888. doi:10.1016/j.sempedsurg.2020.150888

Law, K. J. H., Stuart, A. M., and Zygalakis, K. C. (2015). *Data assimilation: A mathematical introduction*. arXiv:150607825 [math, stat]Available at: http://arxiv.org/abs/1506.07825 (accessed Mar 15, 2022).

Lee, J. M. (2007). Insulin resistance in children and adolescents. *Rev. Endocr. Metab. Disord.* 7, 141–147. doi:10.1007/s11154-006-9019-8

Lee, J. M., Okumura, M. J., Davis, M. M., Herman, W. H., and Gurney, J. G. (2006). Prevalence and determinants of insulin resistance among U.S. Adolescents: A population-based study. *Diabetes Care* 29, 2427–2432. doi:10.2337/dc06-0709

Levine, M. E., Hripcsak, G., Mamykina, L., Stuart, A., and Albers, D. J. (2017). *Offline and online data assimilation for real-time blood glucose forecasting in type 2 diabetes*. arXiv:170900163 [math, q-bio]Available at: http://arxiv.org/abs/1709.00163 (accessed Mar 15, 2022).

Lim, E. L., Hollingsworth, K. G., Aribisala, B. S., Chen, M. J., Mathers, J. C., and TayloR, R. (2011). Reversal of type 2 diabetes: Normalisation of beta cell function in association with decreased pancreas and liver triacylglycerol. *Diabetologia* 54, 2506–2514. doi:10.1007/s00125-011-2204-7

Little, R. R., Rohlfing, C. L., Tennill, A. L., Madsen, R. W., Polonsky, K. S., Myers, G. L., et al. (2008). Standardization of C-peptide measurements. *Clin. Chem.* 54, 1023–1026. doi:10.1373/clinchem.2007.101287

Livhits, M., Mercado, C., Yermilov, I., Parikh, J. A., Dutson, E., Mehran, A., et al. (2012). Preoperative predictors of weight loss following bariatric surgery: Systematic review. *Obes. Surg.* 22, 70–89. doi:10.1007/s11695-011-0472-4

Manley, S. E., Stratton, I. M., Clark, P. M., and Luzio, S. D. (2007). Comparison of 11 human insulin assays: Implications for clinical investigation and research. *Clin. Chem.* 53, 922–932. doi:10.1373/clinchem.2006.077784

Matthews, D. R., Hosker, J. P., Rudenski, A. S., Naylor, B. A., Treacher, D. F., and Turner, R. C. (1985). Homeostasis model assessment: Insulin resistance and beta-cell function from fasting plasma glucose and insulin concentrations in man. *Diabetologia* 28, 412–419. doi:10.1007/BF00280883

Michaliszyn, S. F., Lee, S., Bacha, F., Tfayli, H., Farchoukh, L., Mari, A., et al. (2017). Differences in β-cell function and insulin secretion in Black vs. White obese adolescents: Do incretin hormones play a role? Race, β-cell function, and incretin response. *Pediatr. Diabetes* 18, 143–151. doi:10.1111/pedi.12364

Michaliszyn, S. F., Mari, A., Lee, S., Bacha, F., Tfayli, H., Farchoukh, L., et al. (2014). β-Cell function, incretin effect, and incretin hormones in obese youth along the span of glucose tolerance from normal to prediabetes to type 2 diabetes. *Diabetes* 63, 3846–3855. doi:10.2337/db13-1951

Miller, W. G., Thienpont, L. M., Van Uytfanghe, K., Clark, P. M., Lindstedt, P., Nilsson, G., et al. (2009). Toward standardization of insulin immunoassays. *Clin. Chem.* 55, 1011–1018. doi:10.1373/clinchem.2008.118380

Mingrone, G., Panunzi, S., De Gaetano, A., Guidone, C., Iaconelli, A., Nanni, G., et al. (2015). Bariatric–metabolic surgery versus conventional medical treatment in obese patients with type 2 diabetes: 5 year follow-up of an open-label, single-centre, randomised controlled trial. *Lancet* 386, 964–973. doi:10.1016/S0140-6736(15)00075-6

Montero, P. N., Stefanidis, D., Norton, H. J., Gersin, K., and Kuwada, T. (2011). Reported excess weight loss after bariatric surgery could vary significantly depending on calculation method: A plea for standardization. *Surg. Obes. Relat. Dis.* 7, 531–534. doi:10.1016/j.soard.2010.09.025

Mulgrave, J. J., Levine, M. E., et al. (2020). *Using data assimilation of mechanistic models to estimate glucose and insulin metabolism*. arXiv:200306541 [physics, stat] Available at: http://arxiv.org/abs/2003.06541 (accessed Mar 16, 2021).

Mulla, C. M., Middelbeek, R. J. W., and Patti, M-E. (2018). Mechanisms of weight loss and improved metabolism following bariatric surgery. *Ann. N. Y. Acad. Sci.* 1411, 53–64. doi:10.1111/nyas.13409

Muniyappa, R., and Madan, R. (2018). "Assessing insulin sensitivity and resistance in humans," in *Endotext*. Editors K. Feingold, B. Anawalt, and A. Boyce (South Dartmouth, MA. Available at: https://www.ncbi.nlm.nih.gov/books/NBK278954/.

Nathan, D. M., Davidson, M. B., DeFronzo, R. A., Heine, R. J., Henry, R. R., Pratley, R., et al. (2007). Impaired fasting glucose and impaired glucose tolerance: Implications for care. *Diabetes Care* 30, 753–759. doi:10.2337/dc07-9920

Nowicka, P., Santoro, N., Liu, H., Lartaud, D., Shaw, M. M., Goldberg, R., et al. (2011). Utility of hemoglobin A(1c) for diagnosing prediabetes and diabetes in obese children and adolescents. *Diabetes Care* 34, 1306–1311. doi:10.2337/dc10-1984

Okser, S., Pahikkala, T., and Aittokallio, T. (2013). Genetic variants and their interactions in disease risk prediction – machine learning and network perspectives. *BioData Min.* 6, 5. doi:10.1186/1756-0381-6-5

Olbers, T., Beamish, A. J., Gronowitz, E., Flodmark, C. E., Dahlgren, J., Bruze, G., et al. (2017). Laparoscopic roux-en-Y gastric bypass in adolescents with severe obesity (AMOS): A prospective, 5-year, Swedish nationwide study. *Lancet. Diabetes Endocrinol.* 5, 174–183. doi:10.1016/S2213-8587(16)30424-7

Olson, D. E., Rhee, M. K., Herrick, K., Ziemer, D. C., Twombly, J. G., and Phillips, L. S. (2010). Screening for diabetes and pre-diabetes with proposed A1C-based diagnostic criteria. *Diabetes Care* 33, 2184–2189. doi:10.2337/dc10-0433

Ortega, E., Morínigo, R., Flores, L., Moize, V., Rios, M., Lacy, A. M., et al. (2012). Predictive factors of excess body weight loss 1 year after laparoscopic bariatric surgery. *Surg. Endosc.* 26, 1744–1750. doi:10.1007/s00464-011-2104-4

Ou, X., Chen, M., Xu, L., Lin, W., Huang, H., Chen, G., et al. (2022). Changes in bone mineral density after bariatric surgery in patients of different ages or patients with different postoperative periods: A systematic review and meta-analysis. *Eur. J. Med. Res.* 27, 144. doi:10.1186/s40001-022-00774-0

Pajvani, U. B., and Accili, D. (2015). The new biology of diabetes. *Diabetologia* 58, 2459–2468. doi:10.1007/s00125-015-3722-5

Panunzi, S., De Gaetano, A., Carnicelli, A., and Mingrone, G. (2015). Predictors of remission of diabetes mellitus in severely obese individuals undergoing bariatric surgery: Do BMI or procedure choice matter? A meta-analysis. *Ann. Surg.* 261, 459–467. doi:10.1097/SLA.0000000000000863

Pedersen, H. K., Gudmundsdottir, V., Pedersen, M. K., Brorsson, C., Brunak, S., and Gupta, R. (2016). Ranking factors involved in diabetes remission after bariatric surgery using machine-learning integrating clinical and genomic biomarkers. *NPJ Genom. Med.* 1, 16035. doi:10.1038/npjgenmed.2016.35

Pedregosa, F., Varoquaux, G., and Gramfort, A. (2011). Scikit-learn: Machine learning in Python. *J. Mach. Learn. Res.* 12, 2825–2830.

Pedroso, F. E., Angriman, F., Endo, A., Dasenbrock, H., Storino, A., Castillo, R., et al. (2018). Weight loss after bariatric surgery in obese adolescents: A systematic review and meta-analysis. *Surg. Obes. Relat. Dis.* 14, 413–422. doi:10.1016/j.soard.2017.10.003

Perotte, A., and Hripcsak, G. (2013). Temporal properties of diagnosis code time series in aggregate. *IEEE J. Biomed. Health Inf.* 17, 477–483. doi:10.1109/JBHI.2013.2244610

Prentki, M., and Nolan, C. J. (2006). Islet cell failure in type 2 diabetes. *J. Clin. Investig.* 116, 1802–1812. doi:10.1172/JCI29103

Purnell, J. Q., Dewey, E. N., Laferrère, B., Selzer, F., Flum, D. R., Mitchell, J. E., et al. (2021). Diabetes remission status during seven-year follow-up of the longitudinal assessment of bariatric surgery study. *J. Clin. Endocrinol. Metab.* 106, 774–788. doi:10.1210/clinem/dgaa849

Rackauckas, C., and Nie, Q. (2017). Differentialequations.jl–a performant and feature-rich ecosystem for solving differential equations in julia. *J. Open Res. Softw.* 5, 15. doi:10.5334/jors.151

Radin, M. S. (2014). Pitfalls in hemoglobin A1c measurement: When results may be misleading. *J. Gen. Intern. Med.* 29, 388–394. doi:10.1007/s11606-013-2595-x

Ramos-Levi, A., Sanchez-Pernaute, A., Matia, P., Cabrerizo, L., Barabash, A., Hernandez, C., et al. (2013). Diagnosis of diabetes remission after bariatric surgery may be jeopardized by remission criteria and previous hypoglycemic treatment. *Obes. Surg.* 23, 1520–1526. doi:10.1007/s11695-013-0995-y

Ramos-Levi, A., Sanchez-Pernaute, A., Matia, P., Cabrerizo, L., Barabash, A., Hernandez, C., et al. (2013). Diagnosis of diabetes remission after bariatric surgery may be jeopardized by remission criteria and previous hypoglycemic treatment. *Obes. Surg.* 23, 1520–1526. doi:10.1007/s11695-013-0995-y

Richter, L. R., Wan, Q., Wen, D., Zhang, Y., Yu, J., Kang, J. K., et al. (2020). Targeted delivery of notch inhibitor attenuates obesity-induced glucose intolerance and liver fibrosis. *ACS Nano* 14, 6878–6886. doi:10.1021/acsnano.0c01007

Robert, M., Ferrand-Gaillard, C., Disse, E., Espalieu, P., Simon, C., Laville, M., et al. (2013). Predictive factors of type 2 diabetes remission 1 Year after bariatric surgery: Impact of surgical techniques. *Obes. Surg.* 23, 770–775. doi:10.1007/s11695-013-0868-4

Rouskas, K., Cauchi, S., Raverdy, V., Yengo, L., Froguel, P., and Pattou, F. (2014). Weight loss independent association of TCF7 L2 gene polymorphism with fasting blood glucose after Roux-en-Y gastric bypass in type 2 diabetic patients. *Surg. Obes. Relat. Dis.* 10, 679–683. doi:10.1016/j.soard.2013.12.016

Roy, V. (2019). *Convergence diagnostics for Markov chain Monte Carlo*. arXiv: 190911827 [stat]Available at: http://arxiv.org/abs/1909.11827 (accessed Apr 13, 2022).

Rubino, F., Nathan, D. M., Eckel, R. H., Schauer, P. R., Alberti, K. G. M. M., Zimmet, P. Z., et al. (2016). Metabolic surgery in the treatment algorithm for type 2 diabetes: A joint statement by international diabetes organizations. *Diabetes Care* 39, 861–877. doi:10.2337/dc16-0236

Saisho, Y., Butler, A. E., Manesso, E., Elashoff, D., Rizza, R. A., and Butler, P. C. (2013). β-Cell mass and turnover in humans: Effects of obesity and aging. *Diabetes Care* 36, 111–117. doi:10.2337/dc12-0421

Schauer, P. R., Kashyap, S. R., Wolski, K., Brethauer, S. A., Kirwan, J. P., Pothier, C. E., et al. (2012). Bariatric surgery versus intensive medical therapy in obese patients with diabetes. *N. Engl. J. Med.* 366, 1567–1576. doi:10.1056/NEJMoa1200225

Seeley, R. J., Chambers, A. P., and Sandoval, D. A. (2015). The role of gut adaptation in the potent effects of multiple bariatric surgeries on obesity and diabetes. *Cell. Metab.* 21, 369–378. doi:10.1016/j.cmet.2015.01.001

Shaibi, G. Q., Davis, J. N., Weigensberg, M. J., and Goran, M. I. (2011). Improving insulin resistance in obese youth: Choose your measures wisely. *Int. J. Pediatr. Obes.* 6, e290–e296. doi:10.3109/17477166.2010.528766

Shen, S-C., Wang, W., Tam, K-W., Chen, H. A., Lin, Y. K., Wang, S. Y., et al. (2019). Validating risk prediction models of diabetes remission after sleeve gastrectomy. *Obes. Surg.* 29, 221–229. doi:10.1007/s11695-018-3510-7

Sherman, A. (2022). *Mathematical model of diabetes pathways*. doi:10.6084/m9.figshare.10792412.v9

Sinha, R., Fisch, G., Teague, B., Tamborlane, W. V., Banyas, B., Allen, K., et al. (2002). Prevalence of impaired glucose tolerance among children and adolescents with marked obesity. *N. Engl. J. Med.* 346, 802–810. doi:10.1056/NEJMoa012578

Skelton, J. A., Cook, S. R., Auinger, P., Klein, J. D., and Barlow, S. E. (2009). Prevalence and trends of severe obesity among US children and adolescents. *Acad. Pediatr.* 9, 322–329. doi:10.1016/j.acap.2009.04.005

Stefater, M. A., and Inge, T. H. (2017). Bariatric surgery for adolescents with type 2 diabetes: An emerging therapeutic strategy. *Curr. Diab. Rep.* 17, 62. doi:10.1007/s11892-017-0887-y

Stern, S. E., Williams, K., Ferrannini, E., DeFronzo, R. A., Bogardus, C., and Stern, M. P. (2005). Identification of individuals with insulin resistance using routine clinical measurements. *Diabetes* 54, 333–339. doi:10.2337/diabetes.54.2.333

Sturis, J., Polonsky, K. S., Mosekilde, E., and Van Cauter, E. (1991). Computer model for mechanisms underlying ultradian oscillations of insulin and glucose. *Am. J. Physiol.* 260, E801–E809. doi:10.1152/ajpendo.1991.260.5.E801

Tagi, V. M., Giannini, C., and Chiarelli, F. (2019). Insulin resistance in children. *Front. Endocrinol.* 10, 342. doi:10.3389/fendo.2019.00342

Taylor, R., Al-Mrabeh, A., and Sattar, N. (2019). Understanding the mechanisms of reversal of type 2 diabetes. *Lancet. Diabetes Endocrinol.* 7, 726–736. doi:10.1016/S2213-8587(19)30076-2

Tharakan, G., Scott, R., Szepietowski, O., Miras, A. D., Blakemore, A. I., Purkayastha, S., et al. (2017). Limitations of the DiaRem score in predicting remission of diabetes following roux-en-Y gastric bypass (RYGB) in an ethnically diverse population from a single institution in the UK. *Obes. Surg.* 27, 782–786. doi:10.1007/s11695-016-2368-9

TODAY Study GroupBjornstad, P., Drews, K. L., Caprio, S., Gubitosi-Klug, R., and Nathan, D. M. (2021). Long-term complications in youth-onset type 2 diabetes. *N. Engl. J. Med.* 385, 416–426. doi:10.1056/NEJMoa2100165

Toh, S., Rasmussen-Torvik, L. J., Harmata, E. E., Pardee, R., Saizan, R., Malanga, E., et al. (2017). The national patient-centered clinical research network (PCORnet) bariatric study cohort: Rationale, methods, and baseline characteristics. *JMIR Res. Protoc.* 6, e222. doi:10.2196/resprot.8323

Tohidi, M., Arbab, P., and Ghasemi, A. (2017). Assay-dependent variability of serum insulin concentrations: A comparison of eight assays. *Scand. J. Clin. Lab. Investig.* 77, 122–129. doi:10.1080/00365513.2016.1278260

Tokarz, V. L., MacDonald, P. E., and Klip, A. (2018). The cell biology of systemic insulin function. *J. Cell. Biol.* 217, 2273–2289. doi:10.1083/jcb.201802095

Topp, B., Promislow, K., Devries, G., Miura, R. M., and Finegood, D. T. (2000). A model of β -cell mass, insulin, and glucose kinetics: Pathways to diabetes. *J. Theor. Biol.* 206, 605–619. doi:10.1006/jtbi.2000.2150

Tsilingiris, D., Koliaki, C., and Kokkinos, A. (2019). Remission of type 2 diabetes mellitus after bariatric surgery: Fact or fiction? *Int. J. Environ. Res. Public Health* 16, 3171. doi:10.3390/ijerph16173171

Tsui, S. T., Yang, J., Zhang, X., Tatarian, T., Docimo, S., Spaniolas, K., et al. (2021). Health disparity in access to bariatric surgery. *Surg. Obes. Relat. Dis.* 17, 249–255. doi:10.1016/j.soard.2020.10.015

Wallace, T. M., Levy, J. C., and Matthews, D. R. (2004). Use and abuse of HOMA modeling. *Diabetes Care* 27, 1487–1495. doi:10.2337/diacare.27.6.1487

Wan, E. A., and van der Merwe, R. (2001). "The unscented kalman filter," in *Kalman filtering and neural networks*. Editor S. Haykin (New York, USA: John Wiley & Sons), 221–280.

Wang, G-F., Yan, Y-X., Xu, N., Yin, D., Hui, Y., Zhang, J. P., et al. (2015). Predictive factors of type 2 diabetes mellitus remission following bariatric surgery: A meta-analysis. *Obes. Surg.* 25, 199–208. doi:10.1007/s11695-014-1391-y

Weiner, A., Cowell, A., McMahon, D. J., Tao, R., Zitsman, J., Oberfield, S. E., et al. (2020). The effects of adolescent laparoscopic adjustable gastric band and sleeve gastrectomy on markers of bone health and bone turnover. *Clin. Obes.* 10, e12411. doi:10.1111/cob.12411

Weiskopf, N. G., Hripcsak, G., Swaminathan, S., and Weng, C. (2013). Defining and measuring completeness of electronic health records for secondary use. *J. Biomed. Inf.* 46, 830–836. doi:10.1016/j.jbi.2013.06.010

Yan, W., Bai, R., Yan, M., and Song, M. (2017). Preoperative fasting plasma C-peptide levels as predictors of remission of type 2 diabetes mellitus after bariatric surgery: A systematic review and meta-analysis. *J. Investig. Surg.* 30, 383–393. doi:10.1080/08941939.2016.1259375

Yeckel, C. W., Weiss, R., Dziura, J., Taksali, S. E., Dufour, S., Burgert, T. S., et al. (2004). Validation of insulin sensitivity indices from oral glucose tolerance test parameters in obese children and adolescents. *J. Clin. Endocrinol. Metab.* 89, 1096–1101. doi:10.1210/jc.2003-031503

Yip, S., Plank, L. D., and Murphy, R. (2013). Gastric bypass and sleeve gastrectomy for type 2 diabetes: A systematic review and meta-analysis of outcomes. *Obes. Surg.* 23, 1994–2003. doi:10.1007/s11695-013-1030-z

Frontiers in Endocrinology

Explores the endocrine system to find new therapies for key health issues

The second most-cited endocrinology and metabolism journal, which advances our understanding of the endocrine system. It uncovers new therapies for prevalent health issues such as obesity, diabetes, reproduction, and aging.

Discover the latest Research Topics

See more →

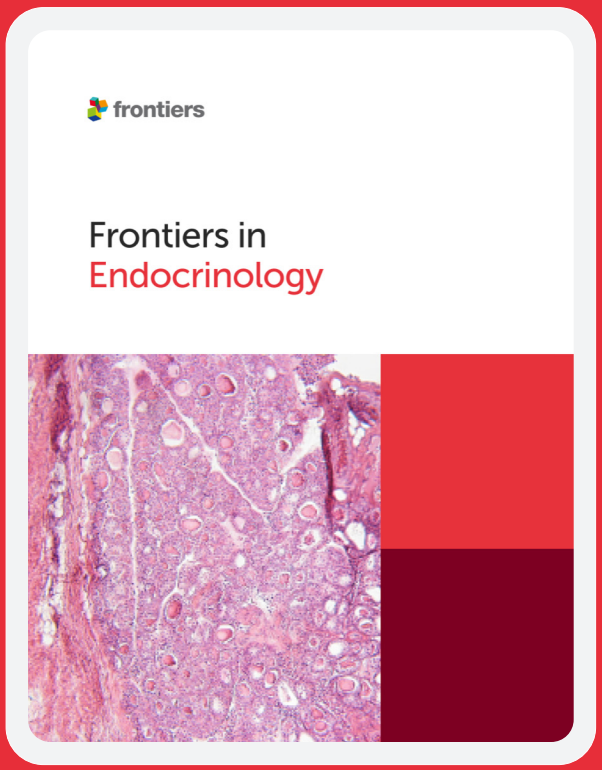

Frontiers

Avenue du Tribunal-Fédéral 34
1005 Lausanne, Switzerland
frontiersin.org

Contact us

+41 (0)21 510 17 00
frontiersin.org/about/contact